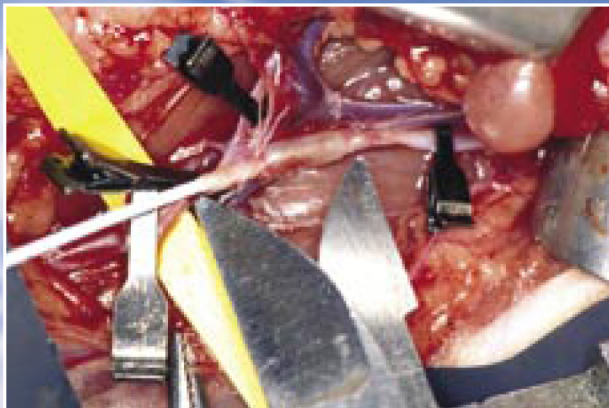


Endovascular Photodynamic Therapy to Prevent Arterial Restenosis



E.E.E. Gabeler

**ENDOVASCULAR PHOTODYNAMIC THERAPY TO
PREVENT ARTERIAL RESTENOSIS**

E.E.E. Gabeler

Financial support by the Netherlands Heart Foundation for the publication of this thesis is thankfully acknowledged.

Additional support of the following companies is very much appreciated:

Lijf & Leven Foundation, Harlan Nederland BV

The studies described in this thesis were performed at the Laboratory for Experimental Surgery and the Department of Biochemistry of the Erasmus Medical Center Rotterdam, The Netherlands.

The studies described in this thesis were supported by a grant of the Netherlands Heart Foundation (NHF 97.181).

Cover : *In front*: Balloon angioplasty of the rat iliac artery. *Background*: Clinical laser therapy.

Print : Optima Grafische Communicatie, Rotterdam

ISBN 90-77595-01-5

©2003, E.E.E. Gabeler, Rotterdam, The Netherlands.

All right reserved. No part of this thesis may be reproduced, stored in a retrieval system of any nature, or transmitted in any form by any means, electronic, mechanical, photocopying, scanning, recording or otherwise, included a complete or partial transcription, without the permission of the author.

ENDOVASCULAR PHOTODYNAMIC THERAPY TO PREVENT ARTERIAL RESTENOSIS

Endovasculaire Fotodynamische Therapie

ter preventie van arteriële restenose

Proefschrift

ter verkrijging van de graad van doctor

aan de Erasmus Universiteit Rotterdam

op gezag van de Rector Magnificus

Prof. Dr. S. W. J. Lamberts

en volgens besluit van het College voor Promoties.

De openbare verdediging zal plaatsvinden op

3 december 2003

om 11:45 uur

door

Edward Emmanuel Euson Gabeler

geboren te Haarlem

Promotie commissie

Promotor : Prof. Dr. H. van Urk

Overige leden : Prof. Dr. P.M.T. Pattynama
Prof. Dr. T.H. van der Kwast
Prof. J.H.P. Wilson

Copromotoren : Dr. R. van Hillegersberg
Dr. W. Sluiter

To my father
In remembrance of my mother
To my sisters Annette, Lydia and Margriet
To Josia, Christian, Dennis-John, Samuël
To Caroline

CONTENTS

SECTION I BACKGROUND

Chapter 1	General introduction..... 1 <i>adapted from Photodynamic News, 2002, Vol.5(1), 6-9.</i>
Chapter 2	Aims and outline of the thesis.....23

SECTION II MODEL REQUIREMENTS

Chapter 3	A Comparison of Balloon Injury Models of Endovascular Lesions.....27 in Rat Arteries. <i>BMC Cardiovascular disorders, 2003,16(1):1-8.</i>
	3.00 Abstract..... 29
	3.01 Introduction..... 30
	3.02 Materials & methods..... 31
	3.03 Results..... 35
	3.04 Discussion..... 42
	3.05 Conclusions..... 43
Chapter 4	Aminolaevulinic acid induced protoporphyrin IX pharmacokinetics 47 in central and peripheral arteries of the rat. <i>Photochemistry & Photobiology, 2003, 78(1):82-87.</i>
	4.00 Abstract..... 49
	4.01 Introduction..... 50
	4.02 Materials & methods..... 51
	4.03 Results..... 53
	4.04 Discussion..... 62

SECTION III ENDOVASCULAR PHOTODYNAMIC THERAPY

Chapter 5	The effect of endovascular photodynamic therapy on the normal rat 67 artery. <i>submitted</i>
	5.00 Abstract..... 69
	5.01 Introduction..... 70
	5.02 Materials & methods..... 70
	5.03 Results..... 72
	5.04 Discussion..... 75
Chapter 6	Endovascular photodynamic therapy with aminolaevulinic acid.....79 prevents balloon induced intimal hyperplasia and constrictive remodelling. <i>Eur J Vasc Endovasc Surg, 2002, 24 :322-331.</i>
	6.00 Abstract 81
	6.01 Introduction..... 82
	6.02 Materials & methods..... 83
	6.03 Results..... 87
	6.04 Discussion..... 92

SECTION IV PDT AND VASCULAR BIOLOGY

Chapter 7	The effect of photodynamic therapy on reendothelialization after balloon injury of the rat iliac artery. <i>submitted</i>	97
	7.00 Abstract	99
	7.01 Introduction	100
	7.02 Materials & methods	100
	7.03 Results	103
	7.04 Discussion	110
Chapter 8	Endovascular photodynamic therapy alters the inflammatory reaction in the arterial response to injury. <i>submitted</i>	115
	8.00 Abstract	117
	8.01 Introduction	118
	8.02 Materials & methods	118
	8.03 Results	122
	8.04 Discussion	127

SECTION V PDT AND VASCULAR PHYSIOLOGY

Chapter 9	Arterial wall strength after endovascular photodynamic therapy. <i>Laser Surg Med, 2003,33(1):8-15.</i>	131
	9.00 Abstract	133
	9.01 Introduction	134
	9.02 Materials & methods	135
	9.03 Results	138
	9.04 Discussion	142

SECTION VI AFTERMATH

Chapter 11	General Discussion and Conclusions	147
Chapter 12	Summary	157
	Samenvatting	164
Appendices	Dankwoord	173
	Curriculum vitae	177

vicit vim virtus

SECTION I

CHAPTER 1

General introduction

1.00 The historical aspects of photodynamic therapy

Since their existence, man has appreciated the benefits of sunlight and described some of its medicinal effects known as heliotherapy. Herodotus in the 6th century BC noticed that sunlight had beneficial effects on bone growth. Hippocrates in 460-375 BC advocated the use of heliotherapy for various human maladies [1]. In 1898, McCall-Anderson described skin photosensitivity due to porphyrin molecules [2]. In 1900, Raab using acridine orange described a photochemical action that led to the killing of protozoa [3]. In 1901, the Dane Niels Rydberg Finsen described the first scientific experiment in animals designated as phototherapy using light from a carbon arc. Phototherapy was defined as the use of visible or near-visible light in the treatment of disease [4]. He noticed that the use of ultraviolet light improved wound healing in smallpox in animals and lupus vulgaris in men. These studies were appreciated with naming a Medical Light Institute after him in Copenhagen and by awarding him the Nobel Prize for Physiology-Medicine in 1903. The Danish Queen Alexandra introduced the technique into the London Hospital in Whitechapel (now the Royal London Hospital) in 1904.

Two medical students in Germany, Jesionek and von Tappeiner, discovered in 1903 that the effect of phototherapy could be amplified by using the light sensitive drug eosin. They found that this so called photodynamic effect made this application suitable for the treatment of tumours in a mouse model [5]. In 1905, they described the eradication of superficial basal carcinoma in humans. In that same year, Albert Einstein discovered the principles of light amplification by stimulated emission of radiation, the acronym for laser [6-7]. With the availability of laser a fundamental tool for successful photodynamic therapy became available. In 1924, Policard in Lyon, described a natural fluorescence of experimental tumours by porphyrins, indicating an association between porphyrins and cancer [8]. In 1942, Auler and Banzer described a tumour reduction in animals using a first generation photosensitizer haematoporphyrin [9]. Some years later, Figge, Wieland and Mangianello in the USA reported that a selective accumulation of haematoporphyrin selectively accumulated in embryonic and regenerating tissue [10]. In 1961, Lipson introduced the haematoporphyrin derivative that could be visualized by its selective red fluorescence upon illumination with ultraviolet light [11]. Later, Diamond and colleagues reported that the photodynamic effect could be obtained by changing the irradiation energy [12]. In 1974, the effectiveness of photodynamic therapy in various animal models was described by Dougherty in Buffalo [13], USA and by Berenbaum in London [14].

The first photodynamic studies in men were published by Kelly and Snell in 1976 [15]. Since then, the development of new photosensitizers increased extensively and PDT became accepted in many medical fields to treat premalignant and malignant lesions, as in the field of dermatology, urology, interventional radiology, neurosurgery, gynaecology, and gastroenterology.

The first regulatory approval for a photodynamic drug was accorded to Photofrin® by the Canadian authorities in 1993. Aminolaevulinic acid (ALA, DUSA Pharmaceuticals, Inc DUSλ) was approved by the British authorities in 2000.

1.01 The fundamental physical principles of photodynamic therapy

Photodynamic therapy (PDT) is a two-step process in which first photosensitive molecules (photosensitizers) localise in target tissue or cells. Secondly, the photosensitizer is activated with appropriate light energy to generate toxic species that mediate tissue or cell destruction <Fig.1.1> [16]. The toxicity is generally oxygen-dependent, but the oxygen dependence varies with the photosensitizer [17].

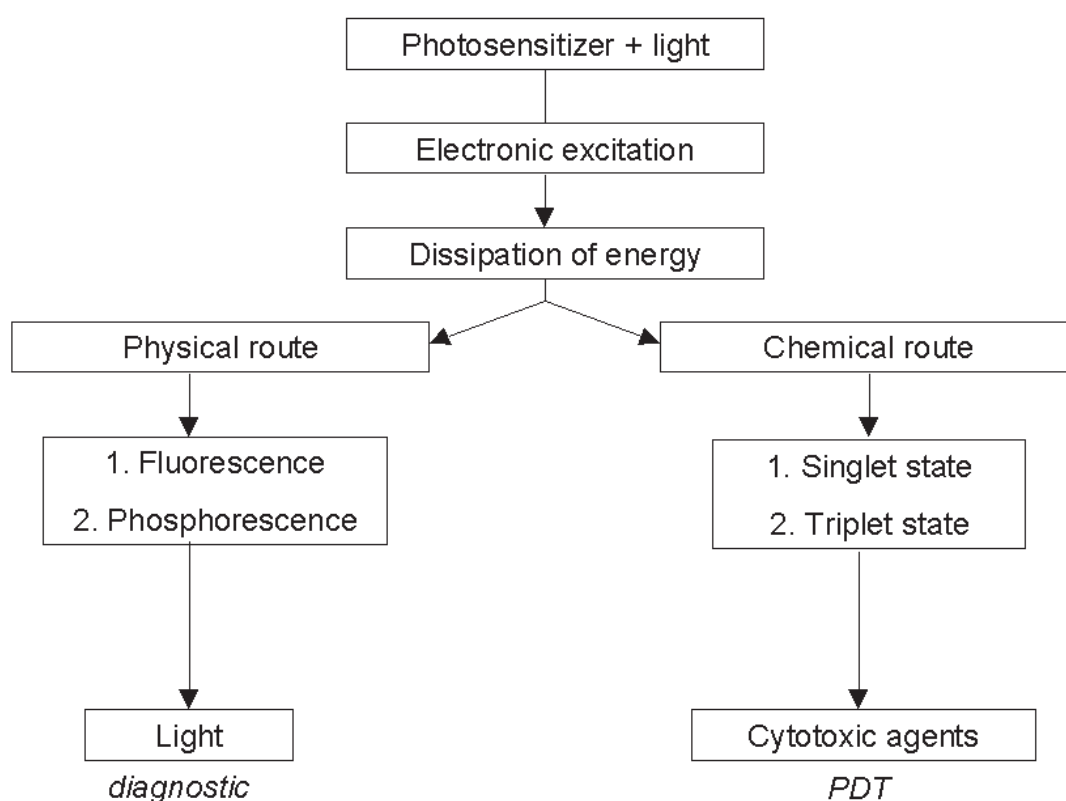


Figure 1.1 A schematic representation of the mechanism of photodynamic therapy. The activation of the photosensitizer with appropriate light results in a electronic excitation (See Figure 3.2) followed by the dissipation of energy via a physical route (fluorescence or phosphorescence) or a chemical route (generation of molecules in the singlet or triplet state). This latter route is responsible for the photodynamic effect.

1.01.1 Light

The use of visible light of one particular wavelength (*monochromatic*) in PDT characterises the core of this treatment. In PDT, it is crucial to think of visible light as energy in the form of sinusoidal electromagnetic radiation expressed as wave and as particle (*quantum, photon*), to perform light-dosimetry.

Fluence is the total radiant energy traversing a small transparent imaginary spherical target containing the point under consideration, divided by the cross sectional area of the target (J/cm^2). External illumination is expressed in J/cm^2 and endovascular illumination is expressed in $\text{J}/\text{cm dl}$. With other words $100 \text{ J}/\text{cm}^2$ is more than $100 \text{ J}/\text{cm dl}$. Due to endovascular spherical abnormalities by stenosis, the cross sectional surface to illuminate is not simple squared. The fluence per cm dl instead of per surface squared cm will avoid the enormous variance in stenosis morphology.

The time needed to arrive at this energy dose or fluence is determined by the fluence rate (irradiance or power density) expressed in W/cm^2 .

1.01.2 The light sources

In PDT the laser is mostly used as the light source. Laser is an acronym for 'light amplification by stimulated emission of radiation'. 'Stimulated' stands for the release of a photon after electronical excitation of the molecule S^* on interaction with a photon, namely: $S^* + h\nu \rightarrow S + 2h\nu$. The used photon has the same properties as the released photon, as described by Townes, Basov and Prokhorov. For this discovery, they were awarded the Nobel Prize in Physics in 1964 [18-20]. The unique properties of laser are that its rays are intense, coherent, so that all the waves are in phase, deliverable in short pulses, wavelength monochromacy, by which all available energy can be focussed at the maximum absorption wavelength of the photosensitizer, and collimated allowing parallel light beam to be transported through a fibre.

1.01.3 The energy states of the photosensitizer

After absorption of electromagnetic radiation, the photosensitizer will be excited to a higher energy state. The transfer of this excitation energy from the excited photosensitizer unto the surrounding molecules (non-ionising decay) may either induce a photochemical reaction (kinetic energy) or be re-emitted as fluorescence. These transitions of electronic energy levels are represented in Jablonski diagrams <Fig.1.2>. The electronic vibrational state of the photosensitizer is represented by the singlet ground state S_0 , which changes into S_1 after absorption with a single photon, S_2 with two or S_3 with 3 photons [21]. These phenomena are known as *internal conversion*. From this energised state, the photosensitizer may relax back to S_0 by the emission of light (fluorescence), may *inter-system cross* to the triplet state, T_1 . This is the more reactive state with a relatively long lifetime and normally, the T_1 by its transition into the ground state initiates direct photochemical reactions (Type 1) or transfers its energy to the ground state oxygen molecules $^3\text{O}_2$ to give rise to excited state oxygen molecules, singlet oxygen $^1\text{O}_2$, that lead to photooxidative reactions (Type 2) [22;23].

1.01.4 The criteria to meet for a photosensitizer

Important criteria for photosensitizers to be suitable for PDT are that they are [24;25] stable and non-toxic without light (low dark-toxicity), accumulate in the target tissue, and can be activated in the absorption spectrum between 600-900 nm, because the most important cellular molecules do absorb light of 200-500 nm. All porphyrin based photosensitizers have a maximum absorption at 400 nm (=Soret or B band) and in the 500-600 nm region usually 4 Q bands if complexed with monovalent metal, and 2 Q bands if complexed with a divalent metal. If the highest Q band is in the 500 nm region than the photosensitizer is called etio-type, at 500 and 600 nm phyllo type, at 550 nm rhodo-type, at 550 and 600 nm oxorhodo-type and at 650 nm retro-etio type. Furthermore, a good photosensitizer must have a high triplet quantum yield, a high singlet oxygen quantum yield and a finite fluorescence quantum yield increasing the cytotoxic potential. Hydrophilicity and electric charge will improve the distribution of the photosensitizer into target tissue or target cells.

Unfortunately, to date, the ideal photosensitizer is not yet discovered.

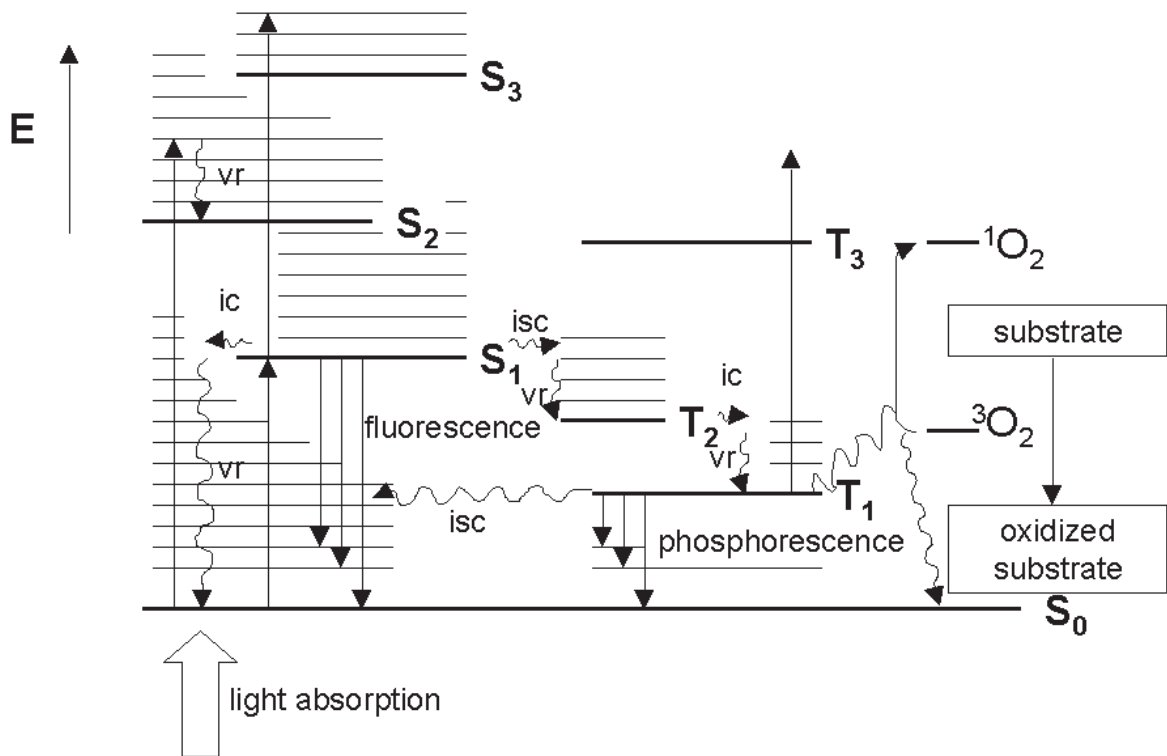


Figure 1.2

Jablonski diagram for an organic molecule, showing the transitions between the singlet (S_0 , S_1 , S_2 , S_3) and triplet (T_1 , T_2 , T_3) electronic levels (heavy horizontal lines). The energy levels of only the vibrational mode are portrayed for each electronic state (light horizontal lines). Radiative transitions are shown as straight arrows. Radiationless relaxation processes are shown as wavy arrows: vr, vibrational relaxation; ic, internal conversion; isc, intersystem crossing. The radiative decay processes depicted are fluorescence and phosphorescence. The diagram exemplifies three spin-allowed absorption processes: 1. the transition from the thermally equilibrated, ground state (S_0), to a vibrational excited level of the second excited singlet state (S_2). 2. The first transition from the thermally equilibrated, first excited singlet state (S_1) to a vibrationally excited level of the third excited singlet state (S_3). 3. The transition from the thermally equilibrated lowest triplet state (T_1) to a vibrationally excited level of the second triplet state (T_3). By so called intersystem crossing the singlet state can be converted into the triplet state with a relatively long half life. The subsequent transition into the ground state S_0 allows a simultaneous type I photochemical reaction or the type II excitation of ground state molecular oxygen (3O_2) into singlet oxygen (1O_2). Fluorescence is a spin-allowed, radiative transition from the thermally equilibrated first excited singlet state (S_1) to different vibronic levels of the ground state (S_0). Phosphorescence is a spin-forbidden radiative transition from the thermally equilibrated lowest triplet state (T_1) to different vibronic levels of the ground state. From fundamentals of photodynamic therapy (T.Hasan SPIE 2000, Sc 031:22).

1.02 The fundamentals of aminolaevulinic acid metabolism

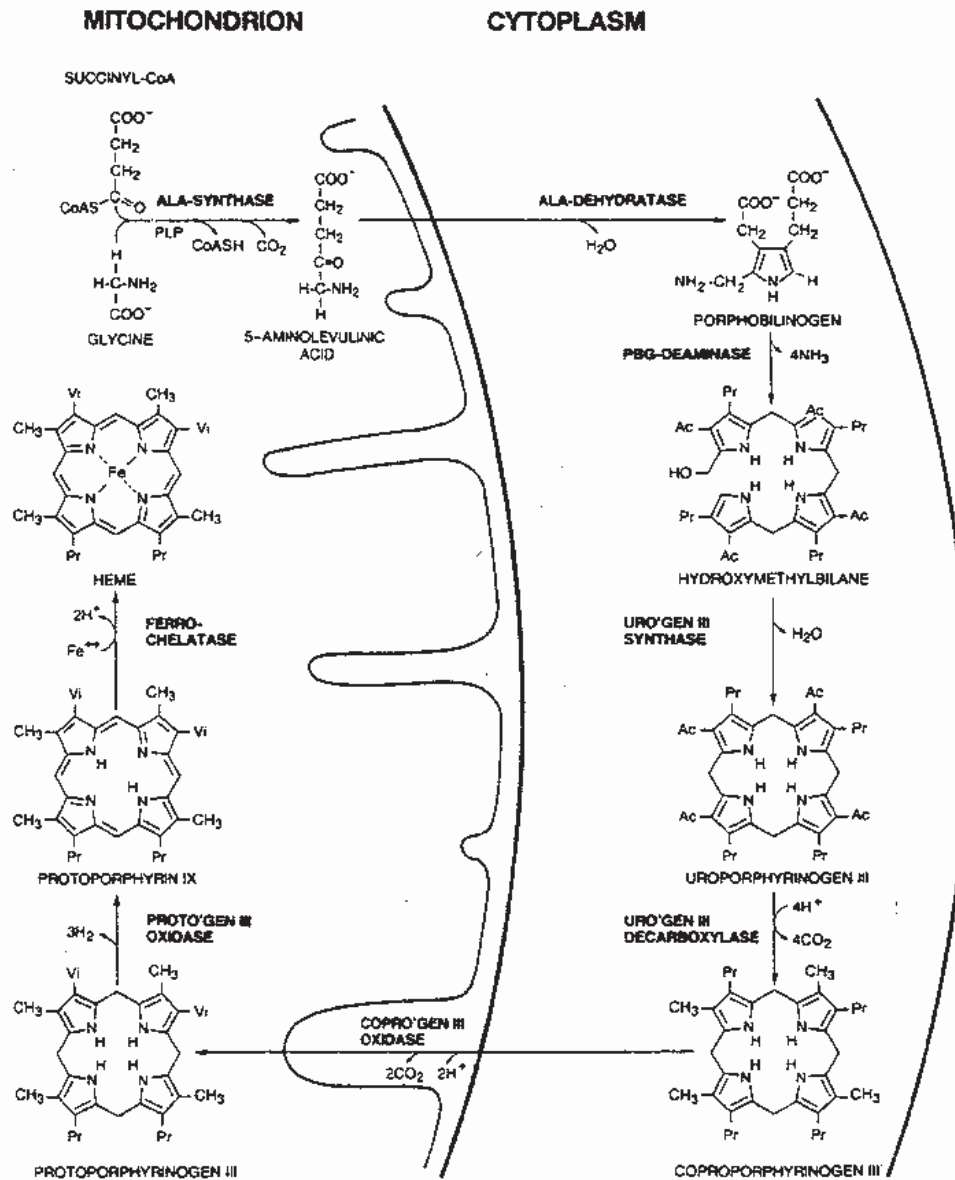
An exception to the second-generation exogenous photosensitizers is the prodrug aminolaevulinic acid, which is an endogenous heme metabolite. Its potential for photodynamic therapy is derived from the induced phototoxicity observed in porphyria. Excessive concentrations in tissue of ALA lead to conversion into heme metabolites, and to in particular the accumulation of the photosensitive protoporphyrin IX. In 1956, Berlin was the first who administered ALA to animals and humans to study the heme and bilirubin synthesis [26]. Our group started experiments with the endogenous photosensitization of liver tumors in rats at the end of the eighties [27]. In 1990, Kennedy described the first clinical experiments with ALA based PDT to treat skin tumours [28]. In 1994, Grant was the first to apply ALA in the prevention of intimal hyperplasia [29].

Heme and porphyrin synthesis

Heme is an essential iron-containing prosthetic group for many important proteins including hemoglobins, myoglobins, catalases, peroxidases and cytochromes [30]. Heme is synthesized from glycine and succinate in a series of reactions occurring in the mitochondria and cytoplasm of the cell.

Glycine and succinyl CoA are condensed to ALA catalyzed by the mitochondrial rate-limiting enzyme ALA synthase, also known as the Shemin pathway <Fig.1.3> [31]. Two ALA molecules when transported into the cytoplasm form one porphobilinogen molecule catalysed by porphobilinogen synthase, four porphobilinogen molecules form uroporphyrinogen 3 that will be converted by PBG deaminase into hydroxymethylbilane (HMB) [27]. Then, HMB may convert spontaneously into uroporphyrinogen 1, and subsequently via decarboxylation into coproporphyrinogen 1 that after oxidation is excreted in the urine as uro- and coproporphyrin. Alternatively, HMB will be converted into uroporphyrinogen 3 by uroporphyrinogen 3 cosynthase, and next by uroporphyrinogen 3 decarboxylase into coproporphyrinogen 3. Coproporphyrinogen is converted by coproporphyrinogen oxidase into protoporphyrinogen IX and subsequently converted into the photosensitizer protoporphyrin IX by the action of protoporphyrinogen oxidase. Finally, heme is formed by the insertion of iron catalyzed by the enzyme ferrochelatase.

Figure 1.3



The heme biosynthetic pathway.

PLP, pyridoxal-5-phosphate; ALA, 5-Aminolevulinic Acid; PBG, Porphobilinogen; URO'gen, Uroporphyrinogen; COPRO'gen, Coproporphyrinogen; PROTO'gen, Protoporphyrinogen; Ac, Acetate; Pr, Propionate; Vi, Vinyl
 (by courtesy of Dr S.S. Bottomley)

1.03 The historical aspects of vascular photodynamic therapy

In 1983, Spears described that the haematoporphyrin derivative (HpD) accumulated selectively in experimental atherosclerotic plaques [32]. In 1985, Litvack presented the first PDT effect with HpD on atherosclerotic arteries and noticed that the selective accumulation of HpD was due to the high mitotic activity of smooth muscle cells (SMC) <Table 3.1>. This started the investigations of using the high energy of lasers in 1987 by Pollock [33], in 1992 by Asahara and in 1993 by Tang to ablate the photosensitive impregnated plaques. Unfortunately, it was impossible to ablate the calcified noncellular coatings of the plaque. In vitro studies performed by Dartsch in 1990 indicated that PDT of SMCs of human atherosclerotic plaques using the photosensitizer Photofrin inhibited their proliferation [34]. On this basis, the rationale to prevent intimal hyperplasia in hyperproliferative restenotic lesions was born. In 1988 and 1991, Mackie published the first successful inhibition of intimal hyperplasia in coronary arteries of dogs using dihaematoporphyrin ester. One year later Eton used external PDT with the first generation photosensitizer Photofrin to inhibit intimal hyperplasia of the rabbit and Ortu used the second generation photosensitizer chloroaluminium sulfonated phtalocyanine (CASPC) for that purpose in the balloon injured carotid artery of the rat. In 1993, LaMuraglia and colleagues described the selective accumulation of CASPC in the proliferative part of the injured rat carotid artery. In 1994, the same group reported that external vascular PDT resulted in inhibition of intimal hyperplasia lasting the observation period of 16 weeks. This beneficial effect was likely due to persistent eradication of smooth muscle cells in the tunica media. In the same year, Grant was the first to use ALA as prodrug for protoporphyrin IX based external PDT in the balloon injured rat femoral artery. In 1996, Gonschior reported for the first time the use of endovascular PDT with Photofrin in the balloon injured femoral pig artery. In 2001, Hayase described the effects of the second-generation photosensitizer texapherin (Antrim®) in the balloon injured rabbit iliac artery <Table 1.1>[28;35-64]. Third generation photosensitizers have an additional targeting system, like monoclonal antibodies, and are in an early stage of development.

1.03.1 The evaluation of vascular PDT in the clinic

In 1999, the UK group led by S. Bown was the first to publish the effects of ALA-PDT in patients with stenosis of the femoral arteries [65]. Promising initial results marked a brake through in the application of PDT. However, no complete eradication of synthetic SMCs was obtained and back-growth of intimal hyperplasia was still the case. The first clinical trial treating patients with stenosis of peripheral arteries using texaphyrin is underway in the USA [66].

1.03.2 The evaluation of vascular PDT in anastomotic models

While inhibition of intimal hyperplasia after balloon injury models in rats, rabbits, dogs, monkeys and pigs was obtained, the inhibition of IH with PDT at the anastomotic site in surgical reconstructions is more difficult to obtain [67]. Further improvements in this field are required before evaluating PDT as a clinical adjuvant tool in anastomotic (by-pass) surgery.

Irradiance mW/cm ²	Fluence J/cm ²	Method	Photo- sensitizer	Dose mg/kg	Wavelength nm	Peak hours	Model design
12-33	32-288	int	HPD	5-20	636	72	rabbits
500	20-410	int 1cm	DHE	2.5	632	24	dogs
nk	2.7	int	HPD	Nk	nk	nk	rabbits+BI
80	7.6	ext 1 cm	Photofrin	5	630	48	rabbits+BI
100	100	ext 2 cm	CASPc	5	675	0.33	rats+BI
32-256	1.6-60	int	Photofrin	2.5-5	630	48	rabbits
100	100	ext 2 cm	CASPc	5	675	24	rats+BI
nk	50	ext	ALS2Pc	0.5-5	675	48	rats
1000	120	int 1 cm	Photofrin	2.5	630	24	swine+BI
150	100	ext 1 cm	ALS2Pc	5	675	1	rats
	250		ALA	200	630	3	
nk	100	ext	ALS2Pc	5	675	1	rabbits
			ALA	200	630	3	
nk	25	ext	AptS	2.5	672	0.5	rabbits+BI
1000	120-240	int 1 cm	Photofrin	5	630	0.33	rabbits+BI
100-180	50	ext 1 cm	ALA	20-200	630	0.5-1.5	rats+BI
70	100	ext	Pheoph	1	647	24	rabbits
100	100	int 1.5 cm	Photofrin/l	5	630	0	pigs
150-200	50	i-ext 1 cm	ALS2Pc	5	675	0.5	rats+BI
100	100	int 1.5 cm	Photofrin/l	5	630	0	pigs+BI
200-400	120	int	HPD	5	630		rabbits+BI
100	100	ext 2 cm	CASPc	5	675	24	rats+BI
10	1.8	int 2 cm	absent		632		rabbits+BI
100	20	ext 2 cm	Chlorine6	2.5	661	4	rats+BI
	40		BSA/e6	2.5		4	
<120	50(20%f)	int 4 cm	ALA	60	635	5-7	patients
100	50-200	ext 2 cm	BPD	0.5-25ug	690	0.25	rats+BI
100	100	ext 1 cm	Met.blue	250	660	0.08	rats+BI
				ug/ml			
180	300	int 2 cm	Zinc-Pc/l	20 ug/ml	6-700	0.5	rabbits+BI
100-200	50(20%f)	int 2 cm	ALA	120	635	4-6	pigs+BI
		int 4 cm					
100/dl	12.5-50	int 2 cm	ALA	200	633	2-3	rats+BI
nk	50-200	int 2-3 cm	Miravant	1-3		2-6	rabbits/swine
250/dl	180/dl	int 3 cm	Antrin	1.2	736	0.25	rabbits+BI

Table 1.1 A summary of chronologically published in vivo studies of photodynamic therapy on restenosis.

The following abbreviations mean:

/ dl= mW/cm diffuser length; 20%(f)=20%; fractionated illumination;
 int 1cm=internal illumination at a spotsize of 1 cm; ext 1 cm= external
 illumination at a spotsize of 1 cm;HPD= hematoporphyrin derivative;DHE=
 dihydroxyphosphyrinester; CASPc= chloroaluminosulfurphthalocyanine; ALS2Pc= alumino
 disulphurphthalocyanine; ALA=aminolaevulinic acid; BPD= bi-porphyrin derivative; +BI= with
 balloon injury

Chl dt	No. N=	Artery type	Groups amount	FU wk	PDT effect on IH mm ²	Media effect mm ²	MLD mm	R
y	15	car/fem	2 PDT	2	damage	fissured	nk	35
n	9	coronary	2 low vs high	4	no IH vs IH	damage vs spasm	nk	36
y	30	iliac	3 BI vs PDT	4	nk	IMR: 3.4vs0.9sd0.7	nk	37
n	10	carotid	3 BI vs PDT	5	24vs16 sd2.1	nk	nk	38
n	Nk	carotid	2 BI vs PDT	2	0.17vs 0.06 sd0.05	ns	nk	39
n	35	aorta	2 BI vs PDT	4	0.7 mm vs0.5 sd0.1	nk	ns	40
n	33	carotid	2 BI vs PDT	16	0.12vs0.03 sd0.02	ns	ns	41
n	75	carotid	4 PDT	24	Depletion	repopulation >24w	nk	42
y	12	iliac	2 pre vs post	4	Nk	nk	39.2vs35.9 sd41%	43
n	Nk	femoral	4 BI vs PDT	24	0.01vs0.02-0.10	nk	nk	44
n	18	carotid	4 BI PDT Al-ALA	3	nk nk	nk nk	bp:5.3 sd0.9 bar 7.0 sd1.7 bar	45
n	120	carotid	4 BI vs PDT	6	0vs0.02	nk	28-143vs22%	46
n	24	iliac	4 BI vs PDT	4	nk	IMR: 1vs0.3 sd0.2	nk	47
n	40	carotid	3 BI vs PDT	4	nk	IMR:0.7vs0	nk	48
y	15	aorta	3 PDT	24 h	denudation	foam cells	nk	49
n	70	femoral	4 BI vs PDT	3	1.57vs0.1 sd0.05	nk	loss 38vs3 %	50
n	100	carotid	4 BI vs PDT	26	100% vs 51% IH	nk	nk	51
n	72	femoral	4 BI vs PDT	3	1.57vs0.1 sd0.05	IMR: 1vs0.3 sd0.2	loss 30vs3%	52
y	20	femoral	2 BI vs PDT	1	nk	IMR:0.5vs0 sd0.02	nk	53
n	24	carotid	2 BI vs PDT	16	0.16vs0.07 sd0.03	0.1vs0.05 sd0.01	0.82vs1.02	54
n	15	aorta	2 BI vs PDT	8	25.3vs4.2 sd0.7	IMR: 2.1vs0.3sd0.0	1.62vs2.32	55
n	15	aorta	2 Chle6 Bcle6	48 h	loss 20-50% loss 60-80%	0% loss 20-40%	nk nk	56
	8	femoral	1	6 m	3:100% success	3:25% rst	2:40%	57
n	32	carotid	4 BI vs PDT	2	0.16vs0.01 sd0.01	0.2vs0.1 sd0.02	0.94vs0.86	58
n	18	carotid	3 BI vs PDT	2	0.19vs0	0.1vs0.06 sd0	ns	59
n	52	femoral	4 BI vs PDT	4	49.4vs40.4 sd7.8	IMR:1.2vs0.6 sd0.2	nk	60
n	13	coronary	4 BI c/i	4	0.7-0.8 sd0.8	2.9-12.5 sd1.1-5.4	1.6-7.9 sd0.7-4.8	61
		iliac	2 BI+PDTc/i		0.4-0.7 sd0.4	2.9vs15.2 sd0.5-4.3	1.4-9.8 sd0.8-3.7	
n	33	iliac	2 BI vs PDT	4	0.15vs0.01 sd0.01	0.13vs0.2 sd0.05	nk	62
n	Nk	per/cor	2 PDT	4	0	nk	nk	63
n	17	iliac	2 BI vs PDT	2	82vs73 sd10 %	3.7vs3.4 sd1	nk	64

Chl dt= cholesterol diet; y=yes; n=no; No.=number; car=carotid; fem=femoral; cor=coronary, per=peripheral; PDT=photodynamic therapy; c/i=coronary and iliac; FU=follow-up; wk= weeks; h=hours; m=months; IH= intimal hyperplasia; vs=versus; sd=standard deviation; nk=not known IMR= intima to media ratio; MLD=maximal lumen diameter; bp=bursting pressure; R=references.

1.04 The pathophysiology of stenosis and restenosis: The phases in restenosis development

Restenosis is defined as the mean narrowing after an initially successful result of vascular intervention [68-70].

Restenosis is initiated indirectly by the combined action of thrombin, platelets, neutrophils or macrophages in the local thrombus that accumulates at the injured arterial segment, or directly through the traumatisation of the artery. Both events change the expression patterns of growth factors, their receptors, release of cytokines and the cell regulating proteins, resulting in a myofibrotic reaction of the artery. Prominent cells involved in the myofibrotic reaction of the artery are endothelial cells, fibroblasts and SMCs. The following phases are distinguished:

1. In the first seconds and minutes the complement-pathway is activated [71].
2. In the first hours after vascular injury, the denudated region by the exposure of fibronectin activates the hemostatic system, causes platelet aggregation and the release of granules by platelets (peaks after several hours and lasts for a day), followed by thrombus formation and thrombolysis (lasts for days to weeks). There is a correlation between the degree of vascular damage and the degree of platelet aggregation and thrombus formation [71-72].
3. In parallel, macrophages, neutrophils and lymphocytes accumulate at the injured site due to chemoattractants. This inflammatory reaction peaks at 24 hours, and lasts for some days [71].
4. The granulation phase overlaps to some extent the inflammatory response and is characterised by cell proliferation lasting for about 3 weeks. This phase is characterized by migration and proliferation of endothelial cells from the wound margins and SMCs or fibroblasts from the adjacent tunica media to cover the wound surface and ultimately leading to intimal hyperplasia. The most prominent cell in the development of intimal hyperplasia is the SMC. Two phenotypes of SMCs exist: 1. Contractile (quiescent) phenotype in the normal tunica media and 2. The synthetic (secretory) phenotype containing abundant synthetic organelles (such as free ribosomes, Golgi-apparatus and rough endoplasmatic reticulum). This type is seen in the injured arterial wall. After 7 days the cell proliferation and migration of SMCs slows down and the deposition of chondriotin-sulfate and dermatan sulfata starts. In fact, 50 to 80% of the volume of the intimal hyperplasia region is composed of extracellular matrix. The sequence of phase 1,2, 3 and 4 is known as 'response-to-injury'[73-74].
5. The formation of the extracellular matrix in the tunica intima and tunica media guided by local and systemic hemodynamics is initiated at 2 weeks after vascular injury and reaches a plateau after 3-4 weeks, possibly lasting for months or even years. This phase of extracellular remodelling is characterized by the deposition of chondroitin-sulfate, dermatan sulfata and the modification of deposited proteoglycans by collagens and elastin after several months. The synthetic SMCs are replaced by contractile SMCs after about 6 months. The 'reactive-adaptive remodelling' phase 5 is the final outcome of the arterial healing [75-76].

1.05 The development of dysplastic intimal hyperplasia

The definition of dysplastic intimal hyperplasia is rather controversial, because it suggests hyperplasia of cells derived from the tunica intima. However, the proliferating synthetic SMCs and fibroblasts are mainly derived from the media and account for 20-50% (vs 50-80% extracellular matrix) of the volume of intimal hyperplasia. The term 'intimal hyperplasia' comprises phase 3 and 4 of the restenosis process and is a morphological rather than a patho-etiological definition. It has been shown that the degree of intimal hyperplasia depends on the degree of arterial injury [73] and on the rate of reendothelialization [76].

1.06 The development of constrictive remodelling

In phase 5 of the restenosis process, constrictive remodelling may occur at long-term. This is characterized by late lumen loss due to a rigorous myofibrotic reaction of the arterial response to injury [77-79]. Under which conditions constrictive or adaptive remodelling will occur is not fully understood [80], but a relation between degree of damage and degree of constrictive remodelling has been reported [73;81].

1.07 The role of shear stress

Many studies described the physiological phenomenon that decreased shear stress in the regions of vascular injury leads to the development of intimal hyperplasia [82-86]. Although the inverse relationship between the shear stress and the degree of intimal hyperplasia may be of importance in the predilection sites of (re)stenosis development, no studies support this hypothesis.

1.08 The experimental models of restenosis

The common method to induce stenosis is balloon-induced damage of the artery, using overstretching of all tunicas and denudation of the tunica intima [87-89].

Other methods like electrocoagulation, cutting off the tunicas, cuffing the artery with silicon and genetic manipulation, were able to initiate restenosis as well. The carotid artery of the rat is widely used to study the development of intimal hyperplasia. However, its different morphology to the human artery makes it less suitable for comparisons with the human condition. Other better comparable arteries are evaluated in Chapter 3. Rabbit and pig models are used to mimic atherosclerosis development, because of their sensitivity to a cholesterol- and lipid-rich diet [90-91].

Despite that the size of their arteries is comparable, the dog model is not frequently used to study the response to arterial injury in humans because of major differences in their metabolism and coagulation. The coagulation pathway in monkeys is very similar to the humans, but their use as laboratory animals is limited because of ethical and financial reasons.

1.09 To date experimental endovascular-based research approaches

Hyperthermia, Microwave therapy and Laser therapy are respectively based on the electro-, microwave or laser coagulation of arterial tissue by the generation of heat [92-94].

PUVA therapy, which name is derived from the use of furocoumarins containing substrates known as psoralens (8-MOP) and light from the ultraviolet 320-400 nm region (=UV-A). This kind of therapy first used to treat a fungoid infection in the skin (vitiligo) by Lerner in 1953 and later to treat the dermatologic autoimmune disease located in the epidermis, known as psoriasis, by Parrish in 1974. Perree described in 1998 PUVA therapy in animals to prevent intimal hyperplasia [95].

Brachy therapy is based on the use of gamma radiation in the range of 12-20 Gray and was for the first time used in animals by Friedman in 1964. In 1990, the first clinical application to treat in-stent stenosis in femoro-popliteal arteries was reported by Liermann. In 1997, Teirstein reported on the first randomised double-blind placebo-controlled intracoronary brachytherapy trial [96].

Directional or rotational atherectomy is based on the use of knives on the balloon to cut the occluding plaque away in order to restore the arterial patency. Clinical trials showed promising results, but the arterial lesions that arose in the arterial wall after cutting are prone to develop restenosis. [97-99].

Cryotherapy is an experimental application, based on the ablation or hibernation of the proliferative smooth muscle cells by freezing using a probe cooled by liquid nitrogen. The initial results are promising and the evaluation of this therapy has just started [100].

Silicon therapy is based on artificial outward remodelling by siliconising the arteries using Albastine [101]. The evaluation of this method is in phase 1.

Gene therapy Since the mapping of the complete genome many studies started to manipulate the arterial healing related genes. However, the results obtained thus far are disappointing because of the low success rate and the low specificity of the present vectors [102-106].

Uncoated/ coated-stents The use of stents in atherosclerotic lesions significantly improved the success rate of vascular interventions. Still, the arterial healing response to the stents can lead to the development of intimal hyperplasia at the edges of these stents. The need to prevent the development of intimal hyperplasia in the stent led to the development of various coatings. With particular coated stents, much better results have been obtained than the conventional stents [107-110].

Photodynamic therapy Since the eighties, the effect of phototoxicity in the prevention of restenosis started. In this thesis, the effects of endovascular photodynamic therapy on the prevention of restenosis is evaluated.

1.10 Conclusions

The effect of endovascular photodynamic therapy is based on the induction of photocytotoxicity in two steps. Activation of the photoactive compound protoporphyrin IX formed via conversion of aminolaevulinic acid using illumination with 633 nm at appropriate irradiance, initiates a cytotoxic type II reaction. It is conceivable that in particular proliferating cells in the vascular lesion may be eradicated by PDT preventing the (re)narrowing of the lumen.

Excessive damage of the artery is believed to initiate an exaggerated healing response resulting in the development of restenosis. Many pathways are involved in the phases of restenosis development, but the leading mechanism is unresolved. Therefore, adjuvant strategies are needed to prevent restenosis. Photodynamic therapy may be a promising tool in that respect.

References

- [1] Bonnett R. Photodynamic therapy in historical perspective. *Rev.Contemp.Pharmacother.* 1999. 10, 1-19.
- [2] McCall-Anderson T. Hydroa aestivale in two brothers complicated with the presence of hematoporphyrin in the urine. *Br.J.Dermatol.* 1898. 10, 1-4.
- [3] Raab O. Über die Wirkung fluoreszierender Stoffe auf Paramaecien. *Z.Biol.* 1900.39, 524-526.
- [4] Finsen NR. *Phototherapy.* London: Arnold, 1901.
- [5] von Tappeiner H, Jesionek A. Therapeutische Versuche mit fluoreszierende Stoffen. *München Med.Wochenschrift* 1903. 47, 2042-2051.
- [6] Einstein A. A new determination of molecular dimensions. *Annalen der Physik* 1905. 17, 549-560.
- [7] Einstein A. On the motion of small particles suspended in liquids at rest required by the molecular-kinetic theory of heat. *Annalen der Physik* 17, 549-560. 1905.
- [8] Policard A. Études sur les aspects offerts par des tumeurs expérimentales examinées a la lumiere de wood. *Comp.Rend.Soc.Biol.* 1924. 91, 1423-1424.
- [9] Auler G, Banzer J. Untersuchungen über die Rolle der Porphyrin bei Geschwulstkranken Menschen und Tieren. *Z.Krebsforschung* 1942.53, 65-68.
- [10] Figge FHD, Wieland GS, Mangiello LOJ. Cancer detection and therapy: affinity of neoplastic embryonic and traumatized tissue for porphyrins and metalloporphyrins. *Proc.Soc.Exp.Biol.Med.* 1948. 68, 640-645.
- [11] Lipson R, Alders E, Olsen A. The use of a derivative of haematoporphyrin in tumor detection. *J.Natl.Cancer Inst.* 1961. 1, 1-11.
- [12] Diamond I, Granelli SG, McDonagh AF, Nielsen SF, Wilson CB, Jaenicke R. Phototherapy of malignant tumours. *Lancet* , 1972. 1175-1177.
- [13] Dougherty TJ. Activated dyes as antitumor agents. *J Natl Cancer Inst* 1974; 52(4):1333-1336.
- [14] Berenbaum MC. Letter: Predicting response of human cancer to chemotherapy. *Lancet* 1974; 2(7889):1141-1142.
- [15] Kelly JF, Snell ME. Hematoporphyrin derivative: a possible aid in the diagnosis and therapy of carcinoma of the bladder. *J Urol* 1976; 115(2):150-151.
- [16] Henderson BW, Dougherty TJ. How does photodynamic therapy work? *Photochem Photobiol* 1992; 55(1):145-157.
- [17] Hasan T. *Fundamentals of photochemistry and Photodynamic therapy.* 1 ed. San Jose: SPIE, 2000.
- [18] Townes CH. *Nobel lectures in physics.* Nobel lectures. Amsterdam: Elsevier, 1972: 58-64.
- [19] Basov G. *Nobel lectures in physics.* Nobel lectures. Amsterdam: Elsevier, 1972: 89-94.
- [20] Prokhorov P. *Nobel lectures in physics.* Nobel lectures. Amsterdam: Elsevier, 1972: 110-116.
- [21] van Hillegersberg R. *Laser treatment for liver metastasis. Thermal and Photodynamic Therapy.* Erasmus Universiteit Rotterdam, 1993.
- [22] Moan J. The photodegradation of porphyrins in cells can be used to estimate the lifetime of singlet oxygen. *J.Photochem.Photobiol.B.* 1991.53, 549-553.

- [23] Moan J. On the diffusion length of singlet oxygen in cells and tissue. *J.Photochem.Photobiol.B.* 1990. 6, 343-344.
- [24] Bonnett R. *Chemical aspects of photodynamic therapy.* 1 ed. London: Gordon and Breach Publishers, 2000.
- [25] Hinnen P. *Biochemical aspects of ALA-PDT. Basic mechanisms and optimization for the treatment of Barrett's oesophagus.* Erasmus Universiteit Rotterdam, 2001.
- [26] Berlin NI, Neuberger A, Scott JJ. The metabolism of 5-aminolevulinic acid. 1normal pathway studied with the aid of ^{15}N . *Biochem.* 1956. *J* 64, 80-100.
- [27] van Hillegersberg R, van den Berg JWO, Kort WJ, Terpstra OT, Wilson JHP. Selective accumulation of endogenously produced porphyrins in a liver metastasis model in rats. *Gastroenterology* 1992c, 103:647-651.
- [28] Kennedy JC, Pottier RH, Pross D. Photodynamic therapy with endogenous protoporphyrin IX: basic principles and present clinical experience. *J Photochem.Photobiol.B* 1990. 6, 143-148.
- [29] Grant WE, Speight PM, MacRobert AJ, Hopper C, Bown SG. Photodynamic therapy of normal rat arteries after photosensitisation using disulphonated aluminium phthalocyanine and 5-aminolaevulinic acid. *Br J Cancer* 1994; 70(1):72-78.
- [30] Kelly WN. Heme and porphyrin metabolism. *Textbook of internal medicine.* J.B. Lippincott Company, 1992: 433-435.
- [31] Gaspar T, Kevers C, Bisbis B, Penel C, Greppin H, Garnier F, Rideau M, Huault C, Billard J, Foidart J. Shemin pathway and peroxidase deficiencies in a fully habituated and fully heterotropic non-organogenic sugarbeet callus: an adaptive strategy or the consequence of modified hormonal balances and sensitivities in these cancerous cells? *Cell Proliferation* 1999. 32[5], 249-70.
- [32] Spears JR, Serur J, Shropshire D, Paulin S. Fluorescence of experimental atheromatous plaques with hematoporphyrin derivative. *J Clin Invest* 1983; 71(2):395-399.
- [33] Pollock ME, Eugene J, Hammer-Wilson M, Berns MW. Photosensitization of experimental atheromas by porphyrins. *J Am Coll Cardiol* 1987; 9(3):639-646.
- [34] Dartsch PC, Ischinger T, Betz E. Responses of cultured smooth muscle cells from human nonatherosclerotic arteries and primary stenosing lesions after photoradiation: implications for photodynamic therapy of vascular stenoses [see comments]. *J Am Coll Cardiol* 1990; 15(7):1545-1550.
- [35] Litvack F, Grundfest W, Forrester J, Fishbein M, Swan H, Corday E, Rider D, McDermid I, Pacala T, Laudenslager J. Effects of hematoporphyrin derivative and photodynamic therapy on atherosclerotic rabbits. *Am.J.Cardiol.* 1985. 56, 667-671.
- [36] Mackie RW, Jr., Vincent GM, Fox J, Orme EC, Hammond EH, Chang-Zong C, Johnson MD. In vivo canine coronary artery laser irradiation: photodynamic therapy using dihematoporphyrin ether and 632 nm laser. A safety and dose-response relationship study. *Lasers Surg Med* 1991; 11(6):535-544.
- [37] Asahara T, Kato T, Amemiya T, Rakue H, Ooike Y, Shiraishi H, Usui M, Oda Y, Naitoh Y, Ibukiyama C. In vivo experimental study on photodynamic therapy for the prevention of restenosis after angioplasty. *Circulation* 86[Suppl. 1992. I], 846-846.
- [38] Eton D, Colburn MD, Shim V, Panek W, Lee D, Moore WS, Ahn SS. Inhibition of intimal hyperplasia by photodynamic therapy using photofrin. *J Surg Res* 1992; 53(6):558-562.
- [39] Ortu P, LaMuraglia GM, Roberts WG, Flotte TJ, Hasan T. Photodynamic therapy of arteries. A novel approach for treatment of experimental intimal hyperplasia. *Circulation* 1992; 85(3):1189-1196.
- [40] Tang G, Hyman S, Schneider JH, Jr., Giannotta SL. Application of photodynamic therapy to the treatment of atherosclerotic plaques. *Neurosurgery* 1993. 32, 438-443.

- [41] LaMuraglia GM, ChandraSekar NR, Flotte TJ, Abbott WM, Michaud N, Hasan T. Photodynamic therapy inhibition of experimental intimal hyperplasia: acute and chronic effects. *J Vasc Surg* 1994; 19(2):321-329.
- [42] Nyamekye I, Grant WE, MacRobert S, Bown S, Adiseshiah M, Bishop C. Photodynamic treatment of normal arteries using a new phthalocyanine and 675-nm laser light. *Br.J.Surg.* 1994. 81, 618-619.
- [43] Hsiang YN, Crespo MT, Machan LS, Bower RD, Todd ME. Photodynamic therapy for atherosclerotic stenoses in Yucatan miniswine. *Can J Surg* 1994; 37(2):148-152.
- [44] Grant WE, Buonaccorsi G, Speight PM, MacRobert AJ, Hopper C, Bown SG. The effect of photodynamic therapy on the mechanical integrity of normal rabbit carotid arteries. *Laryngoscope* 1995; 105(8 Pt 1):867-871.
- [45] Eton D, Borhani M, Spero K, Cava RA, Grossweiner L, Ahn SS. Photodynamic therapy. Cytotoxicity of aluminum phthalocyanine on intimal hyperplasia. *Arch Surg* 1995; 130(10):1098-1103.
- [46] Hsiang Y, Houston G, Crespo T, To E, Todd M, Sobeh M, Bower R. Preventing intimal hyperplasia with photodynamic therapy using an intravascular probe. *Ann Vasc Surg* 1995; 9(1):80-86.
- [47] Nyamekye I, Anglin S, McEwan J, MacRobert A, Bown S, Bishop C. Photodynamic therapy of normal and balloon-injured rat carotid arteries using 5-amino-levulinic acid. *Circulation* 1995; 91(2):417-425.
- [48] Saito T, Hayashi J, Kawabe H, Aizawa K. Photodynamic treatment for atherosclerotic plaques of the rabbit abdominal aorta by the laparoscopic approach using a pheophorbide derivative. *Med.Electron Microsc.* 1996.29[3-4], 137-144.
- [49] Gonschior P, Gerheuser F, Fleuchaus M, Huehns TY, Goetz AE, Welsch U, Sroka R, Dellian M, Lehr HA, Hofling B. Local photodynamic therapy reduces tissue hyperplasia in an experimental restenosis model. *Photochem Photobiol* 1996; 64(5):758-763.
- [50] Nyamekye I, Buonaccorsi G, McEwan J, MacRobert A, Bown S, Bishop C. Inhibition of intimal hyperplasia in balloon injured arteries with adjunctive phthalocyanine sensitised photodynamic therapy. *Eur J Vasc Endovasc Surg* 1996; 11(1):19-28.
- [51] Gonschior P, Vogel-Wiens C, Goetz AE, Huehns TY, Breger F, Gerheuser F, Fleuchaus M, Welsch U, Sroka R, Dellian M, Lehr HA, Hofling B. Endovascular catheter-delivered photodynamic therapy in an experimental response to injury model. *Basic Res Cardiol* 1997; 92(5):310-319.
- [52] Katoh T, Asahara T, Naitoh Y, Nakajima H, Usui M, Rakugi H, Amemiya T, Miyagi M, Ibukiyama C. In vivo intravascular laser photodynamic therapy in rabbit atherosclerotic lesions using a lateral direction fiber. *Lasers Surg.Med.* 1997. 20, 373-381.
- [53] Stadius van Eps RG, ChandraSekar NR, Hasan T, LaMuraglia GM. Importance of the treatment field for the application of vascular photodynamic therapy to inhibit intimal hyperplasia. *Photochem Photobiol* 1998; 67(3):337-342.
- [54] Kipshidze N, Sahota H, Komorowski R, Nikolaychik V, Keelan MH, Jr. Photoremodeling of arterial wall reduces restenosis after balloon angioplasty in an atherosclerotic rabbit model. *J Am Coll Cardiol* 1998; 31(5):1152-1157.
- [55] Nagae T, Louie AY, Aizawa K, Ishimaru S, Wilson SE. Selective targeting and photodynamic destruction of intimal hyperplasia by scavenger-receptor mediated protein-chlorin e6 conjugates. *J Cardiovasc Surg (Torino)* 1998; 39(6):709-715.
- [56] Jenkins MP, Buonaccorsi GA, Raphael M, Nyamekye I, McEwan JR, Bown SG, Bishop CC. Clinical study of adjuvant photodynamic therapy to reduce restenosis following femoral angioplasty. *Br J Surg* 1999; 86(10):1258-1263.

- [57] Adili F, Stadius van Eps RG, LaMuraglia GM. Significance of dosimetry in photodynamic therapy of injured arteries: classification of biological responses. *Photochem Photobiol* 1999; 70(4):663-668.
- [58] Heckenkamp J, Adili F, Kishimoto J, Koch M, LaMuraglia GM. Local photodynamic action of methylene blue favorably modulates the postinterventional vascular wound healing response. *J Vasc Surg* 2000; 31(6):1168-1177.
- [59] Visona A, Angelini A, Gobbo S, Bonanome A, Thiene G, Pagnan A, Tonello D, Bonandini E, Jori G. Local photodynamic therapy with Zn(II)-phthalocyanine in an experimental model of intimal hyperplasia. *J Photochem.Photobiol.B* 2000. 57, 94-101.
- [60] Jenkins MP, Buonaccorsi GA, Mansfield R, Bishop CC, Bown SG, McEwan JR. Reduction in the response to coronary and iliac artery injury with photodynamic therapy using 5-aminolaevulinic acid [In Process Citation]. *Cardiovasc Res* 2000; 45(2):478-485.
- [61] Gabeler EEE, Hillegersberg van R, Stadius van Eps RG, Sluiter W, Urk van H. Endovascular photodynamic therapy inhibits intimal hyperplasia after PTA in a rat model. *Proceedings of SPIE: Lasers in surgery: Advanced characterization,therapeutics and systems X* 2000.1:3907[1], 575-581.
- [62] Hayase M, Woodburn KW, Perloth J, Miller R, Baumgartner W, Yock PG, Yeung A. Photoangioplasty with local motexafin lutetium delivery reduces macrophages in a rabbit post-balloon injury model. *Cardiovasc.Res.* 2001. 49, 449-455.
- [63] Grove R, Rychmovsky S, Purter M, Heath R, Leitch I, Walker J. The photopoint catheter based system for the treatment of intimal hyperplasia. 2002.
- [64] Gabeler EEE. Photodynamic therapy for restenosis: The search for the optimal protocol. *Photodynamic News* 2002. 5[1], 6-9.
- [65] Jenkins MP, Buonaccorsi GA, Raphael M, Nyamekye I, McEwan JR, Bown SG, Bishop CC. Clinical study of adjuvant photodynamic therapy to reduce restenosis following femoral angioplasty. *Br J Surg* 1999; 86(10):1258-1263.
- [66] Rockson SG, Lorenz DP, Cheong WF, Woodburn KW. Photoangioplasty: An emerging clinical cardiovascular role for photodynamic therapy. *Circulation* 2000; 102(5):591-596.
- [67] LaMuraglia GM, Klyachkin ML, Adili F, Abbott WM. Photodynamic therapy of vein grafts: suppression of intimal hyperplasia of the vein graft but not the anastomosis. *J Vasc Surg* 1995; 21(6):882-890.
- [68] Bauters C, Meurice T, Hamon M, McFadden E, Lablanche JM, Bertrand ME. Mechanisms and prevention of restenosis: from experimental models to clinical practice. *Cardiovasc Res* 1996; 31(6):835-846.
- [69] Ross R. The pathogenesis of atherosclerosis: a perspective for the 1990s. *Nature* 1993. 362, 801-809.
- [70] Ross R. Atherosclerosis: An inflammatory disease. *N Engl J Med* 1999; 340:115-125.
- [71] Houston M. *Vascular biology in clinical practice*. 1 ed. Philadelphia: Hanley and Belfus, 2002.
- [72] Ip JH, Fuster V, Israel D, Badimon L, Badimon J, Chesebro JH. The role of platelets, thrombin and hyperplasia in restenosis after coronary angioplasty. *J Am Coll Cardiol* 1991; 17(6 Suppl B):77B-88B.
- [73] Indolfi C, Esposito G, Di Lorenzo E, Rapacciuolo A, Feliciello A, Porcellini A, Avvedimento VE, Condorelli M, Chiariello M. Smooth muscle cell proliferation is proportional to the degree of balloon injury in a rat model of angioplasty. *Circulation* 1995. 92[5], 1230-1235.
- [74] Amann JF, Branson K, Myers PR. The microvascular cell and ischemia-reperfusion injury. *J Cardiovasc Pharmacol* 1996; 27 Suppl 1(1):S26-S30.

- [75] Pasterkamp G, de Kleijn DP, Borst C. Arterial remodeling in atherosclerosis, restenosis and after alteration of blood flow: potential mechanisms and clinical implications. *Cardiovasc Res* 2000; 45(4):843-852.
- [76] A.W.Clowes, M.E.Reidy, M.M.Clowes. Kinetics of cellular proliferation after arterial injury;3.Endothelial and smooth muscle growth in chronically denuded vessels. *Laboratory Investigation* 1986. 54 [3], 295-303.
- [77] Post MJ, Borst C, Kuntz RE. The relative importance of arterial remodeling compared with intimal hyperplasia in lumen renarrowing after balloon angioplasty. A study in the normal rabbit and the hypercholesterolemic Yucatan micropig [see comments]. *Circulation* 1994; 89(6):2816-2821.
- [78] Post MJ, Borst C, Pasterkamp G, Haudenschild CC. Arterial remodeling in atherosclerosis and restenosis: a vague concept of a distinct phenomenon. *Atherosclerosis* 1995; 118 Suppl:S115-23:S115-S123.
- [79] Martin J. Learning from vascular remodelling. *Clin Exp Allergy* 2000; 30 Suppl 1:33-6:33-36.
- [80] Gertz SD, Gimple LW, Banai S, Ragosta M, Powers ER, Roberts WC, Perez LS, Sarembock IJ. Geometric remodeling is not the principal pathogenetic process in restenosis after balloon angioplasty. Evidence from correlative angiographic-histomorphometric studies of atherosclerotic arteries in rabbits [see comments]. *Circulation* 1994; 90(6):3001-3008.
- [81] Faxon DP, Coats W, Currier J. Remodeling of the coronary artery after vascular injury. *Prog Cardiovasc Dis* 1997; 40(2):129-140.
- [82] Caro C, Fitz-Gerald J, Schroter R. Atheroma and arterial wall shear. Observation, correlation and proposal of a shear dependent mass transfer mechanism for atherogenesis. *Proc R Soc Lond B Biol Sci* 1971. 177, 109-159.
- [83] Hazel AL, Pedley TJ. Alteration of mean wall shear stress near an oscillating stagnation point. *J Biomech Eng* 1998; 120(2):227-237.
- [84] Kleinstreuer C, Lei M, Archie JP, Jr. Flow input waveform effects on the temporal and spatial wall shear stress gradients in a femoral graft-artery connector. *J Biomech Eng* 1996; 118(4):506-510.
- [85] Levesque M, Liepsch D, Moravec S. Correlation of endothelial cell shape and wall shear stress in stenosed dog aorta. *Arteriosclerosis* 1986; 6:220-229.
- [86] Topper JN, Gimbrone Jr MA. Blood flow and vascular gene expression: fluid shear stress as a modulator of endothelial phenotype. *Mol Med Today* 1999; 5:40-46.
- [87] Schwartz RS. Neointima and arterial injury: dogs, rats, pigs, and more. *Lab Invest* 1994; 71(6):789-791.
- [88] Kantor B, Ashai K, Holmes DR, Schwartz RS. The experimental animal models for assessing treatment of restenosis. *Cardiovasc.Rad.Med.* 1999. 1[1], 48-54.
- [89] Narayanaswamy M, Wright KC, Kandarpa K. Animal models for atherosclerosis, restenosis, and endovascular graft research. *J Vasc Interv Radiol* 2000; 11(1):5-17.
- [90] Hayashi K, Ide K, Matsumoto T. Aortic walls in atherosclerotic rabbits--mechanical study. *J Biomech Eng* 1994; 116(3):284-293.
- [91] Caramori PR, Eggers EE, Silva Filho AP, Uchoa DM, Jung F, Zago AC, Cerski CT, Schwartzmann G, Zago AJ. Postangioplasty restenosis: a practical model in the porcine carotid artery. *Braz J Med Biol Res* 1997; 30(9):1087-1091.
- [92] Henderson BW, Waldow SM, Potter WR, Dougherty TJ. Interaction of photodynamic therapy and hyperthermia: tumor response and cell survival studies after treatment of mice in vivo. *Cancer Res* 1985; 45(12 Pt 1):6071-6077.
- [93] Tomaru T, Uchida Y, Nakamura F, Miwa AY, Kawai S, Okada R, Sugimoto T. Loss of vasoreactivity by laser thermal energy or argon laser irradiation. *Jpn Heart J* 1993; 34(3):341-353.

- [94] Landau C, Currier JW, Haudenschild CC, Minihan AC, Heymann D, Faxon DP. Microwave balloon angioplasty effectively seals arterial dissections in an atherosclerotic rabbit model. *J Am Coll Cardiol* 1994; 23(7):1700-1707.
- [95] Perree J, van Leeuwen TG, Velema E, Borst C. Psoralen and long wavelength ultraviolet radiation as an adjuvant therapy for prevention of intimal hyperplasia and constrictive remodeling after balloon dilation: a study in the rabbit iliac artery. *Lasers Surg Med* 1998; 23(5):281-290.
- [96] Teirstein PS, Massullo V, Jani S, Popma JJ, Mintz GS, Russo RJ, Schatz RA, Guarneri EM, Steuterman S, Morris NB, Leon MB, Tripuraneni P. Catheter-based radiotherapy to inhibit restenosis after coronary stenting. *N Engl J Med* 1997; 336(24):1697-1703.
- [97] Garratt KN, Holmes DR, Jr., Bell MR, Bresnahan JF, Kaufmann UP, Vlietstra RE, Edwards WD. Restenosis after directional coronary atherectomy: differences between primary atheromatous and restenosis lesions and influence of subintimal tissue resection. *J Am Coll Cardiol* 1990; 16(7):1665-1671.
- [98] Teirstein PS, Warth DC, Haq N, Jenkins NS, McCowan LC, Aubanel-Reidel P, Morris N, Ginsburg R. High speed rotational coronary atherectomy for patients with diffuse coronary artery disease [see comments]. *J Am Coll Cardiol* 1991; 18(7):1694-1701.
- [99] Ahn SS, Eton D, Yeatman LR, Deutsch LS, Moore WS. Intraoperative peripheral rotary atherectomy: early and late clinical results. *Ann Vasc Surg* 1992; 6(3):272-280.
- [100] Sotiropoulos G, Kilagblian T, Dougherty W, Henderson SO. Cold injury from pressurized liquid ammonia: a report of two cases. *J Emerg Med* 1998; 16(3):409-412.
- [101] Hartmann DAP. Siliconen slagaders: Levensbedreigende aneurysma's repareren met Albastine. *Wetenschap en onderzoek* 2001. 4, 11-16.
- [102] Taubman MB. Gene induction in vessel wall injury. *Thromb Haemost* 1993; 70(1):180-183.
- [103] Ohno T, Gordon D, San H, Pompili VJ, Imperiale MJ, Nabel GJ, Nabel EG. Gene therapy for vascular smooth muscle cell proliferation after arterial injury. *Science* 1994; 265(5173):781-784.
- [104] Nabel EG. Gene therapy for vascular diseases. *Atherosclerosis* 1995; 118 Suppl:S51-6:S51-S56.
- [105] Feldman LJ, Tahlil O, Steg G. Perspectives of arterial gene therapy for the prevention of restenosis. *Cardiovasc Res* 1996; 32(2):194-207.
- [106] Kibbe MR, Billiar TR, Tzeng E. Gene therapy for restenosis. *Circ Res* 2000; 86(8):829-833.
- [107] Muller DW, Golomb G, Gordon D, Levy RJ. Site-specific dexamethasone delivery for the prevention of neointimal thickening after vascular stent implantation. *Coron Artery Dis* 1994; 5(5):435-442.
- [108] Ozaki Y, Violaris AG, Serruys PW. New stent technologies. *Prog Cardiovasc Dis* 1996; 39(2):129-140.
- [109] Kornowski R, Hong MK, Tio FO, Bramwell O, Wu H, Leon MB. In-stent restenosis: contributions of inflammatory responses and arterial injury to neointimal hyperplasia. *J Am Coll Cardiol* 1998; 31(1):224-230.
- [110] Morice MC, Serruys PW, Sousa JE. A randomised comparison of the Sirolimus-eluting stent with a standard stent for coronary revascularization. *N.Engl.J.Med.* 2002. 346, 1773-1780.

CHAPTER 2

Aims and outline

2.00 The aims and outline of the studies in this thesis

The aim of this thesis was to evaluate in an animal model the applicability of endovascular ALA-PDT as adjuvant strategy to prevent vascular intervention-induced restenosis. The main theme is the changes in histo-morphometry as a means, 1. to elucidate the arterial ‘response-to-injury’ and the ‘reactive-adaptive remodelling’ after endovascular ALA-PDT in vivo, and 2. to find the optimisation criteria for endovascular ALA-PDT. The outline of this thesis illustrates a step-wise approach from background information, via the model requirements to study endovascular PDT, and the effects of PDT on the vascular biology, and finally to the effects of PDT on the vascular physiology. The section heading applied in this thesis indicates the level at which the research in studying endovascular photodynamic therapy is. Thus, the information obtained from the first described studies has been integrated in the successive studies.

2.01 SECTION I BACKGROUND

In **Chapter 1** background information about photodynamic therapy (PDT), its fundamental principles, the conversion of the applied prodrug aminolaevulinic acid (ALA) into the photosensitizer protoporphyrin IX (PpIX) and information about the application of PDT in the field of (cardio)vascular interventions is given. In this chapter the questions like ‘What is PDT?’ and ‘What is known about PDT in the field of vascular interventions?’ are answered. Additional information about the pathophysiology of restenosis is given. A question like ‘What do we presently know about restenosis?’ is dealt with. The insights in this matter will help to understand the challenge of the performed studies in this thesis, namely ‘Can endovascular PDT prevent restenosis?’.

In **Chapter 2** the aims and outline of the thesis are given. This chapter elucidates the rationale of the studies in this thesis

2.02 SECTION II MODEL REQUIREMENTS

In **Chapter 3** the arterial healing response to injury is thoroughly evaluated to form the basis in the evaluation of the effects of endovascular PDT in the following studies. Therefore, the first aim was to validate a reproducible model for the induction of intimal hyperplasia and constrictive remodelling. The second aim was to compare the histo-geometric healing response to balloon injury in central and peripheral arteries as a measure for the normal-compensatory potential after standardised-balloon injury. The third aim was to describe the arterial healing after balloon injury per artery type as reference to compare the effects induced by ALA-PDT in later studies on ALA-PDT. The question ‘Why did we use the rat model?’ is answered.

In **Chapter 4** we deal with the question ‘What do we know about the photosensitizer accumulation in the arterial wall?’. To answer this, the first aim was to determine the time-intervals at which ALA converted into PpIX in arteries for optimisation of endovascular PDT. The second aim was to compare the time-intervals and peak concentrations between the artery-types as reference to compare the effects induced by ALA-PDT.

2.03 SECTION III ENDOVASCULAR PHOTODYNAMIC THERAPY

In **Chapter 5** we answer the question ‘How does the healthy artery respond to PDT in the validated model?’. Therefore, the first aim was to describe the normal histo-geometric healing response after endovascular PDT in normal arteries. The second aim was to use this information as reference for ALA-PDT after balloon injury.

In **Chapter 6** the key question of this study, namely ‘Does PDT prevent the development of restenosis?’ is answered and evaluated in an interventional model for the prevention of intimal hyperplasia and constrictive remodelling. In this chapter, the first aim was to evaluate the histo-geometric effect of endovascular PDT in this model. The second aim was to find the optimal light-dose for ALA-PDT. The third aim was to describe the effect of ALA-PDT on the cholinergic innervation.

2.04 SECTION IV PDT AND VASCULAR BIOLOGY

In **Chapter 7** the challenge is to find an answer to the question ‘How does endovascular PDT prevent restenosis?’. In this chapter, the first aim was to evaluate the effect of endovascular PDT on the reendothelialisation of the injured vascular wall. The second aim was to describe the role of transforming growth factor beta (TGF- β) in the reendothelialisation process, the development of intimal hyperplasia and of constrictive remodelling after ALA-PDT.

In **Chapter 8** we evaluate the question ‘What is the role of the inflammatory response in the prevention of restenosis by endovascular PDT?’. Therefore, the first aim was to evaluate the effect of endovascular PDT on the inflammatory response upon vascular injury.

2.05 SECTION V PDT AND VASCULAR PHYSIOLOGY

In **Chapter 9** we answer the question ‘Does endovascular PDT alter the strength of the arterial wall?’. Therefore, our aim was to evaluate the long-term effect of endovascular PDT on the bursting pressure of the treated artery.

2.06 SECTION VI AFTERMATH

In **Chapter 10** we discuss the questions that are answered and new questions that have arisen in this thesis, followed by the conclusions of this thesis.

In **Chapter 11** a summary of this thesis in english and dutch is given.

SECTION II

CHAPTER 3

A Comparison of Balloon Injury Models of Endovascular Lesions in Rat Arteries

¹Edward E.E. Gabeler, ¹Richard van Hillegersberg, ¹Randolph G. Statius van Eps,
²Wim Sluiter, ³Elma Gussenhoven, ⁴Paul Mulder, ¹Hero van Urk

¹Dept. of Surgery, Erasmus MC, Rotterdam, The Netherlands

²Dept. of Biochemistry, Erasmus MC, Rotterdam, The Netherlands

³Dept. of Experimental echocardiology (ICIN), Erasmus MC, Rotterdam, The Netherlands

⁴Dept. of Epidemiology and Biostatistics, the Netherlands Institute for Health Sciences

Key Words: balloon injury, rats, remodelling, restenosis

BMC Cardiovascular Disorders 2003, 16(1):1-8.

Abbreviations: AA, abdominal aorta; BI, balloon injury; CCA, common carotid artery; CIA, common iliac artery; CVR, constrictive vascular remodelling; EEL, external elastic lamina; IEL, internal elastic lamina; IH, intimal hyperplasia; LD, lumen diameter; MLD, maximal lumen diameter; MWD, maximal wall diameter; PT(C)A, percutaneous transluminal (coronary) angioplasty; SEM, standard error of the mean; SMC, smooth muscle cell; WALLC, wall circumference.

3.00 Abstract

Background: Balloon injury (BI) of the rat carotid artery (CCA) is widely used to study intimal hyperplasia (IH) and decrease in lumen diameter (LD), but CCA's small diameter impedes the evaluation of endovascular therapies. Therefore, we validated BI in the aorta (AA) and iliac artery (CIA) to compare it with CCA.

Materials & Methods: Rats underwent BI or a sham procedure (control). Light microscopic evaluation was performed either directly or at 1, 2, 3, 4 and 16 weeks follow-up. The area of IH and the change in LD (LD at 16 weeks minus LD post BI) were compared.

Results: In the BI-groups the area of IH increased to 0.14 ± 0.08 mm² (CCA), 0.14 ± 0.03 mm² (CIA) and 0.12 ± 0.04 mm² (AA) at 16 weeks (NS). The LD decreased with 0.49 ± 0.07 mm (CCA), compared to 0.22 ± 0.07 mm (CIA) and 0.07 ± 0.10 mm (AA) at 16 weeks ($p<0.05$). The constrictive vascular remodelling (CVR=wall circumference loss combined with a decrease in LD) was -0.17 ± 0.05 mm in CIA but absent in CCA and AA. No IH, no decrease in LD and no CVR was seen in the control groups.

Conclusions: BI resulted in: a decrease in LD in 1. CCA due to IH, 2. CIA due to IH and CVR, 3. no change in LD in AA. 4. Comparable IH development in all arteries, 5. CCA has no vasa vasorum compared to CIA and AA, 6. The CIA model combines good access for 2F endovascular catheters with a decrease in LD due to IH and CVR after BI.

3.01 Introduction

It is acknowledged that restenosis is the ‘Achilles’ heel of angioplasty [1]. In vascular interventions like percutaneous transluminal (coronary) angioplasty (PT(C)A), it is well-known that balloon injury (BI) to the arterial wall induces restenosis with a typical decrease in lumen diameter (LD) as a result of dysplastic intimal hyperplasia (IH) with or without constrictive vascular remodelling (CVR), shrink or recoiling [2-7].

To improve the long-term success rate of vascular interventions, restenosis must be prevented. Many strategies have already been evaluated on their potential to prevent restenosis. Interestingly, strategies based on local endovascular techniques adjuvant to PT(C)A and stenting, like experimental brachytherapy and photodynamic therapy (PDT), showed promising results in the prevention of restenosis [8], while microwave or cryotherapy, are presently gaining interest [9].

The common animal models for the evaluation of strategies to prevent restenosis are the carotid rat artery, the dog-, the baboon-, the monkey-, the rabbit-, and the pig carotid or coronary arteries [10].

Since the early eighties, the common carotid artery (CCA) in the rat model is widely applied to study molecular mechanisms and the role of smooth muscle cells in the arterial healing after arterial injury, but it has been criticised as not representative for restenosis development [11]. This is more than likely due to abuse or misinterpretation of the rat carotid artery studies, like unjustifiably comparing various artery types. The dog model has been explored mainly because of their arterial size comparable to humans, low cost and ready availability, but they are not very reactive to diets or mechanical injury. The thrombotic activity of baboons and monkeys is more close to humans but they are expensive, difficult to handle and to maintain in the laboratory.

The larger rabbit and pig models are widely accepted models of restenosis development that mimic human disease, because they are sensitive to develop atherosclerosis after cholesterol-rich diets in large injured arteries [12;13]. However, the evaluation of endovascular strategies to prevent restenosis in the rat may be cost-effective because of a wide experience and availability of tested antibodies in contrast to other models, but data about injury in other arteries than the

carotid artery are not extensive. Comparisons of the effect of balloon injury between various arteries in the rat may add to a better understanding of the arterial healing to injury.

A practical point of attention is that the relatively large diameters of the presently available local delivery devices that are used in endovascular therapies cannot be introduced in the rat CCA without causing major vascular wall injury. Until smaller and more flexible fibres and devices are produced, the present relatively large devices determine the arterial criteria of the animal model. Therefore, we developed a rat model using larger vessels with better access such as the abdominal aorta (AA) as earlier reported and common iliac artery (CIA) as never reported.

A comparison was made with the widely used CCA model to validate the model and to assess artery-type-dependent differences in the healing after injury that may be of value in closely related research topics.

3.02 Materials & methods

The experimental protocol was approved by The Committee on Animal Research of the Erasmus University of Rotterdam, The Netherlands and complied with ‘Principles of Good Laboratory Practice’ and ‘The guide for the Care and Use of Laboratory Animals’. Ninety-five inbred Wistar rats (Harlan CPB, Austerlitz, The Netherlands) weighing 250-300 grams (g) were used. The animals had free access to rat chow (AM II, Hope Farms, Woerden, The Netherlands) and tap water acidified to pH 4.0, and were maintained in a standard 12-hr light/dark cycle.

3.02.1 Study design

The rats were randomly subdivided into 4 groups. In 3 groups a balloon injury was performed of either the right CCA-group (n=30), the AA-group (n=30) or the right CIA-group (n=30). A fourth group (=untreated controls; n=5) underwent a sham procedure without BI to serve as a baseline control in the CCA, AA and CIA. The animals were sacrificed immediately after intervention or after 1, 2, 3, 4 or 16 weeks for pressure fixation of the artery. Cross-sections were used for planimetric analysis. The weight of the rat was determined pre-operatively and at the time of harvesting.

3.02.2 Pre-operative procedure

Ketamine (35 mg/kg), atropine (40 ug/kg) and xylazine (5 mg/kg) were given intramuscularly for general anaesthesia.

3.02.3 Surgical techniques

Before the study was started, extensive experiments were executed to gain skill in handling the operative procedure.

3.02.4 The common carotid-group

A median neck incision was performed and the wound area was kept wet with gauzes embedded in 0.9% NaCl. The skin, sternocleidomastoid and omo-/thyrohyoid muscles were retracted with 2 Luer retractors. Then, 20 mm of the right CCA was isolated from the carotid sheath. The internal, external and the proximal CCA were temporarily occluded with vascular clamps (B-2 Hemoclips) to prevent retrograde blood loss. After proximal arteriotomy, the lumen was flushed with 1ml heparin solution (50 IU/ml) and antegrade balloon inflation of a 15 mm long CCA segment performed. Xylocaine (5 mg/kg) was applied to prevent vasospasm. The arteriotomy was closed in 2 layers (interrupted 8-0 prolene sutures) and the clamps removed to restore perfusion. Finally, the neck wall was closed in 1-layer (continuous 2-0 Vicryl sutures).

3.02.5 The abdominal aorta-group

A medial laparotomy was performed and the intestines were wrapped in a wetted gauze (0.9% NaCl). The retroperitoneal fascia was opened medially to expose 20 mm of AA from the right renal artery to the iliac bifurcation. Then, the AA was isolated from the inferior caval vein, followed by temporary occlusion of the left and right ilio-lumbar arteries, the proximal and caudal abdominal aorta, respectively. After the arteriotomy of the AA, a 15-mm segment from the renal artery to the bifurcation was balloon injured (see balloon injury). The lumen was flushed with heparin, followed by a 1-layer closure (Prolene 8-0, interrupted) of the arteriotomy and a 2-layer closure (continuous 4-0 and 2-0 Vicryl sutures) of the abdominal wall.

3.02.6 The common iliac artery-group

The surgical procedure was identical to the AA-group. The CIA was prepared from the aortic bifurcation to the femoral bifurcation. Both femoral bifurcations, left lumbosacral, inferior mesenteric and iliac bifurcation were temporarily occluded. After the arteriotomy, balloon-injury of a 15-mm long CIA segment was performed <Fig.3.1>. The lumen was flushed with heparin, followed by a 1-layer closure (Prolene 8-0, interrupted) of the arteriotomy and a 2-layer closure (continuous 4-0 and 2-0 Vicryl sutures) of the abdominal wall.

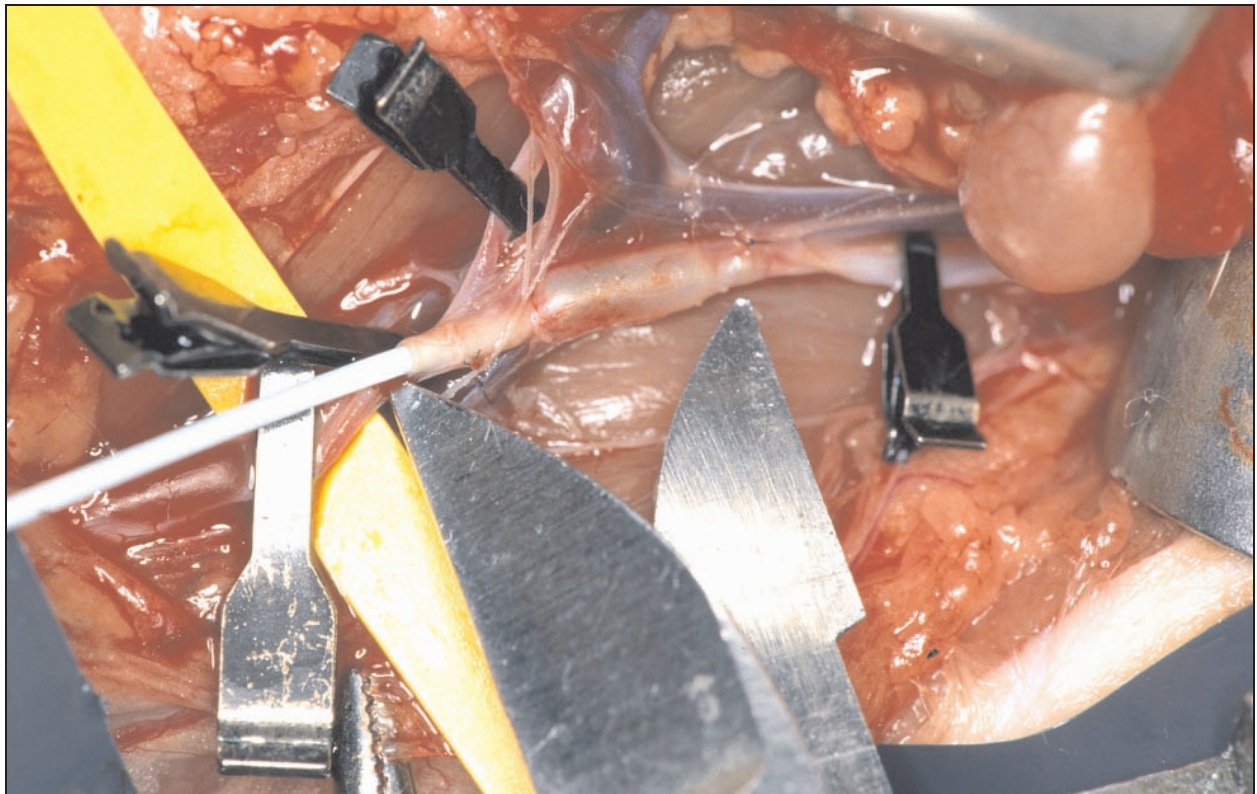


Figure 3.1 A photograph representing the balloon injury at 2 bar of the iliac artery. The metal points (*) demarcate the injured segment of 15 mm (white arrow). The black clips occlude the neighbouring arteries.

3.02.7 Balloon injury

A 2F Fogarty Embolectomy catheter (Baxter Health Care Corp., Edward's Div., Irvin, Ca., USA) was inserted to denude the arterial wall at a pressure of 2 bar (manual barometer) by pulling and rotating the inflated balloon from distally to proximally over a 15-mm long segment for 3 successive times [14]. The balloon was deflated proximally and inflated distally. Then, the arteries were flushed with heparin, closed with Prolene 8-0 and marked halfway the denuded segment with a suture (Prolene 8-0).

3.02.8 Post-operative procedure

The rats recovered under an infrared heater to keep the body temperature at 37°C.

3.02.9 Specimen handling

After sacrifice, a standard perfusion-fixation procedure via the thoracic aorta was performed under ether anaesthesia at respectively 0, 1, 2, 3, 4 and 16 weeks. The lumen was flushed with a phosphate buffer solution (PBS) at pH 7.45 for 2 min and perfusion-fixed with formaldehyde 1.8% for 10 minutes via a silicon tube at 100 mm Hg for paraffin embedding light microscopy. The distally and half-way marked segment (single suture, 8-0 black nylon, B/Braun, München, Germany) of 20 mm long was harvested after length measurement and stored in fresh 1.8% formaldehyde for at least 24 hr.

3.02.10 Planimetric analysis of the cross sections

The entire arterial segment was embedded in paraffin wax and cut into cross-sections of 10 µm at an interval of 3 mm with a microtome. The sections were mounted from distally to proximally on a microscopic slide and stained with haematoxylin and eosin. All cross-sections were video taped with a digital camera and geometrically analysed using a digital manual video-analyser <Fig.3.2> [15]. Each rat accounted for one measurement. Therefore, for calculating time-dependent effects different rats were used. Firstly, a change in LD was calculated using the maximal lumen diameter (MLD) at 0 weeks minus MLD at 16 weeks. Secondly, the absolute area of IH was determined. The IH expressed in mm² was defined as the area between the lumen and the internal elastic lamina. Thirdly, IH-to-media-area ratio was used to compare the extent of IH contributing to the arterial wall composition between the CCA, AA and CIA, using the IH area and media area. Fourthly, the wall circumference (WALLC) was calculated in mm as an approximation of CVR (WALLC before minus WALLC after). Fifthly, the media area expressed in mm² was defined as the area between the internal and external elastic laminae. The maximal thickness was expressed in mm. The role of animal growth during the experiment was corrected with a calculated growth factor, using the formula $G=A * (x*wt)/w_0$, in which A has been iterated, x is the geometric value, w=weight at time 0 or at time t, [16]. Asymmetry was corrected by using the perimeter ($D=$ circumference/ π) assuming a circular configuration to calculate the MLD and MWD.

The number of vasa vasorum was counted in the tunica adventitia.

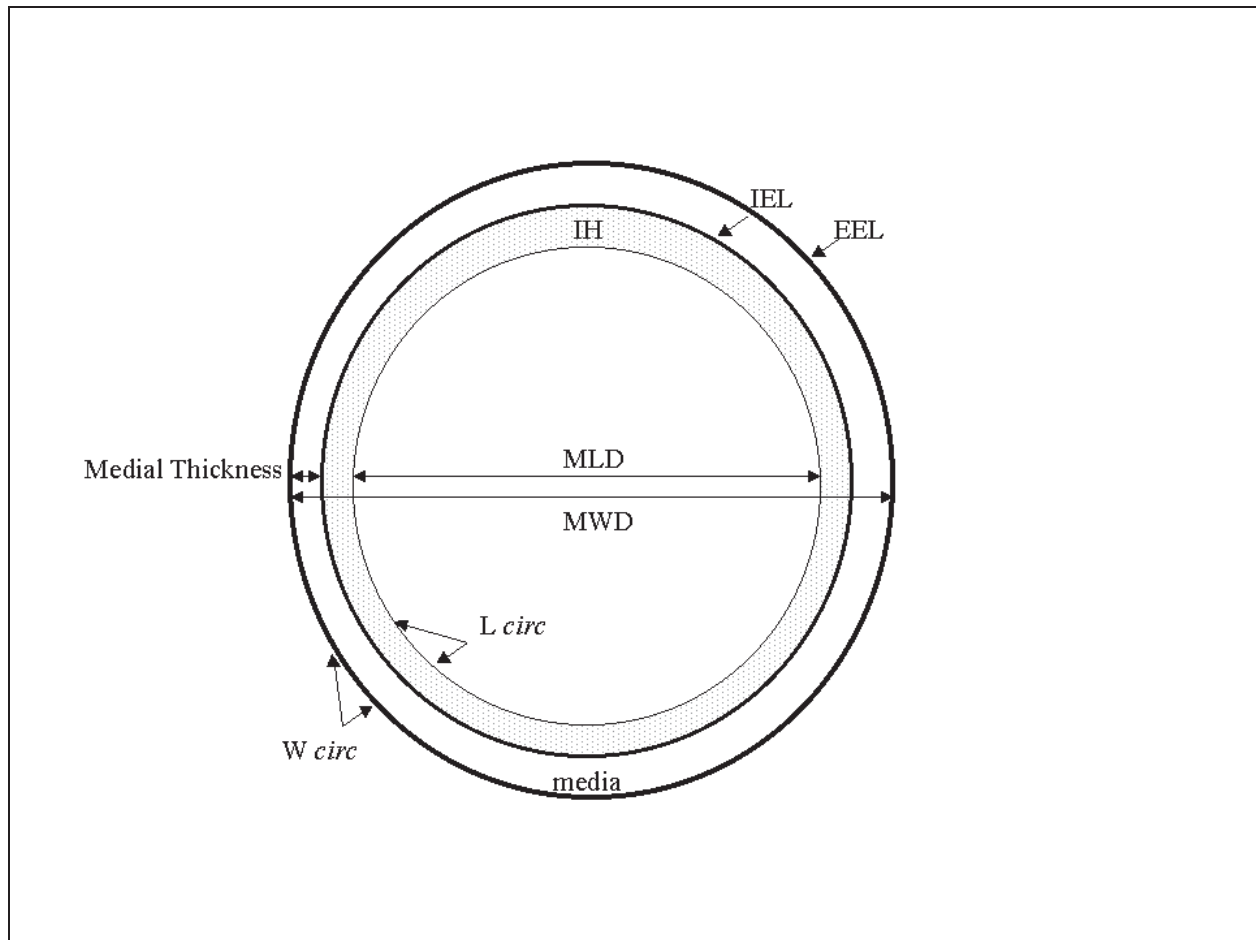


Figure 3.2 Schematic representation of an artery showing the geometric parameters used in this study. IH: Intimal Hyperplasia; media area; MLD: maximal lumen diameter; MWD: maximal wall diameter; maximal medial thickness. IEL: internal elastic lamina; EEL: external elastic lamina. The dotted line represents the lumen circumference (L circ), and the dark line the wall circumference (W circ).

3.02.11 Statistical analysis

Comparisons were made between different groups of rats at different time points. Each rat accounted for one measurement. Data were expressed as means \pm standard error of the mean (SEM). Comparisons including the type*time relations were made using a 2-way ANOVA method with a General Linear Model regression analysis in SAS. Bivariate correlations according Pearson to describe a correlation between type*time and WALLC were used. A difference was considered to be significant at p values less than 0.05.

3.03 Results

All animals appeared healthy without significant weight loss at follow-up. No thrombosis, arterial dissection, aneurysms, paraplegia or paralysis was encountered. The wound areas appeared normal besides some mild fibrosis at the suture side. Adjacent lymph nodes frequently covered the sutured arteriotomy.

3.03.1 Planimetric analysis

On microscopy, the endothelial layer was absent in the arteries immediately after BI and was recovered within 2 weeks after BI. In the control arteries the endothelium layer was continuously present.

3.03.2 Lumen Diameter

At 16 weeks after BI, LD decreased with 0.49 ± 0.11 mm (CCA), 0.22 ± 0.07 mm (CIA) and 0.07 ± 0.10 mm (AA) <Fig.3.3>. The linear association of a decrease in LD in CCA and CIA was significant higher than in AA <Fig.4.4> ($p<0.05$). MLD was 0.86 ± 0.04 mm (CCA), 1.53 ± 0.05 mm (AA) and 0.99 ± 0.02 mm (CIA) at 0 weeks, and was 0.37 ± 0.10 mm (CCA), 1.46 ± 0.09 mm (AA) and 0.77 ± 0.7 mm (CIA) at 16 weeks <Table 3.1>. In time, the overall MLD differed significantly between the CCA, AA and CIA. A significantly decrease was seen at 4-16 weeks (CCA), a temporarily increase at 2 weeks (AA) and a temporarily increase at 1-3 weeks followed by a decrease at 16 weeks (CIA) <Table 3.1>.

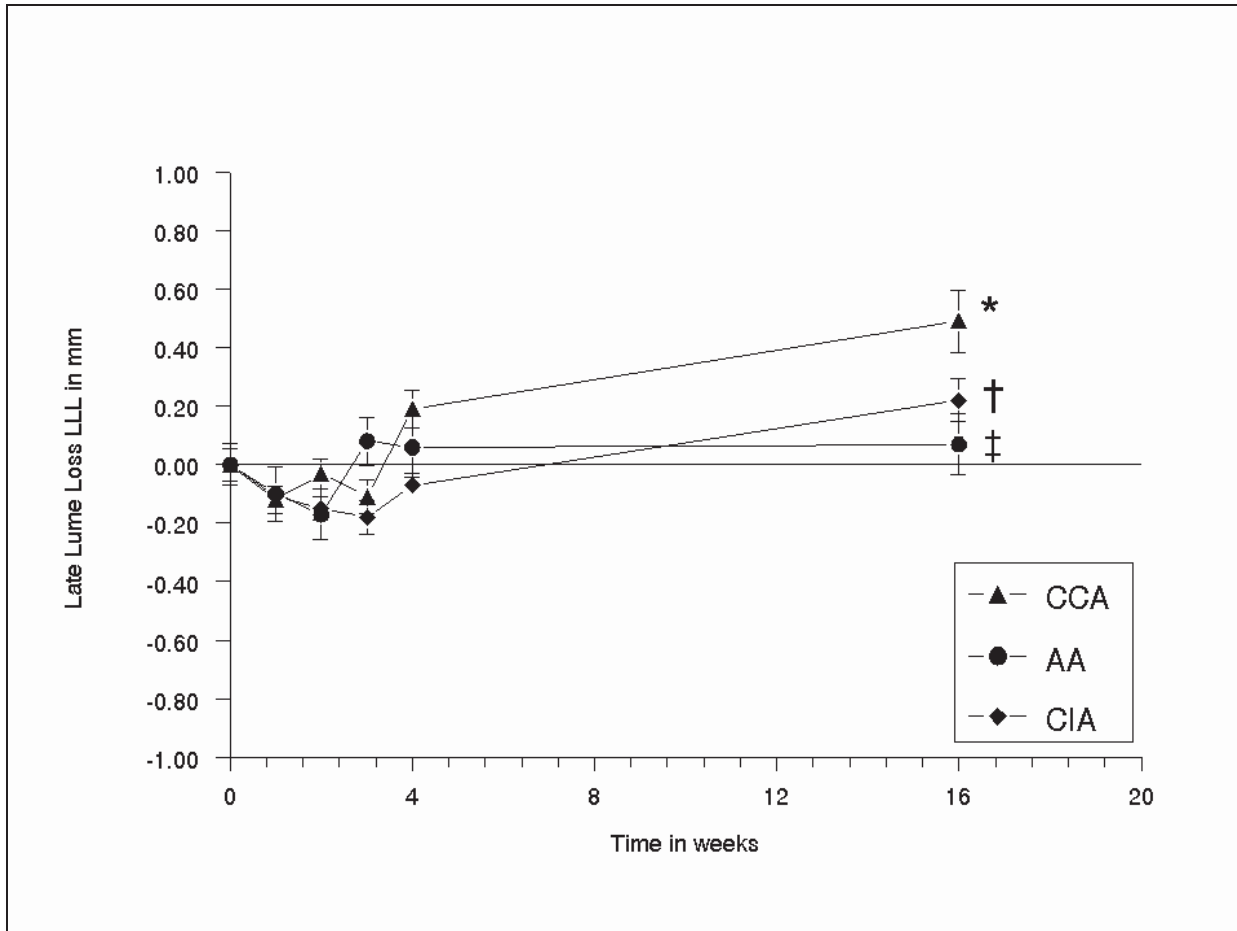


Figure 3.3 Diagram showing the mean difference in lumen diameter (MLD) as the sum of MLD at 0 weeks minus MLD at 16 weeks of the common carotid, abdominal aorta and common iliac artery, plotted against the time in weeks. The error bars are standard errors of the mean ($n=5$ for each time point). At 16 weeks: (*) CCA vs AA $p<0.0002$; (†) CCA vs CIA $p<0.001$; AA vs CIA (‡) $p<0.027$.

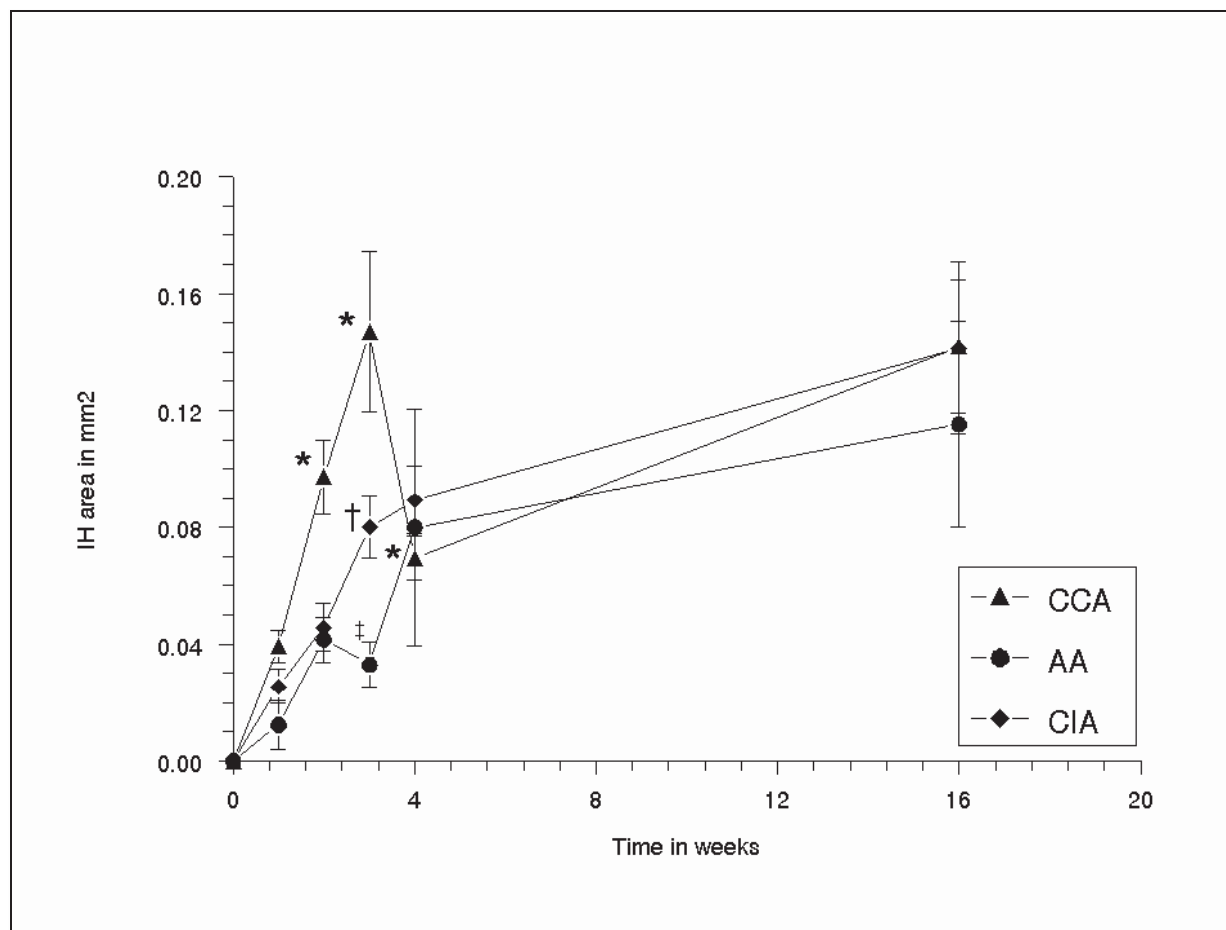


Figure 3.4 Diagram showing the mean area of intimal hyperplasia (IH) of the common carotid, abdominal aorta and common iliac artery, plotted against the time in weeks. The error bars are standard errors of the mean ($n=5$ for each time point).
 Type*Time Difference $p<0.001$: (*) CCA vs AA at 0 and 1 week NS, at 2 weeks $p<0.04$, at 3 weeks $p<0.0001$, at 4 weeks $p<0.0001$, at 16 weeks NS; (†) CCA vs CIA at 0, 1 and 2 weeks NS, at 3 weeks $p<0.007$ and at 4 and 16 weeks NS; (‡) AA vs CIA at 0, 1 and 2 weeks NS, at 3 weeks $p<0.02$, at 4 weeks and at 16 weeks NS.

<i>Parameter</i>	<i>Time</i>	<i>CCA</i>	<i>SEM</i>	<i>AA</i>	<i>SEM</i>	<i>CIA</i>	<i>SEM</i>
MLD in mm	0	0.86±	0.04	1.53±	0.05	0.99±	0.02
	1	0.98±	0.02	1.63±	0.08	1.09±	0.02
	2	0.89±	0.03	1.70±	0.07	1.14±	0.04
	3	0.97±	0.04	1.45±	0.07	1.17±	0.05
	4	0.67±	0.05	1.47±	0.09	1.06±	0.03
	16	0.37±	0.01	1.46±	0.09	0.77±	0.07
Media in mm ²	0	0.10±	0.00	0.25±	0.03	0.13±	0.00
	1	0.13±	0.01	0.32±	0.01	0.18±	0.01
	2	0.13±	0.01	0.35±	0.02	0.21±	0.01
	3	0.14±	0.01	0.40±	0.01	0.21±	0.01
	4	0.11±	0.00	0.32±	0.02	0.19±	0.01
	16	0.13±	0.01	0.28±	0.02	0.15±	0.01
Medial Thickness in mm	0	0.06±	0.00	0.09±	0.01	0.08±	0.00
	1	0.07±	0.00	0.14±	0.02	0.09±	0.00
	2	0.08±	0.00	0.12±	0.01	0.10±	0.01
	3	0.08±	0.01	0.14±	0.00	0.10±	0.00
	4	0.09±	0.00	0.13±	0.01	0.09±	0.01
	16	0.09±	0.00	0.11±	0.01	0.08±	0.00

Table 3.1 A representation of the geometric changes in time expressed in weeks (vertically in ascending order) after balloon injury in respectively (horizontally ordered) the right common carotid artery (CCA), abdominal aorta (AA) and right common iliac artery (CIA). The mean parameters (maximal lumen diameter (MLD), media area and maximal media thickness) are subsequently given. MLD: CCA 16 vs 0 $p < 0.001$; CIA 16 vs 0 $p < 0.0001$; CCA 1 vs 0 $p < 0.0003$; AA 2 vs 0 $p < 0.002$; CIA 3 vs 0 $p < 0.004$. Media area: CCA 3 vs 0 $p < 0.001$; AA 3 vs 0 $p < 0.0001$; CIA 3 vs 0 $p < 0.0001$. THMAX: CCA 16 vs 0 $p < 0.002$; AA 3 vs 0 $p < 0.0001$; CIA 3 vs 0 $p < 0.0001$

3.03.3 Intimal Hyperplasia

In all BI groups, the absolute area of IH increased significantly in time ($p < 0.017$) <Fig.3.5a1-3.5b2>. A significant increase was seen at 2-16 weeks (CCA), at 3-16 weeks (AA) and at 2-16 weeks (CIA). At 16 weeks, the area of IH was $0.14 \pm 0.03 \text{ mm}^2$ (CCA), $0.14 \pm 0.03 \text{ mm}^2$ (CIA) and $0.12 \pm 0.04 \text{ mm}^2$ (AA).

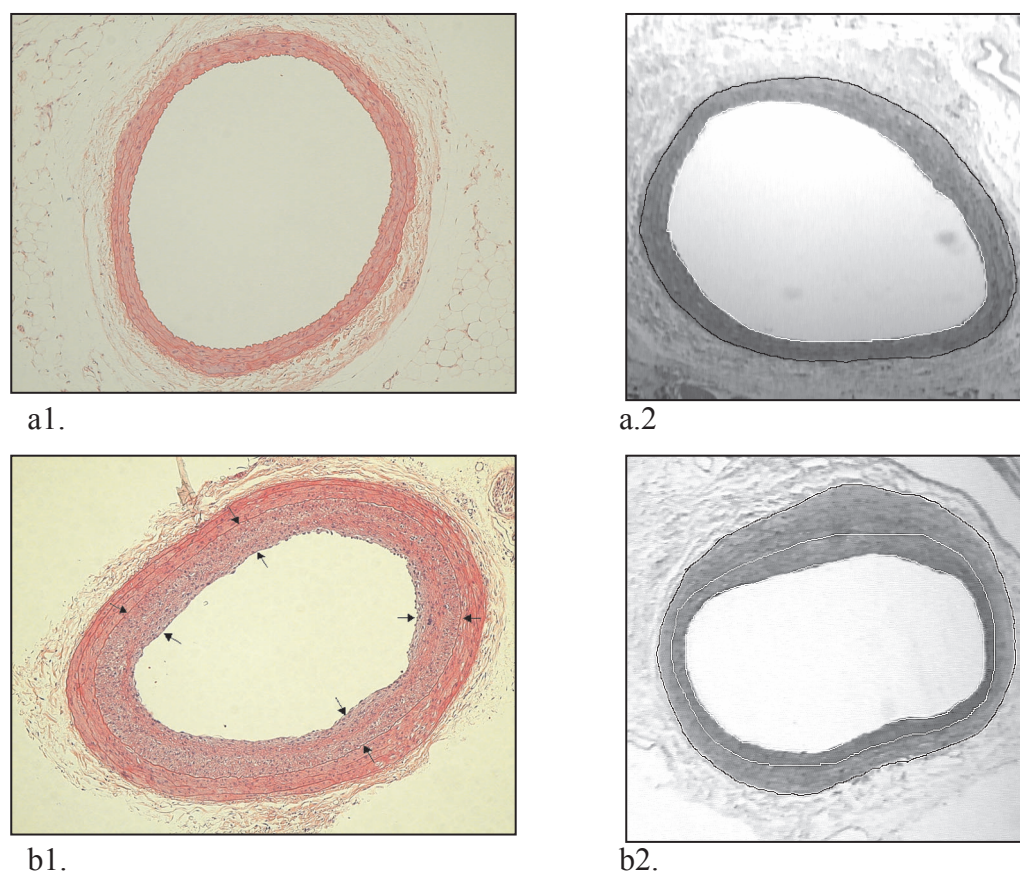


Figure 3.5 Photographs in the left column show HE-stained cross-sections of the iliac artery at 0 weeks (a1) and at 16 weeks (b1) after balloon injury (BI). The area between the black arrows indicate the area intimal hyperplasia. The digital planigraphs in the right column show the iliac artery at 0 weeks (a2) and at 16 weeks (b2) after BI. The white lines demarcate the IH area and the black line represents the external elastic lamina (border medial area=area between black and first white line).

3.03.4 Intimal Hyperplasia to media ratio

In all BI groups, the overall IH to media area ratio increased significantly in time ($p < 0.05$). A significant increase was seen at 1-16 weeks (CCA), at 4-16 weeks (AA) and at 2-16 weeks (CIA) ($p < 0.05$). The IH to media area ratio was higher in CCA (1.09 ± 0.15) than in AA (0.67 ± 0.23) and in CIA (0.95 ± 0.19) at 16 weeks, indicating relatively more IH development in CCA than in CIA and in AA <Fig.3.6>.

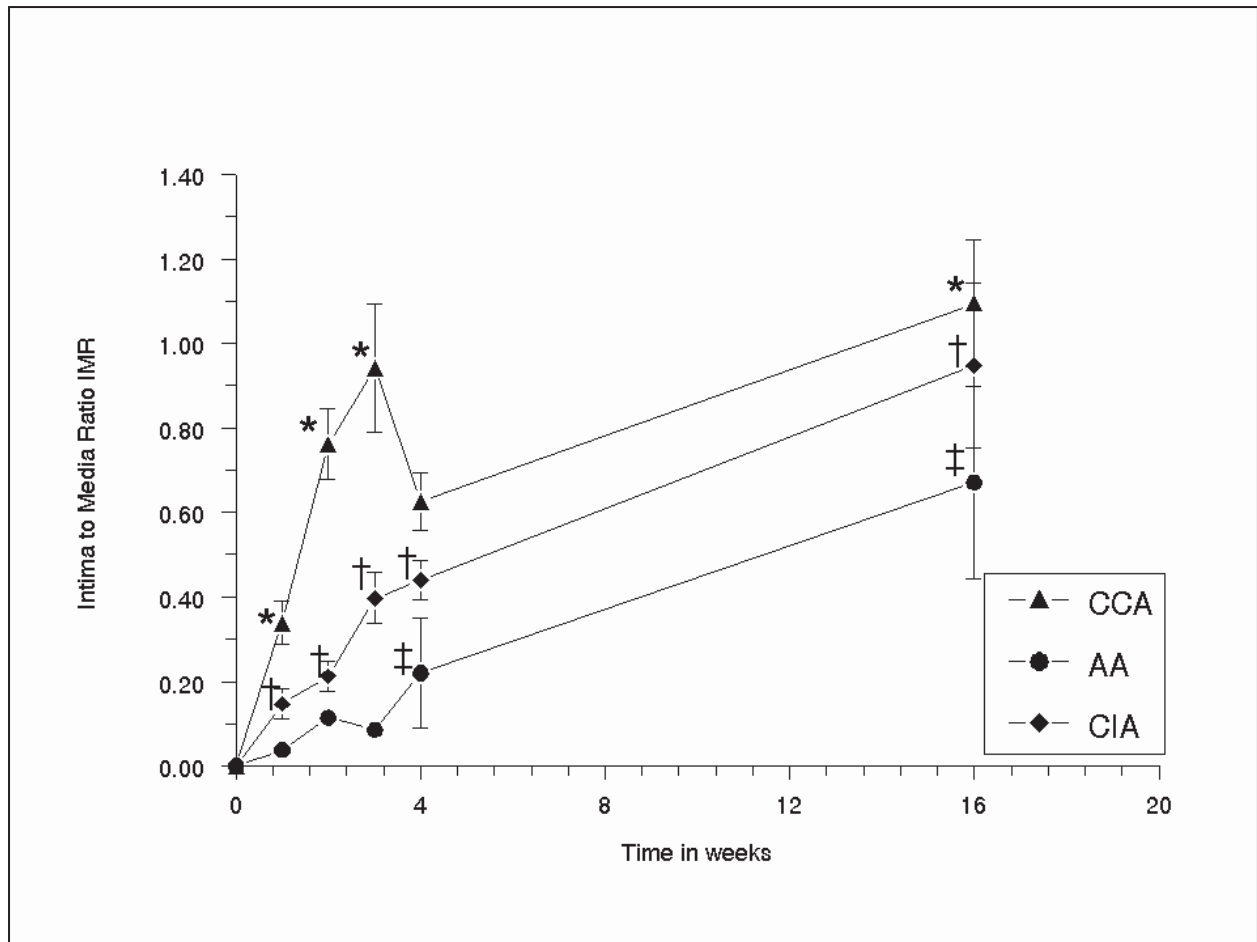


Figure 3.6 Diagram showing the mean-area-of-intimal hyperplasia-to-mean-media area ratio of the right common carotid, abdominal aorta and right common iliac artery, plotted against the time in weeks. The error bars are standard errors of the mean ($n=5$ for each time point). (*) CCA vs AA at 0 and 1 week NS, at 2 weeks $P<0.0001$, at 3 weeks $p<0.0001$, at 4 weeks NS and at 16 weeks $p<0.009$; (†) CCA vs CIA at 0 and 1 week NS, at 2 weeks $p<0.0002$, at 3 weeks $p<0.0004$, at 4 weeks $p<0.007$ and at 16 weeks $p<0.003$; (‡) AA vs CIA at 0, 1, 2 and 3 weeks NS, at 4 weeks $p<0.009$ and at 16 weeks $p<0.003$.

3.03.5 Constrictive vascular remodelling

In all BI groups, the overall wall circumferences (WALLC) varied significantly in artery type and in time <Fig.3.7>. A significant increase was seen at 1-3 weeks in CCA (0.51 ± 0.13 mm), an increase at 1-16 weeks in AA (0.46 ± 0.10 mm) and an increase at 1-4 weeks (0.37 ± 0.05 mm) and a decrease at 16 weeks in CIA (-0.17 ± 0.05 mm). No significant correlation with the time was found (-0.020 ; $p<0.68$).

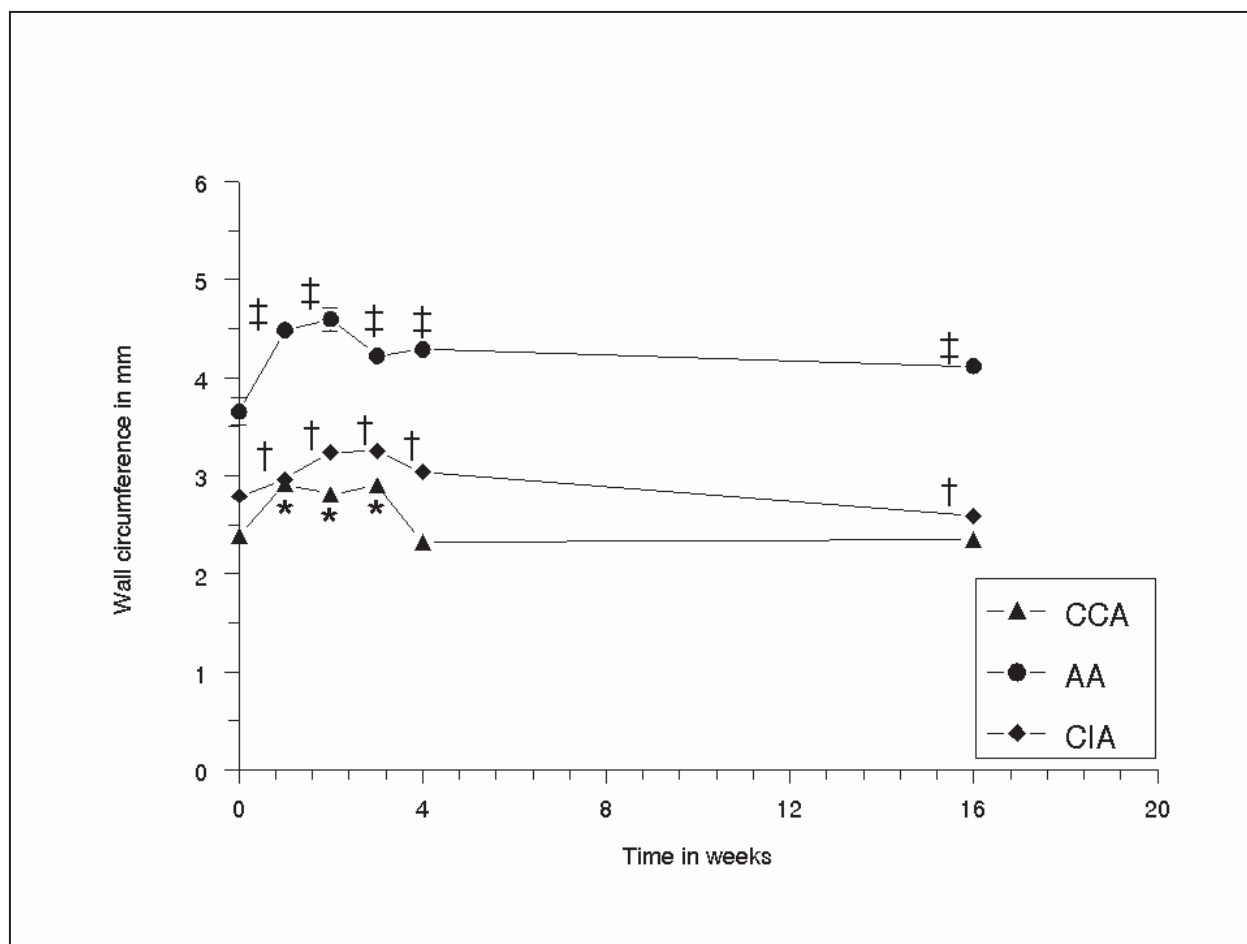


Figure 3.7 Diagram showing the wall circumference of the right common carotid, abdominal aorta and common iliac artery, plotted against the time in weeks. The error bars are standard error of the mean ($n=5$ per time point).
 (*) CCA at 0 vs 1 week $p<0.003$, 0 vs 2 weeks $p<0.004$, 0 vs 3 weeks $p<0.0004$, 0 vs 4 and 16 weeks NS; (†) AA at 0 vs 1 week $p<0.004$, 0 vs 2 weeks $p<0.001$, 0 vs 3 $p<0.001$ and 4 weeks $p<0.001$, 0 vs 16 weeks $p<0.004$; (‡) CIA at 0 vs 1, 2, 3, 4 and 16 weeks $p<0.001$.

3.03.6 Number of vasa vasorum in the tunica adventitia

In the CCA groups, no vasa vasorum were seen, while in the AA and CIA respectively 27 ± 2 and 13 ± 2 vasa vasorum per section at 0 weeks were seen in the tunica adventitia. A significant increase in time was assessed in the AA and CIA groups with respectively 37 ± 2 and 22 ± 2 vasa vasorum/section at 16 weeks ($p<0.05$). Sporadically, some vasa vasorum in the tunica media were seen in the AA and not in the CIA and CCA groups.

3.04 Discussion

Balloon injury of the common carotid artery (CCA) in the rat is a thoroughly studied model that has logistical advantages to evaluate dysplastic intimal hyperplasia (IH) and the decrease in lumen diameter (LD) for the evaluation of strategies to prevent restenosis, like endovascular based interventions. However, CCA does not fit well to evaluate endovascular techniques due to the relatively large diameter of endovascular devices and fibre tips.

Furthermore, in contrast to human arteries, the rat carotid artery has no vasa vasorum, contains a much thinner subintimal layer and a smaller percentage of elastin in the tunica media [17].

In this study the larger –vasa vasorum containing- abdominal aorta (AA) and common iliac artery (CIA) in the rat were validated as an alternative model to be used for the evaluation of endovascular techniques.

In this study, the decrease in LD was higher in CCA and CIA compared to AA after BI. The differences in LD between CCA, AA and CIA are likely explained by an artery-type specific healing response after BI, expressed in the development of IH and constrictive vascular remodelling (CVR), due to differences in the viscoelastic composition, the vasa vasorum in the tunica adventitia and vessel diameter.

Another explanation, however, may be the lower dilatation ratio in the aorta due to its large diameter, causing less IH development and less remodelling. Indeed, we found that in CCA, AA and CIA, IH developed differently at long-term after BI. The extent of CCA IH in our model was similar to that in previous reported rat models [14;18]. Relatively more IH (expressed by the IH to media ratio) developed in CCA and CIA compared to the AA. In CCA and CIA, IH led to a higher decrease in LD.

With regard to CVR, the wall circumference temporarily increased in the CCA and CIA, and remained increased in AA. In CCA and in CIA a decrease of wall circumference was seen in contrast to the increased wall circumference of AA at 16 weeks. Apparently, AA compensated to IH by positive (=outward) remodelling underlining the blood reservoir capacity of AA, but led to shrinkage in the CCA and CIA at 16 weeks underlining the peripheral resistance capacity of CCA and CIA.

Earlier reports, using a PTA catheter or a chain-encircled balloon catheter in pig models described that IH is not correlated to CVR, suggesting that the pathogenesis is not similar [19;20]. In this study, the absence of a decrease in LD and CVR, but still the development of IH in the AA supports these findings, but are in contrast with a decrease in LD, increase in IH and an increase in CVR in the CCA and CIA.

With regard to the media area, no significant difference was found in CCA, AA and CIA in time. With regard to the maximal medial thickness, an increase was seen in CCA but not in CIA and AA after 16 weeks. Apparently the BI caused more damage in the CCA than in AA and CIA, leading to an increased proliferation in the tunica media.

A plausible explanation is likely in the viscoelastic differences between CCA, AA and CIA. The rat CCA in contrast to the human CCA is an integrating part of the circle of Willis and resembles the rat cerebral arteries characterised by a low elastin/ high collagen content and a low contraction potential. In contrast, the systemic AA and CIA have a high elastin/ moderate collagen content and a high contraction potential [21]. Then, the medial content of contractile vs synthetic SMCs varies in CCA, AA and CIA. Their role in remodelling is not fully elucidated but likely adapt the viscoelastic content in the extracellular matrix. Indeed, Goldberg et al showed in rats that an artery-type dependent variation of both synthetic and contractile SMCs determined the vascular wall response [22]. Notably, the attenuated response of the AA could be explained by the lumen diameter to BI pressure ratio as suggested earlier in a rat and rabbit model.

Furthermore, the absence of vasa vasorum in the CCA in the tunica adventitia in contrast to the AA and CIA is strikingly in this study. The increased number in the latter two may favour the arterial healing via reperfusion that may lack in the tunica adventitia of the CCA. The presence of vasa vasorum may explain the difference in arterial healing between the arteries. Indeed, Pels described that the number of vasa vasorum in the tunica adventitia changed after balloon injury in pigs, which may be a component of arterial remodelling after angioplasty [23]. Our data of the CIA, but not of the AA support this conclusion. Badimon described a discrepancy between CCA and the coronary arteries [24], while Ward described a discrepancy between the CIA and coronary artery types after standard BI [25], indicating the importance of an arterial specific healing response as emphasised in our study. Interestingly, the arteries of rabbit, pigs and humans, are also characterised by vasa vasorum in the tunica adventitia. Thus, the CIA and AA of the rat are closer to the arteries the larger models than the CCA of the rat.

A limitation of this study is that no vasodilator was applied. However, geometric analysis of the sections within the groups did not show any significant difference, assuming that the contribution of reversible and chronic vasodilatory spasm was negligible.

Another limitation was the difference in weight between the animals in time. The influence of increased weight on the growth of the artery is well known and was corrected in this model.

Further, the use of balloon catheters that precisely fit with the arterial lumen might be suggested for comparing BI. Indeed, the deflated catheter diameter of the 2F balloon fitted well in CCA, CIA and moderately in AA, but the inflated balloon diameter extended for 45-60% in these arteries (NS: unpublished data). Roubin described that an increased balloon injury resulted in an increased development of restenosis needing bypass surgery in a prospectively randomised clinical trial of 336 patients [26].

In this study, the force to over-stretch the artery was standardised and comparable between the balloon injured arteries. Besides differences in arterial morphology, the severity of injury and strain [27]- and inter-species differences [10] in the healing response and metabolism demand a careful extrapolation to the human situation.

3.05 Conclusions

In conclusion, 1. BI using 2 bar resulted in a decrease in LD in CCA due to IH, 2. In a decrease in LD in CIA due to IH and CVR, 3. no change in LD in AA. 4. Comparable IH development in all arteries, 5. CCA has no vasa vasorum compared to CIA and AA, 6. Discrepancies in changes in LD by IH development and CVR after BI depend on artery type. This should be taken into account in the interpretation of the efficacy of interventional techniques to inhibit IH and a decrease in LD. 7. The CIA model is suitable to evaluate fibre-based therapies, as it combines good access for 2F endovascular catheters with the development of a decrease in LD due to IH and CVR after BI.

Acknowledgements

This study was supported by the Dutch Heart Foundation (project grant NHS 97.181). The authors are grateful to Jan Honkoop for expert technical assistance with the geometric analysis, Dr Marc van Sambeek for freely giving dilation catheters, Patricia Lobe and Manon Holtman for excellent staining of the cross-sections.

References

- [1] Bauters C, Meurice T, Hamon M, McFadden E, Lablanche JM and Bertrand ME, Mechanisms and prevention of restenosis: from experimental models to clinical practice, 1996. *Cardiovasc. Res.* 31, pp. 835-846.
- [2] Giraldo AA, Esposito OM and Meis JM, Intimal hyperplasia as a cause of restenosis after percutaneous transluminal coronary angioplasty, 1985. *Arch. Pathol. Lab Med.* 109, pp. 173-175.
- [3] Glagov S, Intimal hyperplasia, vascular modeling, and the restenosis problem, 1994. *Circulation* 89, pp. 2888-2891.
- [4] Haudenschild CC, Pathogenesis of restenosis, 1989. *Z. Kardiol.* 78 Suppl 3:28-34, pp. 28-34.
- [5] Park JW, Braun P, Mertens S and Heinrich KW, Ischemia: reperfusion injury and restenosis after coronary angioplasty, 1992. *Ann. N. Y. Acad. Sci.* 669:215-36, pp. 215-236.
- [6] Pasterkamp G, de Kleijn DP and Borst C, Arterial remodeling in atherosclerosis, restenosis and after alteration of blood flow: potential mechanisms and clinical implications, 2000. *Cardiovasc. Res.* 45, pp. 843-852.
- [7] Post MJ, Borst C, Pasterkamp G and Haudenschild CC, Arterial remodeling in atherosclerosis and restenosis: a vague concept of a distinct phenomenon, 1995. *Atherosclerosis* 118 Suppl:S115-23, p. S115-S123.
- [8] Teirstein PS, Prevention of vascular restenosis with radiation, 1998. *Tex. Heart Inst. J.* 25, pp. 30-33.
- [9] Landau C, Currier JW, Haudenschild CC, Minihan AC, Heymann D and Faxon DP, Microwave balloon angioplasty effectively seals arterial dissections in an atherosclerotic rabbit model, 1994. *J. Am. Coll. Cardiol.* 23, pp. 1700-1707.
- [10] Schwartz RS, and Holmes DR, Pigs, dogs, baboons and man: lessons for stenting from animal studies. 1994. *J. Intervent. Cardiol.* 7, 355-368.
- [11] Carson SN, Esquivel CO and French SW, Experimental carotid stenosis due to fibrous intimal hyperplasia, 1981. *Surg. Gynecol. Obstet.* 153, pp. 883-888.
- [12] Muller D, Ellis S and Topol EJ. Experimental models of coronary artery restenosis. 1992. *J. Am. Coll. Cardiol.* 19, 418-432.
- [13] French JE, Jennings MA and Florey HW, Morphological studies on atherosclerosis in swine. 1965. *Ann. N. Y. Acad. Sci.* 127, 780-794.
- [14] Indolfi C, Esposito G, Di Lorenzo E, Rapacciuolo A, Feliciello A, Porcellini A, Avvedimento V, Condorelli M, and Chiariello M. Smooth muscle cell proliferation is proportional to the degree of balloon injury in a rat model of angioplasty. 1995. *Circulation* 92[5], 1230-1235.
- [15] Wenguan L, Gussenhoven EJ, Bosch JG, Mastik F, Reiber JHC and Bom N, A computer-aided analysis system for the quantitative assessment of intravascular ultrasound images. 2001. *Proc Computers in Cardiology* 1990, pp. 333-336.
- [16] LaMuraglia GM, Klyachkin ML, Adili F and Abbott M, Photodynamic therapy of vein grafts: suppression of intimal hyperplasia of the vein graft but not the anastomosis, 1995. *J. Vasc. Surg.* 21, pp. 882-890.
- [17] Sims FH, A comparison of structural features of the walls of coronary arteries from 10 different species. 1989. *Pathology* 21, 115-124.

- [18] Schwartz RS, The vessel wall reaction in restenosis, 1997. *Semin. Interv. Cardiol.* 2, pp. 83-88.
- [19] Post MJ, Borst C and Kuntz RE, The relative importance of arterial remodeling compared with intimal hyperplasia in lumen renarrowing after balloon angioplasty. A study in the normal rabbit and the hypercholesterolemic Yucatan micropig, 1994. *Circulation* 89, pp. 2816-2821.
- [20] Holm P, Andersen HO, Nordestgaard BG, Hansen BF, Kjeldsen K and Stender S, Effect of oestrogen replacement therapy on development of experimental arteriosclerosis: a study in transplanted and balloon-injured rabbit aortas, 1995. *Atherosclerosis* 115, pp. 191-200.
- [21] Lee RM, Morphology of cerebral arteries, 1995. *Pharmacol Ther* 1995, pp. 149-173.
- [22] Goldberg ID, Stemerman MB, Ransil BJ, and Fuhro RJ, In vivo aortic muscle cell growth kinetics: Differences between thoracic and abdominal segments after Intimal Injury in the rabbit. 1980. *Circ.Res.* 47, 182-189.
- [23] Pels K, Labinaz M, Hoffert C, and O'Brien ER. Adventitial angiogenesis early after coronary angioplasty: correlation with arterial remodeling. *Arterioscler.Thromb.Vasc.Biol.* 1999. 19[2], 229-238.
- [24] Badimon JJ, Ortiz AF, Meyer B, Mailhac A, Fallon JT, Falk E, Badimon L, Chesebro JH, and Fuster V. Different response to balloon angioplasty of carotid and coronary arteries: effects on acute platelet deposition and intimal thickening. 1998. *Atherosclerosis* 140[2], 307-314.
- [25] Ward MR, Kanellakis P, Ramsey D, Jennings GL and Bobik A, Response to balloon injury is vascular bed specific: a consequence of de novo vessel structure?, 2000. *Atherosclerosis* 151, pp. 407-414.
- [26] Roubin GS, Douglas Jr JS, King 3rd SB, Lin SF, Hutchison N, Thomas RG, and Gruentzig AR. Influence of balloon size on initial success, acute complications and restenosis after percutaneous transluminal coronary angioplasty. A prospective randomized study. 1988. *Circulation* 78[3], 557-565.
- [27] Assadnia S, Rapp JP, Nestor AL, Pringle T, Cerilli GJ, Gunning 3rd WT, Webb TH, Kligman N, and Allison DC, Strain differences in neointimal hyperplasia in the rat. 1999. *Circ.Res.* 84[11], 1252-1257.

SECTION III

CHAPTER 4

Aminolaevulinic Acid Induced Protoporphyrin IX Pharmacokinetics in Central and Peripheral Arteries of the Rat

¹Edward EE Gabeler, ²Wim Sluiter, ³Annie Edixhoven, ¹Richard van Hillegersberg,
²Kees Schoonderwoerd, ¹Randolph G Stadius van Eps, ¹Hero van Urk

¹Dept. of Surgery, Erasmus MC, Rotterdam, The Netherlands

²Dept. of Biochemistry, Erasmus MC, Rotterdam, The Netherlands

³Dept of Internal Medicine, Erasmus MC, Rotterdam, The Netherlands

Keywords: PDT, restenosis, protoporphyrin IX

Photochemistry and Photobiology 2003, 78(1):82-87.

Abbreviations: A. Absorption constant, ALA. Aminolaevulinic acid, COPRO. Coproporphyrin, COPROgen. Coproporphyrinogen, i.v. Intravenous, PBG. Porphobilinogen, PDT. Photodynamic therapy, PpIX. Protoporphyrin IX, SEM. Standard error of the mean, URO. Uroporphyrin, UROgen. Uroporphyrinogen.

4.00 Abstract

Background: Photodynamic therapy (PDT) may prevent restenosis following transluminal angioplasty by inhibiting intimal hyperplasia and vascular constriction. The synthesis of the photosensitive heme intermediate protoporphyrin(Pp)IX in the mitochondrion can be promoted via exogenous administration of aminolaevulinic acid (ALA). Since the number of mitochondria and their activity differ between various tissues, the time-interval to reach the highest PpIX levels may differ among varying arteries.

Materials & Methods: Therefore, we determined the PpIX concentration in various arteries after systemic ALA administration. ALA was administered i.v. (200 mg/kg) to male Wistar rats (n=21). At varying time intervals (0, 1, 2, 3, 6, 12, 24 hr) both central arteries and peripheral arteries were isolated, homogenized and the ALA, porphobilinogen (PBG), uroporphyrinogen (UROgen), coproporphyrinogen (COPROgen), zinc PpIX and PpIX concentration determined by a fluorometric extraction method.

Results: The maximal PpIX concentration was more than two fold higher in peripheral arteries (20.49 ± 3.0 - 24.0 ± 7.5 pmol/mg protein) compared to central arteries (0 - 9.46 ± 0.01 pmol/mg protein) ($p < 0.004$). However, the amount of citrate synthase, reflecting the mitochondrial content of the artery, was lower (0.14 - 0.61 U/mg protein) in the peripheral arteries than in the central arteries (1.87 - 2.32 U/mg protein).

Conclusion: Apparently, the level of PpIX production cannot simply be explained by the mitochondrial content of the arteries of the rat. The time-interval of maximal PpIX accumulation after ALA administration was not statistically significantly different in peripheral versus central arteries (2:27 vs. 2:08 hr) ($p = 0.13$). If the efficacy of PDT in vivo is directly related to the tissue concentration of PpIX, more effect can be expected in peripheral arteries compared to central arteries.

4.01 Introduction

Restenosis, the chronic re-narrowing of a treated stenotic artery, comprises the success rates of vascular interventions in treating symptomatic vascular disease. The incidence of this complication is between 20 and 40% within 6 months after endovascular interventions, which underlines the need for effective preventive strategies [1].

A promising tool in preventing this post-interventional restenosis is vascular photodynamic therapy (PDT) using the endogenous heme intermediate protoporphyrin IX (PpIX) as the photosensitizer [2-5]. To increase the synthesis of PpIX in the arterial wall, its precursor aminolaevulinic acid (ALA) is administered. Key-mechanisms of ALA-PDT as an adjuvant to angioplasty are the eradication of photosensitized proliferating vascular smooth muscle cells [6] and the induction of crosslinks between proteins of the subcellular matrix of the arterial wall [7-9].

After systemic administration, ALA is distributed to most tissues leading to PpIX production and accumulation in specific organ [10]. However, no data are available on the distribution characteristics of ALA and its conversion products in the various artery types following systemic administration. Intrinsic differences between the central visco-elastic arteries and the peripheral muscular arteries could play a role in that respect. Because the products of the heme biosynthetic pathway will contribute to the photosensitization of the blood vessel, knowledge of their accumulation in the vascular wall may be of use to determine the illumination interval following ALA administration. Therefore, the aim of this study was to describe the pharmacokinetics of ALA induced PpIX in various arteries categorized as either central (thoracic aorta, abdominal aorta) or peripheral (carotid-, renal-, iliac artery).

4.02 Materials & methods

4.02.1 Animals

Male inbred Wistar rats (Harlan CPB, Austerlitz, The Netherlands) weighing 200-300g were used. The animals had free access to rat chow (AM II, Hope Farms, Woerden, The Netherlands) and tap water acidified to pH 4.0, while maintained in a standard 12-hr light/dark cycle. The zinc content in food was 5 $\mu\text{mol/day}$ and in drinking water 7.2 $\mu\text{mol/L}$, which is a normal daily intake.

4.02.2 Study design

Twenty-four rats were randomly divided into 8 groups of 3 animals each. Each rat received i.v. 200 mg/kg ALA (Sigma-Aldrich Chemie, Zwijndrecht, The Netherlands) dissolved in phosphate buffered saline (pH 7.45) at 40 mg/ml and was sacrificed at 0, 1, 2, 3, 6, 12 or 24 hr post administration. A control group of 3 rats received phosphate buffer only. The ALA-solution was freshly made for each animal and kept from light exposure. The photosensitized rats were kept in the dark until sacrifice to prevent skin photocytotoxicity. The experimental protocol was approved by The Committee on Animal Research of the Erasmus University of Rotterdam and complied with “the Principles of Good Laboratory Practice”.

4.02.3 Blood samples

At the end of the observation-period, blood samples were taken under ether anesthesia via a cardiac puncture and collected in plastic heparinized tubes wrapped in aluminum foil. All tubes were kept on ice. After centrifugation at 1300xg for 10 min, the plasma was collected, protected from light and stored at $-70\text{ }^{\circ}\text{C}$ until use.

4.02.4 Arterial samples

After collecting the blood samples, all rats underwent a combined thoracotomy and medial laparotomy under ether anesthesia and subdued filtered light (acrylate yellow filter, Wientjes BV, Roden, The Netherlands) [11]. Subsequently, the thoracic aorta and abdominal aorta (central arteries), and the right common-, right renal-, right common iliac- and right femoral artery (peripheral arteries) were harvested and flushed with saline, freeze-dried and stored for at least 24 hr in aluminum reservoirs at $-70\text{ }^{\circ}\text{C}$.

4.02.5 Laboratory assays

Chemicals

PpIX disodium salt, zinc PpIX and PBG were obtained from Porphyrin Products (Logan, UT, USA). Uroporphyrin (URO) and Triton X-100 were obtained from Sigma Aldrich Chemie BV. TRIS was obtained from Boehringer Mannheim (Mannheim, Germany). All other chemicals were obtained from Merck (Darmstadt, Germany).

Sample preparation

The arterial samples were kept on ice and were homogenized in water (1/5, wt/wt) using a Potter Elvehjem homogenizer (Kontess Glass Co, Vineland, NJ, USA). The protein content of the arterial samples was determined according the method of Lowry [12].

Determination of PpIX and its precursors in plasma and arterial samples

Determinations of ALA and PBG in plasma and arterial samples were performed by a fluorimetric enzyme assay as described previously [10]. This assay is based on the conversion of PBG or ALA into uroporphyrinogen (UROgen) I overnight at 37°C, respectively by the addition to the samples of porphobilinogen deaminase (PBG-D) or aminolaevulinic acid dehydratase (ALA-D) and PBG-D. For the determination of UROgen no enzymes were added to the samples. Next, the samples were exposed to UV light (350 nm) for 5 min to convert porphyrinogens into porphyrins, followed by centrifugation for 30 min at 1500xg. The fluorescence of the supernatant was measured at an excitation wavelength of 410 nm and an emission wavelength of 656 nm using a LS-50B spectrofluorometer with a red sensitive photomultiplier (Perkin Elmer, Nieuwerkerk a/d IJssel, The Netherlands). Values were calculated according to a standard line of ALA or PBG converted to UROgen, or of URO. We found that if no enzymes were added to the tissue or plasma samples, no UROgen could be detected.

PpIX and zinc PpIX were extracted by adding to 25 µl of plasma or tissue homogenate 50 µl of Tris-HCl (50 mM, pH 8.0) and 425 µl of a mixture of dimethylsulfoxide and methanol (30:70, v/v). The samples were mixed vigorously using a vortex and left for about 30 min at room temperature. After centrifugation for 30 min at 1500xg, 100 µl of the supernatant was injected on a 10-cm Lichrosorb RP18 column (Chrompack, Middelburg, The Netherlands) for reversed phase HPLC analysis using acetone/methanol/water/formic acid (560:240:200:1.75, by vol.) as the mobile phase [13]. Elution of the porphyrins was detected using a fluorescence detector (LS240, Perkin Elmer, Nieuwerkerk a/d IJssel, The Netherlands) with a red-sensitive photomultiplier operating at excitation and emission wavelengths of 410 nm and 625 nm, respectively. Sporadically, a peak preceded the zinc PpIX peak that could be identified as most likely being coproporphyrin (COPRO). Recovery of porphyrins during the extraction was determined by adding a PpIX or zinc PpIX standard to the samples and amounted to 90-100%. The concentrations of porphyrins in the samples were calculated according to standard lines of zinc PpIX, and PpIX. The porphyrin levels of plasma were expressed in µmol/L and of arterial samples in pmol/mg protein.

A first-order, one-compartment model [14] was used to calculate the time (t_{max}) of maximal concentration (C_{max}) of ALA, PBG, COPROgen (being the reduced counterpart of COPRO in the tissues), zinc PpIX, and PpIX in the arterial wall after i.v. injection of a single dose of ALA. The time course of the concentrations of these compounds in each artery are described according to the standard pharmacokinetic equation 1:

$$C(t) = A * \frac{k1}{k1 - k2} * (e^{(-k2*t)} - e^{(-k1*t)})$$

in which $C(t)$ is the concentration (pmol/mg protein) at time-point t in hours. A represents the absorbed fraction of the dose divided by the distribution volume, $k1$ the absorption rate constant of the metabolite into the compartment under study and $k2$ the elimination rate constant of the metabolite from that compartment expressed in hour⁻¹.

The values of those three parameters were found by iteration using a non-linear regression analysis. Next, the parameters k_1 and k_2 were used to calculate the time-point at which the concentration $C(t)$ is maximal (t_{\max}), using the equation 2:

$$t_{\max} = \frac{\ln\left(\frac{k_1}{k_2}\right)}{k_1 - k_2}$$

After substitution of that time point for t in equation 1 the maximal concentration (C_{\max}) was found. The standard deviations were calculated using the propagation of the errors. The half-time ($t_{1/2}$) in hours was calculated according to the equation 3:

$$t_{1/2} = \frac{0.693}{k_2}$$

Determination of the amount of mitochondria in rat arteries

The number of mitochondria in each artery under study was estimated based on the citrate synthase content of the artery. This is plausible because the enzyme citrate synthase is localized in the mitochondrial matrix. Under saturating substrate concentrations the enzyme activity is equivalent to the enzyme concentration. Citrate synthase activity was determined in homogenates of arterial samples diluted 20 fold (w/v) in 0.25 M sucrose, pH 7.4, according to the method described by Srere et al [15] and expressed in U/mg protein.

The respiratory chain activity was assayed using high-resolution respirometry [16]. In short, after rapid dissection the arteries were permeabilized by treatment with saponin (50 µg/ml) for 60 min. Next, upon the addition of various substrates to each arterial sample the rate of oxygen consumption was measured using a polarographic oxygen sensor (OROBOROS Oxygraph, Anton Paar GmbH, Graz, Austria). Respiration rate was expressed as the amount of oxygen consumed in nmol O₂/sec/mg protein.

4.02.6 Statistical analysis

Data are expressed as means and standard error of the means (SEM). Student's t-test or ANOVA according to Bonferroni's correction for multiple comparisons were used where appropriate to evaluate differences between the artery types as to peak concentrations and corresponding time-intervals of the various porphyrins. The strength of the linear association between the peak concentrations of the various porphyrins and citrate synthase was quantified by calculating the Pearson correlation coefficient. A P-level smaller than 0.05 ($p < 0.05$) was considered statistically significant.

4.03 Results

4.03.1 Courses of the concentrations of ALA and PBG in plasma

The highest concentration of ALA (0.23 ± 0.06 µmol/L) in plasma was found immediately after its intravenous administration <Fig.4.1>. The highest concentration of PBG (0.02 ± 0.003 µmol/L) was detected at 1 hr after intravenous ALA administration.

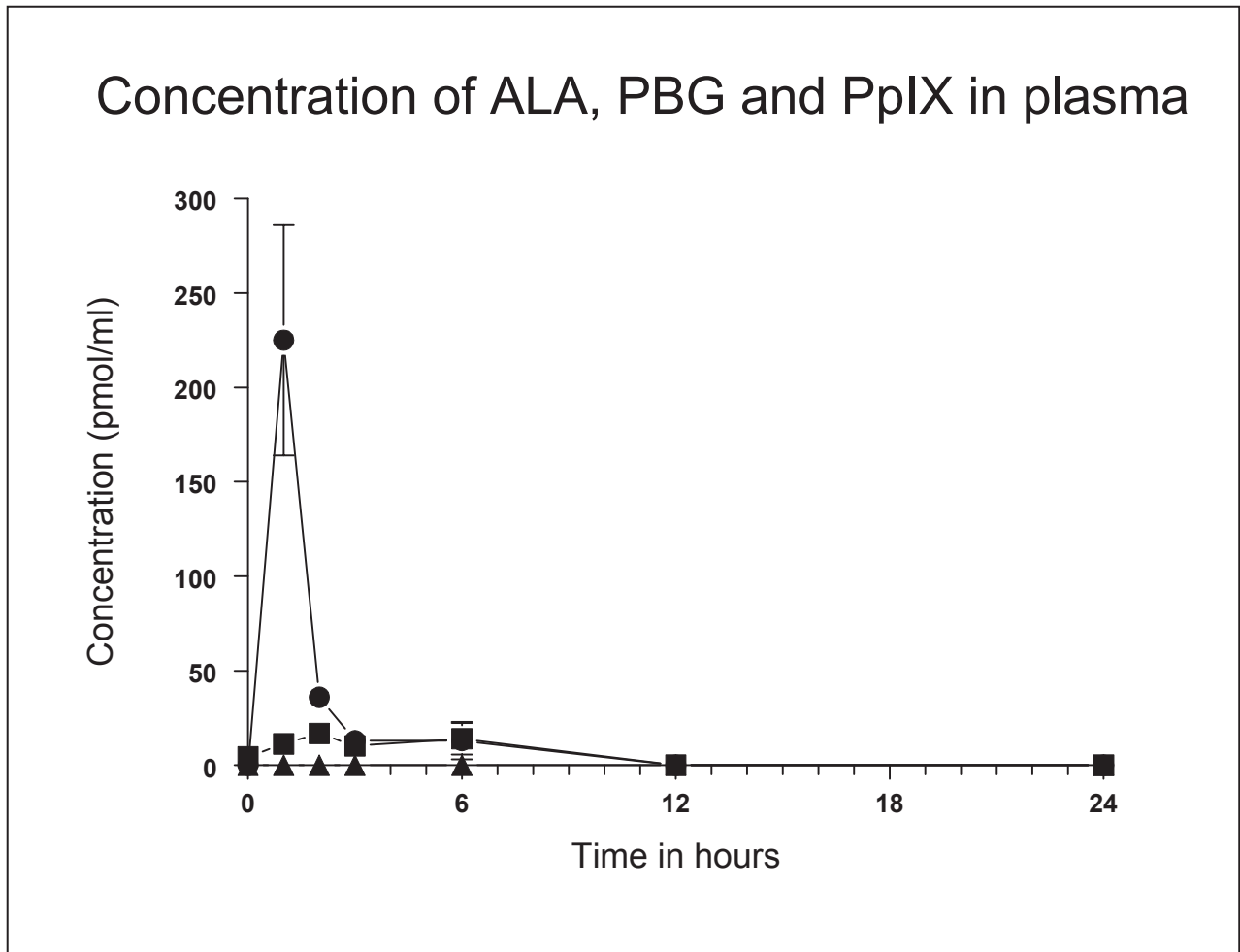
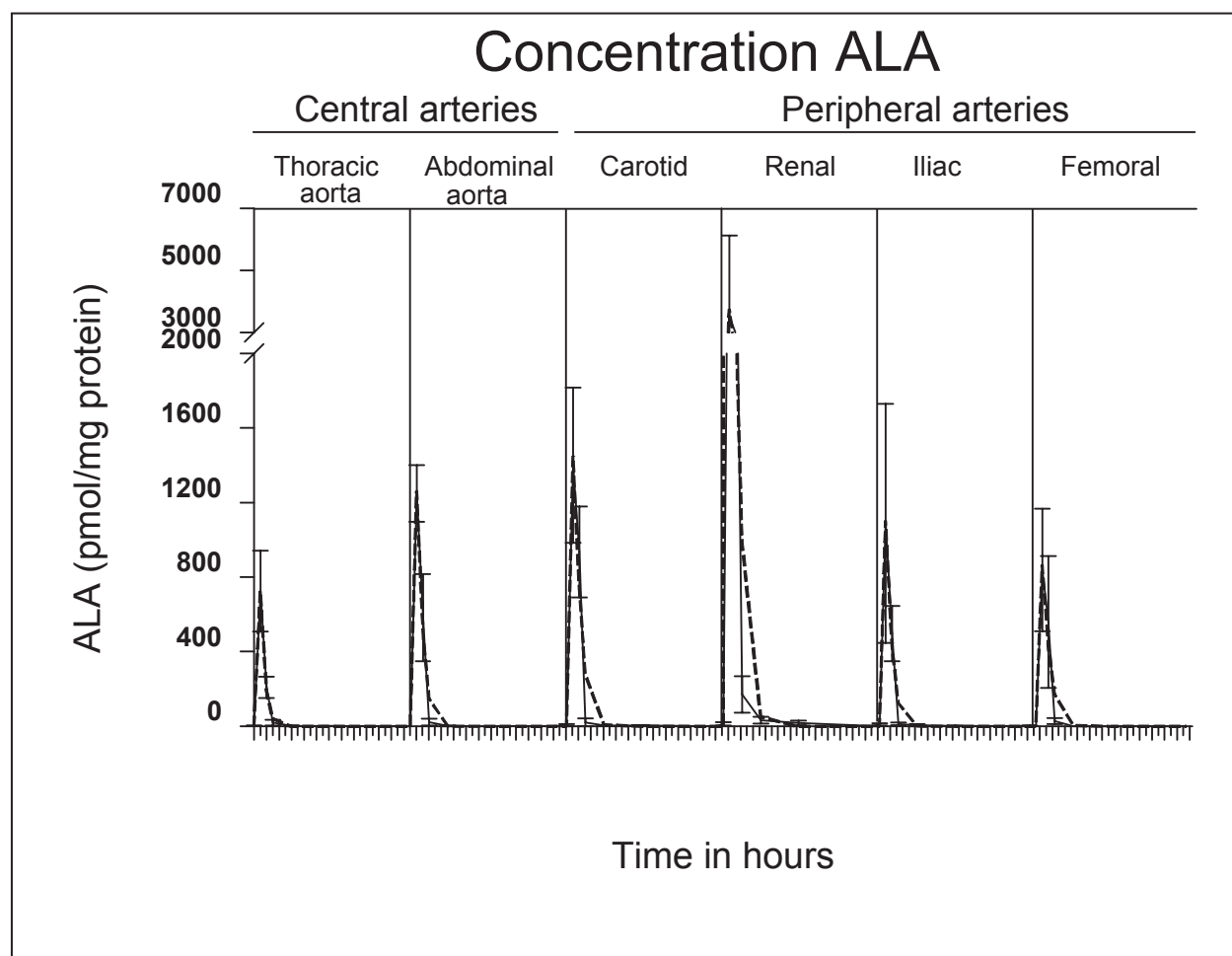


Figure 4.1 Courses of the concentrations of ALA (●), PBG (■) and PpIX (▲) in plasma at various time points after intravenous injection of ALA. Data are means with one standard error.

4.03.2 Courses of the concentrations of ALA and PBG in arteries

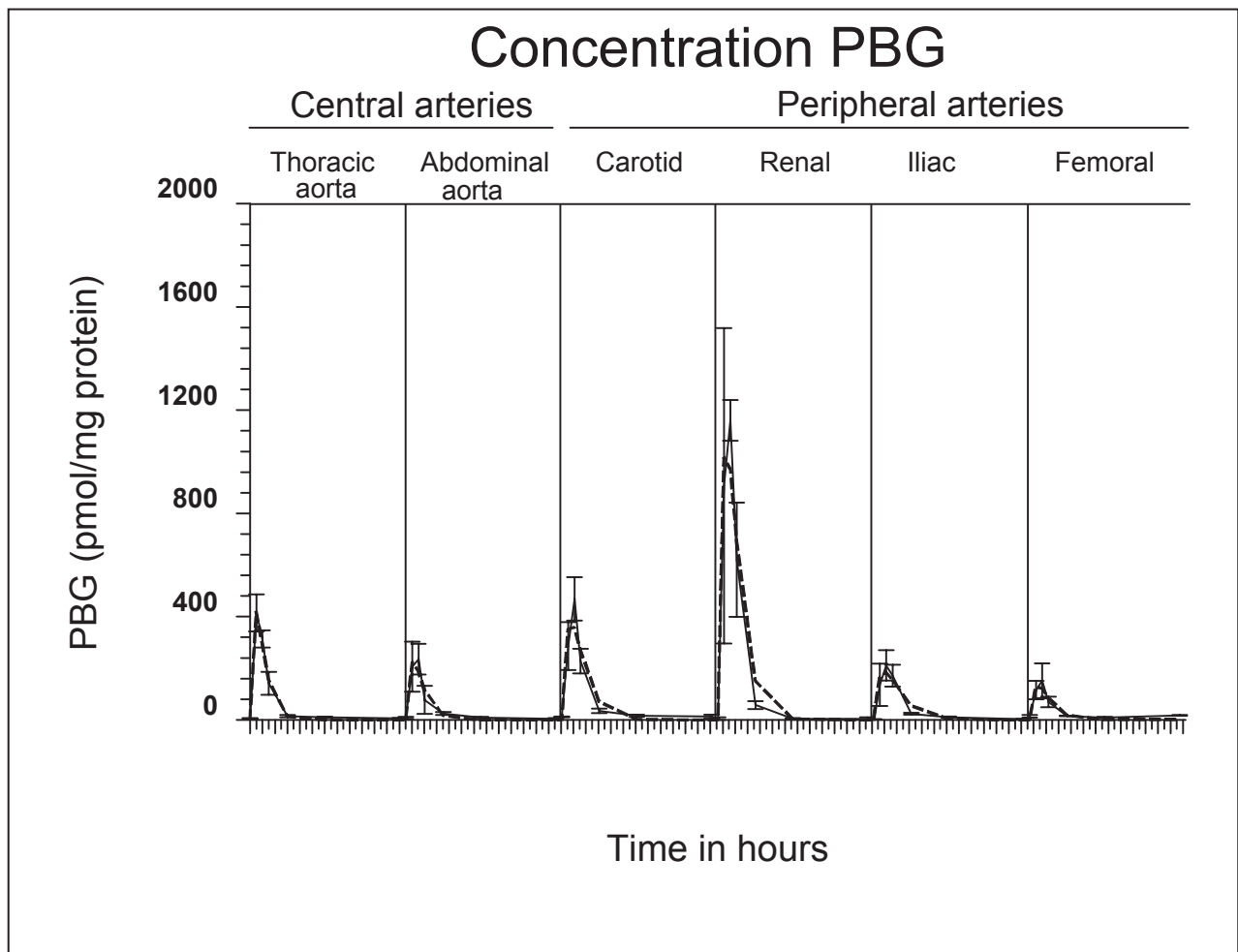
The time at which ALA reached the maximal level was almost similar in central and peripheral arteries <Fig.4.2a>. The same held for PBG <Fig.4.2b>. Of all other arteries, the highest peak concentration of ALA was found in the renal artery ($p < 0.016$). However, the peak concentrations of ALA did not differ significantly between the central and peripheral arteries. The concentration of PBG reached its maximum in all arteries after the peak concentration of ALA. Again, the renal artery showed the highest PBG concentration ($p < 0.007$), but no statistical significant difference was found between the two categories of artery as to the mean peak PBG concentration. Amongst all arteries, the peak concentration of ALA showed a strong, statistically significant association with the peak concentration of PBG ($r = 0.943$; $p = 0.005$).

a.



	Thoracic aorta	Abdominal aorta	Carotid artery	Renal artery	Iliac artery	Femoral artery
<i>C</i> _{max} (pmol/mg protein)	871.1	1290.2	1375	3413.5	1242.7	815.4
SEM	159.3	653.2	556.8	361.9	866	189.7
<i>t</i> _{max} (hr)	0:30	0:37	0:44	0:49	0:37	0:44
SEM	0:12	0:48	0:42	0:36	0:12	0:30
<i>t</i> _{1/2} (hr)	0:21	0:26	0:30	0:34	0:25	0:31

b.



	Thoracic aorta	Abdominal aorta	Carotid artery	Renal artery	Iliac artery	Femoral artery
<i>C</i> _{max} (pmol/mg protein)	377.4	226.7	374.1	1055.9	184.8	134
SEM	72.3	105.7	79.8	95.6	70.5	81
<i>t</i> _{max} (hr)	0:58	1:09	1:29	1:22	1:44	1:20
SEM	0:18	0:24	0:30	0:30	0:36	0:12
<i>t</i> _{1/2} (hr)	0:40	0:47	1:02	0:56	1:13	0:56

4.03.3 Porphyrins in plasma

Plasma contained solely PpIX. The course of PpIX followed first-order kinetics reaching a very small maximum of $0.74 \pm 0.04 \mu\text{mol/L}$ at 4.5 hr after ALA administration <Fig.4.1>. Zinc PpIX and porphyrinogens were not detectable in plasma.

4.03.4 Courses of the concentrations of porphyrins in arteries

The time at which the COPRO(gen) concentration reached its maximum was about similar in the various arteries under study <Fig.4.2c>. Notably, the abdominal aorta did contain the highest COPRO(gen) concentration. The mean peak concentration of COPRO(gen) differed significantly between the two categories of artery ($p=0.025$) being on average a factor of 5.6 higher in the central arteries. With exception of the abdominal aorta, in all arteries PpIX and zinc PpIX were found after ALA administration <Fig.4.2d, 4.2e>. The time-points at which the PpIX \diamond and zinc PpIX concentrations reached their maximum did not differ significantly between the artery types ($p=0.13$ and $p=0.15$, respectively). However, the mean peak PpIX concentration was a factor of 4.2 lower in the central (thoracic and abdominal aorta) than in the peripheral arteries ($p<0.004$) < Fig.4.2d>. If the abdominal aorta was not taken into account, the PpIX concentration of the peripheral arteries remained significantly higher than of the central thoracic aorta ($p<0.05$) <Fig.4.3>. Strikingly, amongst the six different arteries, the peak COPRO(gen) concentrations showed a strong, inverse association with the PpIX concentration ($r=-0.956$; $p=0.003$).

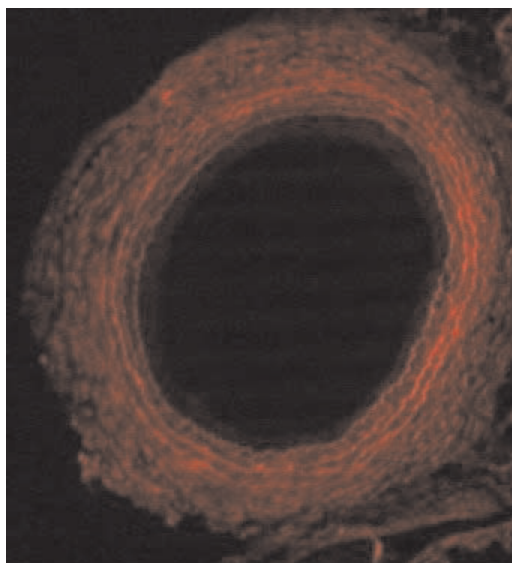
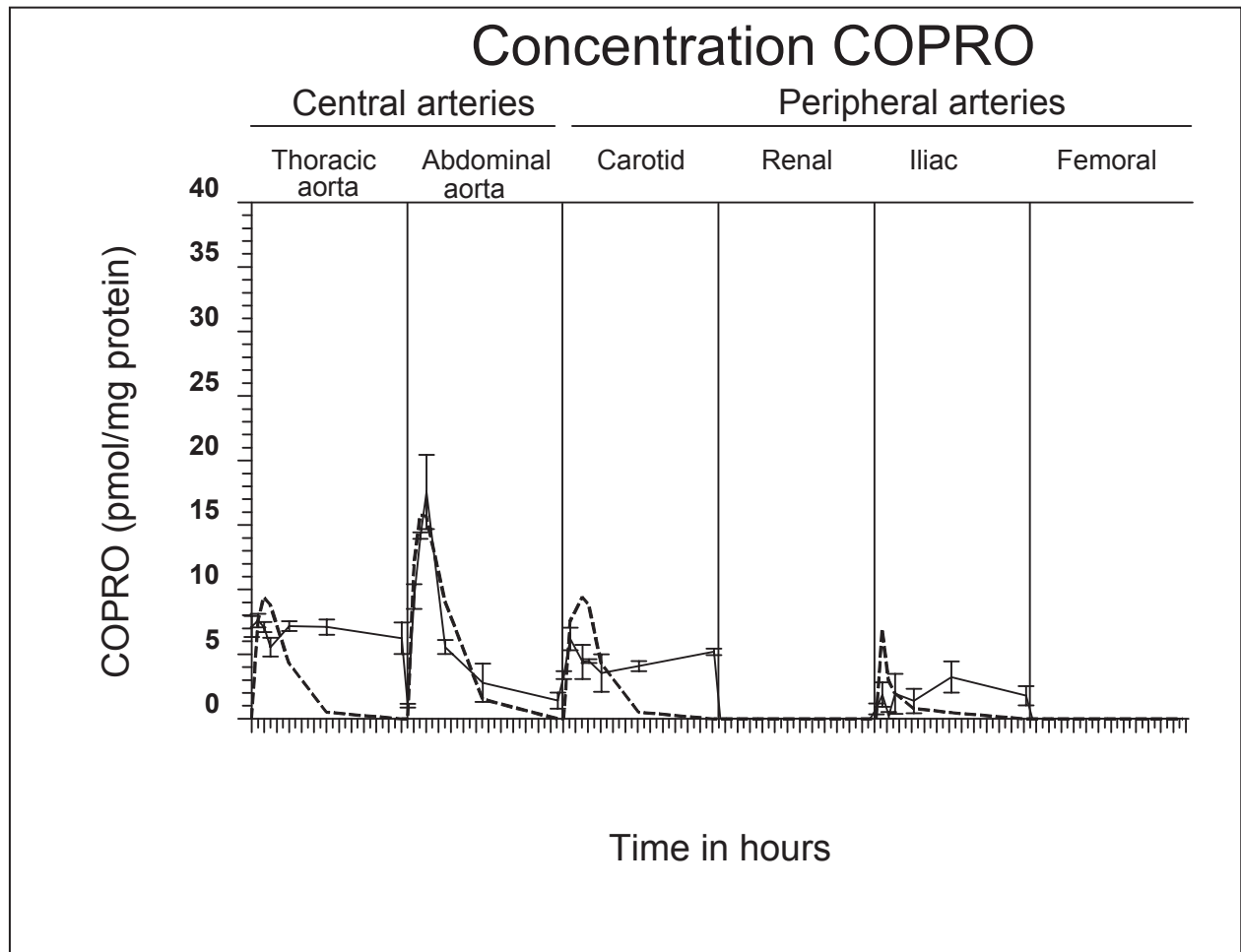


Figure 4.3

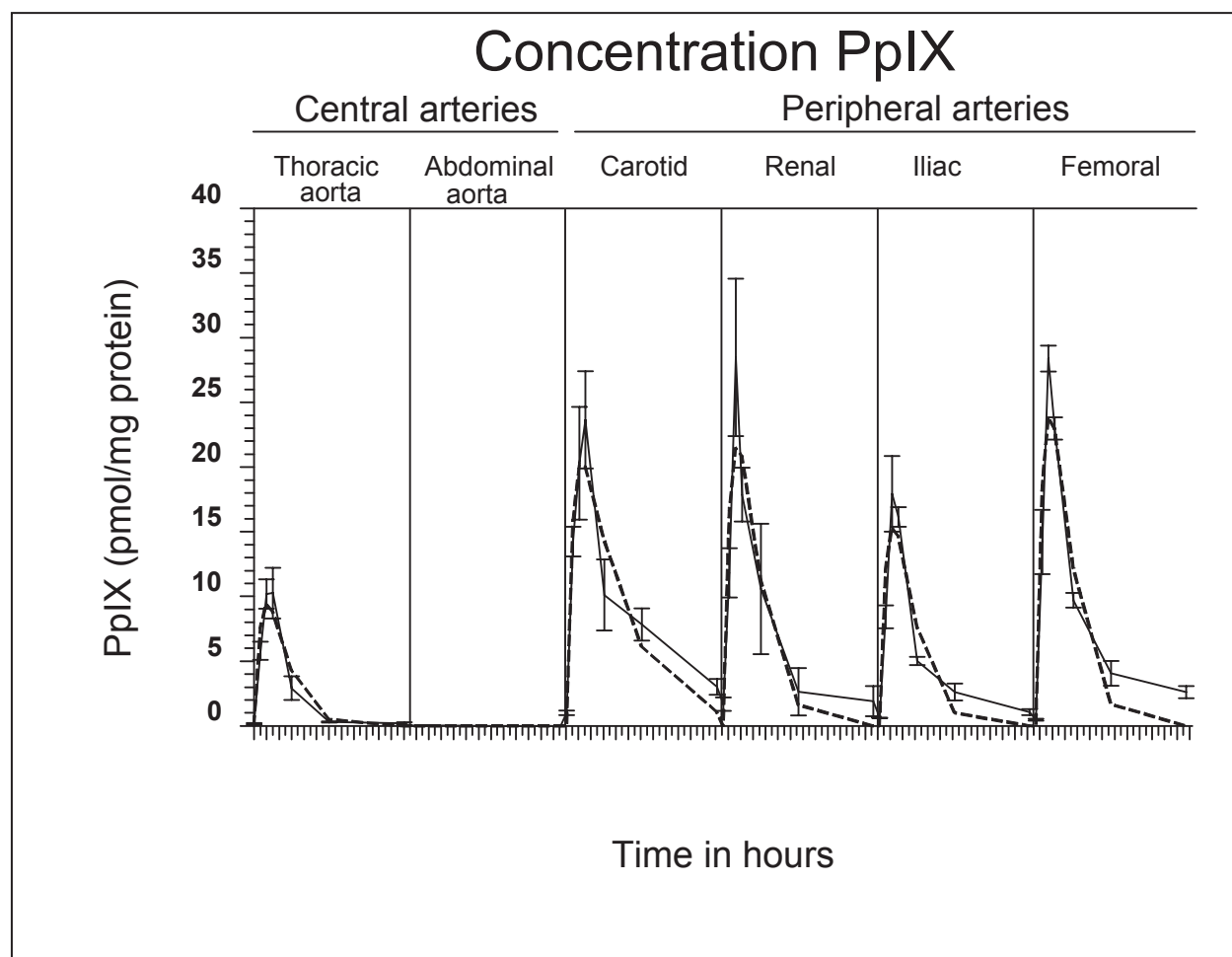
An illustration of the PpIX fluorescence in the iliac artery at 2:30 hours after ALA administration

c.



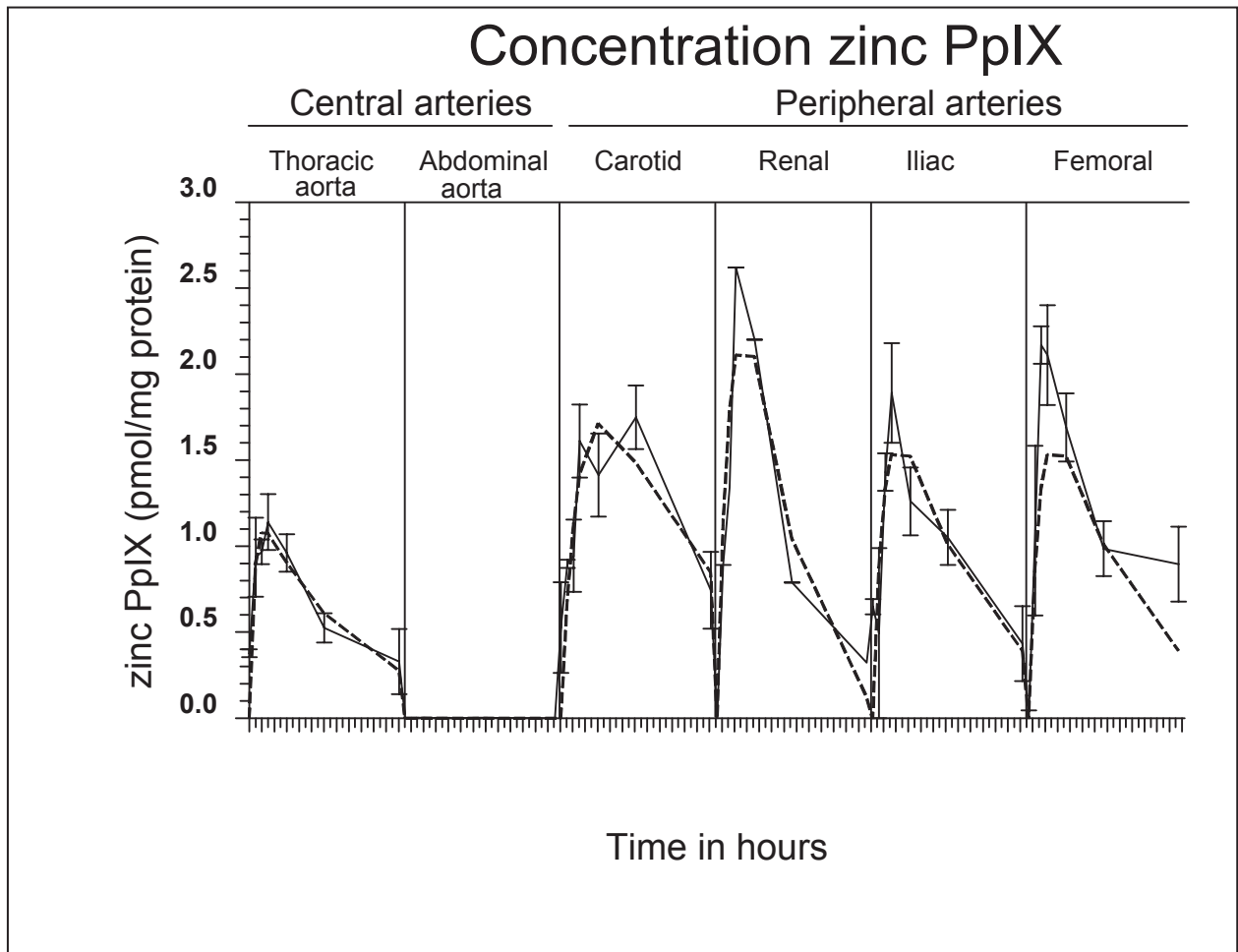
	Thoracic aorta	Abdominal aorta	Carotid artery	Renal artery	Iliac artery	Femoral artery
<i>C</i> _{max} (pmol/mg protein)	9.46	16.05	6.17	0	3.0	0
SEM	0.7	0.2	1.5	0	1.8	0
<i>t</i> _{max} (hr)	2:08	2:26	2:10	0	2:17	0
SEM	-	0:30	-	0	-	0
<i>t</i> _{1/2} (hr)	10:29	1:41	10:23	0	10:35	0

d.



	Thoracic aorta	Abdominal aorta	Carotid artery	Renal artery	Iliac artery	Femoral artery
<i>C</i> _{max} (pmol/mg protein)	9.5	1	20.5	21.7	21.7	24
SEM	0	0	3.0	7.7	13.0	7.5
<i>t</i> _{max} (hr)	2:08	0	2:27	2:18	2:18	2:16
SEM	0:42	0	0:49	0:24	0:24	0:18
<i>t</i> _{1/2} (hr)	1:29	0	4:57	1:35	1:35	1:34

e.



	Thoracic aorta	Abdominal aorta	Carotid artery	Renal artery	Iliac artery	Femoral artery
Cmax (pmol/mg protein)	1.1	0	1.7	2.2	1.6	1.6
SEM	0.6	0	0.9	5.8	1	1
tmax (hr)	2:24	0	6:30	4:18	4:12	4:12
SEM	0:42	0	1:18	0:48	1:06	1:06
t½ (hr)	9:54	0	13:54	3:00	8:48	8:48

Figure 4.2 Diagrams from top to down showing the courses of the concentrations of some components of the heme biosynthetic pathway at 0,1,2,3,6,12 and 24 hr (each tick mark on the abscissa represents 1 hr): a. aminolaevulinic acid (ALA), b. porphobilinogen (PBG), c. coproporphyrin(ogen) (COPROgen), d. protoporphyrin IX (PpIX) and e. zinc protoporphyrin IX (zinc PpIX). Each diagram shows from left to right the concentration courses in the following arteries: the thoracic aorta, abdominal aorta, carotid artery, renal artery, iliac artery and femoral artery. Data are means with one standard error. The predicted data are presented by the dotted line.

4.03.5 The mitochondrial content of the arteries

To find out if the differences in PpIX concentration between the two types of artery were dependent on their mitochondrial mass, we assessed the concentration of the intramitochondrial enzyme citrate synthase in each artery. We found that the citrate synthase content of the various arteries ranged from 0.14 to 2.32 U/mg protein <Table 4.I>. In contrast to the low PpIX concentration of central arteries, the mean citrate synthase concentration of these arteries was about five fold higher ($p=0.002$) than that of the peripheral arteries, i.e., 0.4 (SD: 0.2) and 2.1 (SD: 0.3) U/mg protein, respectively. To further substantiate this difference in mitochondrial mass between the two artery types, as an example we examined the complex I- and II-dependent respiratory chain activity of the thoracic (central) and femoral (peripheral) artery. The results showed that the mean oxygen consumption (in nmol O₂/sec/mg protein) by the thoracic aorta was higher than by the femoral artery, respectively a factor of 2.9 (complex I dependent) and 4.3 (complex II dependent) <Table 4.I>. However, if normalized for the amount of citrate synthase, the respiratory chain activity of both arteries was almost similar <Table 4.I>.

Table 4.I. Mitochondrion-dependent characteristics of various rat arteries

Artery	Citrate synthase (U/mg protein)	Respiratory rate [‡] (nmol O ₂ /sec/mg protein)			
				(nmol O ₂ /sec/U citrate synthase)	
		Complex I	Complex II	Complex I	Complex II
Thoracic aorta	2.32	1.25	6.34	0.54	2.74
Abdominal aorta	1.87				
Carotid artery	0.24				
Renal artery	0.60				
Iliac artery	0.14				
Femoral artery	0.61	0.43	1.49	0.71	2.44

[‡] We determined the respiratory rate in the presence of glutamate and malate (complex I dependent) or succinate (complex II dependent) according to Srere (15). The data were corrected for respiratory state 1.

4.04 Discussion

The aim of this study was to clarify ALA induced PpIX pharmacokinetics in various rat arteries to determine if artery type-dependent differences may play a role in the accumulation of the endogenous photosensitizer PpIX. It is well known that smooth muscle cells produce PpIX from exogenous ALA (4). ALA is normally converted into PpIX in the tissues via PBG, UROgen and COPROgen. This PpIX loses its photosensitivity upon its conversion into heme. However, if excessive amounts of zinc are present, some PpIX will be converted into zinc PpIX that may be photosensitive as well [17].

The results of this study showed that after intravenous injection of ALA, the highest concentration of ALA was found in the wall of the renal artery. However, with exception to the renal artery, the mean peak concentrations of ALA in the central and peripheral arteries were not significantly different.

Furthermore, the time-intervals to reach the peak value did not differ between the various arteries either. Thus, any difference in the formation of PpIX between the artery types cannot be due to a varying availability of the precursor ALA. With regard to the levels of PBG, we measured the highest concentration in the renal artery, but the mean peak concentrations of PBG of the central and peripheral arteries did not differ significantly. PBG peaked in all arteries after at least 1 hr. Noteworthy, the ALA and PBG concentrations in the arterial wall showed synchronous courses. In accordance to earlier reports, the short time interval between the peaks indicates that the zinc-dependent enzyme ALA dehydratase is not rate limiting [18].

Remarkably, the mean peak concentration of COPRO(gen) was significantly higher in the central arteries than the peripheral arteries, and showed a strong inverse association with the peak concentration of PpIX in the various arteries. PpIX was not even detectable in the abdominal aorta and was significantly lower in the thoracic aorta as compared to the peripheral arteries. Apparently, in the central arteries the conversion of COPROgen into PpIX was inhibited. Normally, COPROgen produced in the cytosol is converted first into protoporphyrinogen by coproporphyrinogen oxidase. This enzyme is located in the intermembrane space of the mitochondrion [19,20] and uses oxygen as the only oxidant [21].

Protoporphyrinogen is converted next into PpIX by protoporphyrinogen oxidase that is anchored within the lipid bilayer of the inner membrane of the mitochondrion [22]. Therefore, a simple explanation for the low amounts of PpIX, but high amounts of COPROgen in the central arteries may be that those arteries contain only few mitochondria. The study of Gibson et al. [23], which showed a direct relationship of the mitochondrial content in neoplastic cells to the level of PpIX, supports that assumption. Those authors based their conclusion on the selective, fluorescent probe MitoTracker Green that preferentially accumulates in the lipid membranes of the mitochondrion [24].

In seeming contrast, we found that the mitochondrial mass of central arteries, reflected by the amount of citrate synthase, was high. However, if central arteries contain relatively large mitochondria the fact that the surface to volume ratio of large objects is small may unite the seemingly disagreeing results. In apparent support of this hypothesis, a preliminary morphometric study showed that not only the area of mitochondria of the thoracic aorta was about two times larger than of the femoral artery, amounting to 0.41 (SD: 0.17; n=4) and 0.17 (SD: 0.15; n=10) μm^2 , respectively ($p=0.048$), but the morphology of those mitochondria differed as well <Fig.4.4>.

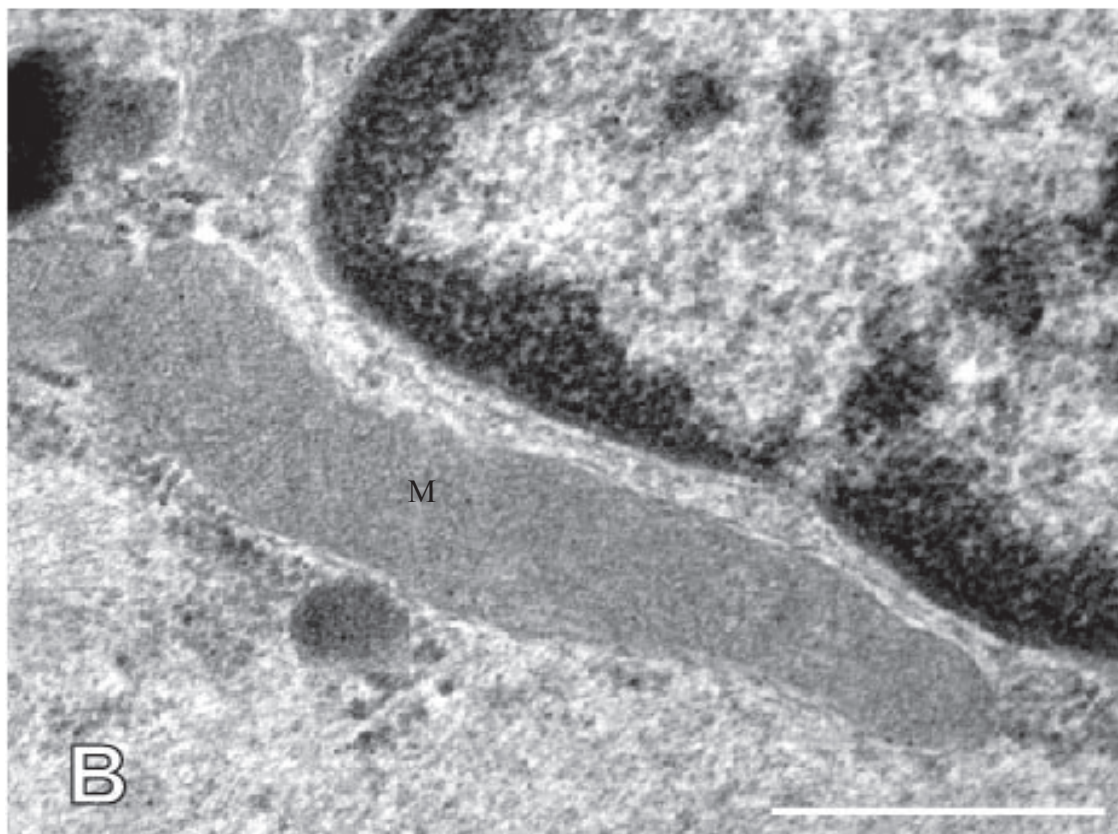
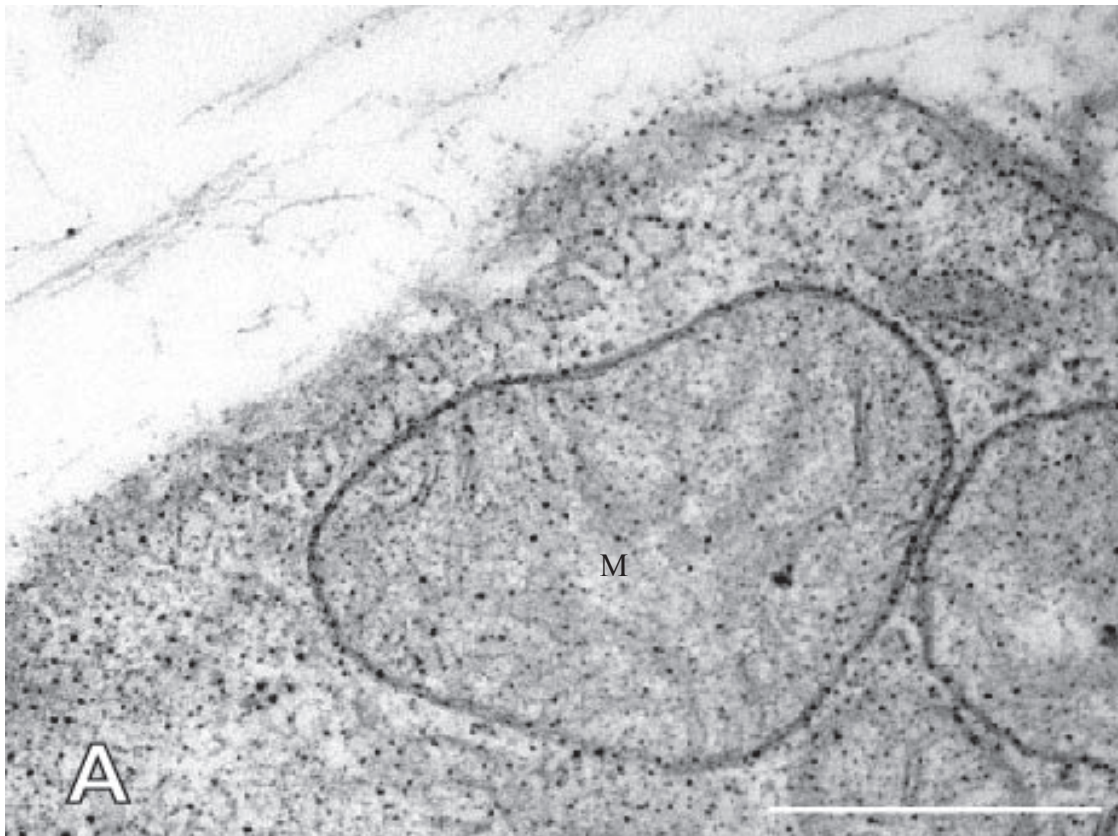


Figure 4.4 Representative electronmicrographs of a mitochondrion (M) in the vascular wall of the thoracic (central)aorta (A) and of the femoral (peripheral) artery (B). Magnification factor: 44 000. The length of the white bars is 500 nm.

Large mitochondria are in a high-energy state [25]. Such mitochondria will not likely accumulate PpIX, because this porphyrin enhances the dissipation of the electrochemical potential gradient across the inner membrane of the mitochondria [26]. However, an alternative explanation of the low PpIX content of central arteries may be a lower coproporphyrinogen oxidase activity in analogy of the imbalance between PBG deaminase and ferrochelatase activities determining the high PpIX concentration of tumor cells [18,27]. Obviously, further study is needed to clarify this issue.

The levels of zinc PpIX and PpIX showed synchronous courses in the arteries under study. Although zinc PpIX is likely photoactive, it will be activated along with PpIX only if the Soret band is used in the treatment, because the shift in the Q-band upon the formation of metalloporphyrins is considerable [28]. However, as shown in the present study, the zinc PpIX levels were only 10% of the PpIX levels and are thus not expected to make a significant contribution to the photodynamic effect.

In the timing of illumination for effective vascular ALA-PDT, the determination of the time-point at which the arterial PpIX content reaches some threshold level seems essential. Iinuma et al. [29] showed for a number of cell lines that a threshold of cellular PpIX is required for PDT-induced cell killing. Cell lines accumulating less than 140 ng PpIX per mg of protein exhibited no phototoxic response. In the present study we have shown that the peak concentrations of PpIX (Mw 562.7) in central arteries varied between 0 and 5.3 ng/mg of protein and in peripheral arteries between 11.5 and 13.5 ng/mg of protein. While the latter PpIX level is about ten times less than the *in vitro* threshold, we recently were able to show that *in vivo* this dose is effective in ALA-PDT of the rat iliac artery to prevent balloon induced intimal hyperplasia [30]. Presently, we do not know if the concentration of PpIX in the central arteries is indeed too low for effective PDT. Nevertheless, these results indicate that more factors beside the PpIX level determine the efficacy of PDT *in vivo*.

In conclusion, ALA accumulation is not artery type dependent, with the exception of the renal artery, but peak concentrations of COPROgen were higher and of PpIX were lower in central compared to peripheral arteries. Central arteries possibly contain relative large mitochondria that are not directed to the synthesis of PpIX. It may be of importance for effective PDT *in vivo* that the time to reach the maximal PpIX level in the peripheral arteries varied between 2:08–2:27 hr.

Acknowledgements

The study was subsidized by the Dutch Heart Foundation Grant 97.181. The authors thank Dr. Felix de Rooy for his hospitality to perform part of this study in his laboratory, Dr. Paul Mulder and Dr. Jan Danser for their advice in the statistical analyses, Anne de Munck for skillful technical assistance and Piet van de Heul for performing the electronmicroscopy.

References

- [1] Bauters, C., T. Meurice, M. Hamon, E. McFadden, J. M. Lablanche, and M. E. Bertrand (1996) Mechanisms and prevention of restenosis: from experimental models to clinical practice. *Cardiovasc. Res.* 31, 835-846.
- [2] Kennedy, J. C. and R. H. Pottier (1992) Endogenous protoporphyrin IX, a clinically useful photosensitizer for photodynamic therapy. *J. Photochem. Photobiol. B* 14, 275-292.
- [3] Grant, W. E., P. M. Speight, A. J. MacRobert, C. Hopper, and S. G. Bown (1994) Photodynamic therapy of normal rat arteries after photosensitisation using disulphonated aluminium phthalocyanine and 5-aminolaevulinic acid. *Br. J. Cancer* 70, 72-78.
- [4] Nyamekye, I., S. Anglin, J. McEwan, A. MacRobert, S. Bown, and C. Bishop (1995) Photodynamic therapy of normal and balloon-injured rat carotid arteries using 5-amino-levulinic acid. *Circulation* 91, 417-425.
- [5] Jenkins, M. P., G. A. Buonaccorsi, M. Raphael, I. Nyamekye, J. R. McEwan, S. G. Bown, and C. C. Bishop (1999) Clinical study of adjuvant photodynamic therapy to reduce restenosis following femoral angioplasty. *Br. J Surg.* 86, 1258-1263.
- [6] Fingar, V. H. (1996) Vascular effects of photodynamic therapy. *J Clin. Laser Med. Surg.* 14, 323-328.
- [7] Horsman, M. R. and J. Winther (1989) Vascular effects of photodynamic therapy in an intraocular retinoblastoma-like tumour. *Acta Oncol.* 28, 693-697.
- [8] Jenkins, M. P., G. Buonaccorsi, A. MacRobert, C. C. Bishop, S. G. Bown, and J. R. McEwan (1998) Intra-arterial photodynamic therapy using 5-ALA in a swine model. *Eur. J. Vasc. Endovasc. Surg.* 16, 284-291.
- [9] Ortu, P., G. M. LaMuraglia, W. G. Roberts, T. J. Flotte, and T. Hasan (1992) Photodynamic therapy of arteries. A novel approach for treatment of experimental intimal hyperplasia. *Circulation* 85, 1189-1196.
- [10] van den Boogert J., R. van Hillegersberg, F. W. de Rooij, R. W. de Bruin, A. Edixhoven-Bosdijk, A. B. Houtsmuller, P. D. Siersema, J. H. Wilson, and H. W. Tilanus (1998) 5-Aminolaevulinic acid-induced protoporphyrin IX accumulation in tissues: pharmacokinetics after oral or intravenous administration. *J. Photochem. Photobiol. B* 44, 29-38.
- [11] Hinnen, P., F. W. de Rooij, G. Voortman, H. W. Tilanus, J. H. Wilson, and P. D. Siersema (2000) Acrylate yellow filters in operating lights protect against photosensitization tissue damage. *Br. J. Surg.* 87, 231-235.
- [12] Lowry, O. H., N. J. Rosebrough, A. L. Farr, and R. J. Randall (1951) Protein measurement with the folin phenol reagent. *J. Biol. Chem.* 193, 265-275.
- [13] van Hillegersberg, R., J. W. van den Berg, W. J. Kort, O. T. Terpstra, and J. H. Wilson (1992) Selective accumulation of endogenously produced porphyrins in a liver metastasis model in rats. *Gastroenterology* 103, 647-651.
- [14] Ritschel, W. A. (1980) Pharmacokinetics of single dose administration. In *Handbook of basic pharmacokinetics*. pp. 230-247. Drug Intelligence Publications Inc., Hamilton, Ill, USA.
- [15] Srere, P. A. (1969) Citrate synthase. *Meth. Enzymol.* 13, 3-11.
- [16] Haller, T., M. Ortner, and E. Gnaiger (1994) A respirometer for investigating oxidative cell metabolism: toward optimization of respiratory studies. *Anal. Biochem.* 218, 338-342.
- [17] Greenbaum, N. L. and A. Kappas (1991) Comparative photoactivity of tin and zinc porphyrin inhibitors of heme oxygenase: pronounced photolability of the zinc compounds. *Photochem. Photobiol.* 54, 183-192.

- [18] van den Boogert J., A. B. Houtsmuller, F. W. de Rooij, R. W. de Bruin, P. D. Siersema, and R. van Hillegersberg (1999) Kinetics, localization, and mechanism of 5-aminolevulinic acid-induced porphyrin accumulation in normal and Barrett's-like rat esophagus. *Lasers Surg. Med.* 24, 3-13.
- [19] Elder, G. H. and J. O. Evans (1978) Evidence that the coproporphyrinogen oxidase activity of rat liver is situated in the intermembrane space of mitochondria. *Biochem. J.* 172, 345-347.
- [20] Grandchamp, B., N. Phung, and Y. Nordmann (1978) The mitochondrial localization of coproporphyrinogen III oxidase. *Biochem. J.* 176, 97-102.
- [21] Yoshinaga, T. and S. Sano (1980) Coproporphyrinogen oxidase. I. Purification, properties, and activation by phospholipids. *J. Biol. Chem.* 255, 4722-4726.
- [22] Deybach, J. C., V. da Silva, B. Grandchamp, and Y. Nordmann (1985) The mitochondrial location of protoporphyrinogen oxidase. *Eur. J. Biochem.* 149, 431-435.
- [23] Gibson, S. L., M. L. Nguyen, J. J. Havens, A. Barbarin, and R. Hilf (1999) Relationship of delta-aminolevulinic acid-induced protoporphyrin IX levels to mitochondrial content in neoplastic cells in vitro. *Biochem. Biophys. Res. Commun.* 265, 315-321.
- [24] Keij, J. F., C. Bell-Prince, and J. A. Steinkamp (2000) Staining of mitochondrial membranes with 10-nonyl acridine orange, MitoFluor Green, and MitoTracker Green is affected by mitochondrial membrane potential altering drugs. *Cytometry* 39, 203-210.
- [25] Muscatello, U., V. Guarriera-Bobyleva, and P. Buffa (1972) Configurational changes in isolated rat liver mitochondria as revealed by negative staining. II. Modifications caused by changes in respiratory states. *J. Ultrastruct. Res.* 40, 235-260.
- [26] Romslo, I. and P. Husby (1980) Iron, porphyrin and heme transport in mitochondria. *Int. J. Biochem.* 12, 709-712.
- [27] Hinnen, P., F. W. de Rooij, M. L. van Velthuysen, A. Edixhoven, R. van Hillegersberg, H. W. Tilanus, J. H. Wilson, and P. D. Siersema (1998) Biochemical basis of 5-aminolaevulinic acid-induced protoporphyrin IX accumulation: a study in patients with (pre)malignant lesions of the oesophagus. *Br. J. Cancer* 78, 679-682.
- [28] Garbo, G. M. (1996) Purpurins and benzochlorins as sensitizers for photodynamic therapy. *J. Photochem. Photobiol. B* 34, 109-116.
- [29] Iinuma, S., S. S. Farshi, B. Ortel, and T. Hasan (1994) A mechanistic study of cellular photodestruction with 5-aminolaevulinic acid-induced porphyrin. *Br. J. Cancer* 70, 21-28.
- [30] Gabeler, E., R. van Hillegersberg, R. G. Stadius van Eps, W. Sluiter, P. Mulder, and H. van Urk (2002) Endovascular photodynamic therapy with aminolaevulinic acid prevents balloon induced intimal hyperplasia and constrictive remodelling. *Eur. J. Vasc. Endovasc. Surg.* 24, 322-331.

SECTION IV

CHAPTER 5

The Effect of Endovascular Photodynamic Therapy on the Normal Rat Iliac Artery

¹Edward E. E. Gabeler, ¹Richard van Hillegersberg, ¹Randolph G. Stadius van Eps, ²Wim Sluiter, ¹Hero van Urk

¹Department of Surgery, Erasmus MC, Rotterdam, The Netherlands

²Department of Biochemistry, Erasmus MC, Rotterdam, The Netherlands

Keywords: ALA, photodynamic therapy, restenosis, arteries

submitted

Abbreviations: ALA. Aminolaevulinic acid, FO. Fiber only, IH. Intimal hyperplasia, LO. Light only, PDT. Photodynamic therapy, PpIX. Protoporphyrin IX

5.00 Abstract

Background: PDT can prevent the development of intimal hyperplasia (IH) and negative remodelling after angioplasty. The effect of PDT on the adjacent normal artery may influence the treatment outcome. Therefore, we assessed the vascular geometry in time after endovascular PDT at varying light doses in the normal artery.

Materials & Methods: Rats were subdivided into experimental, reference and baseline groups. The experimental PDT groups were illuminated with 12.5, 25, 50 or 100 J/cm diffuser length (dl). The reference light only (LO) groups animals underwent illumination. The fiber only (FO) groups served as baseline control. Histogeometric analysis was performed after 2hrs, 4 and 16 weeks.

Results: After 16 weeks, a thin layer of IH had developed (0.01-0.02 mm²) in the PDT groups, whereas no IH had developed in the LO and FO groups (p<0.05). The medial area size was increased (0.05±0.03 mm²) in the PDT groups at 12.5, 25 and 50 J/cm and in the LO and FO groups (0.09±0.02 mm²). In the PDT groups, a fluence of 12.5-25 J/cm dl resulted in partial transient medial acellularity while at 50-100 J/cm dl complete transient medial acellularity occurred. After 16 weeks, the media was completely repopulated and did not show constriction. The maximal lumen diameter (MLD) in the PDT groups was comparable with the LO and FO groups.

Conclusion: PDT of the normal iliac artery induced a transient medial acellularity and minor IH development. As the normal lumen diameter was preserved, no consistent adverse effects of PDT to adjacent normal vessel are expected.

5.01 Introduction

Endovascular photodynamic therapy (PDT) is a new treatment modality for the prevention of vascular restenosis following surgical interventions or percutaneous transluminal angioplasty. PDT is based on the generation of high amounts of the oxidising singlet oxygen after light activation of an accumulated light sensitive substrate (photosensitization) in the target cells [1-3].

This treatment-modality aims at the inhibition of fibrocellular induced arterial constriction (restenosis) by killing of activated arterial cells and deactivating cytokines bound to the subcellular matrix. Successful intermediate-term results after PDT have been described, but varying in long-term success rates exist [4-6]. Only two reports described the importance of the normal arterial response to aminolaevulinic acid (ALA)-based PDT, but used external illumination, various light-dosimetry and various arteries [4-5]. Local cytotoxicity after external PDT in combination with balloon angioplasty has also been reported [7]. Because the response of the adjacent healthy part of the artery to PDT may have an impact on the outcome of treating the adjacent lesion area [8], which is of clinical importance, we examined the effect of endovascular PDT and fiber-insertion in normal iliac arteries in a rat model.

5.02 Materials & methods

The experimental protocol was approved by The Committee on Animal Research of the Erasmus University of Rotterdam and complied with “Principles of Good Laboratory Practice”. Male inbred Wistar rats (Harlan CPB, Austerlitz, The Netherlands) weighing 200-300 g were used. The animals had free access to rat chow (AM II, Hope Farms, Woerden, The Netherlands) and tap water acidified to pH 4.0, while maintained in a standard 12-hour light/dark cycle.

5.02.1 Study design

A hundred and eight rats were randomly assigned to respectively the experimental PDT, reference Light Only (LO) groups or baseline fiber only (FO) group. Both PDT and LO groups underwent a fiber-introduction in the right common iliac artery, and were subdivided into their corresponding illumination parameters (n=4 per fluence parameter), 12.5, 25, 50 and 100 J/cm diffuser length (dl). In the PDT-group (n=48), δ -Aminolaevulinic Acid (ALA) was administered 2 ½ hours before illumination. The LO-groups were only illuminated (LO: n=48). In the FO (n=12) group only a fiber was inserted. The animals were sacrificed 2 hours after the procedure, 4 or 16 weeks later.

5.02.2 Photosensitization

The PDT groups received intravenous 200 mg/ kg ALA (Sigma-Aldrich Chemie, Zwijndrecht, The Netherlands) dissolved in phosphate buffered saline (PBS, Merck) of pH 7.45 at 40 mg/ml. The solution was freshly made for each animal and kept from light exposure. The photosensitized rats were kept in the dark 2 ½ hours prior to surgery and 12 hours after surgery to prevent photosensitivity. The time interval after ALA administration is based on a previous study, where it was found that at that time-point the accumulation of the photosensitive protoporphyrin IX (PpIX) became maximal [9].

5.02.3 Laser

A dye laser (600 Series Dye Module, Laserscope, Surgical Systems, San Jose, CA, USA), pumped by a 532 KTP surgical laser (Laserscope, Surgical Systems, San Jose, CA, USA), was used to generate monochromatic light of 633 nm. The power emitted from the cylindrical diffusing tip (core diameter 200 μm , outer diameter 1.0 mm, tip length 20 mm: LightsticTM, Cardiofocus, West Yarmouth, MA, USA) <Fig.5.1> [10] was calibrated with an in-built power meter, and verified with an external linear diffuser in an integrating cylindrical sphere (Optometer Model 370, Graseby Optronics, Orlando, FL, USA). A spectroscope (WaveMate, Coherent, Auburn, CA, USA) was used to verify the accuracy of the wavelength.

Temperature

The real-time temperature during endovascular PDT was checked at a fluence of 100 J/cm dl using an irradiance of 100 mW/cm dl. Fiber-optic thermosensors with a diameter of 0.5 mm were coupled to a Luxtron thermometry unit (Luxtron Corp., Santa Clara, CA, USA) and were approximated parallel to the laser fiber both outside the artery at an axial distance of 10 mm in the fiber tip. The temperature was determined every second and stored using a computer.

Linear fluence calibration with an isotropic probe

The linear fluence of 100 J/cm dl from the cylindrical diffuser in the arterial wall was measured at an irradiance of 100 mW/cm dl (illumination time of 1000 seconds). An isotropic probe was approximated parallel to the laser fiber outside the artery at axial distances of 10 mm from and 0, 10 and 20 mm in the fiber tip.

5.02.4 Surgical technique

A median laparotomy was performed under general anaesthesia with intramuscular injection of ketamine (Ketalar, Parke Davis and Co., Inc., 40 mg/kg) and xylazin (Rompun Bayer Ag, Leverkusen, Germany; 5 mg/kg). Subdued light using a yellow filter (620-650 nm Kodak) was applied during the procedure [11]. The right common iliac artery was cranially and caudally temporarily occluded with vascular clamps (Haemostat B1, Stöpler, Utrecht, The Netherlands). To create a blood free lumen, the artery was flushed with 1.0-ml heparin (50 IU/ml 0.9% NaCl, Infusion solution Baxter) through an arteriotomy 5 mm cranially from the abdominal aortal bifurcation. Hereafter, the clamps were removed. Reperfusion of the treated section was observed directly after flushing with heparin and two layer closing (interrupted 9-0 prolene sutures). The abdominal wall was closed in two layers (continuous 2-0 prolene sutures).

5.02.5 Endovascular Photodynamic Therapy (PDT)

A 400 μm fiber (Lightstic 360, Rare Earth Medical Inc., West Yarmouth, MA, USA) with a 20 mm long cylindrical diffusing tip was applied. The fiber tip was centred endovascularly to illuminate 20 mm <Fig.5.1>. Because of the cylindrical illumination, the fluence rate was expressed in Joule per cm diffuser length (J/cm dl). The target area was illuminated at 100 mW/cm dl. After treatment, the lumen was thoroughly flushed with 1ml heparin (50 IU/ml). Abdominal organs were protected from light exposure with a light absorbing plastic folium during illumination. The animals recovered in subdued light after treatment.

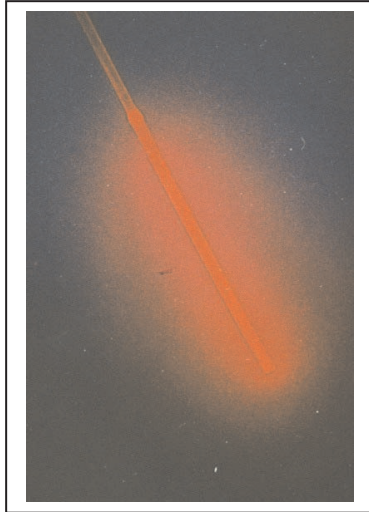


Figure 5.1 A photograph of the laser fiber at the target area illustrating the illuminated segment.

5.02.6 Specimen handling

A standard perfusion-fixation procedure via the thoracic aorta was performed under ether anaesthesia, in which the lumen was flushed with PBS for 2 min, followed by a 10-min perfusion with formaldehyde (3.7%) at 100 mm Hg. The distally marked segment of 20 mm was carefully harvested after length measurement and stored in formaldehyde (3.7%) for at least 24 hours. Thereafter, the specimens were embedded in paraffin.

Three cross sections of 10 μm each were cut with a microtome from distal to proximal at 3, 5 and 10 mm, mounted on a microscopic object glass and stained with haematoxylin and eosin for conventional light microscopy. All mounted sections were video taped with a digital camera for geometrical analysis. A digital video analyser system (IBM Corp., Boca Raton, USA) was used for the assessment of the absolute intimal and medial area in mm^2 [12]. Intimal hyperplasia (IH) was defined as the area of the cell layer between the lumen and the internal elastic lamina. The medial area was defined as the area between the internal and external elastic lamina (EEL). The maximal lumen diameter (MLD in mm) was measured to evaluate arterial remodelling. Asymmetry was corrected by using the perimeter ($D = \text{circumference} / \pi$) assuming a circular configuration to calculate the MLD.

5.02.7 Statistics

The area of IH, the tunica media and MLD were expressed as mean \pm standard error of the mean (SEM). Comparisons were made using the Student's T-test. A difference was considered to be significant at P-values less than 0.05.

5.03 Results

In 2 rats diarrhoea occurred during 2 days after PDT 50 J/cm dl. Other animals appeared healthy, without significant weight loss during the study. No skin photosensitivity reactions were noted in the rats exposed after PDT. All right common iliac arteries were patent at harvesting. All sutured arteriotomies were covered with peri-adventitial fat and adjacent lymph nodes. No aneurysms were noted. During the PDT procedure, the vessel temperature of 33.5 ± 0.18 $^{\circ}\text{C}$ (n=4 at 100 J/cm dl) and the room temperature of 20.1 ± 1.9 $^{\circ}\text{C}$ did not increase. Our previous study showed that the linear fluence in the vascular wall at the applied irradiances matched with the output (100 to 110 %) without loss or significant backscatter interference [13].

5.03.1 Histological and Morphological Analysis

5.03.1.1 Histology

No histological and morphological abnormalities were found in the FO, LO 12.5, 25, 50 and 100 J/cm dl group at 0, 4 and 16 weeks. Ruptures of the arterial wall were not seen microscopically in the PDT and LO groups. Inflammation in the tunica intima and tunica media was microscopically absent in all groups. LO at 12.5, 25, and 50 J/cm dl, did not affect the appearance of SMC's in the media. However, directly after illumination with 100 J/cm dl superficial SMC eradication was seen. PDT at 12.5 and 25 J/cm dl showed partial cellular eradication of the media. Immediately after illumination with 50 and 100 J/cm dl the media was found acellular in the PDT groups. Endothelial cells also disappeared. The media was completely repopulated after 16 weeks.

5.03.1.2 Histo-geometry of the intima

No IH was seen 2 hours after PDT. Sporadic IH developed during the following 16 weeks in all PDT treated groups ($p < 0.05$) (12.5 J/cm dl: $0.01 \pm 0.007 \text{ mm}^2$; 25 J/cm dl: $0.02 \pm 0.007 \text{ mm}^2$; 50 J/cm dl: $0.01 \pm 0.006 \text{ mm}^2$ and 100 J/cm dl: $0.02 \pm 0.009 \text{ mm}^2$), whereas no IH developed in the LO groups. IH development in the PDT groups was not significantly different than in the LO groups.

5.03.1.3 Histo-geometry of the media

In none of the groups immediately following LO or PDT any significant changes of the medial area were seen in comparison with FO (mean medial area $0.12 \pm 0.02 \text{ mm}^2$) <Fig.5.2a>. At 4 weeks, the medial area of the LO groups was not significantly different <Fig.5.2b> and not higher than at immediately after treatment <Fig.5.2a>. PDT treatment tended to increase the medial area at fluences of 25 J/cm dl and higher <Fig.5.2b>, but these increases did not reach statistical significance. Another 12 weeks later, the medial area did not change significantly after PDT at 100 J/cm dl compared to the LO and FO groups. However, the medial area was significantly higher than at immediately after treatment in the PDT groups at lower fluences, (12.5: $0.17 \pm 0.03 \text{ mm}^2$ $p < 0.02$; 25: $0.20 \pm 0.05 \text{ mm}^2$ $p < 0.02$; 50: $0.19 \pm 0.04 \text{ mm}^2$ $p < 0.01$) and LO groups (12.5: $0.26 \pm 0.03 \text{ mm}^2$ $p < 0.004$; 25: $0.18 \pm 0.03 \text{ mm}^2$ $p < 0.03$; 50: $0.21 \pm 0.02 \text{ mm}^2$ $p < 0.001$; 100: $0.18 \pm 0.01 \text{ mm}^2$ $p < 0.01$) <Fig.5.2c>.

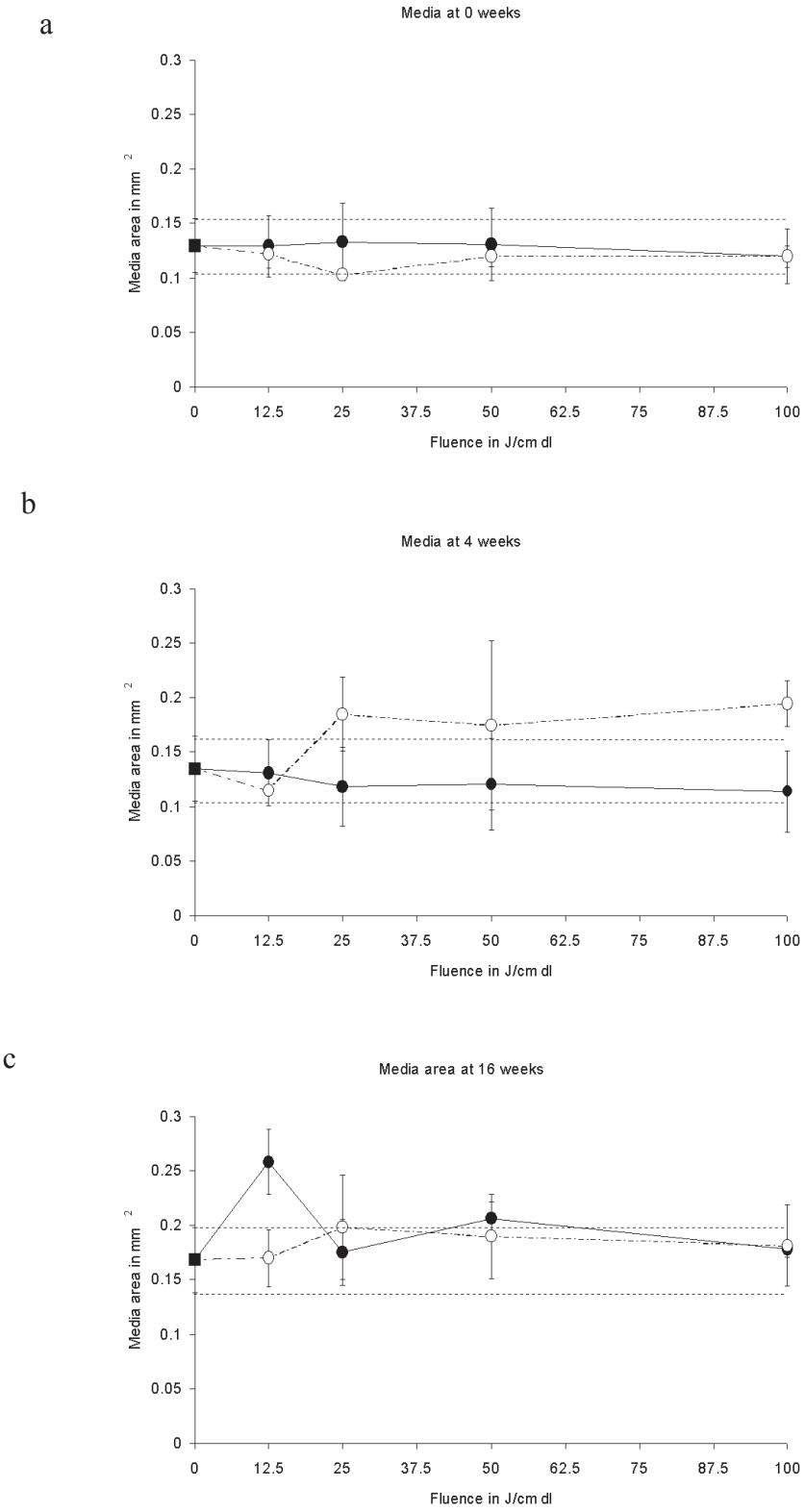


Figure 6.2 Diagrams a,b,c representing the mean media area at 0, 4 and 16 weeks in the LO(●) and PDT(O)groups.

5.03.1.4 Histogeometry of the lumen and the vessel wall

Compared to the FO (MLD: 0.82 ± 0.05 mm), no significant changes in the maximal lumen diameter (MLD) between the PDT groups and the LO groups were seen immediately after the procedure. However, 16 weeks after PDT the MLD increased significantly at 12.5 (1.11 ± 0.13 mm $p < 0.04$) and 50 J/cm dl (1.17 ± 0.06 mm $p < 0.02$) and at 12.5 (1.23 ± 0.23 mm $p < 0.01$), 50 (1.10 ± 0.14 mm $p < 0.05$) and 100 J/cm dl (1.10 ± 0.05 mm $p < 0.01$) in the LO groups compared to 0 weeks. The MLD did not change significantly after 16 weeks in the FO (MLD 0: 0.96 ± 0.10 mm; 16: 1.02 ± 0.45 mm $p < 0.80$), the PDT 25 J/cm dl (16: 1.18 ± 0.09 mm $p < 0.33$), PDT 100 J/cm dl (16: 1.09 ± 0.21 mm $p < 0.80$), FO (16: 1.02 ± 0.45 mm $p < 0.80$) and LO 25 J/cm dl (16: 1.01 ± 0.11 mm $p < 0.58$).

5.04 Discussion

In this study, the aim was to gain insight in the effect of endovascular PDT on the normal iliac artery of the rat. Histo-geometric analysis was used to evaluate the endovascular PDT effect compared to light application only. It was found that endovascular PDT with low fluences of either 12.5-25 J/cm dl resulted in partial media eradication, whereas high fluences of 50-100 J/cm dl (irradiance: 100 mW/cm dl) resulted in complete media eradication in the healthy iliac artery. Remarkably, despite the complete cellular eradication of the media in the PDT groups with high fluences the blood vessels under study were capable to maintain the vascular haemodynamics without long-term constriction. The minimal threshold of endovascular light dose to obtain complete acellularity of the media was 50 J/cm dl at 100 mW/cm dl.

Indeed, early reports described fluences of 50 (at 100-180 mW/cm²), 100 (at 150 mW/cm²) and 250 J/cm² (at 150 mW/cm²) to be effective external light doses [4-5]. An important difference between the previous reports and our study is that they used external illumination and more importantly, higher fluence rates. Indeed, it has been reported that the fluence rate is a more important determinant in the eradication of cells than the total fluence [18]. This may explain the permanent (6 months) flaccid acellularity [4-5], while under the present conditions we found that the media always repopulated within 16 weeks in all endovascular PDT treated arteries combined with patchy intimal hyperplasia (IH).

Apparently, under the latter conditions PDT did not promote cross-linking of the extra cellular matrix proteins as shown by Van Eps et al preventing the influx of smooth muscle cells into the media. In the low fluence light only groups the media was not affected. However, selective cytotoxicity of the medial cells can also be obtained by high light only doses. It is not unlikely that some protoporphyrin IX (PpIX) is present in the cells and function as endogenous photosensitizer underlying the light only effect on the vascular wall. Indeed, early PpIX-based PDT reports using external illumination support the increased effective depth due to the stimulated accumulation of PpIX [14] compared to the application external light only [15].

With regard to remodelling as the putative cause of long-term constriction [16;17], we found that endovascular PDT of the media with fluences of 12.5, 25 and 50 J/cm dl resulted in a media area increase after 16 weeks. No change of the media area was seen in the PDT group with 100 J/cm dl. Also in the light-only group, fluences of 12.5, 25, 50 and 100 J/cm dl showed a medial increase after 16 weeks. Those increases in medial area could have a negative effect on the diameter of the lumen. However, no significant changes of the maximum lumen diameter (MLD) in time were seen in all groups. Rather, a tendency to a beneficial increased MLD was observed in the PDT and high light only groups.

An important mechanism in the normal vascular healing response to injury is the balanced effect of numerous growth factors, cytokines and other mediators orchestrating an

adequate compensation to the vascular damage to maintain the vascular haemodynamics and to prevent a future event [19]. Endovascular ALA-based PDT is a promising tool to modulate this balance.

In conclusion, it was found that PpIX-based endovascular PDT of normal rat iliac arteries only caused a transient acellularity of the tunica media. This phenomenon did not affect the patency of the blood vessel and appeared even to be beneficial with respect to the MLD in long-term.

Acknowledgements

This study was subsidised by the Dutch Heart Foundation (project grant NHS 97.181). The authors are grateful to Mrs. Elma Gussenhoven PhD and Mr. Jan Honkoop for expert technical assistance with the geometric analysis, Ms. Patricia Lobe and Ms. Manon Holtman for excellent preparation of the cross-sections.

References

- [1] Stadius van Eps RG, Adili F, LaMuraglia GM. Photodynamic therapy inactivates cell-associated basic fibroblast growth factor: a silent way of vascular smooth muscle cell eradication. 1997. *Cardiovasc Res*; 35(2):334-340.
- [2] Stadius van Eps RG, Adili F, Watkins MT, Anderson RR, LaMuraglia GM. Photodynamic therapy of extracellular matrix stimulates endothelial cell growth by inactivation of matrix-associated transforming growth factor-beta. 1997. *Lab Invest*; 76(2):257-266.
- [3] Gabeler EEE, van Hillegersberg R, Stadius van Eps RG, Sluiter W, Verbakel CAE, van Urk H. The effect of photodynamic therapy on reendothelialization after balloon injury of the rat iliac artery. 2003. Submitted.
- [4] Nyamekye I, Anglin S, McEwan J, MacRobert A, Bown S, Bishop C. Photodynamic therapy of normal and balloon-injured rat carotid arteries using 5-amino-levulinic acid. 1995. *Circulation*; 91(2):417-425.
- [5] Grant WE, Speight PM, MacRobert AJ, Hopper C, Bown SG. Photodynamic therapy of normal rat arteries after photosensitisation using disulphonated aluminium phthalocyanine and 5-aminolaevulinic acid. 1994. *Br J Cancer*; 70(1):72-78.
- [6] Jenkins MP, Buonaccorsi GA, Raphael M, Nyamekye I, McEwan JR, Bown SG et al. Clinical study of adjuvant photodynamic therapy to reduce restenosis following femoral angioplasty. 1999. *Br J Surg*; 86(10):1258-1263.
- [7] Ortu P, LaMuraglia GM, Roberts WG, Flotte TJ, Hasan T. Photodynamic therapy of arteries. A novel approach for treatment of experimental intimal hyperplasia. 1992. *Circulation*; 85(3):1189-1196.
- [8] Adili F, Stadius van Eps RG, Karp SJ, Watkins MT, LaMuraglia GM. Differential modulation of vascular endothelial and smooth muscle cell function by photodynamic therapy of extracellular matrix: novel insights into radical-mediated prevention of intimal hyperplasia. 1996. *J Vasc Surg*; 23(4):698-705.
- [9] Gabeler EEE, Sluiter W, Edixhoven-Bosdijk A, van Hillegersberg R, Stadius van Eps RG, Schoonderwoerd C, van Urk H. Amino Laevulinic Acid Induced Protoporphyrin IX Dosimetry: Optimum Time-Interval of Photosensitization for Photodynamic Therapy in Central and Peripheral Arteries of the Rat. 2003. In press.
- [10] Heisterkamp J, van Hillegersberg R, Sinofsky E, IJzermans J. Heat resistant cylindrical diffuser for interstitial laser coagulation: Comparison with a bare-tip fibre in ex vivo porcine liver. 1997. *Lasers in Surg. Med.* 20, 304-309.
- [11] Hinnen P, de Rooij FW, Voortman G, Tilanus HW, Wilson JHP, Siersema PD. Acrylate yellow filters in operating lights protect against photosensitization tissue damage. 2000. *Br.J.Surg*; 87, 231-235.
- [12] Wenguang L, Gussenhoven EJ, Bosch JG, Mastik F, Reiber JHC, Bom N. A computer-aided analysis system for the quantitative assessment of intravascular ultrasound images. *Proc Computers in Cardiology*; 1990:333-336.
- [13] Gabeler EEE, van Hillegersberg R, Stadius van Eps RG, Sluiter W, Mulder P, van Urk H. Endovascular Photodynamic Therapy with Amino Laevulinic Acid Prevents Balloon Induced Intimal Hyperplasia and Constrictive Remodelling. 2002. *Eur J Vasc Endovascular Surgery*;
- [14] Jenkins MP, Buonaccorsi GA, Mansfield R, Bishop CC, Bown SG, McEwan JR. Reduction in the response to coronary and iliac artery injury with photodynamic therapy using 5-aminolaevulinic acid. 2000. *Cardiovasc Res*; 45(2):478-485.
- [15] Kipshidze N, Sahota H, Komorowski R, Nikolaychik V, Keelan MH, Jr. Photoremodeling of arterial wall reduces restenosis after balloon angioplasty in an atherosclerotic rabbit model. 1998. *J Am Coll Cardiol*; 31(5):1152-1157.

- [16] Serruys PW, Strauss BH, Beatt KJ, Bertrand ME, Puel J, Rickards AF et al. Angiographic follow-up after placement of a self-expanding coronary-artery stent. 1991. *N Engl J Med*; 324(1):13-17.
- [17] Post MJ, Borst C, Pasterkamp G, Haudenschild CC. Arterial remodelling in atherosclerosis and restenosis: a vague concept of a distinct phenomenon. 1995. *Atherosclerosis*; 118 Suppl:S115-23:S115-S123.
- [18] Karu TI, Pyatibrat LV, Kalendo GS, Essenaliev RO. Effects of monochromatic low-intensity light and laser irradiation on adhesions of He-La cells in vitro. 1996. *Lasers Surg Med*; 18:47-50.
- [19] Lusis AJ, Yancopoulos G, Davis S, Gale NW, Rudge JS, Wiegand SJ et al. Nature insight: vascular biology. 2000. *Nature*; 407:218-257.
- [20] Carmeliet P, Jain RK. Angiogenesis in cancer and other diseases. 2000. *Nature*; 407:249-257.

CHAPTER 6

Endovascular Photodynamic Therapy with Amino Laevulinic Acid Prevents Balloon Induced Intimal Hyperplasia and Constrictive Remodelling

Edward E.E.Gabeler MD^{1*}, Richard van Hillegersberg MD PhD¹, Randolph G. Statius van Eps MD PhD¹, Wim Sluiter PhD², Paul Mulder PhD³, Hero van Urk MD PhD¹

¹Dept. of Surgery, Erasmus MC, Rotterdam, The Netherlands

²Dept. of Biochemistry, Erasmus MC, Rotterdam, The Netherlands

³Dept. of Epidemiology and Biostatistics, International Health Care Institute, Faculty of Health Sciences, Erasmus MC, Rotterdam, The Netherlands

Keywords: ALA, endovascular PDT, IH, light dosimetry, cholinergic innervation, remodelling, stenosis model

Adapted from European Journal for Endovascular and Vascular Surgery 2002, 24:322-331.

Abbreviations: ALA, aminolaevulinic acid; BI, balloon injury; CEF, circular elastic fibres between the smooth muscle cells of the tunica media; CVR, constrictive vascular remodelling; EEL, external elastic lamina; IEL, internal elastic lamina; IH, intimal hyperplasia; iv, intravenous; LO, light only; MLD, maximal lumen diameter; MWD, maximal wall diameter; PDT, photodynamic therapy; PpIX, protoporphyrin IX; SEM, standard error of the mean; SMC, smooth muscle cell.

6.00 Abstract

Background and Objective: Intimal hyperplasia (IH) and constrictive remodelling are important causes of restenosis following endovascular interventions, such as percutaneous transluminal angioplasty. Photodynamic therapy (PDT) with 5-aminolaevulinic (ALA) may prevent restenosis by cellular depletion and eliminating the cholinergic innervation.

Materials & Methods: Rats (n=90) were subdivided into 4 main groups. In the experimental group (n=36: 3 replications x 4 doses x 3 examination time-points), ALA was administered (200 mg/kg iv.) 2-3 hr before balloon injury (BI) of the common iliac artery followed by endovascular illumination with 633 nm at either 12.5, 25, 50 or 100 J/cm diffuser length (dl)(BI+PDT group). As control groups served the BI+Light only (LO) group (n=36) that received no ALA, the BI only group (n=9) (BI), and a group (n=9) that received a Sham procedure (Sham group).

Results: Planimetric analysis showed IH of $0.18 \pm 0.12 \text{ mm}^2$ (BI), $0.15 \pm 0.12 \text{ mm}^2$ (BI+LO at 100 J/cm dl) in contrast to $0.02 \pm 0.02 \text{ mm}^2$ after BI+PDT at 100 J/cm dl at 16 weeks ($p < 0.05$). In the BI+PDT groups, a light-dose increase of a factor 2 led to an IH decrease of 17.2% ($p < 0.05$). In the BI and BI+LO groups constrictive remodelling was found, in contrast to BI+PDT treated groups at 16 weeks. The staining of cholinergic innervation of the tunica media of the blood vessel wall in BI+PDT showed no damage at the highest fluence.

Conclusion: Endovascular ALA-PDT prevents IH and constrictive remodelling after BI without damage of cholinergic innervation of the tunica media. The effective light fluence rate in the rat is 50-100 J/cm dl.

6.01 Introduction

The long-term success rate of (endo)vascular interventions to treat stenosed or occluded peripheral arteries, is determined by arterial lumen preservation, which results in the maintenance of flow and reperfusion of tissue [1]. Unfortunately, the success rate is limited by restenosis, a constriction of the artery due to either an inadequate compensation to injury or a progression of the arterial disease itself [2]. Therefore, re-interventions are still required in 20-40% of the treated patients within 6 months [3].

In the development of restenosis, two pathophysiological determinants play a pivotal role: 1. intimal hyperplasia (IH)†, characterised by a fibrocellular hyperproliferation that obstructs the lumen, and 2. constrictive vascular remodelling (CVR)[4].

The initiation of restenosis occurs when the clotting cascade is activated after endothelial denudation, fibronectin exposure and over-stretching of the tunica media. Then, the thrombogenicity is increased and smooth muscle cells (SMC) start to proliferate and migrate from the tunica media into the tunica intima. With time, IH develops and the ultrastructure of the extracellular matrix reorganises [5].

With regard to the development of IH, a positive correlation to the migration of SMCs from the tunica media into the tunica intima has been described [6]. Therefore, the tunica media plays a pivotal role in IH development.

In iliac arteries, the cholinergic innervation of the tunica intima seems to be upregulated after balloon injury [7]. A possible hypothesis is that the innervation of the tunica media may regulate the development of IH and the rearrangement of the extracellular ultrastructure in peripheral arteries as well [8-15].

With regard to the prevention of IH, numerous experimental models described various degrees of success [16-24]. Brachy therapy with gamma irradiation shows promise as a means to inhibit restenosis [25;26]. Presently, coated-stenting has the best long-term outcome [27], but in-stent restenosis [28], stent-dislocation and stent-wire failure compromises it.

Alternatively, adjuvant vascular photodynamic therapy (PDT) may prevent restenosis by eradicating proliferating SMCs. PDT is based on illumination of an accumulated inert light-sensitive compound (photosensitizer) in the SMCs of the target artery. Subsequently, the use of monochromatic light activates the photosensitizer and generates free radicals, which eradicate the SMCs [29]. In this study, the endogenous pro-drug amino laevulinic acid (ALA) was used, which is a naturally occurring intermediate in the heme biosynthetic pathway. Then, ALA is tissue-dependently metabolised to the photosensitizer, protoporphyrin IX (PpIX).

Experimental studies described the effectiveness of photosensitizer based PDT with either external or internal illumination to prevent IH after balloon injury (BI), but permanent focal ablation of IH without CVR has not been accomplished [30-33]. Already, clinical studies have recently been described. A phase II trial in the USA (Antrim-based with external illumination [34] and a phase III trial in the UK (ALA-based with endoluminal illumination [35]) have been initiated.

The aim of our study was to establish the dosage-effect relationship between light treatment and the prevention of unfavourable arterial remodelling using endovascular ALA-PDT in a rat model.

6.02 Materials & Methods

6.02.1 Animals

The experimental protocol was approved by The Committee on Animal Research of the Erasmus University of Rotterdam and complied with “Principles of Good Laboratory Practice”. Male inbred Wistar rats (Harlan CPB, Austerlitz, The Netherlands) weighing 200-300g were used. The animals had free access to rat chow (AM II, Hope Farms, Woerden, The Netherlands) and acidified tap water, while maintained at a standard 12-hour light/dark cycle.

6.02.2 Study design

Ninety rats were randomly assigned to 4 groups <Table 6.1>. Balloon injury (BI) was used to induce intimal hyperplasia (IH) in 3 groups. In the first group (BI+PDT; n=36: 3 rats (per rat, the mean was determined using 3 heights of the damaged area) x 4 doses x 3 examination time-points), ALA was administered 3 hours before BI, followed by endovascular illumination of the occluded artery at a fluence of 12.5 (n=9), 25 (n=9), 50 (n=9) and 100 (n=9) J/cm diffuser length (dl). In the second and third groups, either light only (LO) without ALA (BI+LO: n=36) or BI only (BI: n=9) was performed. The BI and BI+LO groups served as references to study the inhibitory effect of PDT on the IH development. A fourth group underwent a Sham procedure to serve as baseline control (Sham group: n=9). The animals were sacrificed after either 0 hours, 4 or 16 weeks for pressure fixation of the artery (at each fluence in the group: n=3 per time-point). Cross sections were evaluated using light microscopic planimetric analysis.

Sham		9						Sham n=9
Balloon injury without light	0	3		3		3		BI n=9
Balloon injury + light	12.5	3	3	3	3	3	3	BI + LO (-ALA)
	25	3	3	3	3	3	3	n=36
	50	3	3	3	3	3	3	BI + PDT (+ALA)
	100	3	3	3	3	3	3	n=36
Method	Fluence J/cm dl	- ALA	+ ALA	- ALA	+ ALA	- ALA	+ ALA	GROUP
		0 weeks		4 weeks		16 weeks		

Table 6.1 The study-design of randomised rats in the Sham, balloon injury, balloon injury with light and balloon injury with PDT groups.

6.02.3 Photosensitization

All groups received either iv 200 mg/ kg ALA (Sigma-Aldrich Chemie, Zwijndrecht, The Netherlands) dissolved in phosphate buffered saline (PBS) at 40 mg/ml or PBS only of pH 7.45. The ALA solution was freshly made and kept from light exposure. The photosensitised rats were kept in the dark 2 hours prior to microsurgery, and 12 hours after the operation to prevent uncontrolled phototoxicity.

6.02.4 Laser

A dye laser (600 Series Dye Module, Laserscope, Surgical Systems, San Jose, CA, USA), pumped by a 532/KTP surgical laser (Laserscope, Surgical Systems, San Jose, CA, USA), was used to generate monochromatic light at 633 nm wavelength. The power emitted from the cylindrical diffusing tip (core diameter 200 μm , outer diameter 1.0 mm, tip length 20 mm: LightsticTM, Cardiofocus, West Yarmouth, MA, USA)[36] was calibrated with a built-in power meter, and verified with an external linear diffuser in an integrating cylindrical sphere (Optometer Model 370, Graseby Optronics, Orlando, FL, USA). A spectroscope (WaveMate, Coherent, Auburn, CA, USA) was used to verify the accuracy of the wavelength.

Temperature

The real-time temperature during endovascular PDT was checked at 100 mW/cm dl for 16 minutes and 40 seconds (100 J/cm dl) to exclude high-energy induced hyperthermal effects instead of low-energy induced phototoxicity. Two fibre-optic thermosensors with a diameter of 0.5 mm were coupled to a Luxtron thermometry unit (Luxtron Corp., Santa Clara, CA, USA). One was approximated parallel to the laser fibre along the artery at an axial distance of 10 mm in the fibre tip and the other next to the rat. The temperature was determined continuously.

Linear fluence with an isotropic probe

The linear fluence from the cylindrical diffuser in the arterial wall was measured at an output of 100 mW/cm dl for 16 minutes and 40 seconds (100 J/cm dl) . An isotropic probe was approximated parallel to the laser fibre outside the artery at axial distances of 10 mm from and 0, 10 and 20 mm in the fibre tip.

6.02.5 Surgical technique

A median laparotomy was performed under general anaesthesia with intramuscular injection of ketamine (Ketalar, Parke Davis and Co., Inc., 40 mg/kg) and xylazine (Rompun Bayer Ag, Leverkusen, Germany; 5 mg/kg). The procedure was performed in subdued light using a yellow filter (620-650 nm Kodak). The right common iliac artery was cranially and caudally temporarily occluded with vascular clamps. To create a blood free lumen, the arteries were flushed with 1.0 ml heparin (50 IU/ml 0.9% NaCl) through an arteriotomy 5 mm cranially of the abdominal aortal bifurcation. Then, a balloon catheter (Fogarty arterial embolectomy catheter, 2F, 60 cm, Baxter BV, Utrecht, The Netherlands) was inserted and inflated with deionised water to 2.0 bar with a manometer (Basix25TM, Medioterm, USA) [37]. A right iliac artery section of 15 mm from the bifurcation was damaged by inflating the balloon distally of the bifurcation. Then, after simultaneously pulling and rotating at 120° towards the bifurcation, the balloon was deflated at the end of the section. This procedure was consecutively performed 3 times. A single external suture in the vascular sheet marked the middle of the denuded area. After flushing the lumen with heparin and a two layer closing (interrupted 9-0 prolene sutures) of the arteriotomy,

both the caudal and the cranial clamp were removed. The abdominal wall was closed in two-layers (continuous 2-0 prolene sutures).

6.02.6 Endovascular Photodynamic Therapy (PDT)

In the BI+LO- and BI+PDT group, immediately after BI the fibre tip was centred endovascularly in the denuded area to illuminate 15 mm of the damaged and 2.5 mm of the untreated arterial wall both cranially as caudally. PDT was given when the artery was occluded (no blood flow present). Because of the cylindrical illumination, the fluence (J) and fluence rate (mW) was expressed per cm diffuser length (J or mW/cm dl). An output power of 100 mW/cm dl was used in all experiments. After treatment, the lumen was thoroughly flushed with 1ml heparin solution (50 IU/ml). Abdominal organs were protected from light exposure with light-absorbing plastic during illumination. The animals recovered in subdued light after treatment.

6.02.7 Specimen handling

A standard perfusion-fixation procedure via the thoracic aorta was performed during ether intoxication, in which the lumen was flushed with PBS (pH 7.45) for 2 minutes, followed by a 10-minute perfusion with formaldehyde (3.7%) at 100 mm Hg. The distally marked segment of 20 mm was carefully harvested after length measurement and stored in formaldehyde (3.7%) for at least 24 hours. Thereafter, the specimens were embedded in paraffin. Three cross sections of 10 μ m each were cut with a microtome from the distal end to the proximal direction at 3, 5 and 10 mm from the distal end, mounted on a slide and stained with haematoxylin and eosin for conventional light microscopy. All mounted sections were video-taped with a digital camera for geometrical analysis at a magnification of 100x. A digital video analyser system (IBM Corp., Boca Raton, USA) was used for the assessment of the absolute intimal and medial cross-sectional area in mm^2 . Intimal hyperplasia (IH) was defined as the cross-sectional area of the cell layer between the lumen and the internal elastic lamina. The medial area was defined as the cross-sectional area between the internal and external elastic lamina (EEL). The maximal lumen diameter (MLD in mm) and maximal wall diameter (MWD in mm) were measured to evaluate the remodelling process. Asymmetry was corrected by using the perimeter ($D = \text{circumference}/\pi$) assuming a circular configuration to calculate the MLD and MWD. The amount nuclei of SMCs represented the amount of SMCs per cross-section and were counted using frame grabber-software (Leica analysis, Germany).

6.02.8 Cholinergic unmyelinated innervation staining of the media

Six rats from the BI (n=3) and the BI+PDT at 100 J/cm dl (n=3) groups were sacrificed after 1 day for acetylcholinesterase staining (Schwann cell staining S-100 polyclonal, Dako, Kluströp, Denmark) of the frozen transverse sections from the iliac segment (38). The presence of cholinergic nerves adjacent to respectively the intima, internal elastic lamina (IEL), circular elastic fibres (CEF) in the media between the smooth muscle cells (SMC), external elastic lamina (EEL) and adventitia of the cross-sections were graded using a scoring-scheme to plot the mean layer score. The following scoring-grade was used: 0 indicated absent staining, 1 sporadic hypodense staining (<5 dots per microscopic field at a magnification of 200x) and 2 hyperdense staining (>10 dots, nerve fibre staining).

6.02.9 Statistical analysis

The area of intimal hyperplasia (IH), media, the maximal lumen diameter (MLD), the maximal wall diameter (MWD) and the amount of SMCs were expressed as averages of three measurements. Each of these variables was analysed separately after natural logarithmic transformation as dependent variable in a multiple linear regression analysis. The independent variables in this analysis were light dose (after \log_2 transformation), ALA (Y/N) and the time of sacrificing as categorical variable (weeks 4 or 16 for IH; weeks 0, 4 or 16 for MLD and MWD). Interest is in the regression coefficient B of light dose, expressing a dosage-effect trend relationship. The formula $100(e^B - 1)$ represents the mean percentage of change in the dependent variable as a consequence of doubling the light dose. The light dose by ALA interaction term in the regression model allows one to estimate and test a difference in mean percentage of change between the groups with and without ALA.

With regard to the cholinergic anti-S-100 staining, the Spearman rank correlation coefficient between the treatment and staining score was used. Effects were considered to be significant at p-values less than 0.05 ($p < 0.05$).

6.03 Results

One rat developed thrombosis within 24 hours following balloon injury in the BI+PDT group (100 J/cm dl) and was excluded from further analysis. All other animals appeared healthy, without significant weight loss during the study. No skin photosensitivity reactions were noted in the rats exposed after ALA injection. Omental adhesions along the abdominal scar were seen after harvesting the iliac arteries. All right common iliac arteries were patent at harvesting. All sutured arteriotomies were covered with peri-adventitial fat and an adjacent lymph node. No true or spurious aneurysms were noted.

6.03.1 Temperature and applied irradiance

During the PDT procedure no hyperthermia in the treated arterial segment was measured. The arterial wall temperature of 32.5 ± 0.18 °C (100 J/cm dl) and the room temperature of 19.4 ± 1.8 °C did not change. The linear fluence in the vascular wall at the applied irradiance matched with the output (100 to 110 %) and no loss or significant backscatter interference was measured.

6.03.2 Histological and Morphological Analysis

6.03.2.1 Histology

No histological and morphological abnormalities were found in the Sham group at 0 hours. Besides disruptions of the internal elastic lamina caused by BI, no signs of complete ruptures of the arterial wall were seen microscopically in all groups. Inflammation of the intima and media was absent at the microscopic level in all groups.

6.03.2.2 The tunica intima

BI+PDT statistically significantly inhibits IH compared to the control BI and BI+LO groups ($p < 0.0001$). If the light-dose is increased with a factor 2 than an inhibition of 17.7% was obtained compared to the control BI and BI+LO groups <Fig.6.1>. At 16 weeks, a statistically significant decrease of 65.5% was obtained compared to the controls ($p < 0.009$) <Fig.6.2a,6.2b,6.2c>.

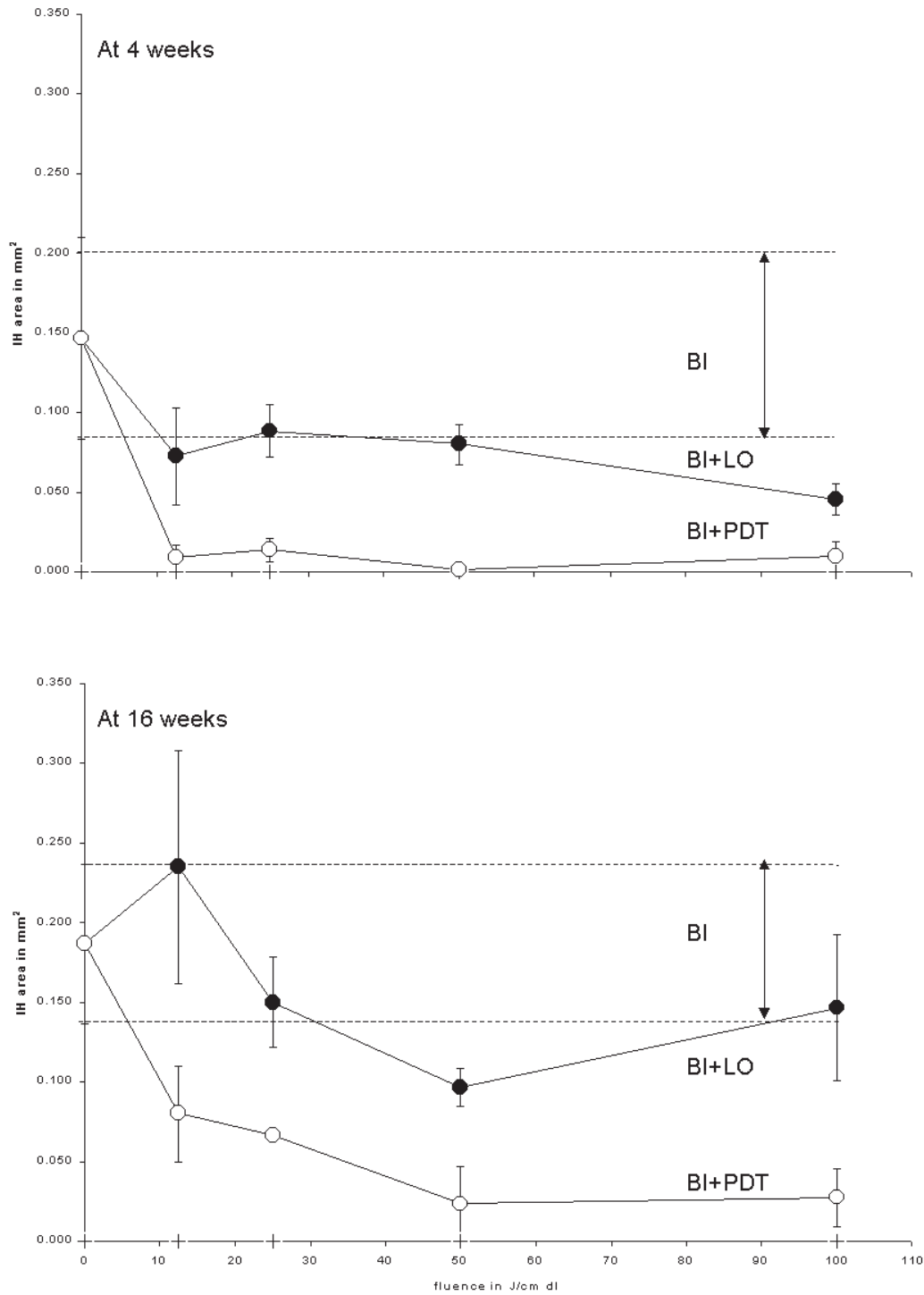


Figure 7.1 The absolute area of intimal hyperplasia (IH) formation expressed in mm^2 in the BI(--), BI+LO(\bullet) and BI+PDT(\circ) groups plotted against the fluence in Joule/cm diffuser length at time 4 weeks (up) and 16 weeks (bottom). The dotted reference lines of the BI group are based on the means of $n=3$. In all groups, no IH was seen at 0 weeks.

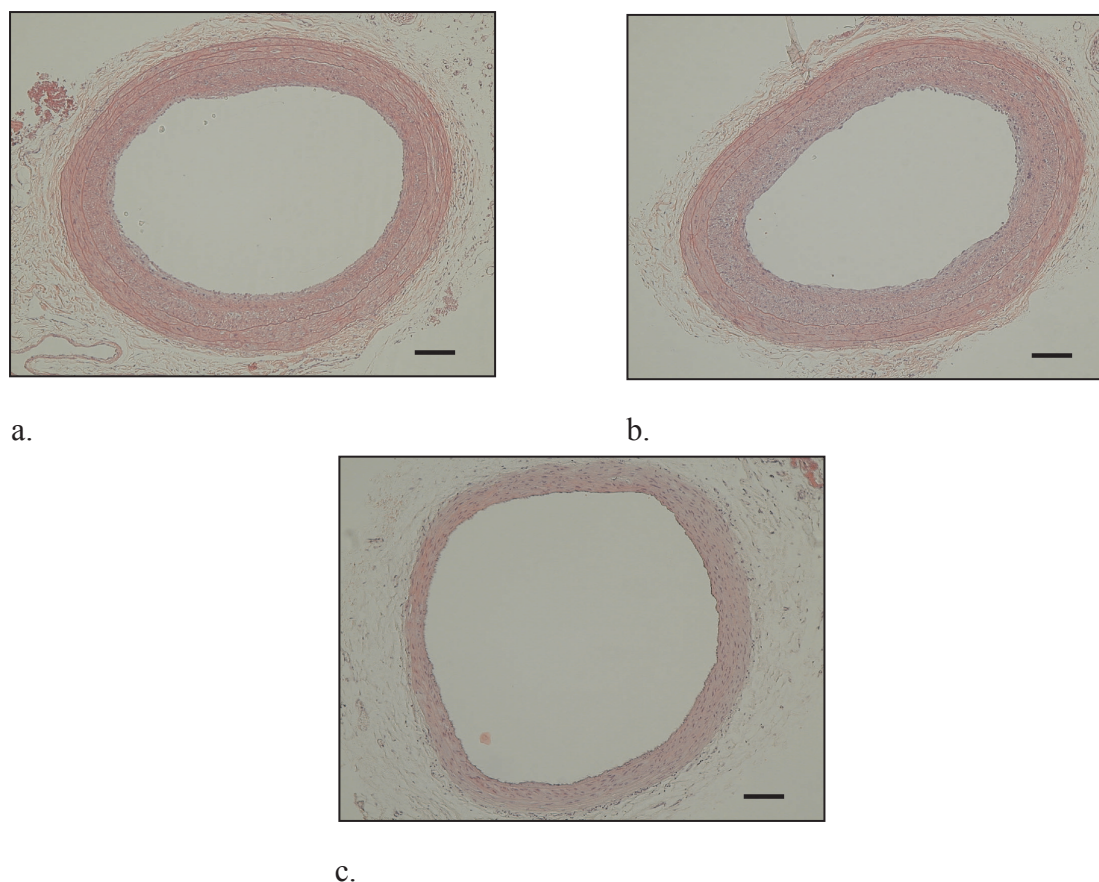


Figure 6.2 Photomicrographs of HE stained cross sections of IH development in the right iliac artery at 100x magnification. The geometric characteristics in relation to IH are illustrated. The scale bar represents 0.1 mm. a. BI (16 weeks). IH area reduced the maximal lumen diameter (MLD), b. BI+LO 50-100 J/cm dl (16 weeks), c. BI +PDT 50-100 J/cm dl (16 weeks).

6.03.2.3 The tunica media

BI+PDT did not statistically significantly change the area of the tunica media in 16 weeks compared to the control BI and BI+LO groups (overall mean: $0.14 \pm 0.04 \text{ mm}^2$).

6.03.2.4 Lumen and vessel wall

BI+PDT statistically significantly inhibits a decrease of the maximal lumen diameter compared to the control BI and BI+LO groups in 16 weeks ($p < 0.01$) <Table 6.2>. In general, if the light dose increased a factor 2 in the BI+PDT groups than the maximal lumen diameter (MLD) increased statistically significantly with 9.8% compared to the control BI and BI+LO groups ($p < 0.04$). At 16 weeks, a statistically significant increase of 72.3% was found in the BI+PDT groups compared to the control BI and BI+LO groups in 16 weeks. No significant difference within the control BI and BI+LO groups was found.

	MLD			MWD		
	0 wk	4 wk	16 wk	0 wk	4 wk	16 wk
Sham	0.92	0.93	1.11	1.06	1.11	1.29
BI+LO						
0	1.01	1.23	0.49	1.24	1.24	0.66
12.5	1.01	1.04	0.60	1.24	1.24	0.66
25	1.06	1.03	0.64	1.24	1.16	1.02
50	1.24	1.28	0.72	1.47	1.52	0.76
100	0.92	1.19	0.85	0.87	1.36	1.10
BI+PDT						
12.5	1.01	0.97	0.86	1.16	0.99	1.08
25	1.16	1.00	1.20	1.35	1.14	1.34
50	1.09	1.37	0.96	1.24	1.52	1.11
100	0.99	0.98	0.97	1.07	0.90	1.07

Table 6.2 The mean maximal lumen diameter (MLD) in mm and the maximal wall diameter (MWD) of the Sham, BI, BI+LO and BI+PDT groups at 0, 4 and 16 weeks (wk) with n=3 per group per time-point.

Likewise, BI+PDT statistically significantly inhibits a decrease of the maximal wall diameter (MWD) compared to the control BI and BI+LO groups in 16 weeks ($p<0.03$) <Table 6.2>. If the light dose was increased with a factor 2 than a MWD increase of 3.9% was seen ($p<0.02$). While no statistically significant difference was seen at 0 weeks, an MWD increase of 43.3% was seen in the BI+PDT groups compared to the BI and BI+LO groups in 16 weeks ($p<0.01$). No significant difference between the control BI and BI+LO groups was found ($p<0.34$).

7.03.3 Amount of SMCs in the tunica media

BI+PDT significantly decreased the amount of SMCs with 73.4% compared to the control BI and BI+LO groups ($p<0.05$) at 0 weeks <Table 6.3>. If the light dose increased a factor 2 than a decrease of 26.9% SMCs was seen ($p<0.01$). A decrease of 30% was seen in the BI+PDT groups compared to the BI and BI+BI+LO groups in 16 weeks ($p<0.008$). The tunica media repopulated in the BI+PDT groups in 16 weeks.

Groups	0 wk	4 wk	16 wk
0	173	189	348
12.5	177	220	357
25	169	194	350
50	185	200	318
100	133	169	290
BI+PDT			
12.5	123	163	233
25	97	180	281
50	7	33	241
100	3	25	196

Table 6.3 The mean amount of SMCs of the BI, BI+LO and BI+PDT groups at 0, 4 and 16 weeks (wk) with $n=3$ per group per time-point.

6.03.4 Effect of PDT on the cholinergic innervation

The cholinergic innervation of the tunica media was seen in all layers of all groups (mean 1.15 ± 0.01). A slight decrease of the anti-S-100 staining in the IEL and CEF between the SMCs was seen in the BI+PDT groups compared to the control BI and BI+LO groups ($r: -0.187$; $p < 0.01$). However, a statistically significantly increase was seen in the tunica adventitia ($r: 0.204$; $p < 0.001$) of the BI+PDT group compared to the control BI and BI+LO groups <Fig.6.4a,6.4b>.

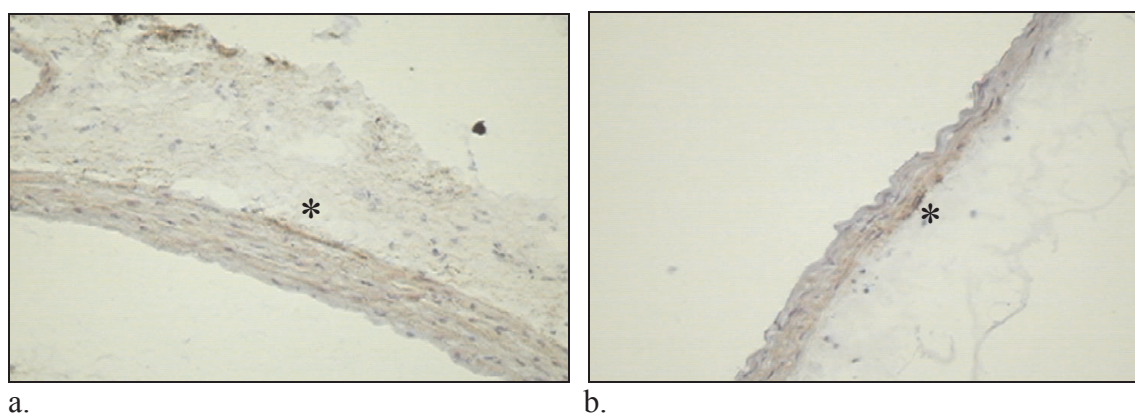


Figure 6.4 Photomicrographs of M-100 stained cross-sections of the right iliac artery at 200x magnification. The cholinergic nerves are stained black-brownish (*).
a. BI (0 weeks), b. BI + PDT 50-100 J/cm dl (0 weeks).

6.04 Discussion

In this study, the use of endovascular aminolaevulinic acid (ALA)-based photodynamic therapy (PDT) to prevent balloon-induced (BI) stenosis was evaluated in a rat model. Our data show that BI+PDT with light fluences of 50 and 100 J/cm dl at the fluence rate of 100 mW/cm dl, inhibits intimal hyperplasia (IH) and constrictive vascular remodelling at long-term (16 weeks). In the BI+PDT groups, a light-dose increase of a factor 2 led to an IH decrease of 17.2%. However, fluences of 12.5 and 25 J/cm dl at 100 mW/cm dl were inappropriate for IH inhibition. To our knowledge this is the first report that describes the inhibition of constrictive vascular remodelling in relation to light-dosimetry as a possible mechanism of the PDT induced inhibition of restenosis after BI.

Both the maximal lumen diameter (MLD) and maximal wall diameter (MWD) were unchanged at long-term at 50 and 100 J/cm dl in the BI+PDT group, compared to the untreated arteries. The BI-damaged arteries not only showed IH, but also a reduction of both MLD and MWD, reflecting late lumen loss due to constrictive remodelling after balloon injury <Table 6.2>. It became clear that restenosis of blood vessels resulting from angioplasty is mainly determined by constrictive remodelling of the vascular wall and not only by the occurrence of IH [39]. This could explain why treatment modalities that are only directed against the development of IH were clinically not successful in preventing restenosis so far. Presently, new treatment modalities are under development to prevent constrictive remodelling by inhibiting matrix metallo-proteinases that are involved in remodelling the subcellular matrix [40].

The presence of cholinergic staining was semi-quantitatively evaluated because we were mainly interested whether or not nerve damage occurred after PDT. For evaluating the cholinergic function, a quantitative analysis would have been required. As the toxic effect of PDT occurs immediately and depletion of acetylcholinesterase from a damaged nerve is fast process, the impact on vascular innervation was studied on the first day after treatment. This study shows that ALA-PDT inhibits IH as well as constrictive vascular remodelling without innervation damage of the tunica media. In fact, this treatment appeared to decrease cholinergic staining of the tunica media and increase the cholinergic innervation staining of the tunica adventitia. As described by Furchgott, cholinergic innervation causes dilation in the presence of endothelial cells in the tunica intima and constriction of SMCs if acetylcholine is directly exposed to smooth muscle cells in the tunica media [41]. The not responding of SMCs in the tunica media to cholinergic stimulation may be due to SMC eradication after BI+PDT, which explains the absence of arterial constriction. The underlying mechanism is not completely elucidated, but warrants further study. A direct cytotoxic effect resulting in permanent focal acellularity of the area of the tunica media is one of the mechanisms previously described with external PDT [32;42].

However, in this study only focal acellularity of the tunica media in the BI+PDT groups with 50 and 100 J/cm dl from 0 up to 4 weeks was found and the tunica media was completely repopulated after 16 weeks. Grant and Nyamekye [43;44] described acellularity of the tunica media upto 6 months after external illumination of damaged and undamaged ALA-photosensitised arteries in a rat without giving any explanation for this phenomenon. Additionally, earlier reports described that in vitro innervation of the tunica media stimulated hyperplasia [8], which may be source for IH. This finding may also be relevant for our observation of repopulation of the tunica media. Another possible explanation is that in our study the vascular wall was illuminated from the luminal side, whereas most previous experimental studies used external illumination [32;44;45]. In that manner the ultrastructure of the extracellular matrix may not so severely and permanently be altered by endovascular PDT treatment and therefore, the tunica media could be repopulated. Notably, we found that light alone at high fluence can prevent IH to some extent as well, which was also described by others

[46]. Presumably intracellular photosensitizers mediate this selective cytotoxicity in the arterial wall.

How BI+PDT led to the inhibition of constrictive vascular remodelling is unknown. In a previous study on PDT in the rat oesophagus we found that PDT dependent damage to the nerve plexus caused dilation of the oesophagus [38]. In this study no nervous damage at the microscopic level could be observed, but the function of the nerves in the tunica media was not evaluated. This makes it less likely that permanent constriction of the blood vessel is prevented by switching-off the nerves. Because innervation of the tunica media likely plays an important role in the repopulation of the media and extracellular ultrastructure organisation, the stimulatory effect of BI+PDT on the innervation of the tunica adventitia may underlie the beneficial outcome of this treatment. The problem of compensatory back-growth of IH and constrictive remodelling with time will need further studies, because despite significant inhibition, slight IH development was seen at 16 weeks in the experimental groups.

Acknowledgements

This study was subsidised by the Dutch Heart Foundation (project grant NHS 97.181). The authors are grateful to E. Gussenhoven and J. Honkoop for expert technical assistance with the geometric analysis, H. Marijnissen for the isotropic linear fluence measurements, P. Lobe, M. Holtman for excellent preparation of the cross-sections and D.P. Hayes for evaluating the HE cross-sections and J.M. Kross for critically evaluating the cholinergic stained cross-sections.

References

- [1] Currier JW, Faxon DP. Restenosis after percutaneous transluminal coronary angioplasty: have we been aiming at the wrong target? [editorial]. *J Am Coll Cardiol* 1995; 25(2):516-520.
- [2] Ross R. The pathogenesis of atherosclerosis: a perspective for the 1990s. *Nature* 362, 801-809. 1993.
- [3] Bauters C, Meurice T, Hamon M, McFadden E, Lablanche JM, Bertrand ME. Mechanisms and prevention of restenosis: from experimental models to clinical practice. *Cardiovasc Res* 1996; 31(6):835-846.
- [4] Guzman LA, Mick MJ, Arnold AM, Forudi F, Whitlow PL. Role of intimal hyperplasia and arterial remodeling after balloon angioplasty: an experimental study in the atherosclerotic rabbit model. *Arterioscler Thromb Vasc Biol* 1996; 16(3):479-487.
- [5] Williams B. Mechanical influences on vascular smooth muscle cell function. *J Hypertens* 1998; 16(12 Pt 2):1921-1929.
- [6] A.W.Clowes, M.E.Reidy, M.M.Clowes. Kinetics of cellular proliferation after arterial injury; 1. Smooth muscle growth in the absence of endothelium. *Laboratory Investigation* 1983; 49[3], 327-333.
- [7] Chen JC, Hsiang YN, Buchan AM. Somatostatin receptor expression in rat iliac arteries after balloon injury. *J Invest Surg* 1997; 10(1-2):17-23.
- [8] Gilad GM, Kagan HM, Gilad VH. Lysyl oxidase, the extracellular matrix forming enzyme in rat brain injury sites. *Neuroscience letters* 2001; 310:45-48.
- [9] Hiltunen JO, Laurikainen A, Airaksinen MS, Saarna M. GDNF family receptors in the embryonic and postnatal rat heart and reduced cholinergic innervation in mice hearts lacking Ret or GFRa2. *Dev Dynamics* 2000; 219:28-39.
- [10] Lee JHM, Peuler JD. A possible indirect sympathomimetic action of metformin in the arterial vessel wall of spontaneously hypertensive rats. *Life Sciences* 2001; 69:1085-1092.
- [11] Lindauer U, Kunz A, Schuh-Hofer S, Vogt J, Dreier JP, Dirnagl U. Nitric oxide from perivascular nerves modulates cerebral arterial pH reactivity. *Am J Physiol Heart Circ Phys* 2001; 281:H1353-H1363.
- [12] Milner P, Loesch A, Burnstock G. Neural endothelin in hypertension: increased expression in ganglia and nerves to cerebral arteries of the spontaneously hypertensive rat. *J Vasc Res* 2000; 37:39-49.
- [13] Monahan KD, Tanaka H, Dinunno FA, Seals DR. Central arterial compliance is associated with age- and habitual exercise-related differences in cardiovascular baroreflex sensitivity. *Circulation* 2001; 104:1627-1632.
- [14] Spilker MH, Asano K, Yannas IV, Spector M. Contraction of collagen-glycosaminoglycan matrices by peripheral nerve cells in vitro. *Biomaterials* 2001; 22:1085-1093.
- [15] Tsuchida A, Handa Y, Nojyo Y, Kubota T. Ultrastructure of NADPH diaphorase-positive nerve fibres and their terminals in the rat cerebral arterial system. *J Chem Neuroanatomy* 2001; 21:267-275.
- [16] Herrman JP, Hermans WR, Vos J, Serruys PW. Pharmacological approaches to the prevention of restenosis following angioplasty. The search for the Holy Grail? (Part I). *Drugs* 1993; 46(1):18-52.
- [17] Castronuovo JJ, Jr., Guss SB, Mysh D, Sawhney A, Wolff M, Gown AM. Cytokine therapy for arterial restenosis: inhibition of neointimal hyperplasia by gamma-interferon. *Cardiovasc Surg* 1995; 3(5):463-468.

- [18] Eriksen UH, Amtorp O, Bagger JP, Emanuelsson H, Foegh M, Henningsen P et al. Randomised double-blind Scandinavian trial of angiopeptin versus placebo for the prevention of clinical events and restenosis after coronary balloon angioplasty. *Am Heart J* 1995; 130(1):1-8.
- [19] Feldman LJ, Tahlil O, Steg PG. Adenovirus-mediated arterial gene therapy for restenosis: problems and perspectives. *Semin Interv Cardiol* 1996; 1(3):203-208.
- [20] Kalinowski M, Tepe G, Schieber A, Brehme U, Bruck B, Erley CM et al. Local administration of ramiprilat is less effective than oral ramipril in preventing restenosis after balloon angioplasty in an animal model. *J Vasc Interv Radiol* 1999; 10(10):1397-1404.
- [21] Miyauchi K, Kawai S, Okada R, Yamaguchi H. Limitations of angiotensin-converting enzyme inhibitor in restenosis of a deep arterial injury model. *Jpn Circ J* 1998; 62(1):53-60.
- [22] Miyazawa N, Umemura K, Kondo K, Nakashima M, Steg PG, Tahlil O et al. Effects of pemirolast and tranilast on intimal thickening after arterial injury in the rat. *J Cardiovasc Pharmacol* 1997; 30(2):157-162.
- [23] Ohsawa H, Noike H, Kanai M, Yoshinuma M, Mineoka K, Hitsumoto T et al. Preventive effects of an antiallergic drug, pemirolast potassium, on restenosis after percutaneous transluminal coronary angioplasty. *Am Heart J* 1998; 136(6):1081-1087.
- [24] Wu KK. Prostacyclin and nitric oxide-related gene transfer in preventing arterial thrombosis and restenosis. *Agents Actions Suppl* 1997; 48:107-23:107-123.
- [25] Teirstein PS, Massullo V, Jani S, Popma JJ, Russo RJ, Schatz RA et al. Three-year clinical and angiographic follow-up after intracoronary radiation : results of a randomized clinical trial [see comments]. *Circulation* 2000; 101(4):360-365.
- [26] Verin V, Popowski Y. Intraarterial beta irradiation to reduce restenosis after PTCA. Experimental and clinical experience. *Herz* 1998; 23(6):347-355.
- [27] Strecker EP, Gabelmann A, Boos I, Lucas C, Xu Z, Haberstroh J et al. Effect on intimal hyperplasia of dexamethasone released from coated metal stents compared with non-coated stents in canine femoral arteries. *Cardiovasc Intervent Radiol* 1998; 21(6):487-496.
- [28] Mehran R, Dangas G, Abizaid AS, Mintz GS, Lansky AJ, Satler LF et al. Angiographic patterns of in-stent restenosis: classification and implications for long-term outcome. *Circulation* 1999; 100(18):1872-1878.
- [29] Henderson BW, Dougherty TJ. How does photodynamic therapy work? *Photochem Photobiol* 1992; 55(1):145-157.
- [30] LaMuraglia GM, Ortu P, Flotte TJ, Roberts WG, Schomacker KT, ChandraSekar NR et al. Chloroaluminum sulfonated phthalocyanine partitioning in normal and intimal hyperplastic artery in the rat. Implications for photodynamic therapy. *Am J Pathol* 1993; 142(6):1898-1905.
- [31] Nyamekye I, Anglin S, McEwan J, MacRobert A, Bown S, Bishop C. Photodynamic therapy of normal and balloon-injured rat carotid arteries using 5-amino-levulinic acid. *Circulation* 1995; 91(2):417-425.
- [32] Ortu P, LaMuraglia GM, Roberts WG, Flotte TJ, Hasan T. Photodynamic therapy of arteries. A novel approach for treatment of experimental intimal hyperplasia. *Circulation* 1992; 85(3):1189-1196.
- [33] Grant WE, Speight PM, MacRobert AJ, Hopper C, Bown SG. Photodynamic therapy of normal rat arteries after photosensitisation using disulphonated aluminium phthalocyanine and 5-aminolaevulinic acid. *Br J Cancer* 1994; 70(1):72-78.
- [34] Rockson SG, Lorenz DP, Cheong WF, Woodburn KW. Photoangioplasty: An emerging clinical cardiovascular role for photodynamic therapy. *Circulation* 2000; 102(5):591-596.

- [35] Jenkins MP, Buonaccorsi GA, Raphael M, Nyamekye I, McEwan JR, Bown SG et al. Clinical study of adjuvant photodynamic therapy to reduce restenosis following femoral angioplasty. *Br J Surg* 1999; 86(10):1258-1263.
- [36] Heisterkamp J, Hillegersberg van R, Sinofsky E, Ijzermans J. Heat resistant cylindrical diffuser for interstitial laser coagulation: Comparison with a bare-tip fibre in ex vivo porcine liver. *Lasers Surg. Med.* 1997; 20, 304-309.
- [37] Indolfi C, Cioppa A, Stabile E, Di Lorenzo E, Esposito G, Pisani A et al. Effects of hydroxymethylglutaryl coenzyme A reductase inhibitor simvastatin on smooth muscle cell proliferation in vitro and neointimal formation in vivo after vascular injury. *J Am Coll Cardiol* 2000; 35(1):214-221.
- [38] van den Boogert J, van Hillegersberg R, van Staveren HJ, de Bruin RW, van Dekken H, Siersema PD et al. Timing of illumination is essential for effective and safe photodynamic therapy: a study in the normal rat oesophagus. *Br J Cancer* 1999; 79(5-6):825-830.
- [39] Post MJ, Borst C, Kuntz RE. The relative importance of arterial remodeling compared with intimal hyperplasia in lumen renarrowing after balloon angioplasty. A study in the normal rabbit and the hypercholesterolemic Yucatan micropig [see comments]. *Circulation* 1994; 89(6):2816-2821.
- [40] Overhaus M, Heckenkamp J, Kossodo S, Leszczynski D, LaMuraglia GM. Photodynamic therapy generates a matrix barrier to invasive vascular cell migration. *Circ Res* 2000; 86(3):334-340.
- [41] Furchgott RF, Zawadski JV. The obligatory role of endothelial cells in the relaxation of arterial smooth muscle by acetylcholine. *Nature* 1980; 288, 373-376.
- [42] Stadius van Eps RG, ChandraSekar NR, Hasan T, LaMuraglia GM. Importance of the treatment field for the application of vascular photodynamic therapy to inhibit intimal hyperplasia. *Photochem Photobiol* 1998; 67(3):337-342.
- [43] Grant WE, Speight PM, MacRobert AJ, Hopper C, Bown SG. Photodynamic therapy of normal rat arteries after photosensitisation using disulphonated aluminium phthalocyanine and 5-aminolaevulinic acid. *Br J Cancer* 1994; 70(1):72-78.
- [44] Nyamekye I, Anglin S, McEwan J, MacRobert A, Bown S, Bishop C. Photodynamic therapy of normal and balloon-injured rat carotid arteries using 5-amino-levulinic acid. *Circulation* 1995; 91(2):417-425.
- [45] LaMuraglia GM, Ortu P, Flotte TJ, Roberts WG, Schomacker KT, ChandraSekar NR et al. Chloroaluminum sulfonated phthalocyanine partitioning in normal and intimal hyperplastic artery in the rat. Implications for photodynamic therapy. *Am J Pathol* 1993; 142(6):1898-1905.
- [46] Kipshidze N, Sahota H, Komorowski R, Nikolaychik V, Keelan MH, Jr. Photoremodeling of arterial wall reduces restenosis after balloon angioplasty in an atherosclerotic rabbit model. *J Am Coll Cardiol* 1998; 31(5):1152-1157.

CHAPTER 7

The Effect of Photodynamic Therapy on Reendothelialization after Balloon Injury of the Rat Iliac Artery

Edward E.E. Gabeler¹, Randolph G. Stadius van Eps¹, Richard van Hillegersberg¹, Caroline A.E. Verbakel¹, Hero van Urk¹, Wim Sluiter²

¹Department of Surgery, Erasmus MC, Rotterdam, The Netherlands

²Department of Biochemistry, Erasmus MC, Rotterdam, The Netherlands

Keywords: ALA, photodynamic therapy, reendothelialization, remodelling, restenosis, TGF-beta

This article has been adapted from and is submitted as 'Photodynamic therapy reduces the expression of transforming growth factor- β after balloon injury of the rat iliac artery'

Abbreviations: AED, area of endothelial denudation; ALA, aminolaevulinic acid; BI, balloon injury; EC, endothelial cell; EEL, external elastic lamina; IEL, internal elastic lamina; IH, intimal hyperplasia; PDT, photodynamic therapy; PpIX, protoporphyrin IX; SEM, standard error of the mean; TGF- β , cytokine transforming growth factor-beta.

7.00 Abstract

Background: Photodynamic Therapy (PDT) effectively inhibits IH after angioplasty, but induces endothelial cell (EC) injury and may interfere with EC regrowth. To study these effects, reendothelialization, and transforming growth factor-beta (TGF- β) protein expression were determined after PDT of balloon injured (BI) rat iliac arteries.

Materials & Methods: In the experimental groups, PDT was performed 2.5 h after i.v. administration of 200 mg/kg aminolevulinic acid (ALA) with 633 nm light at either 50 or 100 J/cm (100 mW/cm) diffuser length just after balloon injury (BI) with 15 mm length of denudation. In the control group, BI was performed only. Normal iliac arteries served as untreated reference. The animals (n=5 per time-point) were sacrificed after 2 hours, 1, 3 and 6 weeks for assessment of the remaining area of endothelial denudation using Evans blue staining and after 2 hours and 3 weeks for TGF- β expression using immunohistochemistry.

Results: In the experimental groups IH was prevented effectively at 50 J/cm ($p < 0.05$). Complete reendothelialization occurred after 6 weeks both in the control group and in the experimental groups. Immediately after BI and BI+PDT, there was increased TGF- β expression on the internal border of the tunica adventitia. After 3 weeks, the TGF- β was mostly expressed in the external border of intimal hyperplasia in the control-group, while in the experimental groups, no TGF- β expression was detected.

Conclusion: PDT significantly reduces the TGF- β expression in the vessel wall, but does not significantly delay EC regrowth following BI in rat iliac arteries. This implies that PDT may be a safe method of inhibiting IH following endovascular interventions.

7.01 Introduction

Endovascular PDT prevents restenosis by inhibiting intimal hyperplasia (IH) and fibrocellular constrictive remodelling following angioplasty [1]. Although this phenomenon has been proved by several authors in various experimental set-ups, the underlying mechanisms are not well understood [1-5]. PDT is based on a photocytotoxic reaction induced by local illumination of a light sensitive substrate (photosensitizer) after its accumulation in the arterial wall [6-7]. The pro-drug aminolaevulinic acid (ALA) is a naturally occurring hydrophilic intermediate in the heme biosynthetic pathway, that is artery type-dependently metabolised to photoactive porphyrins like protoporphyrin IX (PpIX)[4]. Vascular PDT results in a transmural eradication of photosensitised vascular cells and superficial EC's.

The pace and extent of reendothelialization is known to be a major factor in determining the outcome of the arterial healing response to vascular injury [8]. Because of the antithrombotic properties of endothelial cells (EC) and their inhibitory effect on the proliferation of smooth muscle cells (SMC), proper reendothelialization is thought to inhibit IH development [9].

We have previously found a PDT dependent stimulation of EC growth by inactivation of the cytokine transforming growth factor-beta (TGF- β), a potent inhibitor of EC growth *in vitro* [10]. *In vitro*, the cells involved in both the development of IH and fibrosis, like EC's, SMC's, platelets and monocytes, produce TGF- β [11]. On the contrary, [12] *in vivo* the SMC's are the major source of TGF- β and thus different effects may occur [13].

In this study, the effect of PDT on reendothelialization was examined *in vivo* in a balloon injury model of the rat iliac artery. Because of the important role of TGF- β in regulating endothelial cell growth, the PDT effects on TGF- β staining in the vascular wall were assessed [14].

7.02 Materials & Methods

The experimental protocol was approved by The Committee on Animal Research of the Erasmus University of Rotterdam and complied with "Principles of Good Laboratory Practice". Male inbred Wistar rats (Harlan CPB, Austerlitz, The Netherlands) weighing 200-300g were used. The animals had free access to rat chow (AM II, Hope Farms, Woerden, The Netherlands) and acidified tap water, while maintained in a standard 12-hour light/dark cycle.

7.02.1 Study design

The first part of this study focused on the endothelial regrowth after balloon injury (BI) and PDT using Evans blue staining. Seventy rats were assigned to 4 groups and underwent a laparotomy. In the experimental groups, PDT with a fluence of at random 50 (n=20) or 100 J/cm diffuser length (dl) (n=20) at an irradiance of 100 mW/cm dl was delivered after intravenously ALA administration. In the control group, rats (n=20) underwent BI without PDT. In each group, the animals were sacrificed after 2 hours (n=5), 1 week (n=5), 3 (n=5) and 6 weeks (n=5) for Evans Blue staining of the artery. The untreated reference group underwent only a laparotomy (n=10).

Secondly, in a separate series of experiments, the TGF- β protein expression in the vascular wall was assessed using immunohistochemistry. Forty rats were assigned to 4 groups: BI+PDT 50 J/cm dl (n=10), BI+PDT 100 J/cm dl (n=10); BI only (n=10) and an untreated

reference group (n=10). In each group, the animals were sacrificed after 2 hours (n=5) and after 3 weeks (n=5) for harvesting the arterial segment for staining of the TGF- β protein expression.

7.02.2 Photosensitization

All groups received either 200 mg/kg ALA (Sigma-Aldrich Chemie, Zwijndrecht, The Netherlands) dissolved in phosphate buffered saline at 40 mg/ml or an equal volume of phosphate buffer (PBS, Merck; pH 7.45) administered intravenously. The solution was freshly made for each animal and kept from light exposure. The photosensitised rats were kept in the dark 2 ½ hours prior to surgery and 12 hours after the operation to prevent skin phototoxicity.

7.02.3 Laser

A dye laser (600 Series Dye Module, Laserscope, Surgical Systems, San Jose, CA, USA), pumped by a 532/KTP surgical laser (Laserscope, Surgical Systems, San Jose, CA, USA), was used to generate monochromatic light at 633 nm. The power emitted from the cylindrical diffusing tip (core diameter 200 μ m, outer diameter 1.0 mm, tip length 20 mm: Lightstic™, Cardiofocus, West Yarmouth, MA, USA)[15] was calibrated with a built-in power meter, and verified with an external linear diffuser in an integrating cylindrical sphere (Optometer Model 370, Graseby Optronics, Orlando, FL, USA). A spectroscope (WaveMate, Coherent, Auburn, CA, USA) was used to verify the accuracy of the wavelength.

Temperature

The real-time temperature during endovascular PDT was checked at a fluence of 100 J/cm dl with an irradiance of 100 mW/cm dl (illumination time of 1000 sec) to rule out hyperthermic lesions. Two fibre-optic thermosensors with a diameter of 0.5 mm were coupled to a Luxtron thermometry unit (Luxtron Corp., Santa Clara, CA, USA). One was approximated parallel to the laser fibre along the artery at an axial distance of 10 mm in the fibre tip and the other next to the rat. The temperature was determined continuously and measurements saved using a computer [7].

Linear fluence calibration with an isotropic probe

The linear fluence of 100 J/cm dl from the cylindrical diffuser in the arterial wall was measured at an irradiance of 100 mW/cm dl (illumination time of 1000 seconds). An isotropic probe was approximated parallel to the laser fibre outside the artery at longitudinal distances of 10 mm from and 0, 10 and 20 mm in the fibre tip.

7.02.4 Surgical technique

A median laparotomy was performed under general anaesthesia with intramuscular injection of ketamine (Ketalar, Parke Davis and Co., Inc., 40 mg/kg) and xylazine (Rompun Bayer Ag, Leverkusen, Germany; 5 mg/kg). Subdued light using a yellow filter [16](620-650 nm Kodak) was applied during the procedure. The right common iliac artery was cranially and caudally temporarily occluded with vascular clamps (Haemostat B1, Stöpler, Utrecht, The Netherlands). To create a blood free lumen, the arteries were flushed with 1.0 ml heparin (50 IU/ml 0.9% NaCl, Infusion solution Baxter) through an arteriotomy 5 mm proximal to the abdominal aortal bifurcation. Then, a 2F balloon catheter was inserted and inflated with deionized water to 2.0 bar using a manometer that caused a dilatation of 45% [17]. A right iliac

artery section of approximately 15 mm was damaged by inflating the balloon distal from the bifurcation. Then, after simultaneously pulling and rotating at 120° towards the bifurcation, the balloon was deflated at the end of the section. This procedure was repeated 2 times. Then, only in the BI+PDT groups, endovascular PDT was performed directly after BI. A single suture in the vascular sheet marked the middle of the denuded area. After flushing the lumen with heparin and closing of the arteriotomy (interrupted 9-0 prolene sutures), both the caudal and the cranial clamp were removed. Directly thereafter, reperfusion of the dilated section was observed. The abdominal wall was closed in two layers.

7.02.5 Endovascular Photodynamic Therapy (PDT)

In the BI+PDT groups, a 400 µm fibre (Lightstic 360, Cardiofocus, West Yarmouth, MA, USA) with a 20 mm long cylindrical diffusing tip was applied directly after BI. The fibre tip was centred in the denuded area to illuminate 15 mm of the damaged and 2.5 mm of the untreated arterial wall both cranially and caudally. The clamps were not included in the treatment field. Because of the cylindrical illumination, the fluence was expressed in Joule per cm diffuser length (J/cm dl). The target area was illuminated at random with either 50 or 100 J/cm dl, applied with 100 mW/cm dl. After treatment, the lumen was thoroughly flushed with 1ml heparin (50 IU/ml). Abdominal organs were protected from light exposure with a light absorbing plastic folium during illumination.

7.02.6 Specimen handling- Evans blue staining

Thirty minutes before the animals were sacrificed, an intravenous injection of 6 ml of 0.5% Evans blue dye was delivered intravenously via the penile vein to identify the remaining nonendothelialized area. The area of the intimal surface that was stained blue after opening the treated section longitudinally depicted the denuded area. These vessel segments were videotaped and measured to determine the area of endothelial denudation (AED) using a digital video analyser system (IBM Corp., Boca Raton, USA)[18]. Thereafter, these 20-mm sections were carefully harvested and stored in formaldehyde (3.7%) for at least 24 hours. The specimens were embedded in paraffin. Longitudinal sections of 10 µm each were cut with a microtome, mounted on a microscopic object slide and stained with haematoxylin and eosin for conventional light microscopy. All mounted sections were scored for the presence of endothelium, and damage (scored for laminal microruptures, cell eradication/ necrosis or hyperplasia) of the tunica media and tunica adventitia. The area of IH was measured using a digital analyser system.

7.02.7 Specimen handling- staining of TGF-β protein expression

Staining of TGF-β (Serotec mouse anti human cross-reacting with rat pan-TGF-β MCA 797, 0.1 mg, batch NR 210301) was performed using the following protocol: Frozen sections were thawed at room temperature for 1 night, fixed with acetone for 3 minutes and air dried for 10 minutes. With a Peroxidase Anti Peroxidase (PAP)-pen lines were drawn around the tissue sections and washed 3x4 minutes with Tris-buffered saline (TBS; pH 7.4). Next, in a humidified atmosphere the sections were incubated for 30 minutes with TBS containing 10% normal goat serum and 10% normal human to block non-specific antigenic epitopes. Then, primary antibody against TGF-β, diluted 1:200 in TBS containing 1% normal human plasma was added to the sections, following an incubation period of 60 minutes in humidified atmosphere. Thereafter, the sections were rinsed 3x3 minutes with TBS containing 0.1% Tween 20, and incubated for 60 minutes with secondary rabbit anti mouse (biotin) antibody, 1:400 diluted in TBS containing 5%

BSA, 2% normal rabbit serum, 2% normal human plasma and 1% rat serum (2nd stepbuffer). The sections were rinsed 3x3 minutes with TBS containing 0.1% Tween 20, and incubated for 60 minutes with ABC complex (1:100 diluted in 2nd stepbuffer). Then, the sections were first rinsed for 3 minutes with TBS followed by TBS at pH 8.5, and next incubated in the dark for 30 minutes using chromogen solution. After rinsing with tap water, the sections were counterstained using Mayer's Hematoxylin for 10-15 seconds, flushed with water again. Finally, after covering with Imsol-Mount, the sections were kept at 40 °C for 20 minutes. The cross-sections were microscopically analysed. To correct for normal growth, control arteries at each time period were included in the analysis. Because of TGF- β 's laminal ordering, its expression was described as percentage of the total perimeter of the elastic lamina (EL).

7.02.8 Statistical analysis

The data were expressed as mean \pm standard error of the mean (SEM). Differences between the means of various groups were evaluated for statistical significance by linear regression analysis and analysis of variances where appropriate. A difference was considered to be significant at p values less than 0.05.

7.03 Results

All animals appeared healthy without significant weight loss during the study. No skin photosensitivity reactions occurred in the rats exposed to PDT. No temperature changes were seen during PDT and the linear fluence in the vascular wall at the applied irradiance matched with the output (100 to 110%)[7].

7.03.1 Area of endothelial denudation

Two hours after BI, the area of endothelial denudation (AED) was 60 ± 5 mm² in the BI, and 75 ± 8 mm² in the BI+PDT 50 group and 77 ± 6 mm² in the BI+PDT 100 J/cm dl group compared to 0 mm² in the untreated control. The AED did not significantly differ between the BI and PDT groups ($p < 0.59$) <Fig.7.1, 7.2a, 7.2b>. There was reendothelialization with a rapid decrease of the AED in all groups <Fig.7.1, 7.2c, 7.2d>. The AED in the BI+PDT 100 J/cm dl group was higher compared to BI at 3 weeks but this did not reach statistical significance ($p < 0.06$). Complete reendothelialization was found in the BI, BI+PDT 50 J/cm dl and BI+PDT 100 J/cm dl groups after 6 weeks <Fig. 7.2e, 7.2f>. Before complete reendothelialization, endothelial growth was more pronounced distally than proximally in all groups, but in general to a slightly lesser degree in the BI+PDT 100 J/cm dl group compared to BI and BI+PDT 50 J/cm dl group.

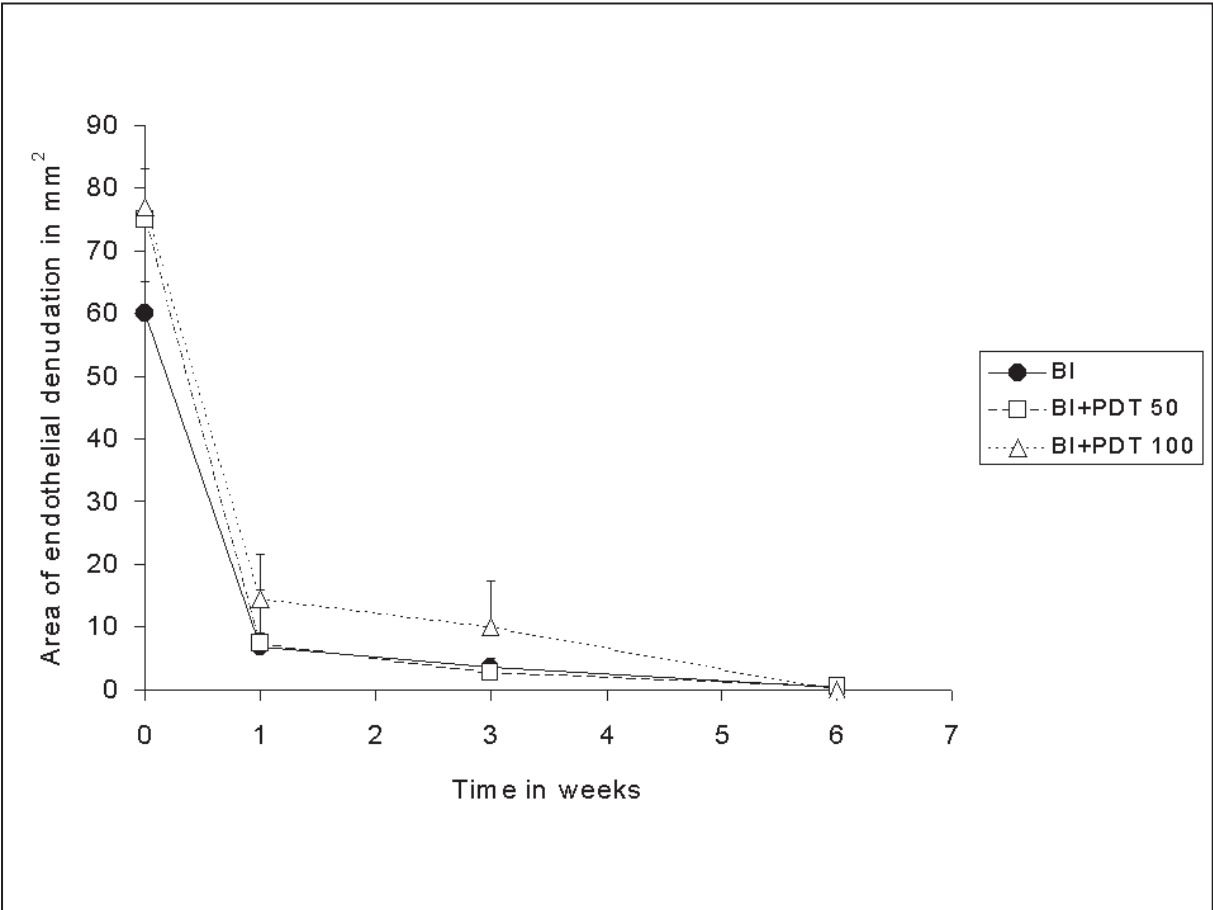
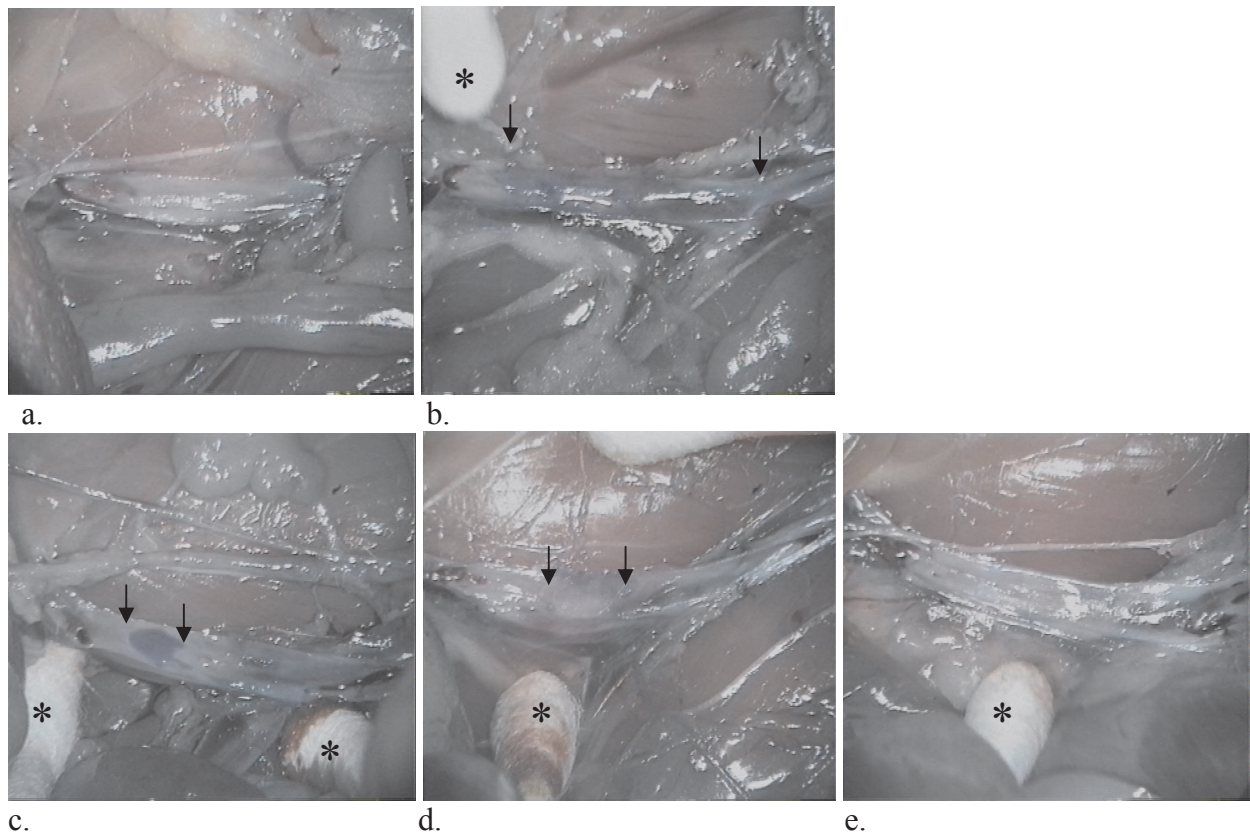


Figure 7.1 A graph showing the area of endothelial denudation in mm² on the y-axis, plotted against the time in weeks on the x-axis. The BI, BI+PDT 50 J/cm dl and BI+PDT 100 J/cm dl are expressed as means±SEM (n=5 per time-point).



*Figure 7.2 Photographs showing the Evans Blue stained areas of denudation in longitudinally opened right common iliac arteries: a. the untreated control at 0 weeks, b. the BI and BI+PDT treated artery at 0 weeks. The denudated area is blue (arrows) and cotton buds are marked with *, c. the BI artery at 3 weeks, d. the BI+PDT 50 J/cm dl at 3 weeks, e. the untreated control at 6 weeks and f. the BI and BI+PDT treated artery at 6 weeks.*

7.03.2 Light microscopic evaluation

Complete EC denudation with dehiscence of the basal lamina of the tunica intima and minor interruptions of elastic lamina in the tunica media was found directly after balloon injury. BI+PDT with 50 and 100 J/cm dl resulted in an acellular tunica media at 2-3 hr after the intervention <Fig.7.3a, 7.3b, 7.3c>. There was a time dependent IH development in the BI group whereas PDT resulted in a significant inhibition of IH up to 6 weeks <Fig. 7.3d, 7.4>. Noteworthy is the increased accumulation of IH at the laminal microruptures in the BI group compared to the fibrin deposition or proteoglycan accumulation at the laminal microruptures in the BI+PDT groups at 6 weeks <Fig. 7.3e, 7.3f, 7.3g>. The tunica media was repopulated with SMC's and fibroblasts in all groups after 6 weeks. Cellular hyperplasia and fibrin deposition in the tunica adventitia was more pronounced in the BI+PDT groups compared to the untreated control and BI group. Reendothelialization combined with a sealed basal and elastic lamina was seen during follow-up and completed after 6 weeks in all groups.

7.03.2 Light microscopic evaluation

Complete EC denudation with dehiscence of the basal lamina of the tunica intima and minor interruptions of elastic lamina in the tunica media was found directly after balloon injury. BI+PDT with 50 and 100 J/cm² resulted in an acellular tunica media at 2-3 hr after the intervention <Fig.7.3a, 7.3b, 7.3c>. There was a time dependent IH development in the BI group whereas PDT resulted in a significant inhibition of IH up to 6 weeks <Fig. 7.3d, 7.4>. Noteworthy is the increased accumulation of IH at the laminal microruptures in the BI group compared to the fibrin deposition or proteoglycan accumulation at the laminal microruptures in the BI+PDT groups at 6 weeks <Fig. 7.3e, 7.3f, 7.3g>. The tunica media was repopulated with SMC's and fibroblasts in all groups after 6 weeks. Cellular hyperplasia and fibrin deposition in the tunica adventitia was more pronounced in the BI+PDT groups compared to the untreated control and BI group. Reendothelialization combined with a sealed basal and elastic lamina was seen during follow-up and completed after 6 weeks in all groups.

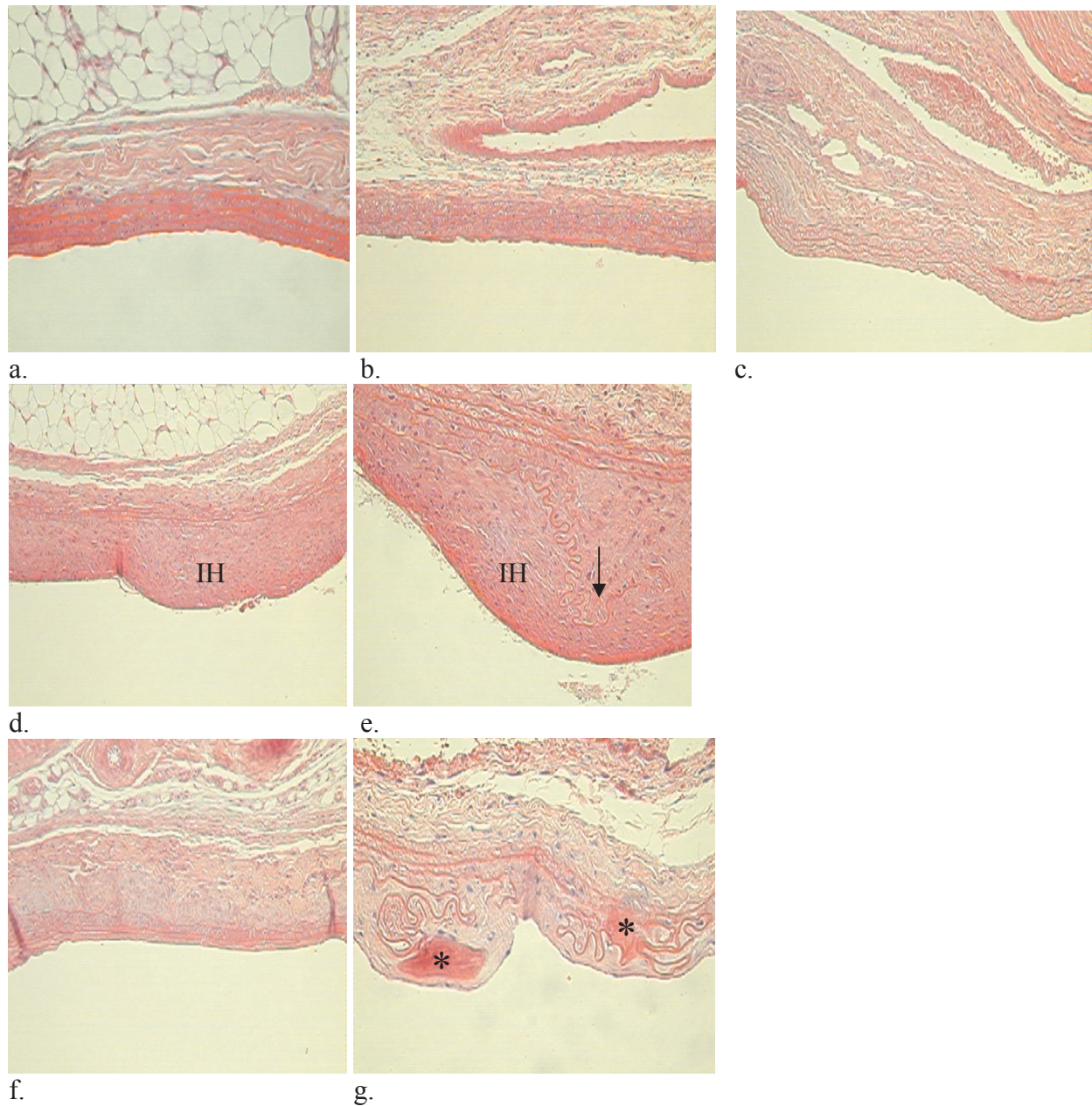


Figure 7.3 Photographs of HE stained longitudinal sections: a. the untreated control at 0 weeks, b. the BI at 0 weeks, c. the BI+PDT section at 0 weeks, d. the BI section at 6 weeks, e. A magnification of the IH. Note the dehiscence marked by a black arrow of the internal elastic lamina covered by hyperplasia, f. the BI+PDT section at 6 weeks, g. A magnification of 200x showing the typically dehiscence laminal fixation by fibrin (*) after PDT.

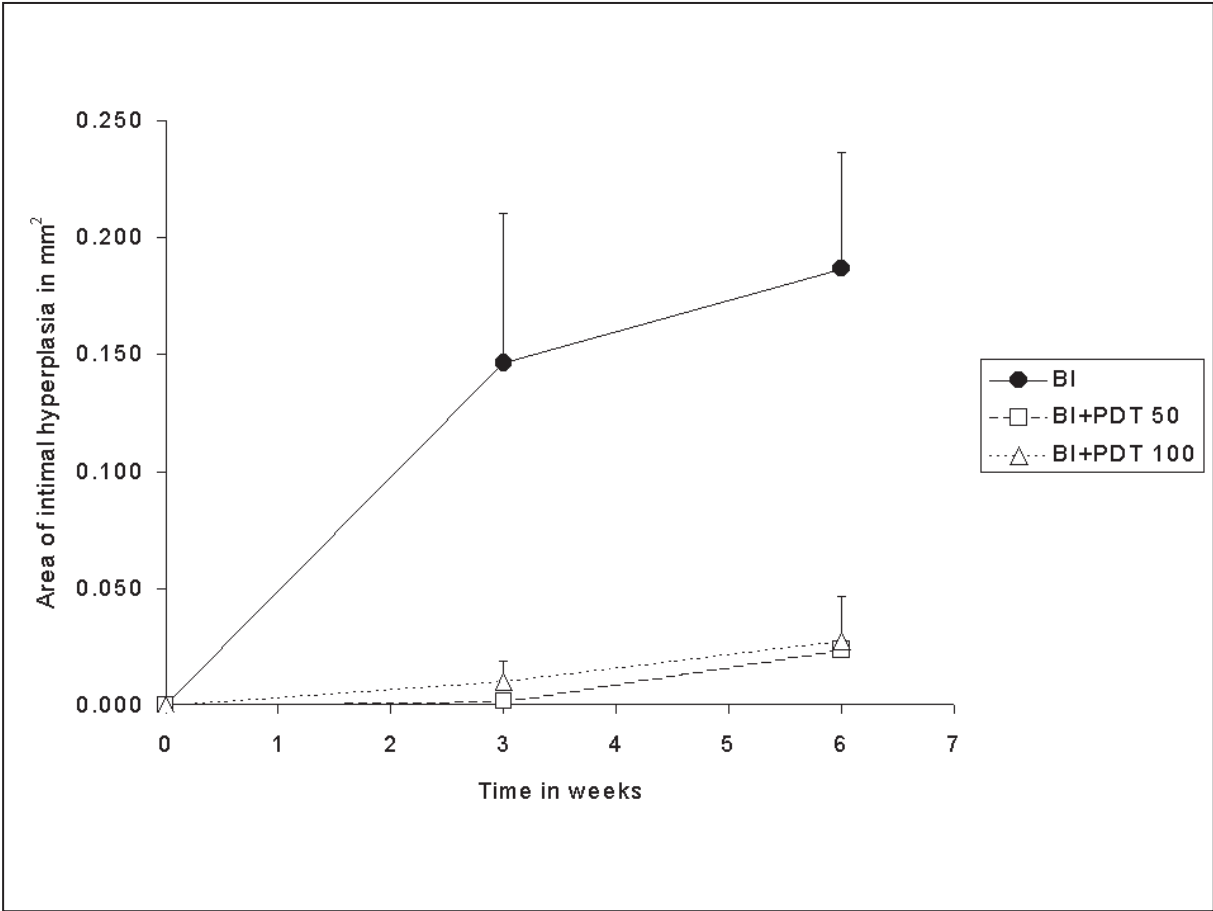


Figure 7.4 A graph showing the area of intimal hyperplasia in mm² on the y-axis plotted against the time in weeks on the x-axis. The BI, BI+PDT 50 J/cm dl and BI+PDT 100 J/cm dl are expressed as means±SEM (n=5 per time-point).

7.03.3 Expression of TGF- β

Immediately after the intervention, there was increased TGF- β expression at the inner border of the tunica adventitia in all treatment groups compared to the untreated group ($p < 0.05$) <Fig.7.5, 7.6a, 7.6b, 7.6c>. In the BI+PDT 100 J/cm dl group the TGF- β expression was significantly higher than in the other groups ($p < 0.05$). At 3 weeks after BI+PDT with both 50 and 100 J/cm dl, TGF- β expression was absent ($p < 0.01$ vs BI), but remained high ($40 \pm 20\%$) at the outer border of intimal hyperplasia in the BI group <Fig.7.5, 7.6d, 7.6e>.

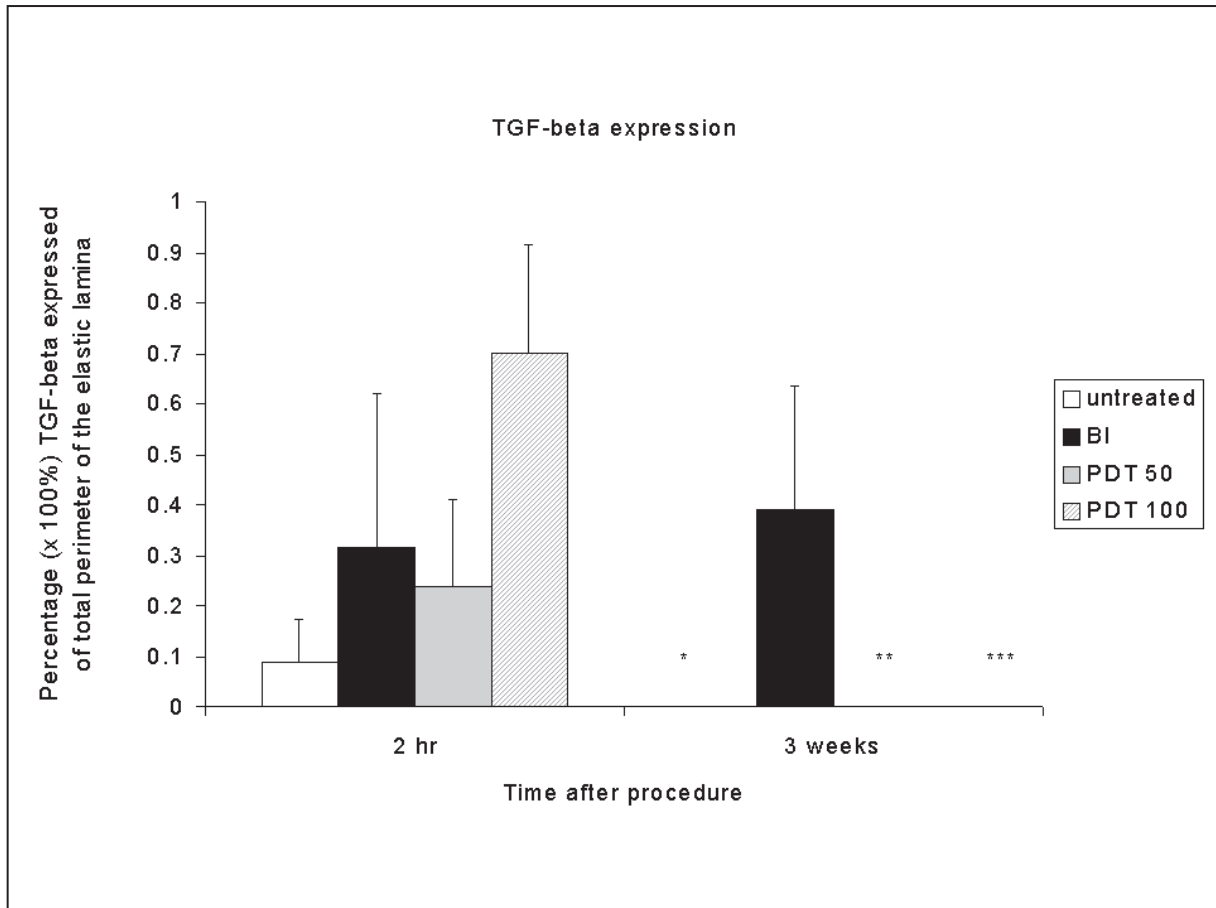


Figure 7.5 Bars showing the percentage TGF- β expression of the total perimeter of the elastic lamina on the y-axis, plotted against the time after the procedure. The untreated, BI, BI+PDT 50 J/cm dl and BI+PDT 100 J/cm dl are expressed as mean \pm SEM ($n=5$ per time-point). At 3 weeks, TGF- β is absent in the untreated (*), BI+PDT 50 (**), and BI+PDT 100 J/cm dl (***) and not in the corresponding group of 2 hr after the procedure.

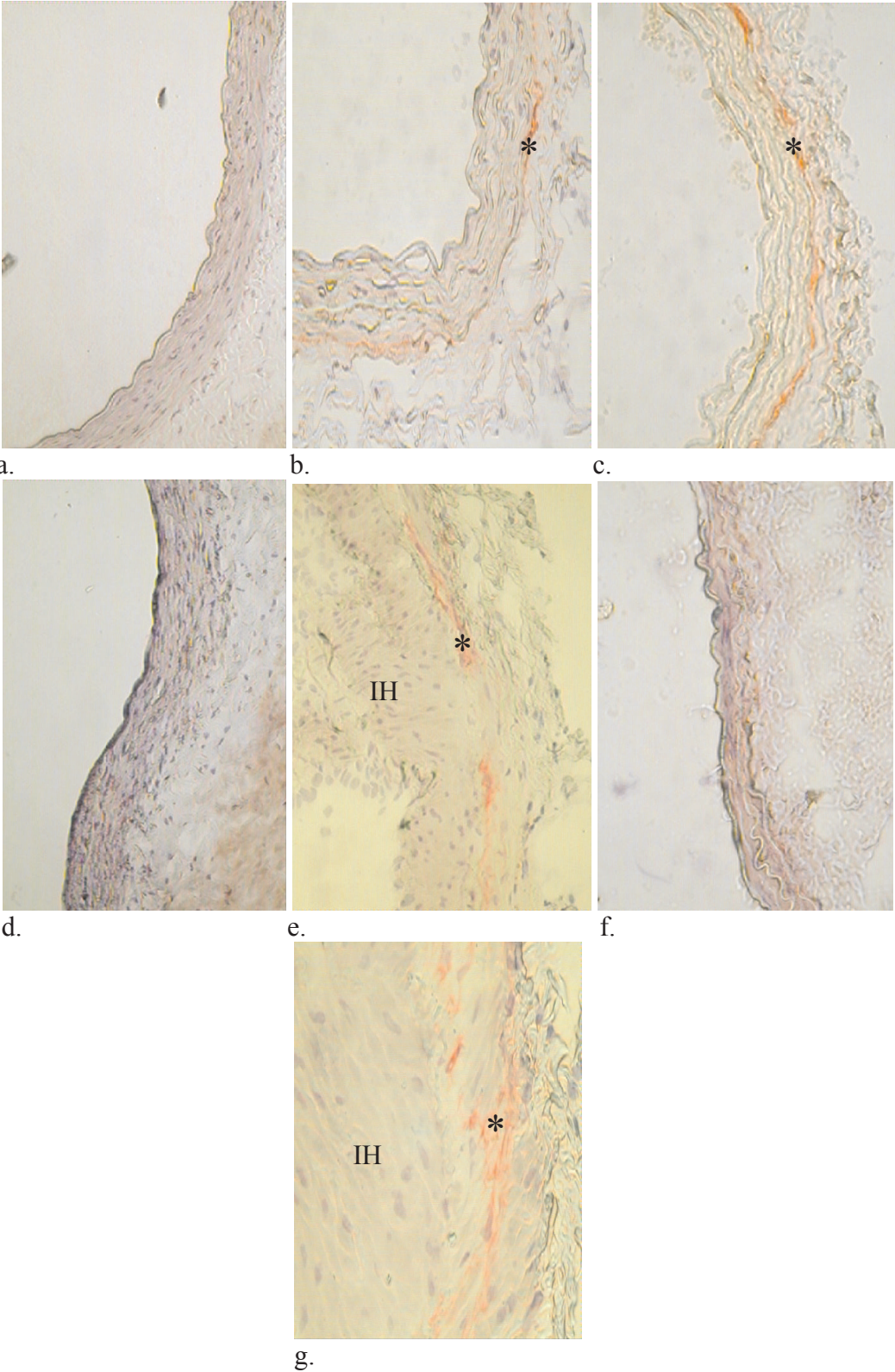


Figure 7.6 Photographs of pan-TGF- β stained (reddish:*) cross-sections. a. the untreated control at 0 weeks, b. the BI section at 0 weeks with TGF- β staining along the external elastic lamina (EEL), c. the BI+PDT section at 0 weeks with an acellular media and TGF- β staining along the EEL, d. the untreated control at 3 weeks, e. the BI section at 3 weeks with persistent TGF- β staining along the external border of IH, f. A magnification showing the TGF- β staining upon the external border of fibrocellular hyperplasia, g. the BI+PDT section at 3 weeks lacking TGF- β expression.

7.04 Discussion

This study examined for the first time the reendothelialization process after endovascular PDT of the rat iliac artery using aminolaevulinic acid (ALA). The pace and extent of endothelial cell (EC) regrowth is assumed to be of major importance in the vascular healing process [9] because lack of EC regrowth is believed to contribute to arterial narrowing [19]. For effective vascular PDT, a small area of uninjured vessel wall should be included in the treatment field to prevent ingrowth of smooth muscle cells from the edges [20]. This study shows that PDT did not impair the reendothelialization process after balloon injury. In all groups, there was a rapid reendothelialization with complete EC regrowth at 6 weeks. As reported earlier, PDT effectively inhibited IH in this study, whereas intimal hyperplasia (IH) developed in the control BI group, as expected in this model [4, 21]. Apparently, the development of IH at the dehiscence in the lamina and the rate or the extent of EC regrowth was not related in this model. It may be relevant in this regard, that fibrin deposition and proteoglycan accumulation was seen at the microruptured sites of the basal and elastic lamina of the BI+PDT treated vessels, instead of IH in the BI only treated vessels.

An earlier report described an incomplete reendothelialization of the balloon injured carotid artery (1-year follow-up) dependent on the length of denudation [8]. As compared to the carotid artery, there are more vasa vasorum in the tunica media and tunica adventitia in the iliac artery, which may affect the rate and extent of reendothelialization via transport of cytokines, chemokines and cells involved in the stimulation of EC growth. Comparisons with other studies related to reendothelialization in the rat iliac after BI could not be done, because of lack of exact reference models.

Because of the important role of TGF- β in regulating EC growth [22], we examined the presence of TGF- β after BI and after BI+PDT. Immediately after BI, there was an increased expression of TGF- β at the inner border of the tunica adventitia along the external elastic lamina. After 3 weeks, TGF- β expression remained high, but was seen at the outer border of intimal hyperplasia along the internal elastic lamina in the tunica media. PDT did not affect this pattern of TGF- β expression immediately after injury, but inhibited the expression of TGF- β after 3 weeks. This is in contrast with our previous *in vitro* study where the acute release of TGF- β by SMCs was inhibited after 100 J/cm² PDT [20], but was increased with a subtherapeutic dose of 10 J/cm², TGF- β activity. The present study indicated that PDT with 100 J/cm dl did not inhibit the acute release of TGF- β . It may well be that the different photosensitizer used in these studies may have been of influence. The photosensitizer chloroaluminum tetrasulfonated phthalocyanine (CASPC) used previously binds mainly to proteins in the extracellular matrix [23], while ALA induced intracellular formation of the photosensitizer protoporphyrin IX.

After 3 weeks, TGF- β expression at the outer border of intimal hyperplasia along the internal elastic lamina in the tunica media in the BI only group was still high. This persistent staining of TGF- β was not seen in the BI+PDT groups. This finding may be explained by the eradication of SMC in the tunica media of the BI+PDT group with only partial repopulation at 4 weeks [11]. However, it can not be excluded that differences in SMC function between the repopulating SMC's in the BI+PDT groups and proliferating SMC's in the BI group account for this phenomenon.

In contrast to the inhibitory effects of TGF- β on EC regrowth as described by Madri et al, the present study did not demonstrate a relation between TGF- β and EC growth [22]. However, we demonstrated here that the expression of TGF- β is far distant from the tunica intima. Therefore, it is conceivable that TGF- β can not exert its action there.

The fact that TGF- β was absent at 3 weeks after endovascular ALA-based PDT, while still present in the BI group, emphasises that PDT affects the vascular healing response in multiple ways. A recent study from our group described the prevention of constrictive remodelling of the iliac artery after endovascular ALA-based PDT [7]. It is tempting to speculate that the rapid down regulation of TGF- β expression plays an important role in the inhibitory effect of PDT on constrictive remodelling.

In conclusion: In this study, it was demonstrated that reendothelialization of the denuded iliac artery did not differ between BI and BI+PDT groups. The development of IH was not related to the pace and the extent of reendothelialization. Additionally, TGF- β appeared not to be directly involved in reendothelialization but its down regulation may be of crucial importance in the PDT dependent remodelling.

Acknowledgements

The authors are grateful for the financial support of the Netherlands Heart Foundation, NHS 97.181. They also would like to thank Patricia Lobe and Manon Holtman of the Department of Pathology for sectioning and HE staining and Marcel Kap of the Department of Internal Medicine for the TGF- β staining protocol.

References

- [1] Gabeler EEE, van Hillegersberg R, Stadius van Eps RG, Sluiter W, Mulder P, van Urk H. Endovascular Photodynamic Therapy with Amino Laevulinic Acid Prevents Balloon Induced Intimal Hyperplasia and Constrictive Remodelling. *Eur.J.Vasc.Endovasc.Surg.* 2002;24[4], 322-331.
- [2] Jenkins MP, Buonaccorsi GA, Raphael M, Nyamekye I, McEwan JR, Bown SG, Bishop CC. Clinical study of adjuvant photodynamic therapy to reduce restenosis following femoral angioplasty. *Br J Surg* 1999; 86(10):1258-1263.
- [3] Nyamekye I, Anglin S, McEwan J, MacRobert A, Bown S, Bishop C. Photodynamic therapy of normal and balloon-injured rat carotid arteries using 5-amino-levulinic acid. *Circulation* 1995; 91(2):417-425.
- [4] Grant WE, Speight PM, MacRobert AJ, Hopper C, Bown SG. Photodynamic therapy of normal rat arteries after photosensitisation using disulphonated aluminium phthalocyanine and 5-aminolaevulinic acid. *Br J Cancer* 1994; 70(1):72-78.
- [5] Jenkins MP, Buonaccorsi GA, Raphael M, Nyamekye I, McEwan JR, Bown SG, Bishop CC. Clinical study of adjuvant photodynamic therapy to reduce restenosis following femoral angioplasty. *Br J Surg* 1999; 86(10):1258-1263.
- [6] Henderson BW, Bellnier DA. Tissue localization of photosensitizers and the mechanism of photodynamic tissue destruction. *Ciba Found Symp* 1989; 146:112-25; discussion 125-30:112-125.
- [7] Henderson BW, Dougherty TJ. How does photodynamic therapy work? *Photochem Photobiol* 1992; 55(1):145-157.
- [8] A.W.Clowes, M.E.Reidy, M.M.Clowes. Kinetics of cellular proliferation after arterial injury;3.Endothelial and smooth muscle growth in chronically denuded vessels. *Laboratory Investigation* 1986. 54[3], 295-303.
- [9] Asahara T, Bauters C, Pastore C. Local delivery of vascular endothelial growth factor accelerates reendothelialization and attenuates intimal hyperplasia in balloon-injured rat carotid artery. *Circulation* 1995; 91:2793-2801.
- [10] Stadius van Eps RG, Adili F, Watkins MT, Anderson RR, LaMuraglia GM. Photodynamic therapy of extracellular matrix stimulates endothelial cell growth by inactivation of matrix-associated transforming growth factor-beta. *Lab Invest* 1997; 76(2):257-266.
- [11] Majesky MW, Lindner V, Twardzik DR, Schwartz SM, Reidy MA. Production of transforming growth factor beta 1 during repair of arterial injury. *J.Clin.Invest* 1991. 88, 904-910.
- [12] Schulick AH, Taylor AJ, Zuo W, Qiu CB, Dong G, Woodward RN, Agah R, Roberts AB, Virmani R, Dichek DA. Overexpression of transforming growth factor beta 1 in arterial endothelium causes hyperplasia, apoptosis, and cartilaginous metaplasia. *Proc Natl Acad Sci U S A* 1998; 95(12):6983-6988.
- [13] Rasmussen LM, Wolf YG, Ruoslahti E. Vascular smooth muscle cells from injured rat aortas display elevated matrix production associated with transforming growth factor-beta activity. *Am J Pathol* 1995. 147, 1041-1048.
- [14] Gabeler EEE, van Hillegersberg R, Stadius van Eps RG, Sluiter W, Gussenhoven EJ, Mulder P, van Urk H. A Comparison of Balloon Injury Models after Endovascular Lesions in the Rat. *BMC Cardiovascular Disorders* 2002; 2(1):16-26.
- [15] Heisterkamp J, Hillegersberg van R, Sinofsky E, IJzermans J. Heat resistant cylindrical diffuser for interstitial laser coagulation: Comparison with a bare-tip fibre in ex vivo porcine liver. *Lasers Surg.Med.* 1997. 20, 304-309.
- [16] Hinnen P, de Rooij FW, Voortman G, Tilanus HW, Wilson JHP, Siersema PD. Acrylate yellow filters in operating lights protect against photosensitization tissue damage. *Br.J.Surg.* 2000. 87, 231-235.

- [17] Indolfi C, Cioppa A, Stabile E, Di Lorenzo E, Esposito G, Pisani A, Leccia A, Cavuto L, Stingone AM, Chieffo A, Capozzolo C, Chiariello M. Effects of hydroxymethylglutaryl coenzyme A reductase inhibitor simvastatin on smooth muscle cell proliferation in vitro and neointimal formation in vivo after vascular injury. *J Am Coll Cardiol* 2000; 35(1):214-221.
- [18] Wenguang L, Gussenhoven EJ, Bosch JG, Mastik F, Reiber JHC, Bom N. A computer-aided analysis system for the quantitative assessment of intravascular ultrasound images. *Proc Computers in Cardiology* 2001; 1990:333-336.
- [19] Davies MGD, Hagen PO. The vascular endothelium: A new horizon. *Ann.Surg.*1993.. 218, 593-609.
- [20] Stadius van Eps RG, Adili F, Watkins MT, Anderson RR, LaMuraglia GM. Photodynamic therapy of extracellular matrix stimulates endothelial cell growth by inactivation of matrix-associated transforming growth factor-beta. *Lab Invest* 1997; 76(2):257-266.
- [21] Ortu P, LaMuraglia GM, Roberts WG, Flotte TJ, Hasan T. Photodynamic therapy of arteries. A novel approach for treatment of experimental intimal hyperplasia. *Circulation* 1992; 85(3):1189-1196.
- [22] Madri JA, Reidy MA, Kocher O, Bell L. Endothelial cell behavior after denudation injury is modulated by transforming growth factor-beta and fibronectin. *Lab Invest* 1989; 60:755-764.
- [23] Stadius van Eps RG, LaMuraglia GM. Photodynamic therapy inhibits transforming growth factor beta activity associated with vascular smooth muscle cell injury. *J Vasc Surg* 1997; 25(6):1044-1052.

SECTION V

CHAPTER 8

Endovascular Photodynamic Therapy Alters the Inflammatory Reaction in the Arterial Response to Injury

¹Edward E.E. Gabeler, ²Wim Sluiter, ¹Richard van Hillegersberg, ³Elly Bruyn, ¹Randolph G. Stadius van Eps, ¹Hero van Urk

¹Department of Surgery, Erasmus MC, Rotterdam, The Netherlands

²Department of Biochemistry, Erasmus MC, Rotterdam, The Netherlands

³Department of Pathology, Daniel den Hoed Oncology Center, Erasmus MC, Rotterdam, The Netherlands

Keywords: leukocytes, photodynamic therapy, remodelling, restenosis

submitted

Abbreviations: ALA. Aminolaevulinic acid, BI. Balloon injury, DAB. Di-amino-benzidin Substrate-Chromogen solution, IH. Intimal hyperplasia, LO. Light only, PDT. Photodynamic therapy, PpIX. Protoporphyrin IX, SMC. Smooth muscle cell, VV. vasa vasorum.

8.00 Abstract

Background: Endovascular Photodynamic Therapy (PDT) prevents intimal hyperplasia following angioplasty. How PDT exerts this beneficial effect is unknown. Since the inflammatory reaction plays a role in the wound healing of the injured artery, we questioned if PDT affected the inflammatory response. Therefore, we studied the accumulation of leukocytes in the artery after treatment.

Materials & Methods: Rats were divided into 2 main groups. 1. The BI, BI+LO 50 J/cm dl and BI+LO 100 J/cm dl groups served as reference. 2. The experimental BI+PDT groups were illuminated with fluences of either 50 or 100 J/cm diffuser length (dl). The rats were sacrificed after either 2 hours or 16 weeks.

Results: Directly after procedure, more leukocytes (mean 309 ± 82 cells/section: 94% neutrophils; 18% mast cells; 6% T-cells; 1% monocytes) were found in the reference groups than in the experimental groups (mean 155 ± 19 cells/section: 22% neutrophils; 13% mast cells; 65% T-cells; 1% monocytes) ($p < 0.05$). After 16 weeks, a significant decrease was seen in all groups, but still more leukocytes 49 ± 12 cells/section (18% neutrophils; 16% mast cells; 56% T-cells; 5% monocytes) were present in the reference than in the experimental groups; 16 ± 3 cells/section (35% neutrophils; 50% mast cells; 16% T-cells; 6% monocytes) ($p < 0.05$). The IH after 16 weeks was significantly less in the BI+PDT groups compared to the BI+LO groups.

Conclusion: Endovascular PDT modifies the inflammatory response after BI. The decrease of the influx of neutrophils into the vessel wall may be one of the mechanisms underlying the inhibition of late lumen loss by PDT after vascular intervention.

8.01 Introduction

Arterial injury-induced restenosis after dilation of a stenotic or occluded artery decreases the long-term success rate to 70 or even 50% [1].

In the development of restenosis, the inflammatory response to arterial injury plays a crucial role [2]. This response begins with the recruitment neutrophils and monocytes [3]. These leukocytes play an ambiguous role at the injured site, and precede the influx of T-cells.

On the one hand, the neutrophils and monocytes eliminate redundant necrotic arterial tissue and apoptotic cells by phagocytosis. On the other hand, the growth of smooth muscle cells and the subsequent deposition of extracellular matrix is stimulated via the release of cytokines. Apparently, these processes are often misbalanced, which leads to fibrocellular stenosis [4].

The first cells to arrive at the lesion site in the vasa vasorum of the tunica adventitia are neutrophils [5;6]. It has been reported that an excessive influx of neutrophils and of activated monocytes after arterial injury is related to late lumen loss [3;7], whereas T-cells are related to medial fibrosis [8].

A successful experimental-adjuvant strategy to prevent restenosis is vascular photodynamic therapy (PDT)[9-13]. It has been shown that this preventive potential of PDT is partly based on the selective killing of excessively proliferating smooth muscle cells (SMC) and partly on structural modifications of the extracellular matrix [14]. This is induced by the generation of highly cytotoxic oxygen radicals upon illumination of a photosensitizer that has accumulated within these cells or in the matrix (15;16).

Since the accumulation of leukocytes at the lesion site of the vascular wall is directly related to arterial stenosis, inhibition of the inflammatory reaction by PDT may underlie the beneficial effect of this treatment modality as well. It could be possible that by decreasing the number of vasa vasorum in the tunica adventitia, PDT hampers the entry of the inflammatory cells into the lesion.

Therefore, the effect of endovascular PDT after balloon injury was assessed on the number and type of infiltrating leukocytes including mast cells in the tunica intima, tunica media and tunica adventitia. Furthermore, the effect of PDT on the vasa vasorum in the tunica adventitia was studied as well.

8.02 Materials & methods

8.02.1 Rats

The experimental protocol was approved by The Committee on Animal Research of the Erasmus University of Rotterdam and complied with “Principles of Good Laboratory Practice”. Male inbred Wistar rats (Harlan CPB, Austerlitz, The Netherlands) weighing 200-300 g were used. The animals had free access to rat chow (AM II, Hope Farms, Woerden, The Netherlands) and tap water acidified to pH 4.0, while maintained in a 12-hr light/dark cycle.

8.02.2 Study design

Fifty rats were randomly assigned to 2 main groups, in which arterial damage was induced via standard balloon injury (BI) of the right common iliac artery (17). The references consisted of the groups BI (n=10), BI+ light only (LO) at 50 J/cm diffuser length (dl) (n=10) and BI+LO at 100 J/cm dl (n=10). In the experimental groups BI+PDT at 50 J/cm dl (n=10) and BI+PDT at 100 J/cm dl (n=10), aminolaevulinic acid (ALA) was administered 2½ hr before BI, followed by endovascular illumination with fluences of either 50 or 100 J/cm diffuser

length (dl). The animals were sacrificed after either 2 hr (n=5 per group) or 16 weeks for perfusion-fixation of the artery. Transverse sections were evaluated by light microscopic planimetric analysis.

8.02.3 Photosensitization

The PDT groups received iv 200-mg/ kg ALA (Sigma-Aldrich Chemie, Zwijndrecht, The Netherlands) dissolved in phosphate buffered saline at 40 mg/ml of pH 7.45. The solution was freshly made for each animal and kept from light exposure. The photosensitised rats were kept in the dark 2½ hr prior to surgery until 12 hr after the operation to prevent uncontrolled phototoxicity.

8.02.4 Laser

A dye laser (600 Series Dye Module, Laserscope, Surgical Systems, San Jose, CA, USA), pumped by a 532/KTP surgical laser (Laserscope, Surgical Systems, San Jose, CA, USA), was used to generate monochromatic light of 633 nm. The power emitted from the cylindrical diffusing tip (core diameter 200 µm, outer diameter 1.0 mm, tip length 20 mm: Lightstic™, Cardiofocus, West Yarmouth, MA, USA)[18] was calibrated with an in-built power meter, and verified with an external linear diffuser in an integrating cylindrical sphere (Optometer Model 370, Graseby Optronics, Orlando, FL, USA). A spectroscope (WaveMate, Coherent, Auburn, CA, USA) was used to verify the accuracy of the wavelength. Temperature and linear fluence measurements in the arterial wall were performed in an earlier study for optimal PDT effect determination. In this study only the irradiance and fluences were calibrated.

8.02.5 Balloon injury

A median laparotomy was performed under general anaesthesia with intramuscular injection of ketamine (Ketalar, Parke Davis and Co., Inc., 40 mg/kg) and xylazin (Rompun Bayer Ag, Leverkusen, Germany; 5 mg/kg). Subdued light using a yellow filter (620-650 nm Kodak) was applied during the procedure [19]. The right common iliac artery was cranially and caudally temporarily occluded with vascular clamps (Haemostat B1, Stöpler, Utrecht, The Netherlands). To create a blood free lumen, the arteries were flushed with 1.0-ml heparin (50 IU/ml 0.9 % NaCl, Infusion solution Baxter) through an arteriotomy 5 mm cranially from the abdominal aortal bifurcation. Then, a balloon catheter (Fogarty arterial embolectomy catheter, 2 F, 60 cm, Baxter BV, Utrecht, The Netherlands) was inserted and inflated to 2.0 bar with a manometer (Basix25™, Medioterm, USA) and deionised water [20]. A right iliac artery section of 15 mm from the bifurcation was damaged by inflating the balloon distally from the bifurcation. Then, after simultaneously pulling and rotating at 120° towards the bifurcation, the balloon was deflated at the end of the section. This procedure was consecutively performed 3 times. Then, in the BI+LO and BI+PDT groups, endovascular illumination was performed. A single suture in the vascular sheet marked the middle of the denuded area. After flushing the lumen with heparin and a two layer closing (interrupted 9-0 prolene sutures) of the arteriotomy, both the caudal and the cranial clamp were removed. Directly thereafter, reperfusion of the dilated section was observed. The abdominal wall was closed in two layers (continuous 2-0 prolene sutures).

8.02.6 Endovascular Photodynamic Therapy (PDT)

In the BI+LO and BI+PDT groups, a 400- μm fibre (Lightstic 360, Rare Earth Medical Inc., West Yarmouth, MA, USA) with a 20 mm long cylindrical diffusing tip was applied immediately after BI(18). The fibre tip was centred endovascularly in the denuded area to illuminate 15 mm of the damaged and 5 mm of the untreated arterial wall both cranially as caudally. Because of the cylindrical illumination, the fluence was expressed in Joule per cm diffuser length ($\text{J}/\text{cm dl}$). The target area was illuminated at a fluence rate of $100 \text{ mW}/\text{cm}^2$. After treatment, the lumen was thoroughly flushed with 1ml heparin solution (50 IU/ml). Abdominal organs were protected from light exposure with a light absorbing plastic folium during illumination. The animals recovered in the dark after treatment

8.02.7 Specimen handling

A standard perfusion-fixation procedure via the thoracic aorta was performed under ether anaesthesia, in which the lumen was flushed with PBS (pH 7.45) for 2 min, followed by a perfusion of 10 min with formaldehyde (3.7 %) at 100 mm Hg. The distally marked segment of 15 mm was carefully harvested after length measurement and stored in formaldehyde (3.7 %) for at least 24 hr. Thereafter, the specimens were embedded in paraffin. Three cross sections of 10 μm each were cut with a microtome from distal to proximal at 3, 5 and 10 mm, mounted on a microscopic object slide and stained for conventional light microscopy. All mounted sections were video taped with a digital camera for histologic analysis. Perivascular arteriole and inflammatory cells in the tunicas intima, media and adventitia were counted at 400x magnification. The tunica adventitia was defined as 2 microscopic fields from the external elastic lamina. A digital video analyser system (IBM Corp., Boca Raton, USA) was used for the assessment of the absolute intimal area in mm^2 .

8.02.8 Immunohistochemistry staining of pan-leukocytes

Following dehydration and paraffin embedding, sections of 4 μm thick were cut and stained for CD-45 (OX-1, Serotec MCA 43 R) using the following protocol: Firstly, the sections were fixed with acetone for 10 min and air dried for 15 min at 37°C . With a Peroxidase-Anti-Peroxidase (PAP) pen circles were drawn around the tissue sections and washed with PBS three times. Then, the endogenous peroxidase activity was blocked with 0.05 % H_2O_2 in PBS for 15 min and rinsed three times with PBS. After preincubation of the sections for 15 min with 0.1 % normal rabbit serum, diluted (1:1000) mouse-anti-rat CD-45 antibody was added for an incubation period of 60 min in humidified atmosphere. Importantly, we found that CD45 of Santa Cruz (35-Z6: sc-1178) was only suitable for FACS analysis of rat leukocytes, but not for their detection in paraffin embedded sections. Next, the sections were rinsed with PBS for three times, incubated with secondary rabbit-anti-mouse antibody for 30 min and again rinsed three times with PBS. Di-amino-benzidin Substrate-Chromogen solution (DAB) was added and sections were incubated for 5-15 min. Rinsing with water for 5 min stopped the DAB-reaction. The sections were put in Mayer's haematoxylin for 40 sec, rinsed and shortly kept in an ammonia-solution. Next, the sections were stepwise dehydrated using a series of 70 %, 90 % and 100 % ethanol, followed by a xylene step. Then, the sections were covered with a coverslip for examination using a light microscope. The intensity of the depositions / expression in the arterial samples was scored blindly via quantitative analysis.

8.02.9 Staining of polymorphonuclear neutrophils and of mast cells

For identifying the neutrophils and mast cells, we used the staining method according to Leder. In short, the sections were deparaffinated, dehydrated using xylene, graded alcohols, rinsed with tap water, and finally one time with distilled water. Next, the sections were incubated in freshly made Leder solution (solution A: 1 drop 4 % pararosaniline, 1 drop 4 % sodium nitrite diluted with 30 ml Veronal buffer pH 7.2, acidified to pH 6.3 with 2M hydrochloric acid, mixed with solution B: 0.1M sodium Veronal and 10 mg of naphthol-AS-D-chloroacetate in 2 ml dimethyl formamide) for 30 min at 37°C, followed by rinsing with tap water for 10 min. The sections were incubated in Mayer haematoxylin for 5 min, followed by rinsing with tap water and next, the sections were covered with a drop IMSOL (IP). After being air-dried at 37°C, the sections were covered with PERTEX.

8.02.10 Staining of pan-T cells

We used a CD-3 antibody (Serotec MAR, CD-3, MCA 772) for pan-T cell staining according to the same protocol as for the CD-45 staining. The marker stained T-helper cells and cytotoxic T-cells only.

8.02.11 Staining of monocytes

For identifying the monocytes the specific esterase 1 staining according to Ornstein was performed. In short, the sections were deparaffinated with xylene, graded alcohols and rinsed with tap water and next, the fixed sections were incubated for 25 min with freshly made Ornstein solution (Solution A: 0.8 ml of 1 g Basic Fuchsin in 30 ml 2M HCl with 0.8 ml of 1 g NaNO₂ in 30 ml water acidified after 30 sec with 4 ml 0.40 M sodium cacodylate, was added to 15 ml distilled water and 0.15 ml of 10 % Tween 20. Then A was mixed with Solution B: 2 ml of 260 mg naphthylbutyrate in 50 ml dioxane was added to 3 ml methanol and diluted with distilled water to 50 ml). After staining with Giemsa for 4 min, the sections were covered with PERTEX. We found that detection of rat monocytes using CD-20 of Santa Cruz (C-20:sc-7733) and of Serotec (MAR ED-1: MCA 341 R) was not possible in paraffin embedded sections, but only by FACS analysis.

8.02.12 Statistical analysis

The area of intimal hyperplasia (IH) was expressed as mean \pm standard error of the mean (SEM). The mean area of IH was compared using a paired Student's t-test. Differences between the means of the number of leukocytes in the tunica intima, tunica media and tunica adventitia, their differential counts, i.e. neutrophils, mast cells, T-cells and monocytes, and the numbers of arteriole were evaluated for significance using a General Linear Multivariate analysis. A difference was considered to be significant at a p-value of less than 0.05.

8.03 Results

All rats were healthy during the study and no side effects of phototoxicity were seen after ALA application. Eosinophils and basophils were not detected in any tissue under study.

8.03.1 Tunica intima

Immediately after BI, the mean number of leukocytes was 1.4 ± 0.4 cells per section in the BI group, 1.6 ± 0.81 cells/section in the BI+LO 50 J/cm dl group and 0.4 ± 0.24 cells/section in the BI+LO 100 J/cm dl group <Fig.8.1a>. After 16 weeks, a significant, but small increase to 5.17 ± 2.56 cells/section in the BI and to 10 ± 6.16 cells/section in the BI+LO 50 J/cm dl was seen ($p < 0.05$). The number of leukocytes remained at 0.4 ± 0.24 cells/ section in the BI+LO 100 J/cm dl after 16 weeks <Fig.8.1a>. Immediately after the procedure and after 16 weeks, no leukocytes with the exception of sporadic leukocytes were seen in the tunica intima of the sections of the BI+PDT 50 J/cm dl and of the BI+PDT 100 J/cm dl groups <Fig.8.1a>. Directly after BI the leukocytes mainly consisted of neutrophils, while sporadic mast cells, T-cells and monocytes were seen after 16 weeks <Fig.8.2a>. Directly after PDT and after 16 weeks, only some T-cells were seen.

With regard to the development of IH after 16 weeks, the mean IH area in the BI group of $0.21 \pm 0.05 \text{ mm}^2$ was significantly ($p < 0.05$) higher than the mean area IH of $0.07 \pm 0.03 \text{ mm}^2$ that occurred in the BI+PDT groups.

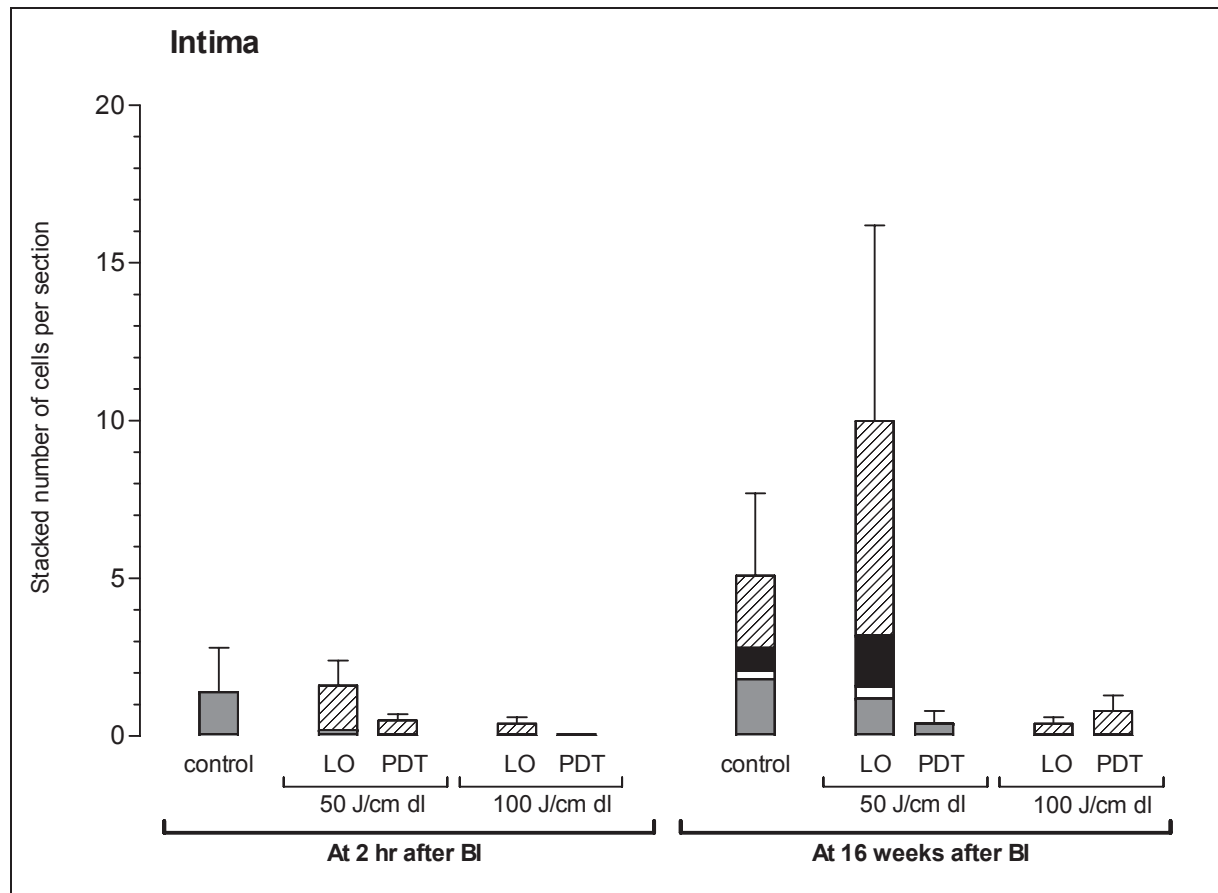


Figure 8.1a A bar diagram representing the amount of neutrophils (stripes), mast cells (white), T-cells (black) and monocytes (gray) per section plotted against the control groups: control, LO and PDT at 2 hrs and at 16 weeks, in the tunica intima.

8.03.2 Tunica media

Immediately after BI, BI+LO 50 J/cm dl and BI+LO 100 J/cm dl, there were no leukocytes in the tunica media with exception of 3.0 ± 1.10 cells/section in the BI+LO 50 J/cm dl group <Fig.8.1b>. After 16 weeks, respectively 1.0 ± 0.45 (BI), 0.8 ± 0.58 (BI+LO 50) and 0.4 ± 0.4 cells/section (BI+LO 100) were seen <Fig.8.1b>. No leukocytes were observed in the BI+PDT 50 J/cm dl or BI+PDT 100 J/cm dl groups immediately after PDT and 16 weeks thereafter <Fig.8.1b>. The few leukocytes present in the tunica intima of the BI, BI+LO 50 J/cm dl or BI+LO 100 J/cm dl groups after 16 weeks, showed that they were neutrophil or T-cell <Fig.8.2b>.

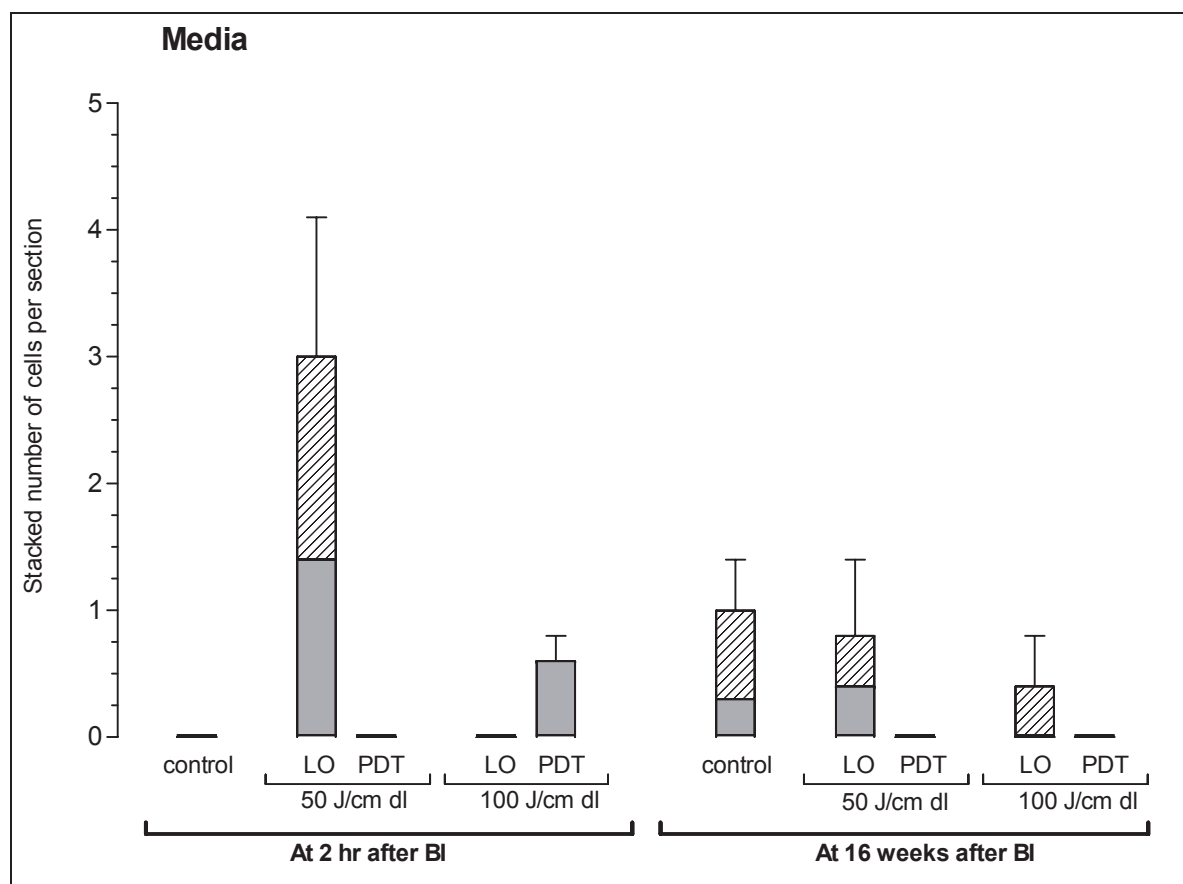


Figure 8.1b A bar diagram representing the amount number of neutrophils (stripes), mast cells (white), T-cells (black) and monocytes (gray) per section plotted against the control groups: control, LO and PDT at 2 hrs and at 16 weeks, in the tunica media.

8.03.3 Tunica adventitia

In the tunica adventitia the number of leukocytes directly after BI, BI+LO 50 or BI+LO 100 J/cm dl was high and amounted to respectively 340 ± 89 , 181 ± 68 and 406 ± 89 cells/ section. After 16 weeks significantly less leukocytes were present in those groups, respectively 84 ± 31 , 30 ± 3 and 33 ± 3 cells/section. Immediately after PDT using 50 J/cm dl (BI+PDT 50 J/cm dl group) the number of leukocytes amounted to 205 ± 28 cells/section, which were similar in the respective BI+LO group. However, after PDT using 100 J/cm dl 104 ± 9 cells/ section were present in the tunica adventitia, which is about a factor 4 less than in the respective BI+LO group <Fig.8.1c>. After 16 weeks the number of leukocytes in both BI+PDT groups significantly decreased to 16 ± 3 and 16 ± 2 cells/section <Fig.8.1c>.

Directly after BI, BI+LO 50 J/cm dl and BI+LO 100 J/cm dl, the infiltrate mainly existed of neutrophils amounting to respectively 313 ± 90 (92%), 153 ± 71 (81%), 393 ± 97 (98 %) per section, and decreased to 29 ± 5 (34%), 3 ± 2 (10%), 3 ± 1 (9 %) per section respectively after 16 weeks <Fig.8.1c>. In the experimental groups, the number of neutrophils was much smaller. Directly after BI+PDT 50 and 100 J/cm dl respectively only 49 ± 26 (24%) and 20 ± 7 (19%) per section were present, but this number decreased after 16 weeks to 11 ± 2 (69%) and 0 per section <Fig.8.1c>.

The number of mast cells directly after BI, BI+LO 50 J/cm dl and BI+LO 100 J/cm dl was small, respectively 6 ± 1 (2%), 11 ± 5 (6%) and 7 ± 1 (2 %) per section. Those numbers did not change much after 16 weeks and were respectively 4 ± 2 (5%), 7 ± 2 (23%), 7 ± 1 (21 %) per section. The number of mast cells directly after PDT using 50 and 100 J/cm dl was slightly higher than after BI+LO, being 15 ± 7 (7%) per section respectively, and 20 ± 1 (19%), and after 16 weeks 4 ± 1 (25%), 12 ± 2 (74%) per section.

The number of T-cells directly after BI, BI+LO 50 J/cm dl and BI+LO 100 J/cm dl was respectively 20 ± 7 (6%), 21 ± 2 (11%), 5 ± 1 (1 %) per section and remained at that level after 16 weeks, respectively 53 ± 27 (42%), 19 ± 1 (63%) and 21 ± 2 (64 %) per section <Fig.8.1c>.

The numbers of T-cells directly after PDT using 50 and 100 J/cm dl were much higher than after BI+LO, respectively amounting to 142 ± 11 (69%), 63 ± 6 (61%) per section, and after 16 weeks decreased to only 1 ± 0.4 (6%), 4 ± 2 (25%) per section <Fig.8.1c>.

The number of monocytes directly after BI, BI+LO 50 J/cm dl and BI+LO 100 J/cm dl was respectively 2 ± 1 (1%), 4 ± 1 (2%), 1 ± 0.2 (0%) per section and after 16 weeks 5 ± 3 (6%), 1 ± 0.2 (3%), 2 ± 1 (6 %) per section. The number of monocytes directly after PDT using 50 and 100 J/cm dl was 0 and 2 ± 1 (1 %) and after 16 weeks 1 ± 0.4 (6%), 1 ± 0.2 (6%) <Fig.8.1c>.

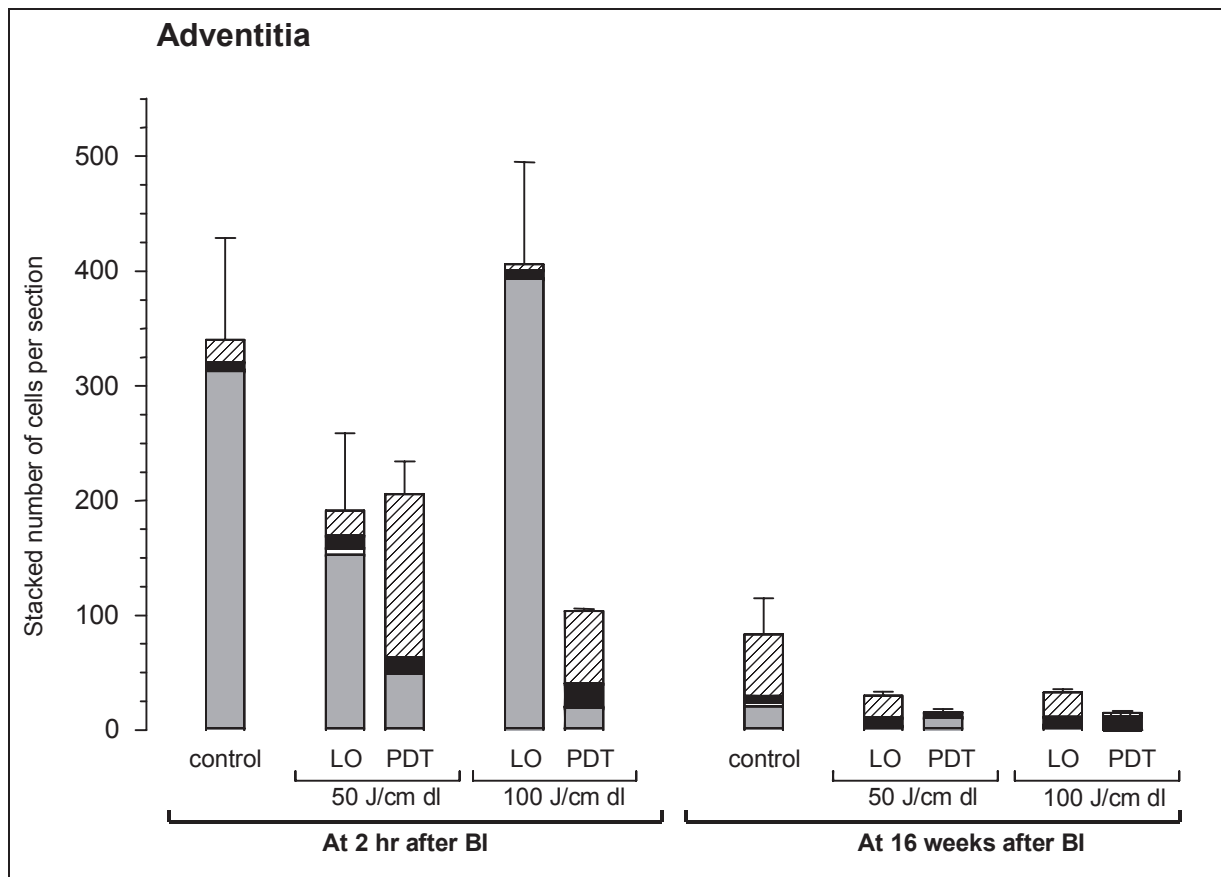


Figure 8.1c A bar diagram representing the amount of number of neutrophils (stripes), mast cells (white), T-cells (black) and monocytes (gray) per section plotted against the control groups: control, LO and PDT at 2 hrs and at 16 weeks, in the tunica adventitia.

8.03.4 Vasa vasorum in the tunica adventitia

The number of vasa vasorum (vv) in the tunica adventitia directly after the procedure <Fig.8.2> was significantly higher ($p < 0.011$) in the reference groups compared to the experimental groups. In the BI, BI+LO 50 and BI+LO 100 J/cm dl groups there were respectively 12 ± 5 , 16.8 ± 3.4 and 13.4 ± 2.2 vv/section compared to the BI+PDT groups having respectively 4.17 ± 1.4 (50 J/cm dl) and no vv/section (100 J/cm dl). However, after 16 weeks, the number of vasa vasorum increased significantly in all groups ($p < 0.001$) and did not differ between the treatments anymore, i.e. in the reference groups (25-36 vv/section) and in the experimental groups (28-31 vv/section).

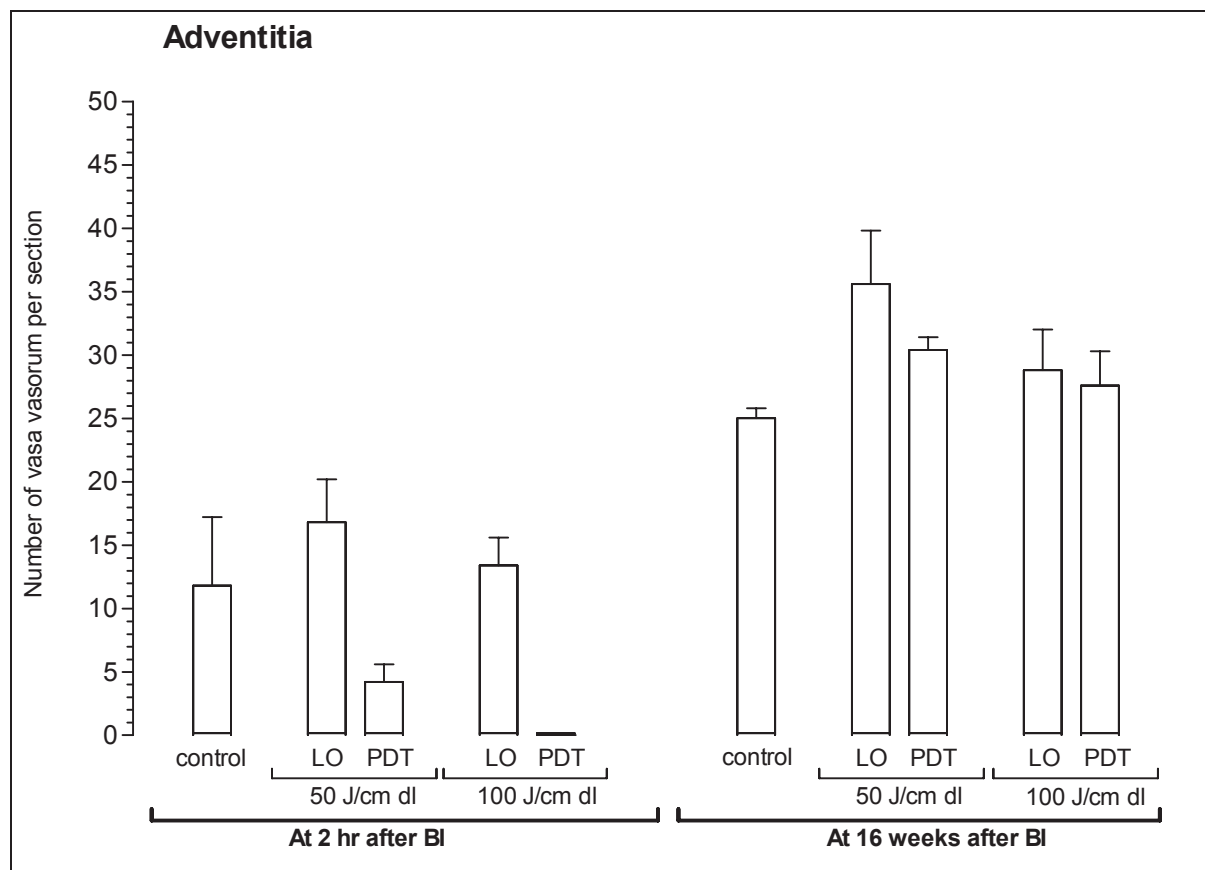


Figure 8.2 A bar diagram representing the number of vasa vasorum in the tunica adventitia plotted against the control group: control, BI and PDT 100 at 2 hours and at 16 weeks. The error bars are standard error of the mean (SEM: n=5 per time-point).

8.04 Discussion

In this study, we evaluated the effect of endovascular aminolaevulinic acid (ALA) based photodynamic therapy (PDT) on the inflammatory response in a standard balloon injured (BI) artery to find an explanation for the earlier reported inhibitory effect of PDT on the occurrence of intimal hyperplasia after interventions [13;21].

The major findings of this study were a significant decrease in accumulation of neutrophils and a significant increase of T-cells in the tunica adventitia directly after balloon injury (BI) followed by PDT compared to BI (+light only), whereas after 16 weeks, the T-cells were significantly reduced compared to the reference groups.

In the reference BI groups, neutrophils accumulated in the tunica intima, tunica media and particularly in the tunica adventitia 2 hours after treatment, preceding the accumulation of T-cells and monocytes in the tunica media and tunica adventitia after 16 weeks. These observations support the classic pattern of inflammatory cell accumulation in response to arterial injury that has earlier been described [3]. It is not unlikely that these neutrophils enter the lesion via the tunica intima, but due to the high shear stress of the blood in the iliac artery permeable vasa vasorum in the tunica adventitia offer a much easier entry site. This is indicated by the increased accumulation of neutrophils in the tunica adventitia.

Most interestingly, in our study, we found that upon endovascular PDT less neutrophils accumulated in the tunicas intima, media, and adventitia, than after BI only. The inhibition of the accumulation of neutrophils by PDT may underlie the prevention of intimal hyperplasia and fibrocellular constriction of the media as shown earlier using antibodies against neutrophil adhesion receptors [22]. Wilson et al. described that antibodies against the neutrophil membrane receptor CD18 reduced myocard damage [23]. That study may indicate the importance of neutrophil adhesion in the development of dysplastic intimal hyperplasia. It is not clear, how PpIX based-PDT prevented the entry of neutrophils into the lesion. Recently, it has been shown that the permeability of the tunica layers decreased after PDT due to cross-linking of [14] extracellular matrix proteins [24]. It may well be that by this PDT dependent phenomenon, the accumulation of neutrophils into the vessel wall is hampered.

Another remarkable finding in this study is the slight increase in the number of mast cells in the tunica adventitia directly after PpIX-based PDT. Interestingly, because mast cells are involved in hypersensitivity reactions [25;26]. Once activated, mast cells secrete TNF- α , chemokines and anti-coagulant heparines to prevent anti-thrombin III- induced coagulation. However, heparin is also a well-known inhibitor of smooth muscle cell proliferation [27;28].

We showed here a relatively fast and strong T-cell accumulation after PpIX based-PDT following BI. Interestingly, it has been reported that the amount of T-cells is related to the amount of medial fibrosis [8]. An in vitro study regarding experimental autoimmune encephalomyelitis described the unique potential of T-cells to penetrate strong basal membranes in contrast to other leukocytes [29]. Since we indeed found less other leukocytes in the vessel wall, this indicates that a strengthening of the arterial wall underlies the altered inflammatory reaction after PDT of the balloon-injured artery.

Relatively few monocytes were present in the tunicas of the arterial wall, after both BI (+LO) only as BI followed by PDT. The decrease in IH after PDT therefore does not likely reside in those phagocytes.

Upon PDT, the number of [13] vasa vasorum in the tunica adventitia decreased. We do not know if increased thrombogenicity, luminal collapse or constriction causes this decrease. It is likely that a decrease in the number of vasa vasorum will hamper the entry of inflammatory cells into the balloon-injured lesion. Indeed, we found that the number of vasa vasorum was inversely associated to the number of leukocytes in the tunica adventitia after injury.

In conclusion, this study underlines the importance of the tunica adventitia in the development of dysplastic intimal hyperplasia. The role of the tunica adventitia in that process had earlier been described by Okamoto in a balloon injured porcine coronary artery model [5], by Völker in a copper-induced rat carotid artery model [30], and by Yutani studying de novo caused by stents in patients [31]. By strengthening the matrix of the vessel wall and transiently decreasing the number of vasa vasorum, PDT specifically inhibits the accumulation of neutrophils in the tunicas intima, media and adventitia. Since it is generally accepted that neutrophils promote IH, the prevention of the accumulation of these cells into the injured vessel wall may be one of the mechanisms by which PDT after vascular intervention favours a beneficial clinical outcome.

Acknowledgements

This study was subsidised by the Dutch Heart Foundation (Grant 97.181). The authors would like to thank Dr. Marc Bakker, Department of Pathology of the Daniel den Hoed Cancer Centre for section typing.

References

- [1] Bauters C, Meurice T, Hamon M, McFadden E, Lablanche JM, Bertrand ME. Mechanisms and prevention of restenosis: from experimental models to clinical practice. *Cardiovasc Res* 1996; 31(6):835-846.
- [2] Ross R. The pathogenesis of atherosclerosis: a perspective for the 1990s. *Nature* 1993. 362, 801-809.
- [3] Welt FG, Edelman ER, Simon DI, Rogers C. Neutrophil, not macrophage infiltration precedes neointimal thickening in balloon-injured arteries. *Arterioscler.Thromb.Vasc.Biol.* 2000. 20, 2553-2558.
- [4] Indolfi C, Esposito G, Di Lorenzo E, Rapacciuolo A, Felicciello A, Porcellini A, Avvedimento VE, Condorelli M, Chiariello M. Smooth muscle cell proliferation is proportional to the degree of balloon injury in a rat model of angioplasty. *Circulation* 1995. 92[5], 1230-1235.
- [5] Okamoto E, Couse T, De Leon H, Vinten-Johansen J, Goodman RB, Scott NA, Wilcox JN. Perivascular inflammation after balloon angioplasty of porcine coronary arteries. *Circulation* 2001. 104, 2228-2235.
- [6] Springer TA. Traffic signals for lymphocyte recirculation and leukocyte emigration: the multistep paradigm. *Cell* 1994. 76, 301-314.
- [7] Moreno PR, Bernardi VH, Lopez-Cuellar J, Newell JB, McMellon C, Gold HK, Palacios IF, Fuster V, Fallon JT. Macrophage infiltration predicts restenosis after coronary intervention in patients with unstable angina. *Circulation* 1996. 94, 3098-3102.
- [8] Legare J-F, Issekutz T, Lee TDG, Hirsch G. CD8+ T lymphocytes mediate destruction of the vascular media in a model of chronic rejection. *Am J Pathol* 2000. 157[3], 859-865.
- [9] Grant WE, Speight PM, MacRobert AJ, Hopper C, Bown SG. Photodynamic therapy of normal rat arteries after photosensitisation using disulphonated aluminium phthalocyanine and 5-aminolaevulinic acid. *Br J Cancer* 1994; 70(1):72-78.
- [10] Jenkins MP, Buonaccorsi GA, Mansfield R, Bishop CC, Bown SG, McEwan JR. Reduction in the response to coronary and iliac artery injury with photodynamic therapy using 5-aminolaevulinic acid [In Process Citation]. *Cardiovasc Res* 2000; 45(2):478-485.
- [11] LaMuraglia GM, ChandraSekar NR, Flotte TJ, Abbott WM, Michaud N, Hasan T. Photodynamic therapy inhibition of experimental intimal hyperplasia: acute and chronic effects. *J Vasc Surg* 1994; 19(2):321-329.
- [12] Nyamekye I, Anglin S, McEwan J, MacRobert A, Bown S, Bishop C. Photodynamic therapy of normal and balloon-injured rat carotid arteries using 5-amino-levulinic acid. *Circulation* 1995; 91(2):417-425.
- [13] Gabeler EEE, van Hillegersberg R, Stadius van Eps RG, Sluiter W, Mulder P, van Urk H. Endovascular Photodynamic Therapy with Amino Laevulinic Acid Prevents Balloon Induced Intimal Hyperplasia and Constrictive Remodelling without Damaging Perivascular Innervation in Rat Iliac Arteries. *Eur.J.Vasc.Endovasc.Surg.* 2002, in press.
- [14] Overhaus M, Heckenkamp J, Kossodo S, Leszczynski D, LaMuraglia GM. Photodynamic therapy generates a matrix barrier to invasive vascular cell migration. *Circ Res* 2000; 86(3):334-340.
- [15] Henderson BW, Dougherty TJ. How does photodynamic therapy work? *Photochem Photobiol* 1992; 55(1):145-157.
- [16] Weishaupt KR, Gomer CJ, Dougherty TJ. Identification of singlet oxygen as the cytotoxic agent in photo-inactivation of a murine tumor. *Cancer Res.* 1976. 36, 2326-2329.
- [17] Gabeler EEE, van Hillegersberg R, Stadius van Eps RG, Sluiter W, Gussenhoven EJ, Mulder P, van Urk H. A Comparison of Balloon Injury Models after Endovascular Lesions in the Rat. Submitted 2002.

- [18] Heisterkamp J, Hillegersberg van R, Sinofsky E, IJzermans J. Heat resistant cylindrical diffuser for interstitial laser coagulation: Comparison with a bare-tip fibre in ex vivo porcine liver. *Lasers Surg.Med.* 1997. 20, 304-309.
- [19] Hinnen P, de Rooij FW, Voortman G, Tilanus HW, Wilson JHP, Siersema PD. Acrylate yellow filters in operating lights protect against photosensitization tissue damage. *Br.J.Surg.* 2000. 87, 231-235.
- [20] Indolfi C, Cioppa A, Stabile E, Di Lorenzo E, Esposito G, Pisani A, Leccia A, Cavuto L, Stingone AM, Chieffo A, Capozzolo C, Chiariello M. Effects of hydroxymethylglutaryl coenzyme A reductase inhibitor simvastatin on smooth muscle cell proliferation in vitro and neointimal formation in vivo after vascular injury. *J Am Coll Cardiol* 2000; 35(1):214-221.
- [21] Jenkins MP, Buonaccorsi G, MacRobert A, Bishop CC, Bown SG, McEwan JR. Intra-arterial photodynamic therapy using 5-ALA in a swine model. *Eur J Vasc Endovasc Surg* 1998; 16(4):284-291.
- [22] Hayashi S, Watanabe N, Nakazawa K, Suzuki J, Tsushima K, Tamatani T, Sakamoto S, Isobe M. Roles of P-selectin in inflammation, neointimal formation, and vascular remodeling in balloon-injured rat carotid arteries. *Circulation* 2000. 102, 1710-1717.
- [23] Wilson I, Gillinov AM, Curtis WE, DiNatale J, Burch RM, Gardner TJ, Cameron DE. Inhibition of neutrophil adherence improves postischemic ventricular performance of the neonatal heart. *Circulation* 1993; 88(5 Pt 2):II372-II379.
- [24] Strauss WS, Sailer R, Schneckenburger H, Akgun N, Gottfried V, Chetwer L, Kimel S. Photodynamic efficacy of naturally occurring porphyrins in endothelial cells in vitro and microvasculature in vivo. *J Photochem Photobiol B* 1997; 39(2):176-184.
- [25] Stevens A, Lowe J. Blood cells. *Histology*. New York: Gower Medical Publisher, 1992: 67-80.
- [26] Holgate ST. The role of mast cells and basophils in inflammation. *Clin.Exp.Allergy* 2000. 30[S1], 28-32.
- [27] Hanke H, Oberhoff M, Hanke S, Hassenstein S, Kamenz J, Schmid KM, Betz E, Karsch KR. Inhibition of cellular proliferation after experimental balloon angioplasty by low-molecular-weight heparin [see comments]. *Circulation* 1992; 85(4):1548-1556.
- [28] Herbert JM, Bono F, Lamarche I, Carmeliet P. The inhibitory effect of heparin for vascular smooth muscle cell proliferation or migration is not mediated by u-PA and t-PA. *Thromb Res* 1997; 86(4):317-324.
- [29] Naparstek Y, Cohen IR, Fuks Z, Vlodaysky I. Activated T-lymphocytes produce a matrix-degrading heparan sulphate endoglycosidase. *Nature* 1984. 310, 241-244.
- [30] Völker W, Dorszewski A, Unruh V, Robenek H, Breithardt G, Buddecke E. Copper-induced inflammatory reactions of rat carotid arteries mimic restenosis/arteriosclerosis-like neointima formation. *Atherosclerosis* 1997. 130, 29-36.
- [31] Yutani C, Ishibashi-Ueda H, Suzuki T, Kojima A. Histologic evidence of foreign body granulation tissue and de novo lesions in patients with coronary stent restenosis. *Cardiology* 1999; 92(3):171-177.

SECTION VI

CHAPTER 9

Arterial Wall Strength after Endovascular Photodynamic Therapy

Edward E.E. Gabeler^{1*}, Richard van Hillegersberg¹, Wim Sluiter², Mike Kliffen³
Randolph G. Stadius van Eps¹, Jan Honkoop⁴, Stephane G. Carlier⁵,
Hero van Urk¹

¹Dept. of Surgery

²Dept. of Biochemistry

³Dept of Pathology

⁴Dept. of Experimental Cardiology

⁵Dept. of Cardiology

from the Erasmus MC, Rotterdam, The Netherlands

Keywords: ALA, arteries, bursting pressure, photodynamic therapy, remodelling, restenosis

Lasers in Medicine and Surgery 2003, 33(1):8-15.

Abbreviations: ALA, amino laevulinic acid; BI, balloon injury; HR, heart rate; IH, intima hyperplasia; J/cm dl, Joule per cm diffuser length; MAP, mean arterial pressure; AD, arterial diameter; PDT, photodynamic therapy; SEM, standard error of the mean; SMC, smooth muscle cell.

9.00 Abstract

Background: Vascular photodynamic therapy (PDT) inhibits intimal hyperplasia induced by angioplasty in rat iliac arteries by eradicating the proliferating smooth muscle cells. This process may jeopardise the structure and strength of the arterial wall, reflected by a decreased bursting pressure.

Materials & Methods: Thirty male Wistar rats of 250-300 g were subdivided into 3 groups (n=10). In all groups intimal hyperplasia was induced by balloon injury (BI). One experimental group received PDT at 50 J/cm diffuser length, the other group at 100 J/cm diffuser length. The third group served as control group and received no PDT. In half of each group the bursting pressure was analysed after 2 hours (n=5), in the other half after one year.

Results: Two hours after the procedure the bursting pressure was 3.37 ± 0.58 (\pm SEM) bar in the BI+PDT 50 and 3.96 ± 0.43 bar in the BI+PDT 100 group, compared to 2.20 ± 0.27 bar in the BI group ($p < 0.05$). After 1 year these values were 3.18 ± 0.87 bar in the BI+PDT 50 ($p < 0.05$) and 2.02 ± 0.31 bar in the BI+PDT 100 group, compared to 2.10 ± 0.30 bar in the BI group (NS). In the BI+PDT 100 group 3 out of 5 rats appeared to have aneurysmal dilatation after one year.

Conclusion: Endovascular PDT increases the arterial wall strength as measured by the bursting pressure at short-term. After one year, wall strength is not diminished as measured by bursting pressure, but aneurysmal dilatation nevertheless developed with 100 J/cm dl. This may limit the use of high energy PDT.

9.01 Introduction

Restenosis due to intimal hyperplasia (IH) and constrictive remodelling decreases the long-term success rates of therapeutic vascular interventions for recanalisation of stenotic or occluded arteries. The incidence of this complication varies between 30 and 50% within 6 months [1], which is still an unfavourable therapeutical outcome that needs to be improved.

In the patho-etiology of restenosis, an excessive proliferation of smooth muscle cells (SMC) after arterial injury leading to IH plays a major role [2]. Remodelling is another important factor [3;4]. The exact contribution of SMCs in the development of constrictive remodelling remains to be elucidated, but various preventive studies showed that the elimination of these SMCs prevent or inhibit restenosis [5-10].

An adjuvant strategy to prevent restenosis may be the use of photodynamic therapy (PDT), a modality based on the light induced cytotoxicity of a light sensitive substrate (photosensitizer) that accumulates in the SMCs of the arterial wall after oral or intravenous administration (photosensitization) [11;12].

Since the first unsuccessful PDT based dose-finding study with Photofrin reported in 1985 [13], the search to find the optimal protocol in PDT studies to prevent restenosis was initiated [14]. Despite the following successful inhibition of IH using this first generation photosensitizer, its use was limited by systemic side effects of photocytotoxicity. This led to the development of second generation photosensitizers like phtalocyanines [15-17]. These photosensitizers are easily absorbed in arterial tissue but with less systemic side effects. However, lipophilic photosensitizers are only activated at high energy levels and are not really tissue specific.

In 1995 the first reports with the pro-drug aminolaevulinic acid (ALA) proved to be successful in the prevention of IH without systemic side effects [18-20] and therefore resulted in the first clinical application [21]. ALA is a naturally occurring intermediate of the heme biosynthetic pathway, which is artery type- and tissue-dependently metabolised to the photosensitizer protoporphyrin IX [22].

It became clear that the dose of the photosensitizer, the timing of illumination, the energy level and the type of artery are important parameters to determine the therapeutical outcome.

However, the direct and long-term effect of PDT induced SMC elimination on the structure of the arterial wall as a safety measure for this strategy is unknown. In this study, the bursting pressure of BI and PDT treated arteries was determined to study the strength of the arterial wall directly after the procedure and one year later.

9.02 Materials & methods

The experimental protocol was approved by The Committee on Animal Research of the Erasmus University of Rotterdam and complied with “Principles of Good Laboratory Practice”. Male inbred Wistar rats (Harlan CPB, Austerlitz, The Netherlands) weighing 200-300 g were used. The animals had free access to rat chow (AM II, Hope Farms, Woerden, The Netherlands) and tap water, while maintained in a standard 12-hr light/dark cycle.

9.02.1 Study design

Thirty male Wistar rats of 250-300 g were subdivided into 3 groups (n=10). In all groups intimal hyperplasia was induced by balloon injury (BI) in the right common iliac artery. One experimental group received PDT at 50 J/cm diffuser length using endovascular laser illumination at 2 ½ hr after the administration of ALA, the other group at 100 J/cm diffuser length. The third group served as control group and received no PDT. In half of each group the bursting pressure was analysed after 2 hours (n=5), in the other half after one year.

9.02.2 Photosensitization

The PDT groups received 200 mg/ kg ALA (Sigma-Aldrich Chemie, Zwijndrecht, The Netherlands) intravenously dissolved in phosphate buffered saline at 40 mg/ml. The solution was freshly made for each animal and kept from light exposure. The photosensitised rats were kept in the dark during 2 ½ hr prior to treatment and 12 hr afterwards to prevent skin reactions from photosensitivity. The time interval after ALA administration is based on a previous study, where we found that at that time point the accumulation of the photosensitive compound protoporphyrin IX became maximal.

9.02.3 Laser

A dye laser (600 Series Dye Module, Laserscope, Surgical Systems, San Jose, CA, USA), pumped by a 532/KTP surgical laser (Laserscope, Surgical Systems, San Jose, CA, USA), was used to generate monochromatic light of 633 nm. The power emitted from the cylindrical diffusing tip (core diameter 200 µm, outer diameter 1.0 mm, tip length 20 mm: Lightstic™, Cardiofocus, West Yarmouth, MA, USA)[23] was calibrated with a built-in power meter, and verified with an external linear diffuser in an integrating cylindrical sphere (Optometer Model 370, Graseby Optronics, Orlando, FL, USA). A spectroscope (WaveMate, Coherent, Auburn, CA, USA) was used to verify the accuracy of the wavelength.

Temperature

The real-time temperature during endovascular PDT was checked at 100 mW/cm dl for 16 minutes and 40 seconds (100 J/cm dl) to exclude high-energy induced hyperthermal effects instead of low-energy induced phototoxicity. Two fibre-optic thermosensors with a diameter of 0.5 mm were coupled to a Luxtron thermometry unit (Luxtron Corp., Santa Clara, CA, USA). One was approximated parallel to the laser fibre along the artery at an axial distance of 10 mm in the fibre tip and the other next to the rat. The temperature was determined every second.

Linear fluence calibration with an isotropic probe

The linear fluence of 100 J/cm dl from the cylindrical diffuser in the arterial wall was measured at an irradiance of 100 mW/cm dl (illumination time of 1000 seconds). An isotropic probe was approximated parallel to the laser fibre outside the artery at axial distances of 10 mm from and 0, 10 and 20 mm in the fibre tip.

9.02.4 Surgical technique

A median laparotomy was performed under general anaesthesia with intramuscular injection of ketamine (Ketalar, Parke Davis and Co., Inc., 40 mg/kg) and xylazin (Rompun Bayer Ag, Leverkusen, Germany; 5 mg/kg). Subdued light using a yellow filter (620-650 nm Kodak) was applied during the procedure to prevent a photodynamic reaction caused by the operating lamp [24]. The right common iliac artery was cranially and caudally temporarily occluded with vascular clamps (Haemostat B1, Stöpler, Utrecht, The Netherlands). To create a blood free lumen, the arteries were flushed with 1 ml heparin (50 IU/ml 0.9% NaCl) infusion solution (Baxter) through an arteriotomy 5 mm proximal to the abdominal aortic bifurcation. The artery was then only balloon injured in the control group and BI +PDT was performed in the experimental groups (see Balloon injury and Endovascular Photodynamic Therapy). Hereafter, the clamps were removed. Reperfusion of the dilated section was observed directly after flushing with heparin and closing the arteriotomy (interrupted 9-0 prolene sutures). The abdominal wall was closed in two layers (continuous 2-0 prolene sutures). The animals recovered in subdued light after treatment.

9.02.5 Balloon injury

A 2F Fogarty embolectomy catheter (Baxter Health Care Corp., Edward's Div., Irvin, Ca., USA) was inserted to denude the arterial wall at a pressure of 2 bar (manometer, Baxter, USA) by pulling and rotating the insufflated balloon from distally to proximally over a 15-mm long segment for 3 successive times [25]. The balloon was desufflated proximally and insufflated distally. Then, the arteries were flushed with 1ml heparin solution, closed with Prolene 8-0 and marked halfway the denuded segment with a suture.

9.02.6 Endovascular Photodynamic Therapy (PDT)

In the PDT group, a 400 µm fibre (Lightstic 360, Rare Earth Medical Inc., West Yarmouth, MA, USA) with a 20 mm long cylindrical diffusing tip was applied. The fibre tip was centred endovascularly in the denuded area to illuminate 10 mm of the balloon damaged arterial wall and 5 mm of the untreated arterial wall both cranially and caudally. Because of the cylindrical illumination, the fluence was expressed in Joule per cm diffuser length (J/cm dl). The target area was illuminated at random with 50 (n=5) or 100 J/cm dl (n=5), applied with a fluence rate of 100 mW/cm dl. After treatment, the lumen was thoroughly flushed with 1 ml heparin solution. Abdominal organs were protected from light exposure with a light absorbing plastic folium during illumination.

9.02.7 Bursting pressure

The bursting pressure was determined in situ. A 2F cannula was fixed proximally in the iliac artery with Vicryl 6-0. At 15 mm distally, the segment was occluded with Vicryl 4-0. The

cannula was connected with a T-piece to an analog pressure transducer (WIKA type Ecotronic) coupled to a converter module matrix. The intra-luminal pressure was gradually increased by pushing a glycol solution (Sigma-Aldrich 5000 MW, 5 g/ml 0.9% NaCl) into the sealed arterial segment via the cannula using a syringe with pressure manometer. Simultaneously, the intra-luminal pressure was digitally displayed on the video screen. The pressures at which the tunica media became transparent due to compression, and at which the tunica adventitia bursted were recorded on S-VHS for analysis <Fig. 9.1>. Just before bursting, the arterial diameter (AD) expressed in mm was determined from the digital images using a scale bar as reference.

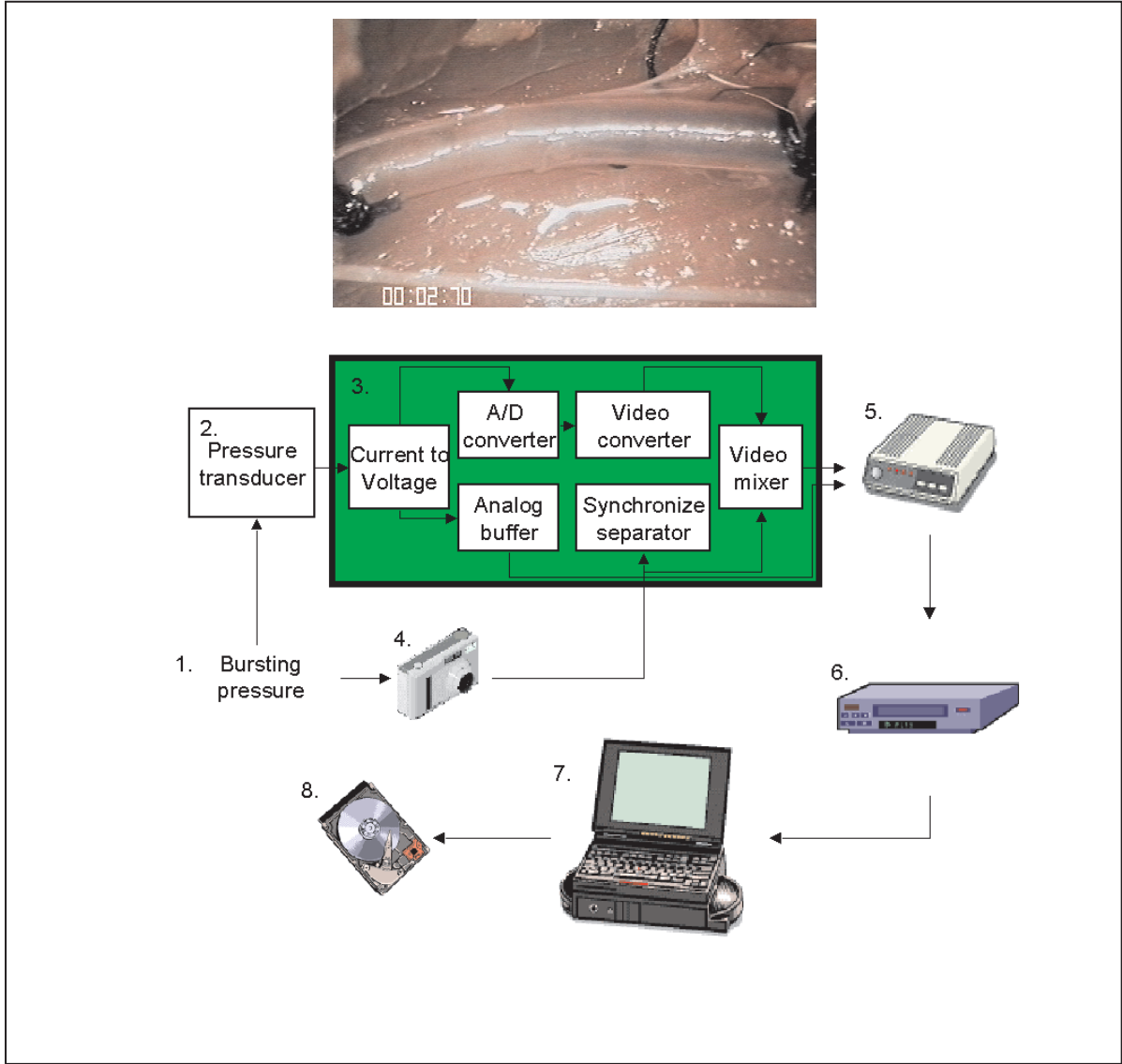


Figure 9.1 A schedule representing the model to determine the bursting pressure of the treated right iliac artery as illustrated in the photograph <1>. The 2F sheet is linked to a pressure manometer and a pressure transducer coupled <2> to a converter module matrix 3>. The analog voltage signal evoked by the pressure is converted to digits in the video screen. These digits are integrated in the display of the bursting pressure analysis using an A/D converter and synchronize separator <1-4>. This signal is incorporated using a video mixer and for tracing a second video mixer <5>. For recording the output of the second video mixer is connected to a S-VHS system <6>. The incorporated signal is displayed on a monitor and digitally converted using a computer <7> and CD <8>.

9.02.8 Histopathology

After the measurement of the bursting pressure the iliac artery was removed and processed for histopathological analysis. The arteries were fixed in formalin, cross-sectioned and embedded in paraffin. 4 μm sections were cut and stained with H&E and Elastic von Gieson.

9.02.9 Statistical analysis

The presence of aneurysmal dilatation after treatment was analysed using a Fisher's exact test. The bursting pressure was expressed as mean \pm standard error of the mean (SEM). ANOVA with a Dunnett's correction was used to compare the experimental means with the means of the control group. ANCOVA was used to study if the arterial diameter (AD) has a significant effect on the outcome of the bursting pressure. A difference was considered to be significant at p values less than 0.05.

9.03 Results

Two rats of the BI+PDT 50 group died directly after the procedure and were excluded from further analysis. All other rats appeared healthy after treatment without significant weight loss or skin phototoxicity during the experiments. In all groups, after 52 weeks macroscopic neo-vascularization in the fascia covering the treated arterial area was seen in contrast to 0 weeks <Fig.9.2>.

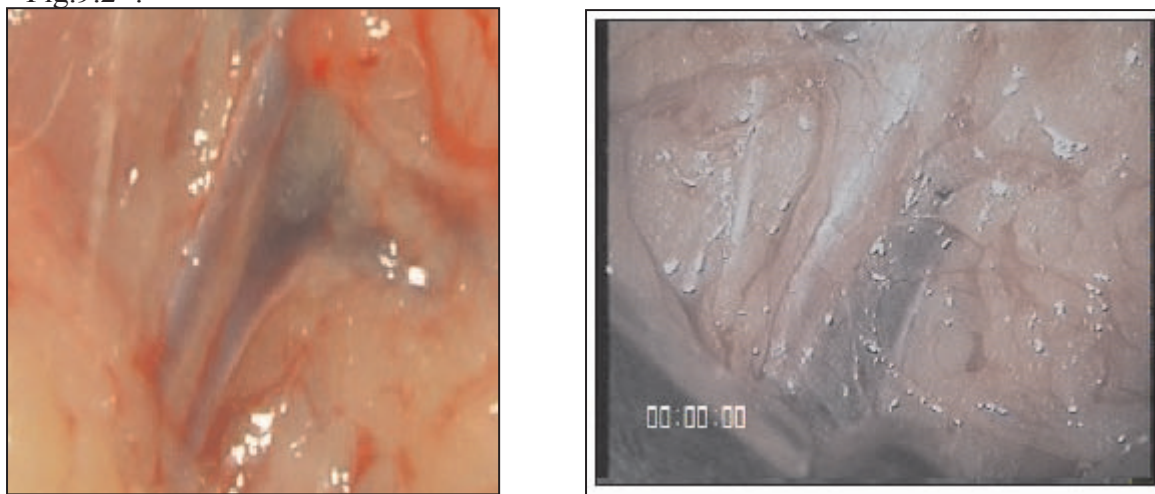


Figure 9.2 Photograph a shows the fascia covering the iliac artery before the procedure. Photograph b shows the increased neo-vascularization in the fascia covering the treated iliac artery seen after 52 weeks in the treated groups. Here an iliac artery treated at 50 J/cm dl using a fluence rate of 100 mW/cm dl.

Strikingly, 3 out of 5 rats of the BI+PDT 100 group developed an aneurysmal dilatation at the proximal site of the PDT treated segment after 52 weeks of which one developed a distally occluded segment <Fig. 9.3>. The fluence of 100 J/cm dl had a significant effect on the development of the aneurysmal dilatation ($p < 0.03$). The temperature in the arterial wall did not increase during illumination and the light fluence was distributed homogeneously in the arterial wall (20).

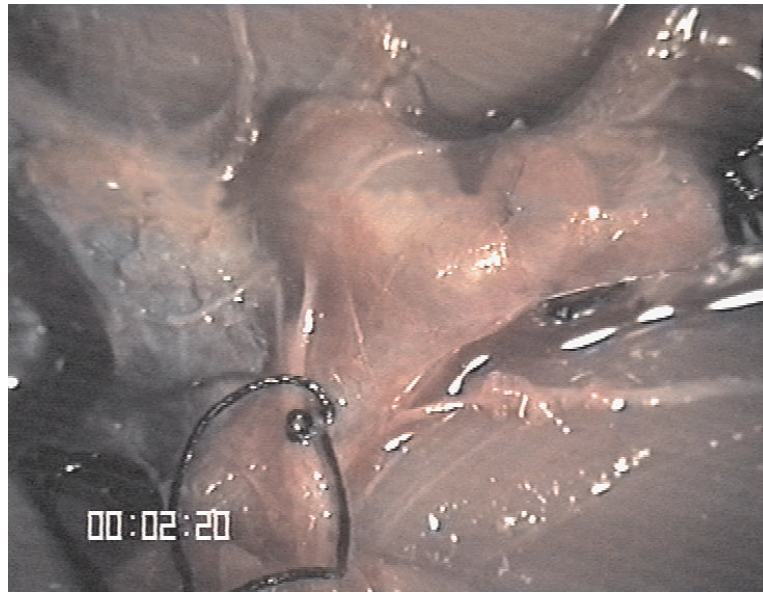


Figure 9.3 A photograph showing the developed aneurysm like dilatation after 52 weeks in the proximal segment of the PDT treated iliac artery at 100 J/cm dl using a fluence rate of 100 mW/cm dl. Bursting pressure digits are given in the photograph.

9.03.1 Bursting pressure of the tunica adventitia

The bursting pressure of the tunica adventitia at 2 hours after the procedure was 2.20 ± 0.27 bar in the control group, compared to 3.37 ± 0.58 bar in the BI+PDT 50 group (*:p<0.05) and compared to 3.96 ± 0.43 bar in the BI+PDT 100 group (**:p<0.05). The bursting pressure of the tunica adventitia at 52 weeks was 2.10 ± 0.30 bar in the control group compared to 3.18 ± 0.57 bar in the BI+PDT 50 group (†:p<0.05) and to 2.02 ± 0.31 bar in the BI+PDT 100 group (NS) <Fig. 9.4>. In general, the tunica media got compressed and became transparent in all groups at a pressure of between 0.22 and 0.46 bar.

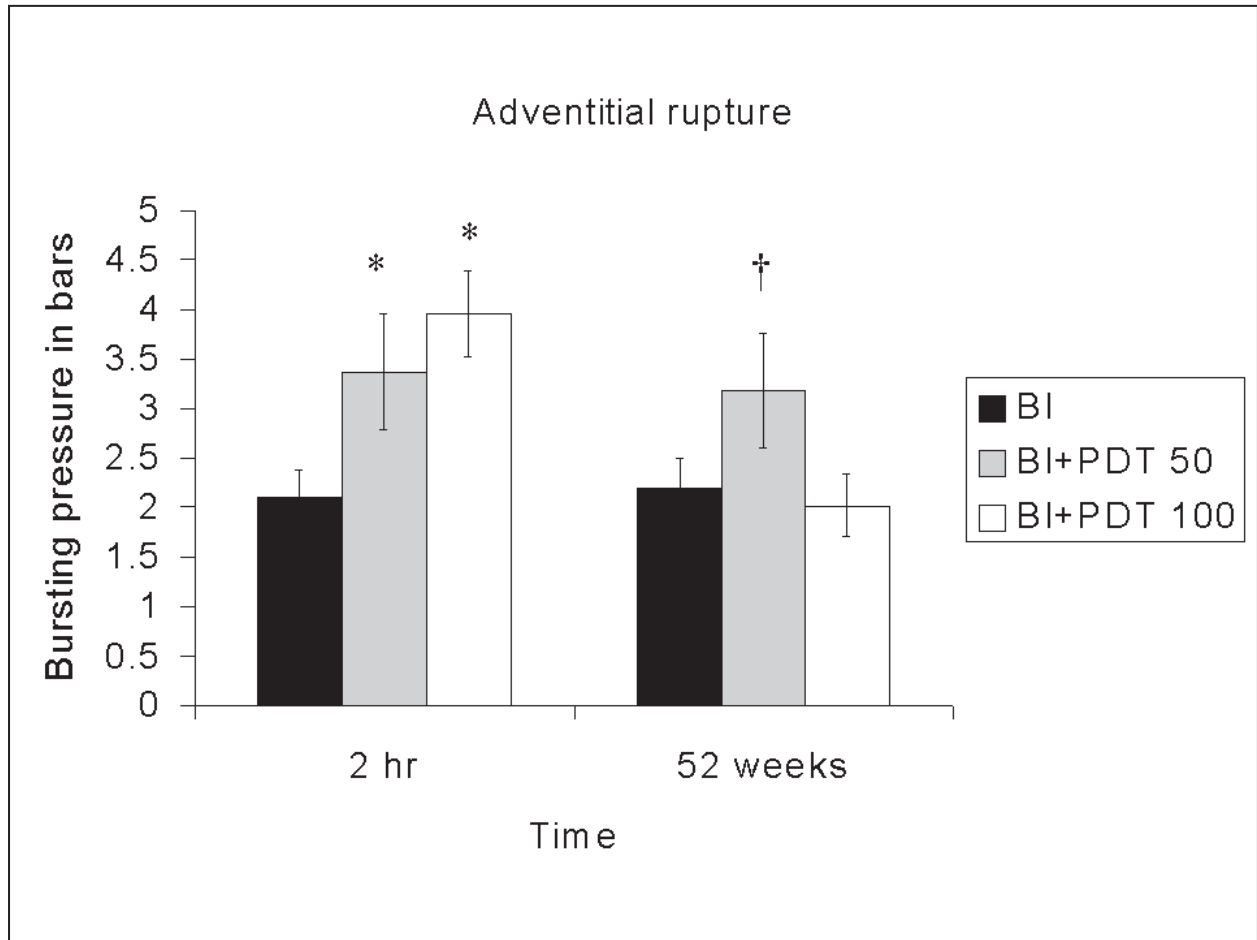


Figure 9.4 A bar diagram representing the mean bursting pressure expressed in bar at which the tunic adventitia ruptures. The control group, BI+PDT 50 and BI+PDT 100 group is plotted against the time at 2 hr and 52 weeks (n=5 per time-point). The error bars are standard errors of the mean (SEM).

9.03.2 The arterial diameter (AD)

After 1 year, the AD just before the bursting pressure had increased significantly in the BI+PDT 50 (1.89±0.04 mm) and 100 group (2.58±0.14 mm) compared to the control group (1.42±0.03 mm) (p<0.05) <Table 9.1>. The AD did not significantly correlate with the mean bursting pressure (c:-0.33, p<0.12).

Groups	Arterial Diameter in mm			
	2 hours	SEM	52 weeks	SEM
Control	1.24±	0.15	1.42±	0.03
BI+PDT 50	1.19±	0.11	1.89±	0.04
BI+PDT 100	1.07±	0.13	2.58±	0.14

Table 9.1 The mean arterial diameter in mm at 2 hours and after 52 weeks in respectively the control group, the BI+PDT 50 J/cm dl group and the BI+PDT 100 J/cm dl group (n=5 per group for each time-point).

9.03.3 Histopathology

In the BI group after 2 hours only slight disruption of the internal area of the vessels was seen. In addition, in both the BT+PDT50 and 100 group, the tunica media became partly acellular <Fig. 9.5a>. The most striking difference was seen after 52 weeks. Intimal hyperplasia was much more prominent in the BI+PDT100 group than in the BI group <Fig.9.5b>. However, the BI+PDT50 group showed no intimal hyperplasia at all. In all groups fragmentation of elastic laminae occurred <Fig. 9.5c1>, but the amount of elastin seemed larger in the PDT groups <Fig. 9.5c2>. Quantitative assessment was not possible with the techniques used. Rupture of the elastic layer with development of aneurysmal dilatation was seen in the PDT100 group <Fig. 9.5d>.

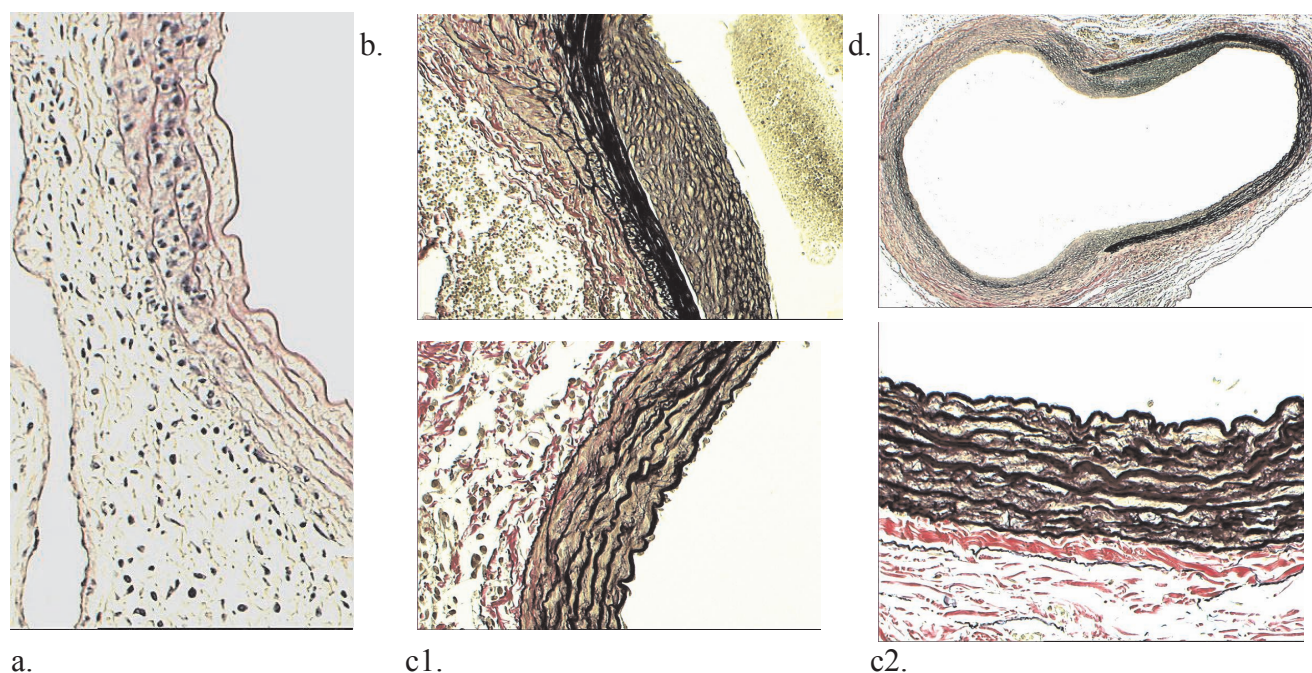


Figure 9.5

Photograph a shows the partial acellularity in the tunica media at 50 J/cm dl after 2 hours at a magnification of 200.

Photograph b shows focal intimal hyperplasia at 100 J/cm dl at a magnification of 200 after one year.

Photograph c1 shows a fragmentation of elastin in the tunica media at 50 J/cm dl after 2 hours at a magnification of 400. An increased density of elastin is shown in photograph c2 at a magnification of 400 in the same group.

Photograph d shows an aneurysmal dilatation in the PDT group at 100 J/cm dl after one year at a magnification of 100.

9.04 Discussion

Vascular PDT, intended to inhibit intimal hyperplasia, eliminates proliferating smooth muscle cells resulting in a temporary acellular arterial wall [20;26]. A concern of this method is the potential formation of aneurysmal dilatation due to weakening of the arterial wall. This would limit the application of PDT as a measure to inhibit IH.

Grant et al. reported that external PDT with a fluence of 100 J/cm² and a fluence rate of 150 mW/cm², did not reduce the arterial wall strength in the carotid artery of rabbits at a follow-up of 21 days using a similar method of measuring, despite of an acellular tunica media [26].

In our study we found that the means of the bursting pressure in all groups were above the normal physiological range (1.0-1.5 bar). The bursting pressure increased significantly at 2 hours after BI+PDT, both at 50 J/cm diffuser length (dl) and 100 J/cm dl. After 52 weeks, the bursting pressure was significantly increased in the BI+PDT 50 J/cm dl group compared to the control and BI+PDT 100 J/cm dl group. Apparently, a fluence of 50 J/cm dl increased the arterial wall strength permanently.

The increase in arterial wall strength shortly after 100 J/cm dl was transient and after one year aneurysmal dilatation developed in this treatment group. This indicates that the light dose for endovascular PDT is limited to a value between 50-100 J/cm dl.

But how can the increase in bursting pressure of the arterial wall be explained after endovascular PDT? Statius van Eps et al. suggested that PDT induces clustering or cross-linking of various protein components in the extracellular matrix, which seals the damaged vascular wall [20]. In a chicken microvascular in vivo model it was also found that ALA based PDT led to an increased deposition of collagens in the arterial wall [27;28]. Furthermore, experiments in rats with methylene blue based PDT showed post treatment a significant increase of the amount of procollagen type I in the vascular wall, which may strengthen the blood vessel wall [29].

An important enzyme of the normal arterial healing response is lysyl oxidase that cross-links (tropo)collagens, fibrils and elastin, and is located in cellular lysosomes and in the extracellular matrix [30-33]. An earlier report described that high laser light output inhibited this particular enzyme in arteries [34]. However, relatively low energy PDT may activate this particular enzyme to induce an increased cross-linking of matrix proteins. In this manner, the vascular PDT-modified healing may form a barrier for smooth muscle cell migration preventing the development of IH [35].

While that latter phenomenon could be beneficial, a possible disadvantage of the vascular PDT-modified healing is that the arterial contractility might be lost. However, the low fluence used in the present study enabled the repopulation of SMCs in the tunica media and tunica adventitia as reported in our earlier study [20]. Furthermore, we found that at long-term follow-up endovascular PDT at 50 J/cm dl resulted in arterial dilatation and at 100 J/cm dl even to an increase in the mean arterial diameter with a factor 2, leading to aneurysmal proportions.

Histopathologically, it seems that the amount of IH development is inversely related to bursting pressure after 52 weeks, with prominent IH in the BI+PDT100 group and no IH in the BI+PDT50 group. This could be due to unequivocal distribution of pressure forces at the arterial wall. In vivo this is probably also reflected by the occurrence of aneurysmal dilatation in the BI+PDT100 group. Histopathologically it is not clear how the differences in bursting pressure after 2 hours can be explained. The only histological difference after 2 hours was the partial acellularity in the vascular wall of the PDT groups.

A relative limitation of the open liquid-based bursting pressure set up used in this study, is the difficulty of fixing the cannula waterproof. However, the location of ruptures at the origins of vasa vasorum in the tunica adventitia in the treated artery could accurately be detected, which can easily be overlooked in models using a balloon catheter for detection of bursts in the tunica adventitia.

In our model, a transient ischemic period was obtained during PDT as similar to the clinical practice of balloon angioplasty and endarterectomy. A relative bloodless environment is necessary to avoid excessive absorption of the laser light by hemoglobine that would prevent light penetration into the vascular wall. This would result in an unpredictable photodynamic effect.

We conclude that PDT at 50 J/cm dl increases the arterial wall strength, maximal wall diameter and lumen diameter permanently in a rat IH model. However, high fluences (100 J/cm dl) promote the development of aneurysmal dilatation. Therefore, the therapeutic window of high energy endovascular PDT is limited.

Acknowledgements

This study was subsidised by the Dutch Heart Foundation (Grant97.181) and the Lijf en Leven Foundation. The authors are grateful to Mr Jan Tuin of the Audio-visual department of the Thorax Centre of the Erasmus MC for digitizing the VHS tapes and Mr Hans Hut, MSc, of the department of Biochemistry, Erasmus MC for the glycol solution.

References

- [1] Bauters C, Meurice T, Hamon M, McFadden E, Lablanche JM, Bertrand ME. Mechanisms and prevention of restenosis: from experimental models to clinical practice. *Cardiovasc Res* 1996; 31(6):835-846.
- [2] A.W.Clowes, M.E.Reidy, M.M.Clowes. Kinetics of cellular proliferation after arterial injury;1.Smooth muscle growth in the absence of endothelium. *Laboratory Investigation* 1983.49[3], 327-333.
- [3] Post MJ, Borst C, Kuntz RE. The relative importance of arterial remodeling compared with intimal hyperplasia in lumen renarrowing after balloon angioplasty. A study in the normal rabbit and the hypercholesterolemic Yucatan micropig [see comments]. *Circulation* 1994; 89(6):2816-2821.
- [4] Mintz GS, Popma JJ, Pichard AD, Kent KM, Satler LF, Chiu Wong S, Hong MK, Kovach JA, Leon MB. Arterial remodelling after coronary angioplasty. *Circulation* 1996. 94[1], 35-43.
- [5] Herrman JP, Hermans WR, Vos J, Serruys PW. Pharmacological approaches to the prevention of restenosis following angioplasty. The search for the Holy Grail? (Part I). *Drugs* 1993; 46(1):18-52.
- [6] Hidaka Y, Eda T, Yonemoto M, Kamei T. Inhibition of cultured vascular smooth muscle cell migration by simvastatin (MK-733). *Atherosclerosis* 1992; 95(1):87-94.
- [7] Choi ET, Engel L, Callow AD, Sun S, Trachtenberg J, Santoro S, Ryan US. Inhibition of neointimal hyperplasia by blocking alpha V beta 3 integrin with a small peptide antagonist GpenGRGDSPCA. *J Vasc Surg* 1994; 19(1):125-134.
- [8] Hanke H, Hanke S, Bruck B, Brehme U, Gugel N, Finking G, Muck AO, Schmahl FW, Hombach V, Haasis R. Inhibition of the protective effect of estrogen by progesterone in experimental atherosclerosis. *Atherosclerosis* 1996; 121(1):129-138.
- [9] Pitsch RJ, Goodman GR, Minion DJ, Madura JA, Fox PL, Graham LM. Inhibition of smooth muscle cell proliferation and migration in vitro by antisense oligonucleotide to c-myb. *J Vasc Surg* 1996; 23(5):783-791.
- [10] Nagler A, Miao HQ, Aingorn H, Pines M, Genina O, Vlodayvsky I. Inhibition of collagen synthesis, smooth muscle cell proliferation, and injury-induced intimal hyperplasia by halofuginone. *Arterioscler Thromb Vasc Biol* 1997; 17(1):194-202.
- [11] Jagger J. The expanding science of photobiology. *Nature* 1981.289, 636-637.
- [12] Henderson BW, Dougherty TJ. How does photodynamic therapy work? *Photochem Photobiol* 1992; 55(1):145-157.
- [13] Litvack F, Grundfest W, Forrester J, Fishbein M, Swan H, Corday E, Rider D, McDermid I, Pacala T, Laudenslager J. Effects of hematoporphyrin derivative and photodynamic therapy on atherosclerotic rabbits. *Am.J.Cardiol.* 1985.56, 667-671.
- [14] Gabeler EEE. Photodynamic therapy for restenosis: The search for the optimal protocol. *Photodynamic News* 2002. 5[1], 6-9.
- [15] Ortu P, LaMuraglia GM, Roberts WG, Flotte TJ, Hasan T. Photodynamic therapy of arteries. A novel approach for treatment of experimental intimal hyperplasia. *Circulation* 1992; 85(3):1189-1196.
- [16] LaMuraglia GM, Ortu P, Flotte TJ, Roberts WG, Schomacker KT, ChandraSekar NR, Hasan T. Chloroaluminum sulfonated phthalocyanine partitioning in normal and intimal hyperplastic artery in the rat. Implications for photodynamic therapy. *Am J Pathol* 1993; 142(6):1898-1905.
- [17] Hsiang YN, Crespo MT, Machan LS, Bower RD, Todd ME. Photodynamic therapy for atherosclerotic stenoses in Yucatan miniswine. *Can J Surg* 1994; 37(2):148-152.

- [18] Grant WE, Speight PM, MacRobert AJ, Hopper C, Bown SG. Photodynamic therapy of normal rat arteries after photosensitisation using disulphonated aluminium phthalocyanine and 5-aminolaevulinic acid. *Br J Cancer* 1994; 70(1):72-78.
- [19] Nyamekye I, Anglin S, McEwan J, MacRobert A, Bown S, Bishop C. Photodynamic therapy of normal and balloon-injured rat carotid arteries using 5-amino-levulinic acid. *Circulation* 1995; 91(2):417-425.
- [20] Gabeler EEE, van Hillegersberg R, Stadius van Eps RG, Sluiter W, Mulder P, van Urk H. Endovascular Photodynamic Therapy with Amino Laevulinic Acid Prevents Balloon Induced Intimal Hyperplasia and Constrictive Remodelling without Damaging Perivascular Innervation in Rat Iliac Arteries. *Eur.J.Vasc.Endovasc.Surg.* 2002. 24[4], 322-330.
- [21] Jenkins MP, Buonaccorsi GA, Raphael M, Nyamekye I, McEwan JR, Bown SG, Bishop CC. Clinical study of adjuvant photodynamic therapy to reduce restenosis following femoral angioplasty. *Br J Surg* 1999; 86(10):1258-1263.
- [22] Malik Z, Lugaci H. Destruction of erythroleukemic cells by photoactivation of endogenous porphyrins. *Br.J Cancer* 1987. 56, 589-595.
- [23] Heisterkamp J, Hillegersberg van R, Sinofsky E, Ijzermans J. Heat resistant cylindrical diffuser for interstitial laser coagulation: Comparison with a bare-tip fibre in ex vivo porcine liver. *Lasers Surg.Med.* 1997. 20, 304-309.
- [24] Hinnen P, de Rooij FW, Voortman G, Tilanus HW, Wilson JHP, Siersema PD. Acrylate yellow filters in operating lights protect against photosensitization tissue damage. *Br.J.Surg.* 2000. 87, 231-235.
- [25] Indolfi C, Esposito G, Di Lorenzo E, Rapacciuolo A, Feliciello A, Porcellini A, Avvedimento VE, Condorelli M, Chiariello M. Smooth muscle cell proliferation is proportional to the degree of balloon injury in a rat model of angioplasty. *Circulation* 1995. 92[5], 1230-1235.
- [26] Grant WE, Buonaccorsi G, Speight PM, MacRobert AJ, Hopper C, Bown SG. The effect of photodynamic therapy on the mechanical integrity of normal rabbit carotid arteries. *Laryngoscope* 1995; 105(8 Pt 1):867-871.
- [27] Stadius van Eps RG, Mark LL, Schiereck J, LaMuraglia GM. Photodynamic therapy inhibits the injury-induced fibrotic response of vascular smooth muscle cells. *Eur J Vasc Endovasc Surg* 1999; 18(5):417-423.
- [28] Strauss WS, Sailer R, Schneckenburger H, Akgun N, Gottfried V, Chetwer L, Kimel S. Photodynamic efficacy of naturally occurring porphyrins in endothelial cells in vitro and microvasculature in vivo. *J Photochem Photobiol B* 1997; 39(2):176-184.
- [29] Heckenkamp J, Adili F, Kishimoto J, Koch M, LaMuraglia GM. Local photodynamic action of methylene blue favorably modulates the postinterventional vascular wound healing response. *J Vasc Surg* 2000; 31(6):1168-1177.
- [30] Huffman MD, Curci JA, Moore G, Kerns DB, Starcher BC, Thompson RW. Functional importance of connective tissue repair during the development of experimental abdominal aortic aneurysms. *Surgery* 2000; 128(3):429-438.
- [31] Li W, Liu G, Chou IN, Kagan HM. Hydrogen peroxide-mediated, lysyl oxidase-dependent chemotaxis of vascular smooth muscle cells. *J Cell Biochem* 2000; 78(4):550-557.
- [32] Quaglino D, Fornieri C, Nanney LB, Davidson JM. Extracellular matrix modifications in rat tissues of different ages. Correlations between elastin and collagen type I mRNA expression and lysyl-oxidase activity. *Matrix* 1993; 13(6):481-490.
- [33] Shanley CJ, Gharaee-Kermani M, Sarkar R, Welling TH, Kriegel A, Ford JW, Stanley JC, Phan SH. Transforming growth factor-beta 1 increases lysyl oxidase enzyme activity and mRNA in rat aortic smooth muscle cells. *J Vasc Surg* 1997; 25(3):446-452.

- [34] Spears JR, Zhan H, Khurana S, Karvonen RL, Reiser KM. Modulation by beta-aminopropionitrile of vessel luminal narrowing and structural abnormalities in arterial wall collagen in a rabbit model of conventional balloon angioplasty versus laser balloon angioplasty. *J Clin Invest* 1994; 93(4):1543-1553.
- [35] Overhaus M, Heckenkamp J, Kossodo S, Leszczynski D, LaMuraglia GM. Photodynamic therapy generates a matrix barrier to invasive vascular cell migration. *Circ Res* 2000; 86(3):334-340.

CHAPTER 10

General discussion

10.00 General discussion

Vascular diseases leading to stenosis of arteries are the primary cause of mortality particularly in the elderly population of the western society [1;2]. The experienced discomfort by patients during the progression of stenosis, depends on the localization and the severity of the stenosis in the arterial network [3-5]. Most of these patients are impaired in their daily activity and suffer from symptoms caused by insufficient blood perfusion. If stenosis progresses and the symptoms become unbearable for the patient, vascular interventions are indicated [6].

In the present clinical policy to treat vascular diseases, a vascular intervention is usually performed at stenosis rates of more than 50%. The overall success rate of these vascular interventions is between 50 to 90% at long-term (>6 months) [7].

Unfortunately, an unwanted side effect after present vascular interventions is the development of restenosis in 30 to 50% within 6 months [8]. This complication impedes the overall success rate and needs to be prevented to improve the outcome of the treatment.

In this thesis, we evaluate endovascular photodynamic therapy as an adjuvant therapy to prevent restenosis in order to improve the outcome of the vascular treatment.

10.01 *What do we presently know about restenosis?*

It is well-known that denudation, overstretching and anastomoses stitches trigger restenosis [9-11], but the mechanism how restenosis develops is still not well-understood.

Typically, 'the cellular and extracellular synthetic repair mode' of the arterial healing response to injury, has difficulties with fine-tuning to the local and systemic hemodynamic requirements [12-17]. This arterial healing response is characterized by 5 phases: 1. the hyperacute phase of complement activation; 2. the acute phase of platelet aggregation; 3. the intermediate phase of leukocyte infiltration; 4. the phase of cellular proliferation and migration, and 5. the chronic phase of cellular and extracellular remodelling.

A logic deduction is that the arterial healing response on one hand depends on the type of artery and arterial injury or pathology and on the other hand on the quality of the local and systemic compensatory mechanisms.

Despite the detection of numerous molecular interactions throughout these phases, the hierarchy in the cascade of events remains to be unraveled in order to find the key target to prevent the development of restenosis. In Chapter 3 we have validated a rat model to study the potential of endovascular PDT as adjuvant therapy of vascular interventions for the prevention of restenosis.

10.02 *Why did we use the rat model?*

We used a rat model for its usefulness in fundamental studies, the ease to handle the animals in the laboratory setting, the existing information on studies in rats and the relative low costs.

Furthermore, we questioned what artery of the rat would be most suitable to evaluate the effects of endovascular PDT. Our challenge was to develop a model in a larger vessel to enable endovascular PDT with the existing laser fiber. Other questions we dealt with were: Does standardised arterial injury induce intimal hyperplasia and constrictive remodelling? Does the 'arterial response to standardised injury' differ between central and peripheral arteries? And if so, will the artery type determine the way to apply PDT?

Remarkably, we found a more excessive accumulation of cells and extracellular material in the peripheral arteries than in the central arteries after standardised balloon injury [18]. Apparently, restenosis developed more easily in the peripheral arteries than in central arteries. With regard to the peripheral arteries after standardised injury, restenosis in the carotid artery consisted of mainly dysplastic intimal hyperplasia, while in the iliac artery the IH was accompanied by constrictive remodeling. Taken the larger initial lumen diameter of the iliac artery and its response to injury, this model suited best to evaluate endovascular PDT.

These findings indicated the differences in the arterial healing between the various arteries that have to be considered in the expected (calculated) outcome after vascular PDT. In other words, the effects of the various PDT dose regimes likely depends on the artery type. Taken together, PDT may be more effective in peripheral arteries than in central arteries, given its important effect on inhibiting IH. The present rat model of standardised balloon injury of the iliac artery appears suitable to evaluate the effect of endovascular photodynamic therapy on dysplastic intimal hyperplasia and constrictive vascular remodelling.

10.03 *What do we know about the photosensitizer accumulation in the arterial wall?*

In Chapter 3 we observed differences in the response to injury between artery type. Next, we questioned if the artery type would determine the accumulation of the photosensitizer in the arterial wall.

As shown, in Chapter 4 the time-intervals for endovascular illumination did not differ significantly between the peripheral and central arteries. However, the maximal amount of PpIX that accumulated in the vascular wall depended on the artery type. More PpIX was formed in peripheral arteries than in central arteries by a lesser mitochondrial content. This contradiction may be explained by our preliminary finding that central arteries contain relatively large mitochondria of which the surface to volume ratio will be smaller than the mitochondria of the peripheral arteries. Since two crucial enzymes that catalyze the final formation of PpIX are located at or in the lipid surface of the mitochondria, i.e. coprogen oxidase and protoporphyrinogen oxidase, the mitochondrion of the central arteries may not be able to generate much PpIX. Alternatively, the activity of these enzymes may be lower in analogy of the imbalance between two other enzymes in the heme synthetic pathway. Thus, the absence of detectable PpIX concentrations in the thoracic aorta but detectable coproporphyrinogen concentrations are indicative for a lower coproporphyrinogen oxidase activity in this central artery type. The ALA dosage should be determined depending on the artery type involved.

An optimal time interval of 2-3 hours between the administration of ALA and the maximal PpIX generation was found.

10.04 *How does the corresponding normal artery of the validated model respond to PDT?*

Given the validated model of Chapter 3 and the corresponding time-interval of the photosensitizer accumulation as described in Chapter 4, we questioned in Chapter 5 what light dose is necessary for effective PDT in the normal artery. These experiments prelude the experiments based on the prevention of restenosis.

We found that light doses lower than 50 J/cm dl at 100 mW/ cm dl caused none to partial eradication of photosensitised cells, while light doses higher than 50 J/cm dl induced eradication of the tunica media. After 16 weeks, the tunica media was completely repopulated without the development of dysplastic intimal hyperplasia. Thus, endovascular ALA-PDT of the normal artery eradicates the cellular content of the tunica intima and tunica media without a significant intimal hyperplasia. What role the eradication of the tunica media has in the prevention of intimal hyperplasia remains to be studied.

10.05 *Does PDT prevent the development of restenosis?*

To answer this crucial question we applied the conclusions of Chapter 3, 4 and 5 in designing a vascular PDT protocol. We questioned what the effective light dose would be in a balloon-injured blood vessel. Furthermore, we wondered if PDT at this effective light dose would effect the hemodynamic regulation system, namely the nerve innervation of the arteries.

In Chapter 6 we showed that PDT prevented restenosis at light doses higher than 50 J/cm dl. Remarkably, PDT resulted in a slight arterial dilation after 4 weeks without any dysplastic IH or constrictive remodeling. The innervation, which regulate arterial constriction and dilation, was not morphologically effected after PDT. After 16 weeks, the tunica media was completely repopulated. The question if the intercellular synapses in the tunica media were damaged after PDT and if the innervation of the tunica media was functionally impaired remained unanswered. Adjuvant endovascular ALA-PDT to balloon injury prevents the development of dysplastic intimal hyperplasia and of the constrictive remodelling. Remarkably, a light dose dependant vessel enlargement was found.

These promising results with vascular PDT in inhibiting dysplastic IH and constrictive remodeling, bear many questions about the crucial step of the arterial healing response that was tackled by PDT.

10.06 *What do we know about mechanisms of restenosis prevention by vascular PDT?*

Strikingly, inhibition of the excessive arterial healing response by PDT, appears to be achieved by the complete eradication of smooth muscle cells in the vascular lesion. Given the many indications from the literature that smooth muscle cell proliferation is inhibited upon reendothelialization of the vascular wall, we questioned whether increasing the rate of reendothelialization is an additional mechanism of PDT in the prevention of restenosis.

In vitro studies showed that PDT induced cross-linking of proteins in the extracellular matrix which may strengthen the extracellular matrix of the treated artery [20-21] and inhibit the repopulation of the lesion. An important enzyme in that respect could be lysyl oxidase [22-27], that facilitates the cross-linking between collagen and elastin. We hypothesized that PDT inhibits transforming growth factor beta (TGF- β) which plays an important role in the regulation of cellular and extracellular matrix synthesis.

In Chapter 7 we found that the time of complete reendothelialization between PDT- and untreated balloon-injured vessels did not differ. Thus, adjuvant endovascular ALA-PDT to balloon injury does not affect the rate of reendothelialisation at the lesion site. Remarkably, the cytokine TGF- β was only temporarily upregulated in the tunica adventitia after PDT in contrast to the sustained high expression after balloon injury only. Adjuvant endovascular ALA-PDT to balloon injury down-regulates the increased expression of TGF-beta upon arterial injury. The expression of TGF-beta in the arterial is associated with the development of dysplastic intimal hyperplasia and the development of constrictive remodelling.

This important finding may indicate that TGF- β plays a key role in the exaggerated vascular repair. It has been shown that TGF- β can stimulate the synthesis of lysyl oxidase [29]. Thus, TGF- β may promote the natural cross-linking of collagen and elastin in the lesion. However, if the expression of TGF- β decreases the subsequent decrease in activity of lysyl oxidase, it will inhibit the abundant synthesis of collagen as seen in arterial restenosis [27-28].

Obviously, further study is needed to clarify the relevance of this issue for PDT.

10.07 *What is the role of the inflammatory response after vascular PDT?*

Normally, in the restenosing artery an inflammatory response is seen, which is characterised by a massive influx of leukocytes particularly into the tunica adventitia. Therefore, we questioned which is the effect of endovascular PDT on the inflammatory response to injury.

We found in Chapter 8 that upon vascular PDT, less neutrophils, but more T-cells and mast-cells were seen in the tunica adventitia. Interestingly, T-cells infiltrate into ‘collagen rich or hyperdense fibrocellular areas’. Thus, these cells may be a marker for strengthening of the injured arterial wall.

Shortly after PDT the number of vasa vasorum decreased. By strengthening the tunica media of the vessel wall and transiently decreasing the number of vasa vasorum, PDT probably inhibits the accumulation of neutrophils into the arterial wall. Since it is generally accepted that neutrophils promote IH, this may be one of the mechanisms by which PDT achieves a beneficial clinical outcome of the vascular intervention.

Thus, adjuvant endovascular ALA-PDT to balloon injury decreased the accumulation of neutrophils at the lesion site which are known to promote IH, by a transient decrease in the number of vasa vasorum.

10.08 *What do we know about the strength of the arterial wall after vascular PDT?*

The eradication of the tunica media may weaken the arterial wall with the consequence of aneurysm formation at long-term. We therefore studied the effect of PDT on the strength of the arterial wall.

In Chapter 9 we found that on the contrary PDT resulted in an immediate strengthening of the arterial wall at high light doses and, in Chapter 7, we found fibrin-like-cross-links at the site of ruptured elastic laminae after PDT.

After a follow-up of 1 year, PDT at the therapeutic light dose range of 50 to <100 J/cm dl still had a positive effect on wall strength. However, a light dose of 100 J/cm dl at 100 mW/cm dl resulted in an aneurysmatic dilatation of the treated artery. Unfortunately, we presently can not a solid explanation why PDT using high fluences led to a weakening of the vessel wall at long-term.

10.09 *What are the disadvantages of our model?*

A major disadvantage of our model is that it is focused on the injured healthy artery and not on the complex atherosclerotic artery with rigid plaques. It can be expected that the reaction of the atherosclerotic plaques to PDT will be far more complex. This merits further study of the suitability of PDT treatment in other models.

10.10 *Which photosensitizer do we use in vascular PDT?*

In general, hydrophilic photosensitizers may diffuse in healthy tissue and are effective to modulate the ‘healthy’ arterial healing response after PDT [30].

The use of ALA induced PpIX as described in Chapters 3-8 proved to be effective in the prevention of dysplastic IH in a peripheral rat iliac artery after standardized balloon injury.

It is likely that this approach will work in patients as well, but as shown in this thesis, the therapeutic window will be narrow and artery type specific.

As the sole treatment of atherosclerotic lesions a successful outcome is less likely: Jenkins and colleagues treated the femoro-iliac arteries of 7 patients in this way, but probably

their treatment was only partially effective because of bad vascularisation of the rigid plaques [31].

However, in rigid lipid rich plaques, lipophilic photosensitizers like chloro-aluminium phtalocyanines (CASPC) [19;32-34] and texaphorins (Antrim)[35-36] may be absorbed more easily and may be more effective to modulate the 'pathologic' arterial healing response. These lipophilic photosensitizers are developed to target the plaques and the macrophages in the plaques, but they face the problem of a non-homogenous distribution and absorption in the arterial plaques and arterial tissue. Obviously, the one ideal photosensitizer is still not available.

10.11 *What type of illumination is preferable in vascular PDT?*

To illuminate the injured vessel there are two options: externally or endovascularly. In external illumination a fibre-tip for spatial divergent illumination is positioned above the tunica adventitia of the arterial lesion. The use of an external reflective mirror under the artery is a prerequisite for circumferential illumination of the artery. It should be taken into account that an important part of the light energy will dissipate via erythrocytes in the circulation because the blood flow is not interrupted during external illumination [37].

In endovascular illumination a transparent cylindrical diffuser fibre-tip for homogenous illumination is endovascularly positioned within the transparent PTA balloon at the arterial lesion. The inflated balloon causes a relative bloodless environment at the illumination site thus preventing the unwanted loss of light energy.

10.12 *What timing do we use in vascular PDT?*

Presently, the timing to illuminate the PpIX-photosensitized artery in vascular PDT is based on the fundamental 2-step concept as described in Chapter 1 at which the fluorescence level is maximal [30;38-42].

Our studies suggest an effective threshold concentration of photosensitive intermediates at which IH is inhibited, but at which the fluorescence level is not necessarily 'maximal'. Apparently, the timing of vascular PDT does not only depend on the time-point at which the concentration of the photosensitizer in the treatment area is maximal, but on the magnitude of the light dose as well. Indeed, the reports of Nyamekye and colleagues [43] and Kipshidze and colleagues support these findings [44].

10.13 *What are the future goals?*

The experimental results described in this thesis and other studies give a solid basis for a phase II clinical trial to evaluate the potential role of ALA-PDT in inhibiting vascular restenosis after PTA or surgical procedures of peripheral arteries.

The clinical challenge is nonetheless to prevent restenosis and to treat atherosclerotic plaques.

References

- [1] Rauwerda JA, Kasteleijn-Nolst Trenité DGA, van Oosterhout-Harmsen MJW. Vaatpatiënten in beeld: knelpunten in de zorg en aanbevelingen. 1 ed. 1998.
- [2] Meijer WT, Hoes AW, Rutgers DM. Peripheral arterial disease in the elderly. The Rotterdam Study. *Arterioscler.Thromb.Vasc Biol* 18, 182-192. 1998.
- [3] Housley E, Leng GC, Donnan PT. Physical activity and risk for peripheral arterial disease in the general population. Edinburgh Artery Study. *J.Epid.Commun.Health.* 47, 475-480. 1993.
- [4] Kaul TK, Fields BL, Wyatt DA, Jones CR, Kahn DR. Surgical management in patients with coexistent coronary and cerebrovascular disease. Long-term results. *Chest* 1994; 106(5):1349-1357.
- [5] Kusaba A. [The significance of the medical research study: hemodynamic and pathophysiological characteristics in peripheral arterial reconstruction]. *Nippon Geka Gakkai Zasshi* 1997; 98(8):697-699.
- [6] Oppat W, Rubin BG. Evaluation of peripheral vascular diseases. In: Doherty GM, Baumann DS, Creswell LL, Goss JA, Lairmore TC, editors. *The Washington manual of Surgery*. Boston, Massachusetts: Little, Brown and Company, 1997: 306-311.
- [7] Nissen SE. Who is at risk for atherosclerotic disease? Lessons from intravascular ultrasound. *Am J Med* 2002; 112 Suppl 8A:27S-33S.:27S-33S.
- [8] Bauters C, Meurice T, Hamon M, McFadden E, Lablanche JM, Bertrand ME. Mechanisms and prevention of restenosis: from experimental models to clinical practice. *Cardiovasc Res* 1996; 31(6):835-846.
- [9] Haudenschild CC. Pathogenesis of restenosis. A correlation of clinical observations with cellular responses. *Z Kardiol* 1990; 79 Suppl 3:17-22:17-22.
- [10] Forrester JS, Fishbein M, Helfant R, Fagin J. A paradigm for restenosis based on cell biology: clues for the development of new preventive therapies. *J Am Coll Cardiol* 1991; 17(3):758-769.
- [11] Brami M, Cote G, Bonan R. [Clinical, experimental and physiopathological aspects of restenosis after coronary angioplasty]. *Arch Mal Coeur Vaiss* 1997; 90(3):385-391.
- [12] Post MJ, Borst C, Kuntz RE. The relative importance of arterial remodeling compared with intimal hyperplasia in lumen renarrowing after balloon angioplasty. A study in the normal rabbit and the hypercholesterolemic Yucatan micropig [see comments]. *Circulation* 1994; 89(6):2816-2821.
- [13] Chen C, Coyle KA, Hughes JD, Lumsden AB, Ku DN. Reduced blood flow accelerates intimal hyperplasia in endarterectomized canine arteries. *Cardiovasc Surg* 1997; 5(2):161-168.
- [14] Azevedo LC, Pedro MA, Souza LC, de Souza HP, Janiszewski M, da Luz PL et al. Oxidative stress as a signaling mechanism of the vascular response to injury: the redox hypothesis of restenosis. *Cardiovasc Res* 2000; 47(3):436-445.
- [15] Berni A, Cavaiola S, Carra A, Fiorellino A, Tombesi T, Tromba L. Control of the operated carotid with ultrasound. Anatomical and hemodynamical modifications, both local and intracranial. *J Cardiovasc Surg (Torino)* 1999; 40(1):27-29.
- [16] Cavalcanti S. Hemodynamics of an artery with mild stenosis. *J Biomech* 1995; 28(4):387-399.
- [17] Hironaka K, Yano M, Kohno M, Tanigawa T, Obayashi M, Konishi M et al. In vivo aortic wall characteristics at the early stage of atherosclerosis in rabbits. *Am J Physiol* 1997; 273(3 Pt 2):H1142-H1147.
- [18] Gabeler EEE, van Hillegersberg R, Stadius van Eps RG, Sluiter W, Gussenhoven EJ, Mulder P et al. A Comparison of Balloon Injury Models after Endovascular Lesions in the Rat. Submitted 2002.

-
- [19] LaMuraglia GM, ChandraSekar NR, Flotte TJ, Abbott WM, Michaud N, Hasan T. Photodynamic therapy inhibition of experimental intimal hyperplasia: acute and chronic effects. *J Vasc Surg* 1994; 19(2):321-329.
- [20] Overhaus M, Heckenkamp J, Kossodo S, Leszczynski D, LaMuraglia GM. Photodynamic therapy generates a matrix barrier to invasive vascular cell migration. *Circ Res* 2000; 86(3):334-340.
- [21] Heckenkamp J, Adili F, Kishimoto J, Koch M, LaMuraglia GM. Local photodynamic action of methylene blue favorably modulates the postinterventional vascular wound healing response. *J Vasc Surg* 2000; 31(6):1168-1177.
- [22] Kagan HM, Tseng L, Trackman PC, Okamoto K, Rapaka RS, Urry DW. Repeat polypeptide models of elastin as substrates for lysyl oxidase. *J Biol Chem* 1980; 255(8):3656-3659.
- [23] Kagan HM, Vaccaro CA, Bronson RE, Tang SS, Brody JS. Ultrastructural immunolocalization of lysyl oxidase in vascular connective tissue. *J Cell Biol* 1986; 103(3):1121-1128.
- [24] Ooshima A, Midorikawa O. Increased lysyl oxidase activity in blood vessels of hypertensive rats and effect of beta-aminopropionitrile on arteriosclerosis. *Jpn Circ J* 1977; 41(12):1337-1340.
- [25] Osborne-Pellegrin MJ, Farjanel J, Hornebeck W. Role of elastase and lysyl oxidase activity in spontaneous rupture of internal elastic lamina in rats. *Arteriosclerosis* 1990; 10(6):1136-1146.
- [26] Quaglino D, Fornieri C, Nanney LB, Davidson JM. Extracellular matrix modifications in rat tissues of different ages. Correlations between elastin and collagen type I mRNA expression and lysyl-oxidase activity. *Matrix* 1993; 13(6):481-490.
- [27] Shanley CJ, Gharaee-Kermani M, Sarkar R, Welling TH, Kriegel A, Ford JW et al. Transforming growth factor-beta 1 increases lysyl oxidase enzyme activity and mRNA in rat aortic smooth muscle cells. *J Vasc Surg* 1997; 25(3):446-452.
- [28] Spear JR, Zhan H, Khurama S, Kavonen RL, Reiser KM. Modulation of beta-aminopropionite of vessel luminal renarrowing, structural abnormalities in arterial wall collagen in a rabbit model of conventional balloon angioplasty versus laser balloon angioplasty. *J Clin Invest* 1994;93:1543-1553.
- [29] Sheridan PJ, Kozar LG, Benson SC. Increased lysyl oxidase activity in aortas of hypertensive rats and effect of beta-aminopropionitrile. *Exp Mol Pathol* 1979; 30(2):315-324.
- [56] Stadius van Eps RG, LaMuraglia GM. Photodynamic therapy inhibits transforming growth factor beta activity associated with vascular smooth muscle cell injury. *J Vasc Surg* 1997; 25(6):1044-1052.
- [30] Hasan T. *Fundamentals of photochemistry and Photodynamic therapy*. 1 ed. San Jose: SPIE, 2000.
- [31] Jenkins MP, Buonaccorsi GA, Raphael M, Nyamekye I, McEwan JR, Bown SG et al. Clinical study of adjuvant photodynamic therapy to reduce restenosis following femoral angioplasty. *Br J Surg* 1999; 86(10):1258-1263.
- [32] Adili F, Stadius van Eps RG, Karp SJ, Watkins MT, LaMuraglia GM. Differential modulation of vascular endothelial and smooth muscle cell function by photodynamic therapy of extracellular matrix: novel insights into radical-mediated prevention of intimal hyperplasia. *J Vasc Surg* 1996; 23(4):698-705.
- [33] LaMuraglia GM, Adili F, Schmitz-Rixen T, Michaud NA, Flotte TJ. Photodynamic therapy inhibits experimental allograft rejection. A novel approach for the development of vascular bioprostheses. *Circulation* 1995; 92(7):1919-1926.
- [34] LaMuraglia GM, Ortu P, Flotte TJ, Roberts WG, Schomacker KT, ChandraSekar NR et al. Chloroaluminum sulfonated phthalocyanine partitioning in normal and intimal hyperplastic artery in the rat. Implications for photodynamic therapy. *Am J Pathol* 1993; 142(6):1898-1905.

- [35] Blumenkranz MS, Woodburn KW, Qing F, Verdooner S, Kessel D, Miller R. Lutetium texaphyrin (Lu-Tex): a potential new agent for ocular fundus angiography and photodynamic therapy. *Am J Ophthalmol* 2000; 129(3):353-362.
- [36] Hayase M, Woodburn KW, Perlroth J, Miller R, Baumgartner W, Yock PG et al. Photoangioplasty with local motexafin lutetium delivery reduces macrophages in a rabbit post-balloon injury model. *Cardiovasc.Res.* 49, 449-455. 2001.
- [37] Ben Hur E, Orenstein A. The endothelium and red blood cells as potential targets in PDT-induced vascular stasis. *Int J Radiat Biol* 1991; 60(1-2):293-301.
- [38] Adili F, Staius van Eps RG, LaMuraglia GM. Significance of dosimetry in photodynamic therapy of injured arteries: classification of biological responses. *Photochem Photobiol* 1999; 70(4):663-668.
- [39] Star WM, Marijnissen JP. Light dosimetry in optical phantoms and in tissues: 1. Multiple flux and transport theory. *Phys.Med.Biol.* 33[4], 437-442. 1988.
- [40] van den Boogert J, van Hillegersberg R, van Staveren HJ, de Bruin RW, van Dekken H, Siersema PD et al. Timing of illumination is essential for effective and safe photodynamic therapy: a study in the normal rat oesophagus. *Br J Cancer* 1999; 79(5-6):825-830.
- [41] Henderson BW, Dougherty TJ. How does photodynamic therapy work? *Photochem Photobiol* 1992; 55(1):145-157.
- [42] van den Boogert J, van Hillegersberg R, de Rooij FW, de Bruin RW, Edixhoven-Bosdijk A, Houtsmuller AB et al. 5-Aminolaevulinic acid-induced protoporphyrin IX accumulation in tissues: pharmacokinetics after oral or intravenous administration. *J Photochem Photobiol B* 1998; 44(1):29-38.
- [43] Nyamekye I, Anglin S, McEwan J, MacRobert A, Bown S, Bishop C. Photodynamic therapy of normal and balloon-injured rat carotid arteries using 5-amino-levulinic acid. *Circulation* 1995; 91(2):417-425.
- [44] Kipshidze N, Sahota H, Komorowski R, Nikolaychik V, Keelan MH, Jr. Photoremodeling of arterial wall reduces restenosis after balloon angioplasty in an atherosclerotic rabbit model. *J Am Coll Cardiol* 1998; 31(5):1152-1157.

CHAPTER 11

Summary

11.00 Summary

1. General introduction.

The concept of photodynamic therapy is based on the local use of light and a photosensitive substrate to generate free reactive radicals. These reactive radicals cause local cytotoxicity. The use of photodynamic therapy in the field of vascular medicine has been derived from the field of oncology and dermatology in treating hyperproliferative disorders. A review of vascular photodynamic therapy and the relevant physics of photodynamic therapy are given. The development of restenosis after vascular interventions to treat stenosis in (cardio) vascular diseased patients remains a problem, because it compromises the success rates of vascular interventions. A baseline problem of restenosis development is the unraveled patho-etiology. Presently, restenosis development is considered as a 'response-to-injury' and a 'reactive-adaptive remodelling' of the vascular wall. The difficulty for the strategies of vascular interventions to prevent restenosis, is to find the key target in the complex multifactorial arterial healing response. Promising results in the prevention of dysplastic intimal hyperplasia are obtained by using vascular photodynamic therapy.

2. Aims and study outline

3. A rat model for the evaluation of endovascular techniques to prevent restenosis.

In this chapter, reference models of standardized balloon injury in peripheral arteries, the right common carotid artery and the right common iliac artery and in a central artery, the abdominal aorta, were compared for the validation of a rat model to evaluate endovascular photodynamic therapy to prevent restenosis. The requirements for the suitability of the rat model were significant late lumen loss, significant dysplastic intimal hyperplasia, significant constrictive remodelling and reproducibility. In this study, rats underwent a standard balloon injury of 15 mm length at 2.0 bar in the carotid-, iliac artery and abdominal aorta. After 16 weeks, late lumen loss was 0.49 ± 0.07 mm, 0.22 ± 0.07 mm and 0.07 ± 0.10 mm in respectively the carotid-, iliac artery and abdominal aorta ($p < 0.05$). Dysplastic intimal hyperplasia was 0.14 ± 0.08 mm², 0.14 ± 0.03 mm² and 0.12 ± 0.04 mm² in respectively the carotid-, iliac artery and abdominal aorta ($p < 0.001$ vs 0 weeks and mutually NS). The constrictive remodelling was only detected in the iliac artery compared to the carotid and abdominal aorta. In this report we concluded that the standardized balloon injury resulted late lumen loss due to dysplastic intimal hyperplasia in the carotid artery, due to dysplastic intimal hyperplasia and constrictive remodelling in the iliac artery, and dilatatory remodelling in the abdominal aorta. Apparently, the occurrence of late lumen loss is artery-type dependent. Therefore, the iliac artery appears to be most suitable artery to evaluate the effect of endovascular photodynamic therapy on dysplastic intimal hyperplasia and constrictive remodelling.

4. Aminolaevulinic acid induced protoporphyrin IX pharmacokinetics: Optimum time interval of photosensitization for photodynamic therapy in peripheral and central arteries of the rat.

In this chapter, the first prerequisite to perform endovascular aminolaevulinic acid (ALA) based PDT in the validated balloon injured iliac artery is photosensitization of the target artery. Therefore, this study focused on the pharmacokinetics of the conversion of ALA into protoporphyrin IX (PpIX) after its systemic application to determine the time-intervals of

maximal PpIX concentrations in the peripheral- and central arteries. The peripheral arteries were represented by the carotid-, renal-, iliac and femoral artery, and the central arteries by the thoracic- and abdominal aorta. In this study, rats underwent photosensitization after intravenous ALA administration at a dose of 200 mg/kg body weight. At varying time-points, respectively 0, 1, 2, 3, 6, 12 and 24 hours both peripheral and central arteries were isolated, homogenized and the PpIX concentration determined by a fluorometric extraction method. The time-interval of maximal PpIX accumulation after ALA administration was not significantly different in the peripheral and central arteries (2:09 vs 2:27 hours). The maximal PpIX concentrations in the peripheral arteries varied between 20.49 ± 3.0 and 24.0 ± 7.5 pmol/mg protein and in the central arteries between 0 and 9.46 ± 0.01 pmol/mg protein. The total protoporphyrin accumulation within 24 hours was significantly higher in the peripheral arteries than in the central arteries ($p < 0.007$). This study demonstrated that as prerequisite for endovascular ALA based photodynamic therapy arteries should be illuminated between 2-3 hours after ALA administration if maximal photosensitizer concentrations are mandatory.

5. The effect of endovascular aminolaevulinic acid-based photodynamic therapy on the normal rat iliac artery.

In this chapter, the baseline histo-geometric effects of endovascular aminolaevulinic acid-based photodynamic therapy (ALA-PDT) on the normal rat iliac artery were evaluated using the specifications of *Chapter 4*. This study described the normal arterial healing response that has to be taken into account when endovascular ALA-PDT as adjuvant strategy to endovascular balloon angioplasty is used during the treatment of the adjacent uninjured arterial segment next to the injured arterial segment. Rats underwent endovascular ALA-PDT at light doses of 12.5, 25, 50 or 100 J/cm dl at an irradiance of 100 mW/cm dl. As a result of endovascular ALA-PDT after 16 weeks, a negligible amount of intimal hyperplasia was seen with values of 0.01 ± 0.007 mm², 0.02 ± 0.007 mm², 0.01 ± 0.006 mm² and 0.02 ± 0.009 mm² at respectively 12.5, 25, 50 and 100 J/cm dl (NS). A fluence of 12.5-25 J/cm dl resulted in partial cellular eradication of the tunica media, while a fluence of 50-100 J/cm dl resulted in complete cellular eradication of the tunica media 3 hours after endovascular ALA-PDT. However, complete repopulation of the tunica media was seen without late lumen loss and constriction after 16 weeks. The observations in this study showed that endovascular ALA-PDT only caused minor and transient damage to the normal iliac arterial wall that fully recovered within 16 weeks keeping its normal functions.

6. Endovascular photodynamic therapy with aminolaevulinic acid prevents balloon induced intimal hyperplasia and constrictive remodelling in rat iliac arteries.

In this chapter, the effects of endovascular ALA-PDT adjuvant to balloon injury are reported on the development of dysplastic intimal hyperplasia and constrictive remodelling by elimination of smooth muscle cells in the tunica media and of elimination of endothelial cells in the tunica intima. Additionally, the effect of endovascular ALA-PDT on the cholinergic innervation of the tunica media was determined, because we hypothesized that the presence of this innervation may be a prerequisite in the arterial healing response for modulating the repopulation and re-configuring the tunica media. The specifications for endovascular ALA-PDT adjuvant to balloon injury were derived from *Chapter 3, 4 and 5*. Rats underwent at random either endovascular ALA-PDT

adjuvant to balloon injury with a light dose of 12.5, 25, 50 or 100 J/cm dl at an irradiance of 100 mW/cm dl in the experimental groups or balloon injury with 0, 12.5, 25, 50 or 100 J/cm dl in the control groups. Planimetric analysis of the arterial cross-sections showed negligible intimal hyperplasia of $0.02 \pm 0.02 \text{ mm}^2$ after adjuvant endovascular ALA-PDT at 100 J/cm dl in the experimental groups, while significant intimal hyperplasia occurred of $0.28 \pm 0.12 \text{ mm}^2$ and $0.27 \pm 0.12 \text{ mm}^2$ in the balloon injury group respectively at 0 and 100 J/cm dl at 16 weeks ($p < 0.05$).

In the experimental endovascular ALA-PDT groups adjuvant to balloon injury, a light-dose increase of a factor 2 led to a decrease of intimal hyperplasia of 17.2% ($p < 0.05$). Constrictive remodelling remained absent in the experimental groups in contrast to the control groups after 16 weeks. The staining of cholinergic innervation of the tunica media of the blood vessel wall in the experimental groups was not decreased at the highest fluence, indicating the preservation of the cholinergic innervation after endovascular ALA-PDT. In this report we concluded that endovascular ALA-PDT prevents dysplastic intimal hyperplasia and constrictive remodelling after balloon injury without damage of cholinergic innervation of the tunica media. The effective light fluence rate in the rat is 50-100 J/cm dl.

7. The effect of aminolaevulinic acid-based endovascular photodynamic therapy on reendothelialization after balloon injury of the rat iliac artery.

In this chapter, the effect of endovascular ALA-PDT on the reendothelialization of the tunica intima during the arterial healing is evaluated because on one hand, reendothelialization of the tunica intima is crucial to preserve laminar blood flow, and on the other hand, it is a well-known inhibitor of intimal hyperplasia.

Furthermore, the effects of endovascular ALA-PDT upon balloon injury on the expression of the multifactorial cytokine TGF- β , an important regulator of endothelial cell growth and intimal hyperplasia development were studied.

Reendothelialization was detected by the exclusion of Evans Blue by the blood vessel (1) and TGF- β expression by immuno-staining (2). In the experimental endovascular ALA-PDT group upon balloon injury, endovascular illumination was performed with 50 J/cm dl or 100 J/cm dl at an irradiance of 100 mW/cm dl. In the control group only balloon injury was performed and untreated arteries served as base-line controls. We found a complete reendothelialization at the lesion site after 3 weeks in the experimental and control groups without a significant difference between the groups.

However, endovascular ALA-PDT upon balloon injury resulted in significant inhibition of intimal hyperplasia and a modification of adventitial morphology as described in *Chapter 6*. There was an immediate increase in the expression of TGF- β without significant differences between the experimental and control groups. Importantly, no TGF- β was detectable in the experimental groups after 3 weeks in contrast to the control balloon injury group.

In this report we concluded that adjuvant endovascular ALA-PDT does not significantly affect the rate of reendothelialization process in vivo. Besides inhibiting dysplastic intimal hyperplasia, endovascular ALA-PDT reduced the increased expression of TGF- β upon balloon injury, which may play a role in the favourable remodelling after endovascular ALA-PDT as described in *Chapter 6*.

8. Endovascular photodynamic therapy altered the composition of leukocyte infiltrate in the arterial response to injury.

In this chapter, the effects of endovascular ALA-PDT upon balloon injury on the inflammatory reaction in the vessel wall, described as phase 3 in *Chapter1* is evaluated. We assessed the number and type of leukocytes that accumulated in the rat iliac artery in the experimental groups, treated with endovascular ALA-PDT using 12.5, 25, 50 or 100 J/cm dl at an irradiance of 100 mW/cm dl after balloon injury and in the control groups with only balloon injury.

Sixteen weeks after treatment, statistically significantly fewer leukocytes of 28 ± 4 were seen in the experimental endovascular ALA-PDT groups than in the control balloon injury group with 91 ± 34 leucocytes ($p<0.004$). In the experimental group the leukocytes consisted of 20% neutrophils, 35% mastcells, 29% T-cells and 18% monocytes compared to the control group with 31% neutrophils, 5% mastcells, 59% T-cells and 5% monocytes. In this study we concluded that 1. Endovascular ALA-PDT after balloon injury decreases the total number of leukocytes that enter the lesion site.
2. Endovascular ALA-PDT altered the composition of the inflammatory exudate after balloon injury: it decreases the percentage neutrophils and increases the percentage of mastcells.

9. Arterial strength after amino-laevulinic acid based endovascular photodynamic therapy.

In this chapter, the effect of endovascular ALA-PDT adjuvant to balloon angioplasty on the arterial wall strength and the local blood flow was evaluated with regard to the functional quality of the treated arterial wall. In this study we determined the mean bursting pressure of the artery and the local blood flow in the experimental groups with endovascular ALA-PDT using 50 or 100 J/cm dl at an irradiance of 100 mW/cm dl upon balloon injury, and in the control balloon injury only group. Two hours after the procedure the mean bursting pressure in the experimental group was 3.37 ± 0.58 bar at 50 J/cm dl and 3.96 ± 0.43 bar at 100 J/cm dl, compared to 2.20 ± 0.27 bar in the control group ($p<0.05$). After 1 year these values were in the experimental groups 3.18 ± 0.87 bar at 50 J/cm dl ($p<0.05$) and 2.02 ± 0.31 bar at 100 J/cm dl (NS), compared to 2.10 ± 0.30 bar in the control group. Remarkably, in the experimental group at 100 J/cm dl 3/5 rats developed an aneurysm proximally in the treated arterial segment. Apparently, endovascular ALA-PDT after balloon injury increases the arterial wall strength as measured by the bursting pressure at short term and at low fluence in longterm. However, at a fluence of 100 J/cm dl aneurysms formed after 1 year. The mean local flow in the treated artery was 5.02 ± 0.09 ml/min and was not significantly different between the experimental and control groups 3 hours after intervention. After 1 year, the flow was significantly decreased in the experimental groups compared to the control group due to dilational enlargement of the arterial segment. In this study we concluded that the light dose is crucial in endovascular ALA-PDT and should be limited to 50 J/cm dl in this model to take full advantage of the beneficial effect of this fluence on the characteristics of the treated blood vessel.

10. General discussion.

In this chapter, the general concepts and challenges are discussed to prevent restenosis after vascular interventions by endovascular ALA-PDT.

Endovascular ALA-PDT is based at least two mechanisms : 1. The eradication of (hyper) proliferative smooth muscle cells, and 2. Strengthening the arterial wall by the induction of protein-protein cross links. Since the patho-etiology of restenosis is characterized by two phenomena, namely dysplastic intimal hyperplasia and constrictive remodelling, it is not surprisingly that PDT is an effective treatment.

In *Chapter 3*, the role of the artery type in the arterial healing response after arterial injury was described to illustrate the importance of the artery type in restenosis prevention. Peripheral arteries appeared to be more prone to develop restenosis by dysplastic intimal hyperplasia or constrictive remodelling than central arteries. Indeed, the incidence of restenosis is higher in peripheral arteries than in central arteries. Therefore, preventive measures are used more frequently in peripheral arteries. The role of artery type for endovascular ALA-PDT in the conversion of ALA into the photosensitive intermediate protoporphyrin IX (PpIX) was described in *Chapter 4*, in which we concluded that the accumulation of PpIX was higher in the peripheral arteries than in the central arteries. For effective endovascular ALA-PDT we hypothesized that the criterion of maximal PpIX concentrations in the target artery is a favorable prerequisite. Indeed, we reported in *Chapter 5 and 6* promising results in the prevention of dysplastic intimal hyperplasia and constrictive remodelling using this criterion, but the question what threshold dose of PpIX or photosensitizer in general is required for effective ALA-PDT remains to be studied. In our *in vivo* study described in *Chapter 7*, an important cytokine in regulating the abundant synthesis of collagens occurring during restenosis was down regulated after endovascular ALA-PDT. Furthermore, probably due to its decreasing effect on the number of vasa vasorum in the tunica adventitia, a likely entry site of inflammatory cells into the lesion site, the influx of leukocytes decreased in magnitude and changed into a more favourable composition (less neutrophils, more T-cells) as was described and discussed in *Chapter 8*. In *Chapter 9* the importance of light-dose in relation to the arterial bursting strength was described. It appeared that endovascular ALA-PDT has a dilatory effect and results in aneurysms if too high light doses are used. Therefore, the application of endovascular ALA-PDT bears some risk of complications if no adequate dosimetry is taken into account. How to integrate endovascular ALA-PDT in the prevention of restenosis in pathologic human arteries will depend on the predictability of the arterial healing response under these circumstances. The issues with regard to the complexity of the arterial healing response and the involved topics and challenges of vascular photodynamic therapy have been discussed.

11. Summary

11.01 Samenvatting

1. Introductie.

Het fundamentele concept van fotodynamische therapie is gebaseerd op het gebruik van een locale lichtbron om een lichtgevoelig substraat in het doelgebied te activeren, hetgeen zal resulteren in de vorming van vrije radicalen. Deze radicalen zijn in principe cytotoxisch, hetgeen lokaal zal leiden tot cel versterf. Het gebruik van fotodynamische therapie in het werkkerrein van de vasculaire geneeskunde is afkomstig uit de oncologische en dermatologische hoek, waar fotodynamische therapie gebruikt wordt om kwaadaardige aandoeningen te behandelen. In dit hoofdstuk wordt een overzicht gegeven van het probleem restenose, de achtergrond van vasculaire fotodynamische therapie en de bijbehorende relevante fysische beginselen van fotodynamische therapie.

Het slagen van een therapeutische vasculaire behandeling van ernstige vaatvernauwende aandoeningen bij patiënten met hart- en vaatziekten, wordt belemmerd door de ontwikkeling van een complicatie genaamd 'restenose'. Restenose wordt gedefinieerd als het opnieuw ontstaan van een vaatvernauwing in het behandelde arteriële traject. Ten gevolge van restenose zullen deze patiënten wederom klachten ondervinden die worden veroorzaakt en uitgelokt door insufficiënte doorbloeding. Het een of meerdere malen herhalen van de belastende en dure therapeutische ingrepen is daarom vaak onvermijdelijk. Echter, het voorkomen van restenose is lastig gezien de onopgehelderde patho-etologie van deze complicatie.

Tot op de dag van vandaag worden twee hypothesen gebruikt om de ontwikkeling van restenose te verklaren, namelijk 1. de 'response-to-injury' hypothese die gestoeld is op de cellulaire en extracellulaire morfologische reacties na arteriële beschadiging en gekarakteriseerd wordt door de ontwikkeling van dysplastische intimale hyperplasie, en 2. de 'reactive-adaptive remodelling' hypothese die beschrijft dat de locale en systemische hemodynamiek de uiteindelijke uitkomst van de arteriële genezingsresponse bepaalt welke gekarakteriseerd wordt door constrictieve remodellering. De ontwikkeling van deze twee hypothesen is niet verwonderlijk omdat intimale hyperplasie en constrictieve remodellering zowel afzonderlijk als in combinatie als reactie op vaatwandschade kunnen optreden. De moeilijkheid voor de te ontwikkelen strategieën om restenose te voorkomen is nu het vinden van een werkbare oplossing in deze complexe multifactoriële reacties van de arteriële genezingsrespons. De beschreven resultaten verkregen met vasculaire fotodynamische therapie hierbij zijn echter veel belovend.

2. De doelstellingen en de indeling van deze dissertatie.

3. Een validatie studie van ratten modellen voor de evaluatie van endovasculaire technieken om restenose te voorkomen.

In dit hoofdstuk worden potentiële referentie modellen om restenose op te wekken na gestandaardiseerde ballon schade van de arteriële vaatwand in perifere en centrale arteriën met elkaar vergeleken om te komen tot een gevalideerd ratten model voor de bestudering van de effectiviteit van endovasculaire fotodynamische therapie ter preventie van restenose. De vereisten waaraan dit ratten model aan moest voldoen waren een significant verlies van de arteriële lumen diameter, de zogenaamde 'late lumen loss', een significante ontwikkeling van dysplastische intimale hyperplasie, een significante ontwikkeling van constrictieve remodellering, gedefinieerd als een afname van de arteriële vaatwand omtrek en luminale diameter, en uiteraard de reproduceerbaarheid van het model. In deze studie werden de

arteria carotis communis, de arteria iliaca communis en de abdominale aorta van de ratten volgens een standaard protocol met behulp van een ballon opgeblazen tot 2.0 bar over een lengte van 15 mm. Na 16 weken was de diameter van het lumen van respectievelijk de arteria carotis communis, de arteria iliaca communis en de abdominal aorta 0.49 ± 0.07 mm, 0.22 ± 0.07 mm and 0.07 ± 0.10 mm kleiner, en de ontwikkeling van dysplastische intimale hyperplasie respectievelijk 0.14 ± 0.08 mm², 0.14 ± 0.03 mm² and 0.12 ± 0.04 mm² ($p < 0.001$ vs 0 weken en onderling NS). Constrictieve remodelering werd alleen gezien in de arteria iliaca communis. In dit rapport concludeerden wij dat de gestandaardiseerde ballonschade van de arteriële vaatwand resulteerde in vermindering van de luminale diameter in de arteria carotis communis ten gevolge van dysplastische intimale hyperplasie, in de arteria iliaca communis ten gevolge van dysplastische intimale hyperplasie en constrictieve remodelering, maar geen vermindering van luminale diameter in de abdominale aorta doordat de geringe intimale hyperplasie gecompenseerd werd door enige verwijdende remodelering. Klaarblijkelijk, is het verlies in luminale diameter afhankelijk van het type arterie. Het arteriële genezingsproces na beschadiging is dus afhankelijk van het vaat type in de rat. Voor ons onderzoek is de gestandaardiseerde ballonschade in de arteria iliaca communis dus het meest geschikt om het effect van endovasculaire fotodynamische therapie ter voorkoming van restenose te bestuderen.

4. De farmacokinetiek van aminolevuline zuur geïnduceerde protoporfyrine IX in perifere en centrale arteriën van de rat.

In dit hoofdstuk is de fotosensitizatie van de te behandelen arterie met behulp van de endogene heem metaboliet aminolevuline zuur (ALA) geevalueerd als eerste voorwaarde om endovasculaire fotodynamische therapie te verrichten. In het ontwerp van deze studie ligt de nadruk op de farmacokinetiek van de omzetting van systemisch toegediend ALA naar protoporfyrine IX (PpIX) om het tijdsinterval te bepalen waarbinnen de concentratie van PpIX in de vaatwand van een aantal perifere arteriën, zoals de arteria carotis communis, arteria renalis, arteria iliaca communis en in de arteria femoralis, en van de centrale arteriën, zoals de thoracale en abdominale aorta, de hoogste waarde bereikt. Daartoe werden ratten gefotosensitizeerd door intraveneuze toediening van 200 mg ALA /kg lichaamsgewicht. Op 0, 1, 2, 3, 6, 12 en 24 uur na ALA toediening werden de arteriën geïsoleerd en gehomogeniseerd. Vervolgens werd de concentratie PpIX in de vaatwand fluorometrisch bepaald met behulp van HPLC. Het bleek dat de tijd waarin de concentratie PpIX maximaal werd niet significant verschilde tussen de perifere en centrale arteriën (2:09 en 2:27 uur). Echter, de concentratie PpIX was hoger in de perifere arteriën, variërend tussen de 20.49 ± 3.0 en 24.0 ± 7.5 pmol/mg eiwit, dan in de centrale arteriën met waarden tussen de 0 en 9.46 ± 0.01 pmol/mg eiwit. Dit verschil in hoogte in de concentratie PpIX tussen de perifere en centrale arteriën was significant ($p < 0.007$). De afwezigheid van detecteerbare concentraties PpIX bij aanwezigheid van coproporphyrinogeen in de thoracale aorta, in tegenstelling tot de aanwezigheid van detecteerbare concentraties PpIX en coproporphyrinogeen in de perifere vaten is dus indicatief voor een arterie type afhankelijke omzetting van ALA. Als een vereiste voor optimale fotodynamische therapie is dat de concentratie van PpIX maximaal is, moet op grond van deze studie belichting tussen de 2-3 uur na systemische toediening van ALA plaatsvinden.

5. Het effect van endovasculaire fotodynamische therapie met aminolevuline zuur op de normale ratten iliacaal arterie.

In dit hoofdstuk worden de histo-geometrische effecten op de normale ratten iliacaal arterie geevalueerd na aminolevuline zuur-gebaseerde endovasculaire fotodynamische therapie (ALA-PDT). De tijdsintervallen voor het belichtingsregime voor een veronderstelde optimale fotodynamische therapie zoals beschreven in *Hoofdstuk 4* zijn hiervoor gebruikt. Deze studie beschrijft het genezingsproces in de gezonde arterie na endovasculaire ALA-PDT. Op grond daarvan zou kunnen worden ingeschat wat het effect is van endovasculaire ALA-PDT op het aangrenzende onbeschadigde arteriële segment bij gebruik van PDT als adjuvante strategie voor de behandeling van het beschadigde arteriële segment na endovasculaire ballon angioplastiek. Hiervoor ondergingen ratten endovasculaire ALA-PDT met een licht dosis van 12.5, 25, 50 of 100 J/cm diffuser lengte (dl) bij een lichtsterkte van 100 mW/cm dl. Het resultaat na 16 weken was een verwaarloosbare ontwikkeling van intimale hyperplasie met waarden van $0.01 \pm 0.007 \text{ mm}^2$, $0.02 \pm 0.007 \text{ mm}^2$, $0.01 \pm 0.006 \text{ mm}^2$ en $0.02 \pm 0.009 \text{ mm}^2$ respectievelijk na 12.5, 25, 50 en 100 J/cm dl (NS). Een lichtdosis van 12.5-25 J/cm dl resulteerde in partiële depletie van het aantal cellen in de tunica media, na een lichtdosis van 50-100 J/cm dl waren alle cellen in de tunica media 3 uur na endovasculaire ALA-PDT verdwenen. Echter, na 16 weken werd weer een normale celdichtheid in de tunica media gezien zonder enige vermindering van de luminale diameter of constrictieve remodelering. Op basis van deze observaties concludeerden wij dat endovasculaire ALA-PDT geen blijvend nadelig effect had op de vaatwand.

6. Endovasculaire fotodynamische therapie met aminolevuline zuur voorkomt ballon geïnduceerde dysplastische intimale hyperplasie en constrictieve remodelering in ratten iliacaal arteriën.

In dit hoofdstuk worden de effecten beschreven van endovasculaire ALA-PDT op de ontwikkeling van dysplastische intimale hyperplasie en constrictieve remodelering na ballon beschadiging van de vaatwand. Verder wordt het effect van endovasculaire ALA-PDT op de cholinerge innervatie van de tunica media bestudeerd, omdat wij veronderstelden dat de aanwezigheid van deze innervatie een voorwaarde kan zijn voor het sturen van de cellulaire reproductie en extracellulaire re-configuratie van de tunica media en tunica intima. De specificaties voor optimale endovasculaire ALA-PDT zijn gebaseerd op de resultaten beschreven in *Hoofdstukken 3, 4 en 5*.

Hiervoor werden ratten gerandomiseerd verdeeld over de experimentele groepen waarin de iliacaal arterie door balloneren werd beschadigd en vervolgens endovasculaire ALA-PDT werd toegepast met een licht dosis van 12.5, 25, 50 of 100 J/cm dl bij een lichtsterkte van 100 mW/cm dl, en over de controle groepen waarin de ballon beschadigde iliacaal arterie niet met PDT werd behandeld maar alleen belicht met een licht dosis van 0, 12.5, 25, 50 of 100 J/cm dl. De resultaten verkregen met behulp van een planimetrische analyse van de arteriële coupes lieten slechts een verwaarloosbare intimale hyperplasie zien met een gemiddelde waarde van $0.02 \pm 0.02 \text{ mm}^2$ in de experimentele groep die behandeld werd met 100 J/cm dl ALA-PDT, terwijl de controle groep van 0 en 100 J/cm dl gekenmerkt werd door dysplastische intimale hyperplasie met waarden van $0.18 \pm 0.12 \text{ mm}^2$ en $0.15 \pm 0.12 \text{ mm}^2$ na 16 weken ($p < 0.05$). Een toename van de licht dosis met een factor 2 in de experimentele endovasculaire ALA-PDT groepen resulteerde in een afname van intimale hyperplasie met 17.2% ($p < 0.05$). Constrictieve remodelering trad in de experimentele groepen niet op in tegenstelling tot de controle groepen. Op grond van immuno-histochemische kleuring kon worden vastgesteld dat de cholinerge innervatie van de tunica media niet tussen de

groepen verschilde, hetgeen erop duidt dat ondanks endovasculaire ALA-PDT de innervatie werd gepreserveerd.

Wij concludeerden in dit rapport dat endovasculaire ALA-PDT dysplastische intimale hyperplasie en constrictieve remodelering voorkomt binnen 4 maanden na ballon beschadiging zonder schade van de cholinergische innervatie van de tunica media. De effectieve licht dosis in dit ratten model was 50-100 J/cm dl.

7. Het effect van endovasculaire fotodynamische therapie op de reendothelialisatie van de ratten iliacaal arterie na ballon beschadiging.

In dit hoofdstuk wordt het effect geëvalueerd van endovasculaire ALA-PDT op de reendothelialisatie van de tunica intima omdat endotheel cruciaal is om de laminaire bloed flow te kunnen garanderen zonder de ontwikkeling van thrombose, en een belangrijke factor is om intimale hyperplasie te voorkomen. Vervolgens werd ook het effect van endovasculaire ALA-PDT na ballon beschadiging van de iliacaal arterie in het gevalideerde ratten model op de expressie van het multifactoriële cytokine ‘transforming growth factor-beta’ (TGF- β) bestudeerd. TGF- β is een belangrijke regulerende factor van endotheliale cel groei en de ontwikkeling van intimale hyperplasie. In de experimentele groep bestond de behandeling na ballon beschadiging van de iliacaal arterie uit een endovasculaire belichting met 100 mW/cm dl tot een totale lichtdosis van 50 of 100 J/cm dl ALA-PDT. In de controle groep werd alleen ballon beschadiging verricht van de rechter iliacaal arterie en de linker onbehandelde arterie gebruikt als controle. Op basis van Evans Blue kleuring kon worden vastgesteld dat na 3 weken zowel in de experimentele als in de controle groepen de beschadigde arterie weer compleet bedekt was met endotheel zonder enig significant verschil tussen de groepen.

In zowel de experimentele als controle groepen nam de expressie van TGF- β direct na beschadiging toe zonder significante verschillen tussen beide groepen.

Echter, in de experimentele groepen was na 3 weken geen TGF- β meer detecteerbaar, maar in de controle groepen bleef de expressie van TGF- β hoog. Endovasculaire ALA-PDT remt dus de verhoogde expressie van TGF-beta na vaatwandschade volledig.

De langdurige expressie van TGF-beta wordt daarom geassocieerd met de ontwikkeling van dysplastische intimale hyperplasie en de ontwikkeling van constrictieve remodelering.

In dit rapport concludeerden wij dat endovasculaire ALA-PDT het proces van reendothelialisatie *in vivo* niet beïnvloedt. Naast de eerder in *Hoofdstuk 6* vermelde remming van de ontwikkeling van dysplastische intimale hyperplasie, concluderen wij ook dat endovasculaire ALA-PDT de verhoogde expressie van TGF- β kleuring in de door ballon behandeling beschadigde arteriële vaatwand op termijn onderdrukt. Of dit effect van invloed is geweest op de gunstige remodelering na endovasculaire fotodynamische therapie valt nog te bezien.

8. Endovasculaire fotodynamische therapie beïnvloedt de grootte en samenstelling van het leucocyten infiltraat in de tunica adventitia na ballon beschadiging.

In dit hoofdstuk wordt het effect van adjuvante endovasculaire ALA-PDT geëvalueerd op de ontstekingsreactie na ballon beschadiging.

In de experimentele groepen werd adjuvante endovasculaire ALA-PDT verricht met een licht dosis van 12.5, 25, 50 of 100 J/cm dl bij een belichting van 100 mW/cm dl na ballon beschadiging, en in de controle groepen werd alleen ballon beschadiging verricht.

Vervolgens werd het ontstekingsinfiltraat in de tunica adventitia van de ratten arteria iliaca communis getypeerd.

Het aantal leucocyten van gemiddeld 28 ± 4 in de vaatwand van de experimentele groepen na endovasculaire ALA-PDT was statistisch significant lager dan in de controle groep met een gemiddelde van 91 ± 34 ($p < 0.004$). Daarvan was in the experimentele groepen 20% neutrofielen, 35% mestcellen, 29% T-cellen en 18% monocytten, en in de controle groep was 31% neutrofielen, 5% mestcellen, 59% T-cellen en 5% monocytten. Op basis van deze studie concludeerden wij dat endovasculaire ALA-PDT de ophoping van leucocyten in de vaatwand na ballon beschadiging vermindert en ook de samenstelling van het leukocyten infiltraat (ten gunste) beïnvloedt: minder neutrofielen, meer T-cellen.

9. Het effect van endovasculaire fotodynamische therapie op de sterkte van de arteriële vaatwand.

In dit hoofdstuk wordt het effect van endovasculaire ALA-PDT op de sterkte van de ballon beschadigde arteriële vaatwand en of de lokale bloed stroming geëvalueerd als maat voor de functionele kwaliteit van de behandelde arteriële vaatwand.

De gemiddelde druk waarbij de arteriële vaatwand ruptureert, de zogenaamde ‘bursting pressure’, en de lokale bloed stroming werden bepaald in de experimentele groepen die endovasculaire ALA-PDT kregen met een licht dosis van 50 of 100 J/cm dl bij een belichting van 100 mW/cm dl na ballon beschadiging, en in de controle groep waarin alleen ballon beschadiging werd verricht. Twee uur na de procedure was de gemiddelde bursting pressure in de experimentele groepen met 3.37 ± 0.58 bar bij 50 J/cm dl en 3.96 ± 0.43 bar bij 100 J/cm dl significant hoger dan in de controle groep met 2.20 ± 0.27 bar ($p < 0.05$).

Endovasculaire ALA-PDT na ballon angioplastiek kent klaarblijkelijk een optimale licht dosis waardoor de arteriële vaatwand stugger wordt. Na 1 jaar was de bursting pressure in de experimentele groepen van 50 J/cm dl nog steeds hoog met een waarde van 3.18 ± 0.87 bar ($p < 0.05$), terwijl deze in de 100 J/cm dl groep gedaald was tot 2.02 ± 0.31 bar, hetgeen niet significant verschilde van 2.10 ± 0.30 bar in de controle groep.

Opmerkelijk was de observatie in de experimentele groep bij 100 J/cm dl na 1 jaar, dat 3 van de 5 behandelde ratten een aneurysma proximaal in het behandelde arteriële segment hadden ontwikkeld. Op korte termijn doet endovasculaire ALA-PDT de arteriële vaatwand na ballon beschadiging dus ongeacht de lichtdosis blijkaar stugger worden. Ook op de langere termijn van 1 jaar bleek de vaatwand ook nog stugger te zijn in de groep die behandeld was met een licht dosis van 50 J/cm dl. Echter in de groep van 100 J/cm dl bleek de keerzijde van endovasculaire PDT uit de ontwikkeling van aneurysmata. Overbelichting van de behandelde arterie na endovasculaire ALA-PDT leidt potentieel tot de ontwikkeling van een aneurysma.

De gemiddelde lokale bloed stroming 3 uur na de interventie in de behandelde arterie

bedroeg 5.02 ± 0.09 ml/min, zowel in de experimentele als in de controle groepen. Na 1 jaar was de bloed stroming significant lager in de experimentele groepen vergeleken met de controle groep door een verwijding van het behandelde arteriële segment. Endovasculaire ALA-PDT na ballon beschadiging heeft een vaatverwijdend effect dat licht- dosis afhankelijk is.

Daarom concludeerden wij op basis van de gegevens uit deze studie dat de licht dosis cruciaal is bij endovasculaire ALA-PDT en in dit gevalideerde ratten model beperkt dient te blijven tot 50 J/cm dl bij een belichting van 100 mW/cm dl.

10. De algemene discussie.

In dit hoofdstuk worden de algemene concepten en uitdagingen voor adjuvante endovasculaire ALA-PDT na vasculaire interventies bediscussieerd om het probleem van restenose en het herintreden van aan hypoperfusie gerelateerde symptomen te kunnen voorkomen. De patho-etilogie van restenose wordt gekarakteriseerd door twee fenomenen, namelijk door dysplastische intimale hyperplasie, en door constrictieve remodelering. Het concept van endovasculaire ALA-PDT is nogal onconventioneel, omdat in eerste instantie (bijna) alle cellen in de tunica intima en in de tunica media erdoor worden gedood en de overblijvende extracellulaire matrix wordt gemodificeerd. Toch blijkt deze radicale aanpak effectief in de arteriële genezing. Het is zeer waarschijnlijk dat endovasculaire ALA-PDT de prikkel wegneemt voor de overmatige reactie van dysplastische intimale hyperplasie en constrictieve remodelering. In *Hoofdstuk 3* werd de reactie van verschillende typen arterie op vaatwandschade beschreven. Hierbij bleken de perifere arteriën van de rat vatbaarder te zijn voor het ontwikkelen van restenose door dysplastische intimale hyperplasie of door constrictieve remodelering dan de centrale arteriën. Ook in patiënten blijkt de algemene incidentie van restenose hoger in perifere arteriën dan in centrale arteriën. Aansluitend werd een tweetal aspecten van de fotosensitizatie van verschillende arterie typen na systemische toediening van ALA beschreven in *Hoofdstuk 4*. Hierin concludeerden wij dat weliswaar het tijdstip waarop de concentratie PpIX maximaal werd niet verschilde tussen de perifere en de centrale arteriën, maar wel de hoogte ten gunste van de perifere arteriën. Als voor effectieve endovasculaire ALA-PDT de hoogte van de PpIX concentratie een criterium is, is de verwachting dat perifere arteriën effectiever met behulp van endovasculaire fotodynamische therapie kunnen worden behandeld. Inderdaad blijkt uit de *Hoofdstukken 5 en 6* dat de ontwikkeling van dysplastische intimale hyperplasie en constrictieve remodelering in de perifere iliacaal arterie door endovasculaire PDT op het moment dat de PpIX concentratie in de vaatwand maximaal was effectief voorkomen kon worden. De vraag wat de effectieve drempel concentratie van PpIX is voor vasculaire ALA-PDT hebben wij nog niet kunnen beantwoorden. In onze in vivo studie beschreven in *Hoofdstuk 7*, bleek de expressie van een belangrijk cytokine dat betrokken is bij de overmatige synthese van matrix eiwitten enige tijd na endovasculaire ALA-PDT niet meer tot expressie te komen in de vaatwand, terwijl in de vaatwand die alleen ballon beschadiging had ondergaan de expressie van dit cytokine onverminderd hoog was. Endovasculaire ALA-PDT bleek ook een afname van het aantal leucocyten in de tunica adventitia te veroorzaken alsmede een gunstige verandering in het type ontstekingscellen waaruit het ontstekingssexudaat bestond, zoals beschreven en bediscussieerd in *Hoofdstuk 8*. In *Hoofdstuk 9* werd het belang van de licht dosis in relatie tot de arteriële vaatwand sterkte beschreven. Daarbij bleek dat endovasculaire ALA-PDT een vaatverwijdend effect heeft en op de korte en lange termijn een versterkend effect heeft op de vaatwand. Bij hoge licht dosis leidt endovasculaire fotodynamische therapie echter uiteindelijk tot aneurysma ontwikkeling. Blijkbaar heeft

endovasculaire ALA-PDT dus een nauw therapeutisch effect in dit gevalideerde ratten model, een gegeven waar bij de humane klinische studies rekening meedient worden te gehouden.

Hoe dit gegeven geïntegreerd dient te worden in de methodiek van endovasculaire ALA-PDT bij patiënten zal volledig afhankelijk zijn van de voorspelbaarheid van het arteriële genezingsproces onder deze omstandigheden. De kern begrippen met betrekking tot de complexiteit van het arteriële genezingsproces, de betrokken raakvlakken en uitdagingen voor vasculaire fotodynamische therapie zijn verder bediscussieerd in dit hoofdstuk.

11. Samenvatting

Appendices

Dankwoord

Ik heb het genoeg gehad om met unieke mensen te kunnen samenwerken waardoor dit proefschrift tot stand kon komen. De expertise en professionaliteit van dezen maakte de studie tot een uiterst leerzame uitdaging. Onmiskenbaar voor het welslagen is de goede onderlinge samenwerking geweest. Daarom wil ik hen bedanken die hierin hebben bijgedragen.

Prof. Dr. H. van Urk, promotor van de studie. Beste professor, alle gezamenlijke inspanningen hebben uiteindelijk kunnen resulteren in dit proefschrift. Uw scherpe kritiek deed een manuscript in de loop van de tijd reduceren tot een heldere boodschap. Bedankt voor de samenwerking. Dr. R. van Hillegersberg, beste Richard, aanvrager van het project en mentor. Je enthousiasme en frisse kijk op de zaken heeft menigmaal de nodige 'boost' gegeven aan het project zodat de studie vlot kon verlopen. Jouw inbreng in de studie naast je eigen opleiding destijds voordat je staf lid op de afdeling Heelkunde te Utrecht werd in combinatie met je eigen gezin verdient veel lof. Voor het feit dat je je ervaring op het gebied van de juiste contact personen, het management, chirurgie (in proefdieren) en o.a de laser fysiologie hebt gedeeld wil ik je bedanken. De momenten dat er iets te vieren viel heb je steeds aangegrepen, een Mac-snack, een Havanna, een Westerpaviljoen, een World congresje, you name it! Lekker lachen en af en toe goed feesten. Bedankt voor je vriendschap. What is your next project?

Dr. W. Sluiter, beste Wim, wetenschapper van het eerste uur en kamergenoot-'genoeg is meer dan veel'. Ik ben je bijzonder dankbaar voor je wetenschappelijke hulp, meer nog je droge humor en bovenal voor wie je bent als mens. Ik heb m.b.t. dit proefschrift 'genoeg' van je geleerd. Bedankt voor je inzicht, de vele discussies en het gestructureerd doornemen van de diverse voorbereidende stappen zodat meerdere malen een effectieve strategie opgebouwd kon worden. Dat we een werkdag samen met Kees konden afsluiten met een goede anekdote onder het genot van iets te drinken en lekker lachen zal ik nooit vergeten. Wanneer doen we de volgende 'one-hundred-and-eighty dart-game championship'?

Dr. R.G. Stadius van Eps, beste Randolph, bedankt voor je inbreng bij de opzet van de studie. Het feit dat je een eigen fotodynamisch onderzoek hebt opgezet en momenteel in Houston te USA bij de afdeling vaatchirurgie werkzaam bent maakt dat je helaas niet bij de promotie aanwezig kunt zijn. Veel succes bij de continuering van de fotodynamische studie, de opleiding en je gezin.

Dr. G.C. Schoonderwoerd, beste Kees, dankzij je kennis en ervaring konden we de rol van mitochondriën bij de synthese van protoporfyrines beschrijven zodat het desbetreffende artikel een hoger wetenschappelijk gehalte kreeg. Je aanwezigheid en betrokkenheid is altijd hand in hand gegaan met veel gezelligheid.

Dr. W.J. Ligetvoet-Gussenhoven, beste 'lady' Elma. Hartelijk dank voor je openhartigheid en gezelligheid. De vanzelfsprekendheid en het gemak waarmee je me de geometrie meetmethoden bijbracht is ronduit super. Ik zal niet vergeten dat ik tijdens de weken, zo niet maanden van aaneenstuk door meten van de histologische coupes, de neiging kreeg om automatisch een schatting te maken van de omtrek, diameter en oppervlakte van elke ronde vorm die ik op weg naar huis tegen kwam. Veel succes in je nieuwe levensfase.

Dr. P. Mulder, beste Paul, een waar genie op het gebied van de statistische toetsen en de strategische significanties. Bedankt voor de heldere toelichtingen en bijdrage bij de diverse publicaties. Zelfs nadat u uw enkel gebroken had was de deadline destijds voor u geen probleem. De kleine commissie: Prof. Dr. P.M.T. Pattynama, Prof. Dr. T.H. van der Kwast en Prof. J.H.P. Wilson. Hartelijk dank voor het beoordelen van dit proefschrift en uw bereidheid om deel te nemen in de kleine commissie. Prof. Dr. P.J. de Feyter, Prof. Dr. H.W. Tilanus, Dr. M.R.H.M. van Sambeek, hartelijk dank voor uw deelname in de grote commissie.

Dr. R. de Bruin, beste Ron. Bedankt voor de goede en professionele werksfeer op het

experimenteel chirurgisch lab, waardoor ik de talrijke microchirurgische operaties probleemloos heb kunnen doen. Met veel plezier zal ik blijven terugdenken aan de tijd van aaneenstuk door opereren in het lab waar menig onderzoeker in opperste concentratie bezig was.

Ir. J. Honkoop. Beste Jan, bedankt voor je technische expertische bij het opzetten van het bursting pressure model. Het gemak waarmee je de technische problemen wist op te lossen verdient alle lof.

Dr. M. Kliffen, beste Mike. Bedankt voor je heldere histologische analyse bij het bursting pressure verhaal waardoor het gepubliceerd kon worden. Dr. J. Kros, Dr. Marc Bakker en Donal Hayes, bedankt voor jullie analyse.

Ir. A. van Edixhoven, beste Annie, een super analiste op het gebied van de protoporfyrine analyses. Bedankt voor je inzet en expertise. Veel succes op je nieuwe werkplek.

Dr. F.W.M. de Rooy, beste Felix, dankzij het meedenken in het begin stadium konden cruciale stappen genomen worden. Bedankt voor de nuttige gesprekken en de rit in de limo te Vancouver. Veel succes met de lopende projecten.

Dr. P.D. Siersema, W. de Vrie, en J. Haringsma. Beste Peter, Wim en Jelle, bedankt voor de goede samenwerking bij de klinische PDT trial ter behandeling van Barret esofagitis. Met de inmiddels opgedane Amerikaanse ervaringen wil ik jullie veel succes wensen bij de vervolg projecten.

Ir. E. Bruyn, beste Elly, dankzij jouw expertise bij de ontstekingskleuringen kon het manuscript uitgewerkt worden, waarvoor mijn dank.

Dr. A. Houtsmuller en Ir. A. Nigg de mannen van de digitale microscopische fluorescentie analyses. Bedankt voor de uitleg en jullie bijdrage bij de fluorescentie analyse.

Dr. Piet van de Heul, hartelijk dank voor de electronen microscopische analyse van de mitochondriën.

Dr. D.Sterenborg, beste Dik, je bent een echte fysicus met hart voor PDT. Bedankt voor de samenwerking en de adviezen. Ik wil je veel succes wensen met de PDT studies.

Ir. R. van der Veen, beste Robert bedankt voor de samenwerking bij de klinische PDT trial en het co-auteurschap in het befaamde dosimetrie artikel. Succes bij jouw promotie.

Van het laboratorium biochemie wil ik Prof. Dr. J.F. Koster bedanken voor de mogelijkheid om op het lab onderzoek te kunnen doen. Prof. Dr. J.M.J. Lamers, Prof. Dr. H.R. Scholte, Prof. Dr. H. Jansen, Prof. Dr. A. van Tol, Prof. Dr. H.R. de Jonge, Dr. A.J.M. Verhoeven, Dr. B.C.Tilly, Karel Bestarosti, Dick H.W. Dekkers, Marcel Edixhoven, Teus van Gent, Lydia van Garstel, Anne de Munck, bedankt voor de nuttige voordrachten en jullie interesse in het onderzoek.

Cecile Hanson bedankt voor je secretariële steun en Rinus Machielsen bedankt voor je belangstelling. De analisten Regina Kraak-Slee en Elly Merbel-de Wit, bedankt voor het werken op jullie lab.

De post-docs Thea van der Wijk, Delfina Vieira en Jet de Jonge veel succes met jullie carrière.

De AIO's Hans Hut (bedankt voor je tip!), Bas F.B. Tomassen, Jessica T. Lie, Gert-Jan Botma veel succes met jullie onderzoek. Wanneer gaan jullie de boel afronden?

Ter nagedachtenis aan Dr. Wil J. Kort en aan Albert Kershof van het laboratorium experimentele heelkunde die hun bijdrage en interesse lieten blijken.

De laser genoten Dr. Joos Heisterkamp, Dr. Jolande van den Boogert en Dr. Petra Hinnen, bedankt voor jullie praktische tips en succes met jullie carrière.

Van de PDT werkgroep wil ik Dr. Hugo van Staveren en Riëtte Bruine bedanken voor de leuke en nuttige gesprekken.

Van het laboratorium experimentele cardiologie wil ik Dr. Rob Krams, Dr. Stephane Carlier, Luc van Damme, Dr. Heleen van Beusenkomp, Prof. Dr. Piet Verdouw en Prof. Dr. Dik J.G.M. Dunckers bedanken voor de interesse en de mogelijkheid te werken op het cath-lab.

Van het laboratorium kinderchirurgie wil ik Patricia Specht bedanken voor de flow metingen.

Coby Peekstok, Manon Holtman, Patricia Lobe, Frida van der Ham en Janine van Leeuwen van het laboratorium pathologie, bedankt voor de histologische kleuringen, waardoor ik de talloze coupes kon gaan analyseren. Lovenswaardig is de vanzelfsprekendheid en het gemak waarop dit altijd ging. Petje af, hoor! Dhr. F.L. van der Panne, bedankt voor de digitale foto instructies.

Ing. Fred Bonthuis, Dr. Timo ten Hagen (hopelijk komt het gezamenlijke artikel ooit), Sandra van Tiel, An Seynhaven, Pim van Schalkwijk, Ton Boymans, Boudewijn van Etten en Dr. Frans Oei, bedankt voor jullie interesse en praktische adviezen.

Mika Vogel, bedankt voor de thermografische analyse en de CT scans van de gefotosensitiseerde ratjes. Veel succes met je promotie onderzoek.

De Raman spectroscopie groep met Tom Bakker Schut, Dr. Kees Maquelin en Ron Wolthuis: Bedankt voor jullie interesse en hulp als ik weer iets voor de YAG laser nodig had.

De technische dienst met Jan van de Berg en Anton Caldehoven. Voor technische zaken omtrend de laser stonden jullie altijd klaar. Keep those lasers running! Veel succes met jullie verdere loopbaan. Dhr. Jan Tuin van de afdeling thorax chirurgie, bedankt voor het digitaliseren!

Van het experimenteel proefdier centrum wil ik vermelden Ed Lansbergen, Esther Fijneman, Albert Kloosterman, Enno Collij, Frans Schreeve, Marijke Lagerman, Henk Dronk, John Mahabier, Roy Spruijt en Piet Kreeft. Bedankt voor jullie goede zorg voor de proefdieren.

Anneke de Zwart, bedankt voor de secretariële steun.

De paranimfen, Dr. Ewout Kouwenhoven en Patrick Fungaloi, twee chirurgen in hart en nieren die het Rotterdamse avontuur hebben meegemaakt. Beste Ewout, bedankt dat je mijn paranimf wilt zijn. Je weet wat het is om te promoveren, te werken als chirurg en een goede balans te vinden tussen werk en het leven daarnaast. Beste Patrick, bedankt dat je mijn paranimf bent. De ervaring met het maken van een anastomose in het varkensmodel komt nu goed van pas in de kliniek. Veel succes met de laatste loodjes van je promotie m.b.t. fotodynamische therapie.

Het thuisfront

Lieve Pa, bedankt voor je goede zorg, vertrouwen en steun. Veel zaken uit het leven lijken inderdaad op een goede schaakpartij. Ervan leren en ook nogeens goed kunnen genieten met de nodige humor lijkt mij geen onaardige conclusie. Op naar de volgende uitdagingen!

Ik heb het echt getroffen met 3 geweldige zussen. Jullie steun is onvervangbaar. Dankzij jullie is het relativeren van een boel zaken altijd weer gegarandeerd pret. Annette, met het credo 'ervoor gaan' kom je inderdaad ver. Jouw scherpe kijk op zaken heeft al menigmaal een verfrissende uitwerking gehad. Lydia, bedankt voor je inspiratie, betrokkenheid en luisterend oor. Volgens mij kun jij inmiddels ook een PDT sessie verrichten na alle verhalen over de gelaserde ratjes.

Wanneer pakken we weer een filmpje? Ha Margriet, in één woord 'Haarlem'. De waarde hiervan weet alleen jij op zijn merites te beoordelen. Het feit dat je afgezien hebt van de opleiding tot jachtvlieger heeft al meerdere malen zijn vruchten afgeworpen, en jou kennende zal dat wel zijn vruchten blijven afwerpen. Wanneer jij je diploma hebt gaan we naar NY! Josia, zwager!

Bedankt voor je vriendschap. Er zijn er maar weinig met wie je lekker kunt door filosoferen over de zaken in het leven. Ik zal jouw support al vanaf dat ik je ken niet vergeten. Mijn neven Christian, Dennis John en Samuël. Kanjers! Bedankt voor jullie spontaniteit! Jullie komen er wel!

Schoonfamilie in spé, bedankt voor jullie interesse en steun. Wonderen bestaan, en ik geloof dat jullie precies weten wat ik bedoel!

Caroline, lieverd, jij weet precies wat het is om te promoveren en arts te zijn! Bedankt voor je steun en je bijdrage, maar bovenal voor wie je bent! Jouw vriendschap, vrolijkheid en enthousiasme is one-of-a-kind. Wat dacht je van het strand, de zee of het bos?

Last but not least, alle dank aan God, immers 'de vreze des Heren is de ware wijsheid'.

Curriculum vitae

Edward E. E. Gabeler was born on January 23, 1973 in Haarlem, The Netherlands.

He graduated in atheneum β in 1991 from the Spaarne Lyceum in Haarlem and continued his studies at the Faculty of Medicine of the University of Amsterdam.

In the summer of 1991 he worked at the laboratory of the GG&GD in Haarlem. Since 1992 he participated in surgical research at the Department of Surgery of the Academic Medical Center of Amsterdam (Prof. Dr. T. M. van Gulik). The studied surgical related topics were respectively:

1. the postoperative morbidity after the Whipple procedure, 2. the effect of Tissucol in the prevention of pancreatic duct leakage, 3. liver ischemia and reperfusion injury in a pig model, and 4. the role of bile acid in the preservation of bile ducts in UW solution. The last study was presented at the European Society of Surgical Research in Padua, Italy. In the summer of 1997, the author went for a short clinical stay at the Department of Urology of the Medical Hospital of Modena, Italy (Dr. G. Berri).

In 1998 the author was qualified as medical doctor and was offered a position as PhD student by Dr. R. van Hillegersberg at the Department of Vascular Surgery of the Erasmus Medical Center of Rotterdam. In this project on 'Endovascular photodynamic therapy to prevent arterial restenosis', he worked with Dr. W. Sluiter of the Department of Biochemistry and with Dr. R.G. Stadius van Eps of the Department of Surgery, under supervision of Prof. Dr. H. van Urk of the Department of Vascular Surgery. As a PhD student he has been qualified for the 'ex-article 9' in 1998 for 'Good Laboratory Practice', the Microsurgery course in 1999, the Oxford examination English, a basic course on Photochemistry and Photobiology in San Jose, California, USA and the Classical methods for data-analysis at the Erasmus MC in 2000. In 2001 he taught fundamentals of Clinical Lasers at the Laser Course organized by EMCO at the Erasmus MC. During the 4 years as a PhD student, he was involved in PDT-related research by Dr. P. Siersema and Dr. J. Haringsma on the project entitled 'PDT in the treatment of Barrett's Esophagitis', by Dr. J. Heisterkamp on 'Interstitial laser coagulation of liver tumors', by Dr. D. Sterenborg and Dr. R. van der Veen in light dosimetry during PDT of Barrett's Esophagitis and by Dr. R. Krams in the induction of restenosis in the cholesterolemic rabbit model.

The author worked as resident under the supervision of Prof. Dr. C. J. Avezaat at the Department of Neurosurgery, Erasmus MC, Rotterdam, The Netherlands.

Het einde ener zaak is beter dan haar begin
Prediker 7:8

